VISCOSITY OF SIMPLE LIQUIDS INCLUDING MEASUREMENT AND PREDICTION AT ELEVATED PRESSURE

A thesis submitted for the degree of

Doctor of Philosophy

of

The University of Strathclyde

Department of Chemical and Process Engineering

by

J D ISDALE

National Engineering Laboratory

1976

ACKNOWLEDGEMENTS

This work has been carried out in Properties of Fluids Division at National Engineering Laboratory, East Kilbride. The author would like to thank Director, NEL, for permission to use the facilities of the Laboratory for this work, and those colleagues who have contributed in various ways.

Particular thanks are due to Dr L Grunberg, CBE, past Superintendent of Fluids Group and visiting Professor at University of Strathclyde, for his continued encouragement, support, and constructive criticism, and also to Mr C M Spence for practical assistance with much of the experimental work.

Thanks are also due to Dr R Hendry and Professor G S G Beveridge of the Department of Chemical Engineering at Strathclyde for their continued interest and advice.

S U M M A R Y

A falling body viscometer with self-centring sinkers has been developed and used to measure the viscosities of benzene, carbon tetrachloride and eight halogenated hydrocarbons at pressures up to 500 MN m^{-2} in the temperature range 25°C to 100°C. Two isotherms of water have also been measured at pressures up to 1000 MN m^{-2}. Details of the viscometer and its pressurising equipment are given together with an analysis of the performance of the system.

The results are estimated to be accurate to within ±2 per cent, and show good agreement with other measured data where available. The change of viscosity with pressure for the halogenated hydrocarbons is generally similar to that of other simple liquids. The results show that liquids having molecules of similar shape also have a similar change in relative viscosity with pressure.

Theories of liquid viscosity are reviewed and constants required by Eyring's significant structure theory are obtained for more than sixty liquids using literature data. Methods are derived for calculating these constants from correlations with readily available critical properties or chemical structure. The correlations are tested using the new measurements and literature data. These tests show that the methods derived work well if one or two values of viscosity at atmospheric pressure can be used but are less reliable if only structural information is available. Since at least one measured viscosity is available for most liquids it is concluded that the method will be useful for predicting viscosities at other temperatures and pressures.

C O N T E N T S

N O T A T I O N

Except where specified otherwise the symbols used have the following meaning:

A	Viscometer constant
A_o	Viscometer constant in equation (6.5)
A_i	Constants in Chebyshev series
B	Viscometer constant in equation (6.5)
g	Gravitational constant
K	Ratio of diameter of sinker to viscometer bore
$\bar{K}$	Isothermal secant bulk modulus
K_o	Isothermal secant bulk modulus at atmospheric pressure
L_s	Sinker length
L_r	Length of measuring section of viscometer tube
m	Sinker mass
m	Slope of bulk modulus against pressure plot in equation (7.4)
N	Constant in equation (6.5)
P	Liquid pressure
P^*	Reduced pressure defined by $P^* = \log(1 + \frac{P}{200})$ with P in MN m^{-2}
P_c	Critical pressure
Re	Reynolds number
r_1	Sinker radius
r_2	Tube radius
T	Time for sinker to fall fixed length
T_c	Critical temperature
$T_i(x)$	Chebyshev series of degree i
t	Liquid temperature
t_o	Temperature at which viscometer is measured
$\bar{U}$	Mean fluid velocity

N O T A T I O N (contd)

V	Terminal velocity of sinker
v	Specific volume
v_o	Limiting specific volume
v_c	Critical volume
Z_c	Critical compressibility factor
α	Linear coefficient of expansion of tube and sinker
β	Coefficient of compressibility of tube and sinker
η	Liquid viscosity
η_o	Liquid viscosity at atmospheric pressure
ρ_L	Liquid density
ρ_s	Sinker density

C H A P T E R 1

INTRODUCTION

1 INTRODUCTION

The AIChE Physical Property Estimation System report (1965) states 'Liquid viscosities are available at low temperatures for many materials. No reliable estimation method is available ... Liquids under pressure and liquid mixtures are in even a worse position. Data are not plentiful and correlations of any kind are scarce and only approximate. This is an area which needs immediate attention.' This investigation was initiated with the object of studying liquid viscosity in order to extend methods for prediction at saturation or elevated pressure.

Existing viscosity theories and empirical methods have been examined since it was decided at an early stage that the best chance of developing a successful method of prediction would come from a method based at least in part on one of the current theories of liquid viscosity.

This decision was taken because it was felt that, while it might be simpler to obtain empirical correlations for homologous series of chemical compounds, the chances of obtaining cross correlations of empirical constants between such series, would be small, and hence any method based on this approach would probably be seriously limited. This point of view is supported by Reid and Sherwood (1966) in the introduction to their book 'The properties of gases and liquids' where they state 'Correlations are of three types: purely empirical, partly empirical but based on some theoretical concept, and purely theoretical. The first is often unreliable and worthless, and the third is seldom adequately developed. Most of the useful correlations are of a form suggested in part by theory, with empirical constants based on experimental data.'

Since existing fundamental and model based theories can strictly only be applied to simple spherical molecules, an attempt has been made here to extend one of these, the significant structure theory, to real molecules. An examination of the variation of structure dependent constants, which occur in the theory, for a wide range of liquids has led to the development of correlations which allow these constants to be predicted for certain types of liquids.

To assist this study a self-centring falling body viscometer has been developed and used to measure the viscosity of ten liquids at pressures up to 500 MN m^{-2}, and water up to 1 000 MN m^{-2}. The data produced have been used to test the correlations. The halogenated hydrocarbons were selected because few have been measured under pressure and because as a group they are becoming increasingly important industrially. To aid the analytical part of the project, the liquids were restricted to those of fairly simple molecular shapes so that the influence of single structural units on the parameters used could be detected.

Three liquids have been included which have been measured by other investigators at pressure. These liquids, water, carbon tetrachloride, and benzene, were included to check the accuracy of the measurement technique, and also to extend the temperature range.

Extensive use has been made of data from the literature both at atmospheric or saturation pressure and under high pressure. To simplify the handling of large numbers of data values were stored on magnetic tape so that they could be easily accessed by computer.

The falling body method was chosen for the experimental measurements. This method has a number of advantages which make it attractive for use

in hostile environments. Viscosity is calculated from the measurement of fall time only and this can be done electrically remote from the viscometer: only one fill with the sample is needed for a series of measurements and the sample is completely enclosed in the viscometer tube.

C H A P T E R 2

REVIEW OF VISCOSITY THEORIES

SUMMARY OF CHAPTER 2

2 REVIEW OF VISCOSITY THEORIES

Newton defined viscosity as the constant of proportionality between applied stress and resulting velocity gradient. Since stress can be considered as momentum flux normal to the net motion it follows that viscosity is that property which describes momentum flux in fluids.

Momentum may be transferred in two ways: firstly by bodily movement of molecules, with their individual momenta, across planes of net motion, and secondly by direct interaction between the force fields of adjacent molecules. The former type of transfer is dominant in gases and the latter in liquids. From simple considerations it is easily deduced that fluid viscosity is the sum of a gas-like and a liquid-like term. However the liquid-like term is a function of the average intermolecular distance usually expressed in terms of a radial distribution function. Since the radial distribution function cannot at present be calculated for real molecules, mainly because of distortion caused by the flow, this fundamental approach does not yet provide a method for calculating viscosity in real fluids in the liquid state.

As the basic approach is still quite far from practical use several models for the flow mechanism in liquids have been proposed in attempts to overcome the difficulties. These are usually based either on the concept of an activation energy for viscous flow or on the availability of free volume in the liquid. The activation energy concept assumes that a molecule requires a certain amount of energy, the activation energy, before it can contribute to the flow process. This method has been used by Eyring, Glasstone, Laidler and Eyring,

Frenkel and others, and usually leads to equations of the well known Arrhenius or Andrade type. By considering free volume Cohen and Turnbull, Matheson and others have derived equations similar in form to that proposed on empirical grounds by Doolittle. Both types of equation are known to fit experimental data well and in fact Barlow, Lamb and Matheson have shown that, for some liquids, the Arrhenius type of equation is best at high temperatures while the free volume equation is best at lower temperatures. Further developments of Eyring's theory by Ree, Ree and Eyring and by Jhon, Klotz and Eyring have led to forms which incorporate the effects of free volume.

Numerous other equations are available, many of which are described by Brush, Partington or Rowlinson. Most of these are either unreliable or are limited to small groups of liquids. The constants required to predict the viscosity of a particular liquid cannot be obtained without experimental viscosity data. Even the better developed model theories can strictly only be applied to spherically symmetric molecules.

It is concluded that the significant structure theory of Eyring and others allows three parameters to be identified which should contain the major part of the effects of chemical structure on viscosity.

CHAPTER 2 - REVIEW OF VISCOSITY THEORIES

2 REVIEW OF VISCOSITY THEORIES

Newton defined the coefficient of viscosity as the constant of proportionality between applied stress and the resulting velocity gradient. In the past three centuries it has been found experimentally that the majority of liquids obey this law. For an elemental volume $\delta x \delta y \delta z$ subject to a force F_{xy} acting in the x direction over a plane normal to the y direction, Newton's law may be expressed by

$$\frac{F_{xy}}{\delta x \delta z} = -\eta \frac{u_x}{\delta y} ,$$

or

$$S_{xy} = -\eta G_{xy} , \qquad (2.1)$$

where u_x is velocity, S is shear stress, G is velocity gradient, and the subscripts x and y have the same meaning associated with force above. Equation 2.1 may be generalised using tensor notation though in fact it is necessary to introduce a second coefficient, the bulk viscosity, to describe the relationship (assumed linear) between normal stresses and velocity gradients. In practice the bulk viscosity is usually assumed to be zero and is certainly undetectable in most simple shearing experiments. While the continuum mechanics approach is useful in defining the relationships between stresses and velocity gradients it does not give any insight into the origin of these relationships or the liquid properties which lead to them. To do this it is necessary to examine equation 2.1 in a slightly different way.

If the shearing force is considered, by Newton's second law, to be rate of change of x momentum in the y direction then equation 2.1 describes the relationship between the total momentum flow and velocity gradient occurring in the elementary volume. On the molecular

scale momentum is transferred as a result of the molecular motions and interactions which occur within the volume considered. The kinetic contribution to momentum transfer due to the bodily movement of molecules is simply given by

$$\frac{1}{V} \sum_i p_{ix} p_{iy}/m \ ,$$

where the summation is taken over all the molecules in volume V. If the molecules interact through central force fields then momentum transfer by interaction is given by

$$\frac{1}{V} \sum_{pairs} F_{ij}(r_{ij}) (x_{ij} y_{ij})/r_{ih} \ ,$$

where the summation is taken over all interacting pairs in volume V.

Summing these two terms to give the shear stress and substituting in equation 2.1 gives

$$\eta = -\frac{1}{VG_{xy}} \sum_i \frac{p_{ix} p_{iy}}{m} - \frac{1}{VG_{xy}} \sum_{pairs} \frac{F_{ij}(r_{ij})(x_{ij} y_{ij})}{r_{ij}} \qquad (2.2)$$

Equation 2.2 then gives viscosity in terms of the properties of the assembly of molecules and can clearly be expressed as mass, velocity, separation, and force field. Classically the whole viscosity problem is centred on solutions to equation 2.2 and the evaluation of the integrals which occur as a consequence of the summation terms.

2.1 Classical Methods

By using the concepts of a mean free path, λ, and a mean square velocity, $\bar{u}$, and by assuming that the second term in equation 2.2 was small, Maxwell was able to show that, for gases at low density the equation could be reduced to the well known form

$$\eta = k \bar{u} \rho \lambda .$$

Maxwell's later more general kinetic theory expressed velocity in terms of a radial distribution function which defined the velocity of molecules within a given radius of one at the origin. For a particular intermolecular force law he was able to carry out the necessary integrations and evaluate the viscosity of gases at low density with considerable success, and later refinements allowed Lennard-Jones to deduce an exact form of intermolecular potential function.

The success of Maxwell's theory has led to attempts to apply the same basic principles to higher density gases and liquids, particularly by Kirkwood (1935) and by Born and Green (1946). The difficulty with this approach lies in the evaluation of the radial distribution functions. In equilibrium both the velocity and number distributions are symmetric, but when a shear stress is present they become distorted by the flow and are difficult to calculate. Kirkwood was able to deduce a function which could be evaluated and which enabled Kirkwood, Buff and Green (1949) to calculate hard sphere viscosities for some liquids. Born and Green later extended this method for molecules with central force fields but were unable to include a suitable distribution function.

Though much effort is devoted to the classical approach (see for example reviews by Green (1952), Bondi (1968), Brush (1962)) it must be concluded that it is likely to take a very long time to produce methods for predicting viscosity of real liquids of complex molecular shape.

2.2 Dense Gas Theories

Dense gas theories rely essentially on attempts to extrapolate dilute gas viscosities to regions of high density by means of a suitable expression. The most successful of these has been developed by Enskog (1922) and is based on a virial type of expansion

$$\eta = \eta_0(y^{-1} + A + By) \qquad (2.3)$$

The theory was developed for hard spheres, with y being a correction factor for the increase in collision frequency with density, though only two body collisions were considered. The coefficients may be calculated from an equation of state and the equation has been used successfully to predict the viscosity of dense gases. It seems unlikely, however, that the theory will deal satisfactorily with liquids for three reasons:

1 the basic assumption of two body collisions has restricted the form of the equation and the effect of multiple collision, which will occur comparatively frequently in liquids, is therefore excluded

2 the hard sphere assumption will be valid only in a few very specific cases

3 it is not clear how the effects of non spherical shape may be introduced.

Nevertheless this theory in a corrected form has recently been used to predict self diffusion coefficients for pseudo spherical molecules with some success (Dymond (1973)).

2.3 Solid-like Liquid Theories

Many currently popular theories and semi-empirical methods fall in this category. Most of these have been severely criticised because they invariably rely on one or more constants which can only be obtained by data fitting (see for example Brush (1962)). They rely mainly on variations of two basic models, the potential barrier mechanism and the free volume mechanism. Most lead to equations of a similar exponential type which can fit the data rather well, so that it becomes difficult to make a choice on objective grounds.

If it is assumed that atoms or molecules are located at the bottom of a potential well, then, for flow to occur, it is necessary for the atom or molecule to possess sufficient energy, W, to overcome the potential barrier. The chance to flow is then governed by the probability of each atom having this energy and, since this probability is proportional to the fluidity of the liquid, it follows that the viscosity is proportional to $e^{W/kT}$ giving

$$\eta = A\, e^{W/kT} \qquad (2.4)$$

A simple theoretical derivation of this equation was given by Frenkel (1955). It has been widely used and is often referred to as the Arrhenius or Andrade equation. It is capable of fitting the experimental data of many simple liquids over quite wide temperature ranges. It has also been used in modified forms to account for deviations from the simple form. The energy constant $W/\underline{k}$ or E_v/R, can be split into two or more parts which allow for the separate contributions of liquid structure, molecular structure, molecular interaction and as many other degrees of freedom as the system possesses. However, it is in general not possible to calculate E_v for any liquid without resorting to data fitting, though studies of

homologous series have shown that E_v does vary in a regular manner within a given series (Grunberg (1955)).

By analogy with chemical reaction rate theory and using the barrier mechanism, Eyring (1936) was able to derive an equation similar to equation 2.4. In this case the energy of activation was assumed to be proportional to the energy of vaporisation, and A in equation 2.4 was calculated as a function of volume, temperature and activation energy.

Another approach using free volume has been developed by Cohen and Turnbull (1959). In this case it is assumed that the chance of a transitional jump taking place is governed by the probability that there is an adjacent vacant site. They were able to deduce that this probability is given by

$$p_j = A\, e^{-Bv/v_f}$$

which in terms of viscosity is

$$\eta = A\, e^{Bv^*/v_f}$$

where v^* is the hole volume required for flow. This form of equation was first suggested by Doolittle (1951) on purely empirical grounds and is known to be capable of fitting the experimental data of many liquids with good accuracy. In fact, Cohen and Turnbull's analysis introduced another factor $T^{\frac{1}{2}}$ in the expression for viscosity, but they neglected it when comparing their equation with experimental data, since its variation is small compared with the variation of the exponential term.

Though this equation produces excellent fits to experimental data, it must be again concluded that it is not possible to predict the constants for a given liquid. The free volume v_f is usually assumed

to be given by the difference between the bulk liquid volume v, and the volume of some hypothetical solid-like state, v_o. If then v is linearly related to temperature by

$$v = v_o\left[1 + \alpha(T - T_o)\right] ,$$

the free volume equation can be written in terms of temperature as

$$\eta = A\, e^{\frac{B}{T - T_o}}$$

This form has been used by a number of workers.

The potential barrier mechanism and the free volume mechanism are not mutually exclusive. On simple physical reasoning one would expect the energy of the molecule to be the governing factor in cases where there is a large proportion of free volume available for flow, and when free volume is scarce the probability of finding available space would be dominant. Barlow, Lamb and Matheson (1966) have shown that this is true for some liquids.

Eyring and others later extended the reaction rate model to include the effects of identified 'significant liquid structures'. The new theory assumes that a liquid is composed of a mixture of 'fluidized vacancies' and liquid molecules in a solid-like state. Each fluidized vacancy of molecular size confers gas-like properties to one molecule so that the viscosity of the liquid is then equal to the sum of the viscosities of the gas-like and solid-like molecules times their respective volume fractions

$$\eta = \eta_g \frac{v - v_s}{v} + \eta_s \frac{v_s}{v}$$

The viscosity of the gas-like molecules can be derived from kinetic theory but at temperatures well below the critical it is small enough to be neglected in comparison with the solid-like viscosity.

This model satisfies some of the criticisms that are made of the Arrhenius and the free volume models since both the availability of free space and the activation energy enter into the calculation of solid-like viscosity. Neglecting the gas-like viscosity term and grouping the constants allows the final equation for liquid viscosity to be written

$$\eta = \frac{T^{\frac{1}{2}}}{v - v_s} e^{\left\{A + \frac{Bv_s}{v - v_s}\right\}} \quad .$$

2.4 Empirical Methods

Empirical and semi-empirical methods of predicting viscosities are numerous. Some of these are described by Reid and Sherwood (1958), Partington (1951), Brush (1962), and Bretsznajder (1971). One method not included in these references is that developed by Roelands (1966) for lubricating oils, which can also be applied to pure liquids. This method is based on two equations, the first of which describes the viscosity at atmospheric pressure in terms of temperature, and the second describes the variations of viscosity with pressure at constant temperature. They are

$$\log(\log \eta_o + 1.200) = -S \log(1 + \frac{T}{135}) + \log G_o$$

and

$$\log(\log \eta + 1.200) = Z \log(1 + \frac{P}{2000}) + \log(\log \eta_o + 1.200)$$

where η_o is the viscosity at atmospheric pressure and S and Z are constants. The third constant G_o is given by

$$G_o = \log(\log \eta_o + 1.200) \text{ at } 0^\circ C \quad .$$

The temperature constant S and the pressure constant Z, can both be obtained for pure liquids from correlations with density or refractive index. The temperature constant can also be obtained

from a correlation with molecular weight. Roelands concluded that his method could be used for pure liquids though for some, particularly ones with high aromatic content, the agreement between predicted and experimental values was rather poor.

This method is limited by the form of the viscosity pressure equation which limits the variation of the slope of a logarithm of viscosity against pressure plot. According to the equation $d(\log \eta)/dP$ can either increase or decrease in the positive pressure region, depending on the appropriate value of Z. In practice this function can both increase and decrease along a single isotherm. Bridgman lists seventeen liquids which show this type of behaviour and it is especially marked in the case of the silicones (ASME 1953).

The real limitation of Roelands' method, however, is that it does not work well for liquids of low viscosity as will be shown later.

2.5 Discussion

From the foregoing it was clear that existing theories of viscosity are either not sufficiently developed, are limited to certain types or groups of liquids, or require that one or more viscosities be known in order to predict viscosities in the liquid region.

Since the principle object of the present work was to develop a method for predicting viscosity, it was therefore clear that a totally novel method had to be developed or an existing method selected and further developed to produce the desired result. The latter approach was chosen to make the maximum use of existing experience.

Classical methods were rejected because it was felt that a great deal

of fundamental work would not necessarily lead to a prediction method. Methods based on the ratio of liquid to gas viscosity such as Enskog's theory, or on residual viscosity (the difference between liquid and gas viscosity) such as those described by Bondi (1968), were also rejected since these are still insensitive in the liquid region. Of the remaining model theories the best developed was Eyring's significant structure. From the correlation and prediction point of view this had three points in its favour:

1 it was known to fit liquid viscosity data well (Jhon, Klotz and Eyring (1969), Hogenboom, Webb, and Dixon (1967))

2 it had predicted viscosities of some liquids with reasonable accuracy by applying the hard sphere assumption (Ree, Ree, and Eyring (1964))

3 its constants, though strictly not calculable for molecules of complex shape, were considered to be comparatively well defined and could reasonably be expected to be closely related to molecular properties.

The significant structure theory was therefore chosen for more detailed examination. The full theory is derived in Appendix I in the form used in the present work.

C H A P T E R 3

LIMITING SPECIFIC VOLUME

SUMMARY OF CHAPTER 3

3 VISCOSITY AND LIMITING VOLUME

Since free volume theories and significant structure theory require a limiting value of specific volume this property is examined in its own right. Values have been calculated from molecular data, critical constants, volume fitting, and viscosity fitting at atmospheric and high pressure. Comparisons of the results shown that limiting volumes obtained by the different methods correlate well with each other though the magnitudes may vary. It is also shown that different values of limiting volume may be obtained for one liquid by fitting viscosity data over different temperature ranges.

It is concluded that limiting volumes may be firmly tied to chemical structure using the critical properties method. Values calculated in this way do not produce significantly less accurate fits to experimental data and are easily obtained.

CHAPTER 3 - LIMITING SPECIFIC VOLUME

LIST OF TABLES

LIST OF FIGURES

3 LIMITING SPECIFIC VOLUME

The significant structure theory the Cohen and Turnbull (1959) theory and the Doolittle (1957) equation each contain a constant parameter, v_o, which corresponds to the specific volume of some condensed state. In most investigations values of v_o have been obtained by fitting viscosity data to the appropriate equation, though Doolittle (1951) earlier used a method based on extrapolation of density data to absolute zero temperature. Since values of these parameters have to be obtained in order to predict viscosity, this part of the work was carried out to find out if suitable values could be obtained without using viscosity data.

Doolittle called v_o the 'limiting specific volume' and defined it as 'the limiting volume to which a real liquid would contract if it were to continue to behave as a non-associated liquid without change of phase all the way to absolute zero'. Cohen and Turnbull defined their free volume as the difference between the volume of a 'cage' containing the molecule and the volume of the molecule, though in practice they used a reference temperature and expansion coefficient in testing their equation. In significant structure theory v_o is the 'specific volume of the solid-like structure'.

Hogenboom, Webb and Dixon (1967) have shown that different values of v_o are obtained for one liquid if viscosity data from different temperature regions are fitted to the significant structure equation, the Cohen and Turnbull equation or the Doolittle equation. In each case the variation of v_o indicated an apparent negative temperature coefficient. Neither the Doolittle definition nor the Cohen and Turnbull definition allow any temperature variation of

v_o, and a negative temperature coefficient is clearly contrary to experience even for a solid-like state unless solid/solid transitions are occurring. It follows that each equation is to some degree deficient in describing temperature variation of viscosity.

3.1 Limiting Specific Volumes Calculated from Molecular Data

The most firmly established limiting volume is of course the van der Waals volume, and values for most molecules may be simply calculated from structural constants tabulated by Bondi (1968). If it were possible for molecules to interlock perfectly with each other without leaving any unoccupied space, then a liquid could contract to the van der Waals volume expressed as a specific volume. This quantity therefore represents the minimum limiting value possible without compressing the molecules themselves, and consequently provides a useful reference state for this work. Values calculated by Bondi's method are given in Table 3.1 for several of the liquids examined here.

The van der Waals volume is not the limiting volume defined by the various viscosity theories though it should be close to the quantity defined by Cohen and Turnbull. Several limiting volumes were obtained by Hogenboom, Webb and Dixon by fitting viscosity data to the Cohen and Turnbull equation. These values are included in Table 3.1 where it can be seen that they are about 40 per cent greater than the corresponding van der Waals volumes.

Another form of limiting volume which has not received much attention in this context is the limiting volume at absolute zero temperature.

According to the van der Waals equation the limiting volume at absolute zero is exactly one-third of the critical volume, but values derived from experimental volume data are greater than this. To take account of this deviation from 'ideal' van der Waals behaviour the product $v_c Z_c$ has been used as an approximation to the value at absolute zero, that is

$$v_c = v_c Z_c = v_c \frac{P_c v_c}{R T_c} \quad .$$

Values of the critical parameters for various equations of state are discussed by Hirschfelder, Curtiss and Bird (1954). This quantity was considered by Doolittle but was rejected on the grounds that it was inaccurate and difficult to obtain. It has also been used by Mathews (1916) who attributed it directly to van der Waals. Many critical properties are now available so that this form of limiting volume is now comparatively easily calculated. The critical compressibility factor can also be estimated from normal boiling point or from structure by the methods of Garcia-Barcena (1953) while the critical volume may be calculated from structure by Lydersen's (1955) method.

Table 3.1 gives values for the liquids examined here.

The ratio of the van der Waals volume to the volume at absolute zero is called by Bondi a packing density and values of this ratio calculated as described above are compared with experimental values given by Bondi for several crystalline materials in Table 3.2. Packing densities on simple cubic lattices can vary from 0.524 for spheres to 0.785 for infinitely long cylinders, and both sets of values fall well within this band. In fact the calculated and experimental values are in quite good agreement though the

calculated values are, with only one exception, a little lower.

3.2 Limiting Specific Volumes from Volume Data

For the normal paraffins Doolittle (1951) was able to calculate volumes at absolute zero by extrapolating atmospheric pressure density data. He then correlated his results with the equation

$$v_o = e^{10/m} \quad ,$$

where m is the molecular weight and v_o the limiting volume in cc/gm. Values so obtained are included in Table 3.1.

If the paraffin chains are treated as cylinders radius R, with an axial carbon-carbon bond length a, an axial extension b due to the two hydrogen atoms at each end, and with N carbon atoms it is easily shown that the molecular volume is given by

$$v_o = \frac{\pi R^2}{m M_H} (a(N - 1) + b)$$

where M_H is the mass of the hydrogen atom. Therefore substituting for N using molecular weight gives

$$v_o = A' + B'/m \quad .$$

Expanding Doolittle's correlation gives

$$v_o = 1 + \left(\frac{10}{m}\right) + \left(\frac{10}{m}\right)^2/2! + \left(\frac{10}{m}\right)^3/3! \ldots\ldots \quad .$$

Clearly if m is much greater than 10 the latter two equations are of the same form and

$$A' \sim 1$$

and

$$B' \sim 10 \quad .$$

Doolittle's correlation therefore rests on the cylindrical molecule assumption being valid and should not be applied to other shapes.

Limiting volumes calculated from high pressure volume data are also shown in Table 3.1. These values were obtained by fitting the equation

$$v = v_o(1 + aP + bP^2)(1 + cT) + dT(1 + fT)(e^{-gP} + {}^{h}/_{P}) \qquad (3.1)$$

to the data of Cutler, McMickle, Webb, and Schiessler (1958) and Hogenboom, Webb, and Dixon. The equation fitted the data well and was later used to calculate volumes under pressure. The constants of the equation have no theoretical significance, though the constants of the first group of terms were allowed to take values characteristic of a solid while those of the second group took values characteristic of a gas. The form of the equation ensures that as the temperature tends to zero the volume tends to a limiting value, v_o, with a solid-like compressibility. The values of v_o obtained were similar to those of Doolittle, but were erratic and difficult to obtain.

3.3 Limiting Specific Volumes from Viscosity Data

Values obtained by Hogenboom, Webb, and Dixon are given in Table 3.1 together with three values (for pentane, hexane, and hexadecane) obtained here by fitting API 44 data to Doolittle's equation.

3.4 Viscosity Equations using Predicted Limiting Volumes

In calculating hard sphere viscosities using the significant structure method Ree Ree and Eyring (1964) assumed that the volume of the solid-like state was 1.6 times the 'closest packing volume', which was defined as $3\sqrt{2}/\pi$ times the molecular volume. The packing density of the closest packed state was therefore 0.740, while that of the

solid-like state was 0.463 if the molecular volume is used in place of the van der Waals volume. The latter value is very low indeed for a solid-like state, for example for liquid benzene the packing density is 0.551 near the melting point and 0.504 near the boiling point. Of the normal paraffins only those with more than twelve carbon atoms have packing densities less than 0.46, but then only near the boiling point. It is clear therefore that the limiting volume of solid-like state used by Ree, Ree and Eyring had a packing density more characteristic of a liquid than a solid, though the magnitude of the limiting volume was corrected to an extent by using equivalent molecular diameters calculated from experimental van der Waals volumes.

To investigate the effect of predicted limiting volumes on viscosity equations, tests were carried out on the liquids listed in Table 3.2 using API 44 viscosity and density data. Van der Waals volumes calculated by Bondi's method and the limiting volume at absolute zero calculated from critical properties, were used in both the Doolittle equation and the significant structure equation. The latter quantity is strictly correct only for the Doolittle definition, but in view of the calculated packing densities it was felt that it should also be suitable for the significant structure equation. Van der Waals volumes were used simply to test the effect of low limiting volumes on the equations.

Doolittle's equation is

$$\ln\eta = A + \frac{Bv_o}{v - v_o} \quad ,$$

and was tested by plotting $\ln\eta$ against $1/(v - v_o)$. The results for benzene, pentane and octadecane are shown in Figs 3.1, 3.2, and 3.3.

The equation works well for benzene over the normal liquid range with both types of limiting volume, though the limiting volume at absolute zero is more accurate at low temperatures. For pentane and octadecane, however, it fails to describe the data accurately with either constant.

Results for the same liquids using the significant structure equation are given in Figs 3.4, 3.5, and 3.6. The significant structure equation can be written

$$\ln\left[\frac{\eta(v - v_o)}{T^{\frac{1}{2}}}\right] = A + \frac{Bv_o}{(v - v_o)T} \quad ,$$

and was tested by plotting the left-hand side of the equation against $1/(v - v_o)T$. The results are excellent for both benzene and pentane with the limiting volume at absolute zero but are less satisfactory for octadecane.

In all the tests carried out the significant structure equation was better than the Doolittle equation, and in each case the limiting volume at absolute zero was clearly closer to the optimum limiting volume than the van der Waals volume. The numerical values given in Table 3.1 also show that the limiting volumes at absolute zero for the longer paraffins fall within the band of values obtained by fitting to viscosity data.

3.5 Discussion

It is concluded from the foregoing that the limiting volume at absolute zero calculated from the critical constants is a satisfactory approximation to limiting volume of the solid-like state required by significant structure theory. It has four main advantages:

1 it can be easily calculated for most liquids

2 its magnitude is similar to that obtained by fitting to viscosity data

3 its packing density is consistent with that of a solid-like state

4 it can be obtained without using viscosity or density data.

The non linearity of the experimental points shown on Figs 3.4, 3.5, and 3.6 is clearly the cause of the apparent variation of v_o with temperature.

T A B L E 3.1

COMPARISON OF LIMITING VOLUMES

Compound	Limiting volumes (cc/gm) obtained from						
	(A) structural or critical data		(B) viscosity data fitted to			(C) volume extrapolation by	
	van der Waals volume v_w	$v_c Z_c$	(1) significant structure equation	(2) Cohen and Turnbull equation	(3) Doolittle equation	Doolittle's correlation	equation 3.1
pentane	0.8043	1.1039	-	-	1.077	1.1487	1.215
hexane	0.7921	1.1335	-	-	1.137	1.1230	1.170
dodecane	0.7611	0.9920	1.05 -0.91	1.098-1.038	1.110-1.048	1.0605	1.043
pentadecane	0.7548	0.9528	1.058-0.91	1.106-1.033	1.116-1.044	1.0482	1.070
hexadecane	0.7532	0.9035	-	-	1.119	1.0451	1.098
octadecane	0.7506	0.7858	1.072-0.78	1.100-1.01	1.110-1.021	1.0401	1.056
cis-decalin	-	0.9277	0.899	0.945	0.953	-	0.873
trans-decalin	-	0.9870	0.897	0.960	0.969	-	0.953
spiro4,5decane	-	0.9519	0.909	0.953	0.963	-	0.946
spiro5,5undecane	-	0.9318	0.911	0.957	0.966	-	0.919
cis-octahydroindene	-	0.9136	0.903	0.955	0.965	-	0.993
trans-octahydroindene	-	0.9729	0.895	0.946	0.960	-	0.962

TABLE 3.2

COMPARISON OF PACKING DENSITIES, v_w/v_o

Compound	Packing density, v_w/v_o		
	Calculated from critical properties	Calculated from Doolittle's correlation	Experimental values from Bondi
ethane	0.650	0.653	0.684
propane	0.677	0.678	0.695
butane	0.685	0.694	0.725
pentane	0.729	0.700	0.711
hexane	0.699	0.705	0.722
octane	0.698	0.713	0.735
nonane	0.712	0.715	0.727
benzene	0.689	-	0.697
toluene	0.733	-	0.675

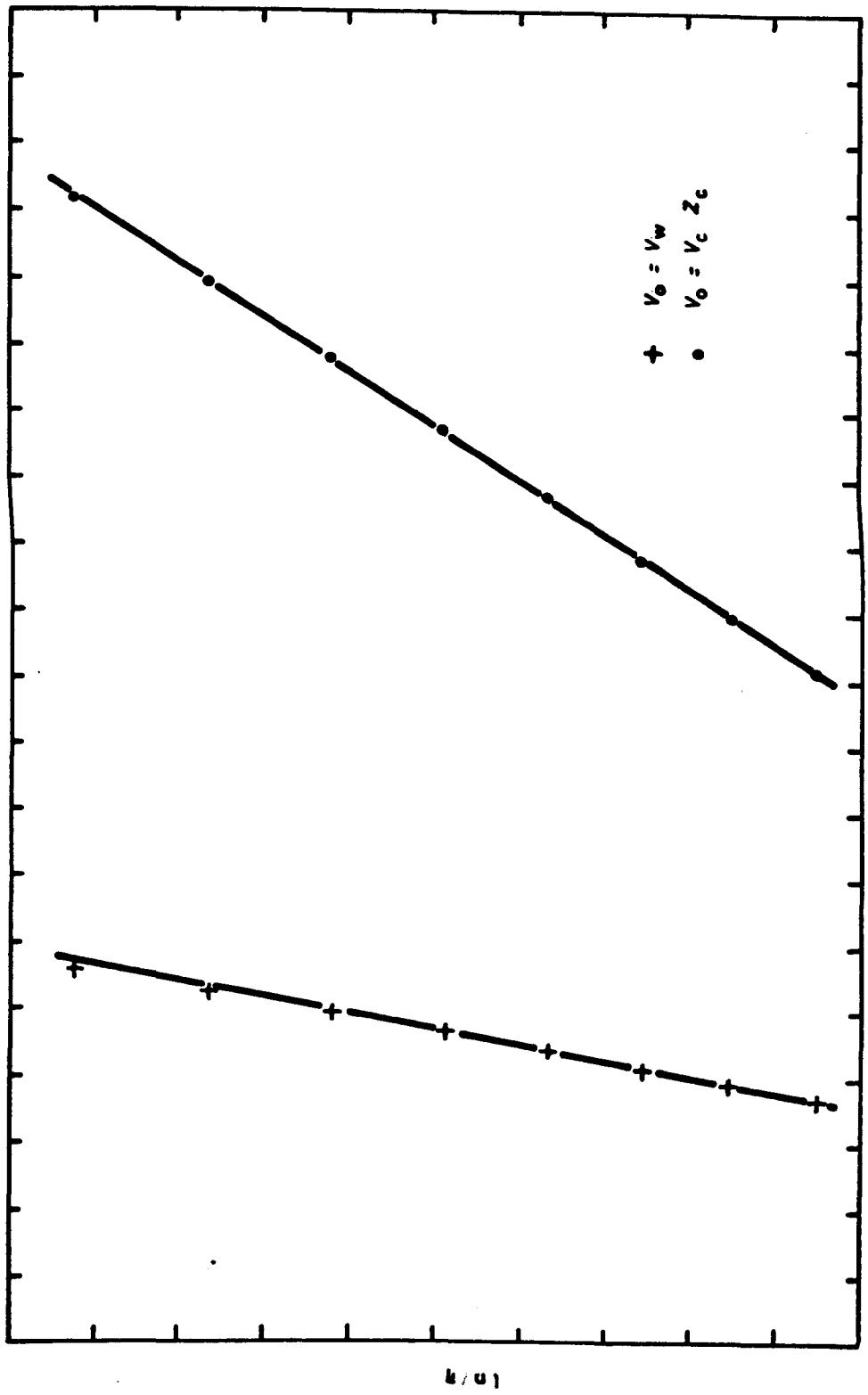

FIG 3.1 TEST OF DOOLITTLE'S EQUATION WITH BENZENE DATA

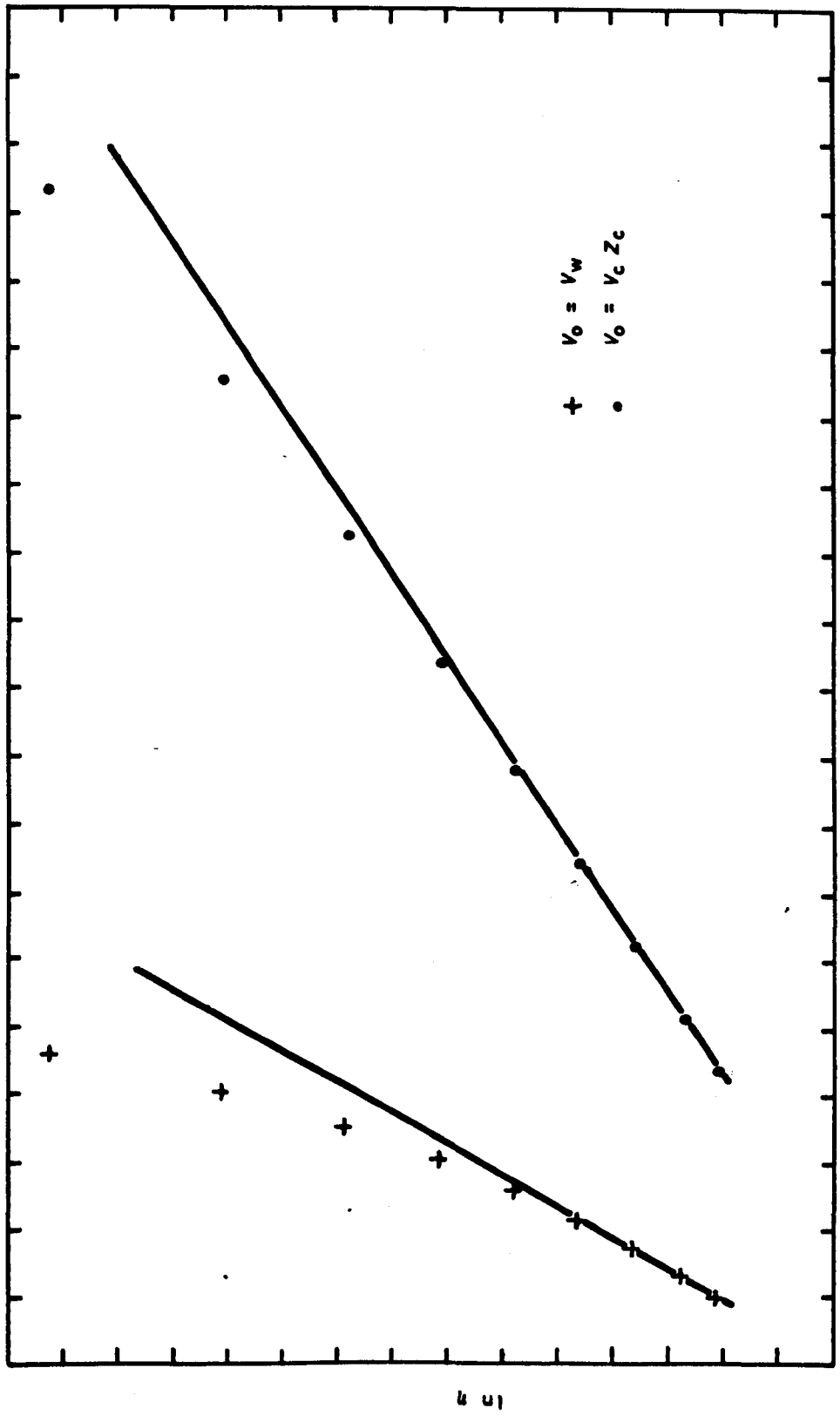

FIG 3.2 TEST OF DOOLITTLE'S EQUATION WITH PENTANE DATA

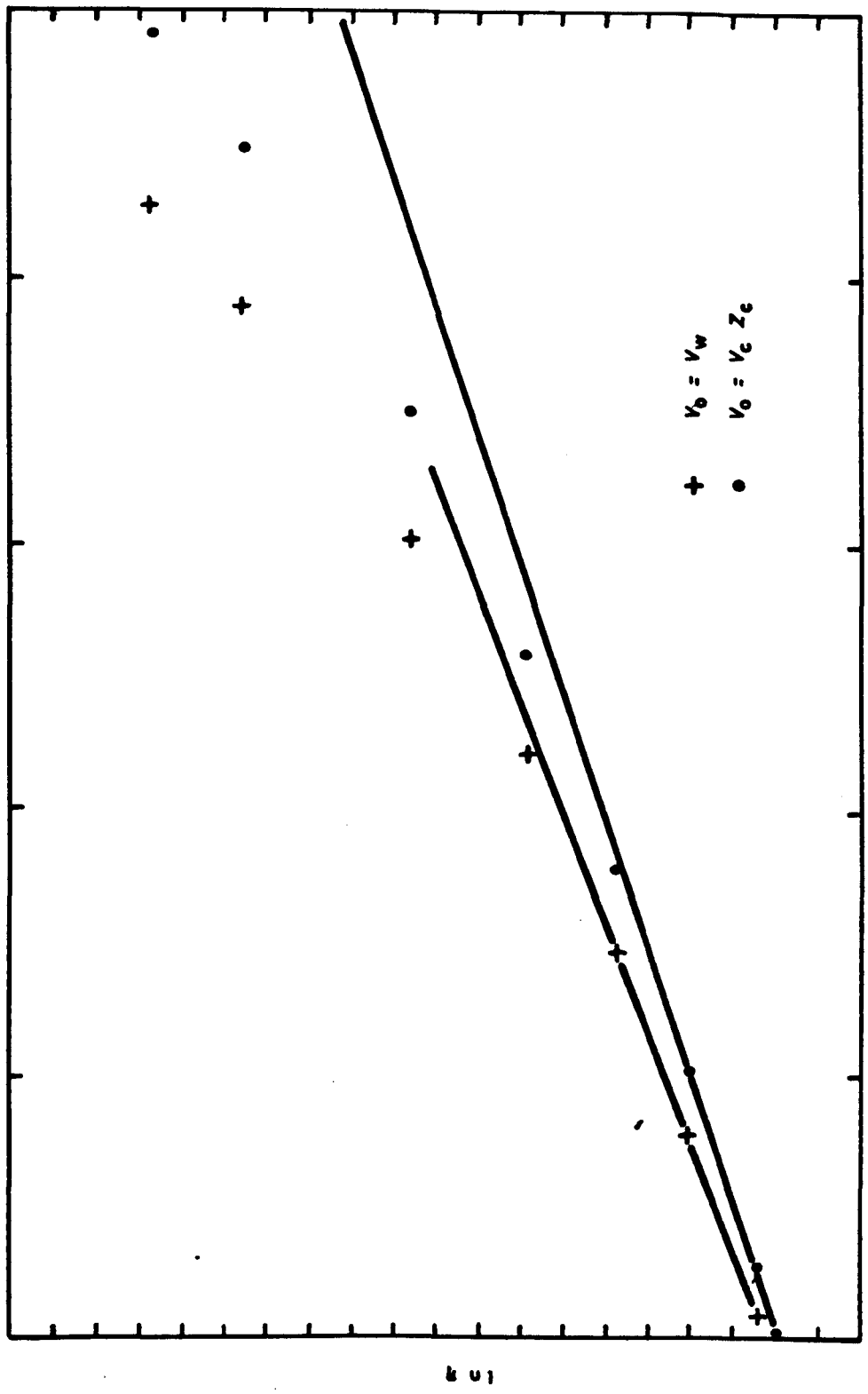

FIG 3.3 TEST OF DOOLITTLE'S EQUATION WITH OCTADECANE DATA

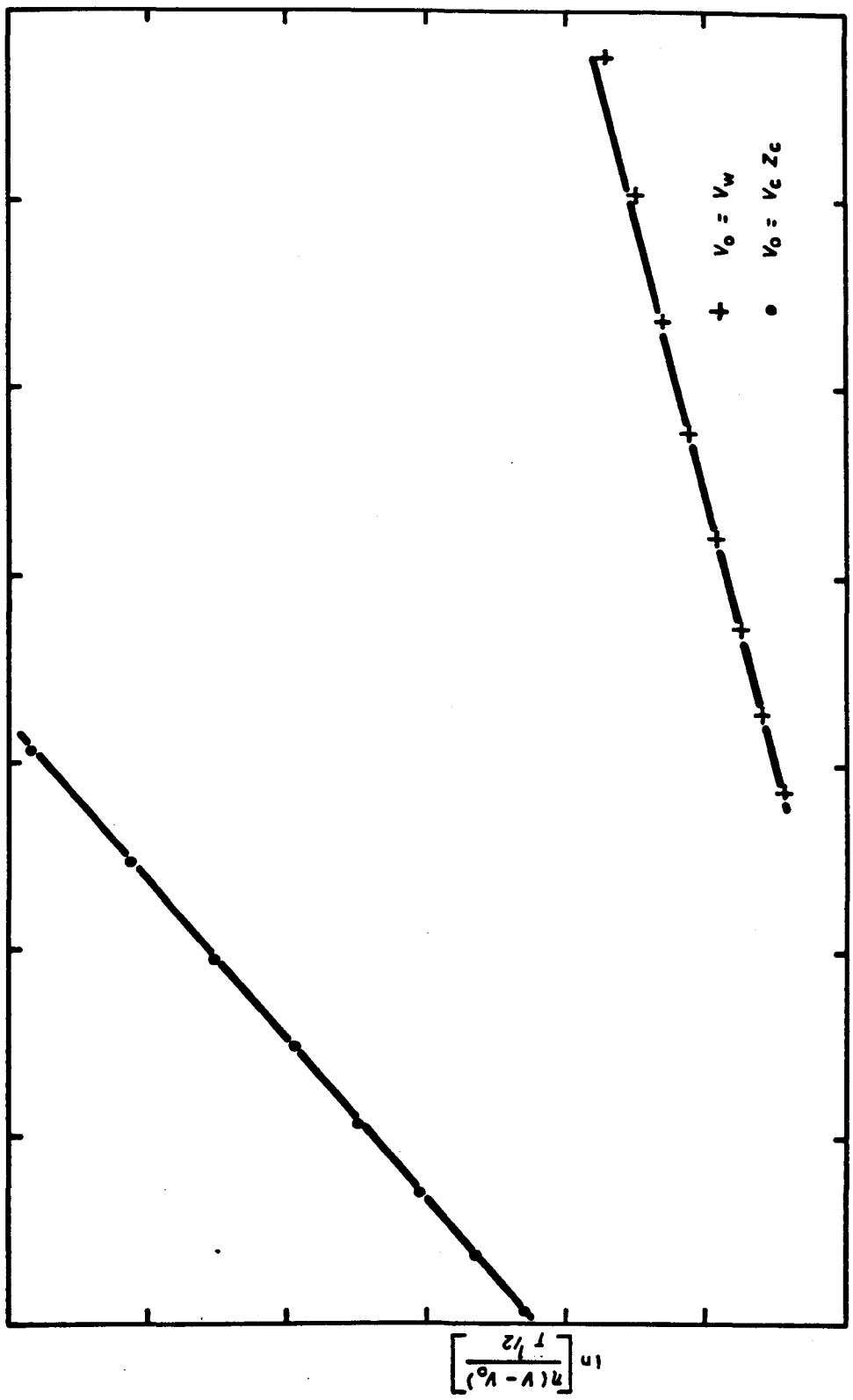

FIG 3.4 TEST OF SIGNIFICANT STRUCTURE EQUATION WITH BENZENE DATA

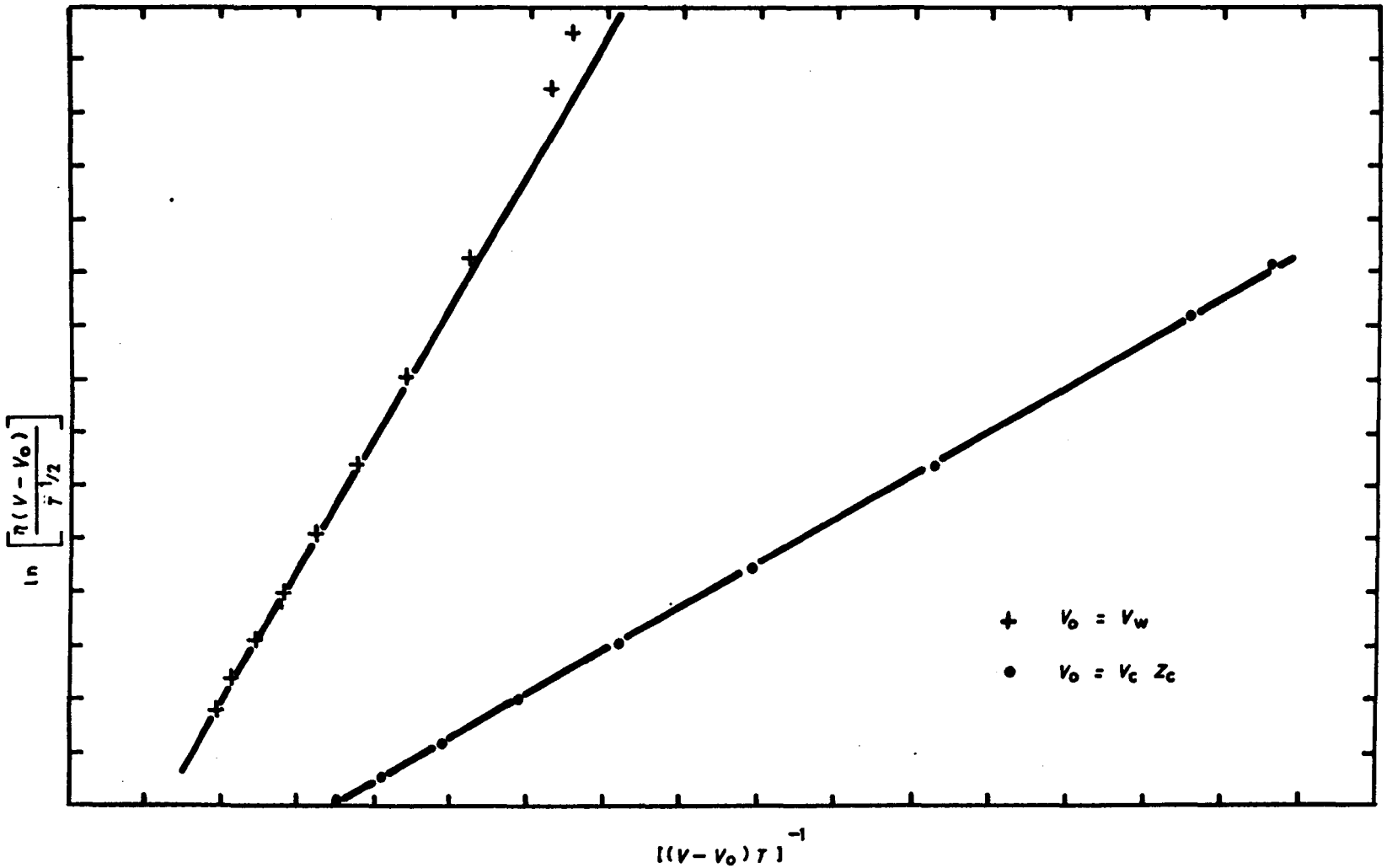

FIG 3.5 TEST OF SIGNIFICANT STRUCTURE EQUATION WITH PENTANE DATA

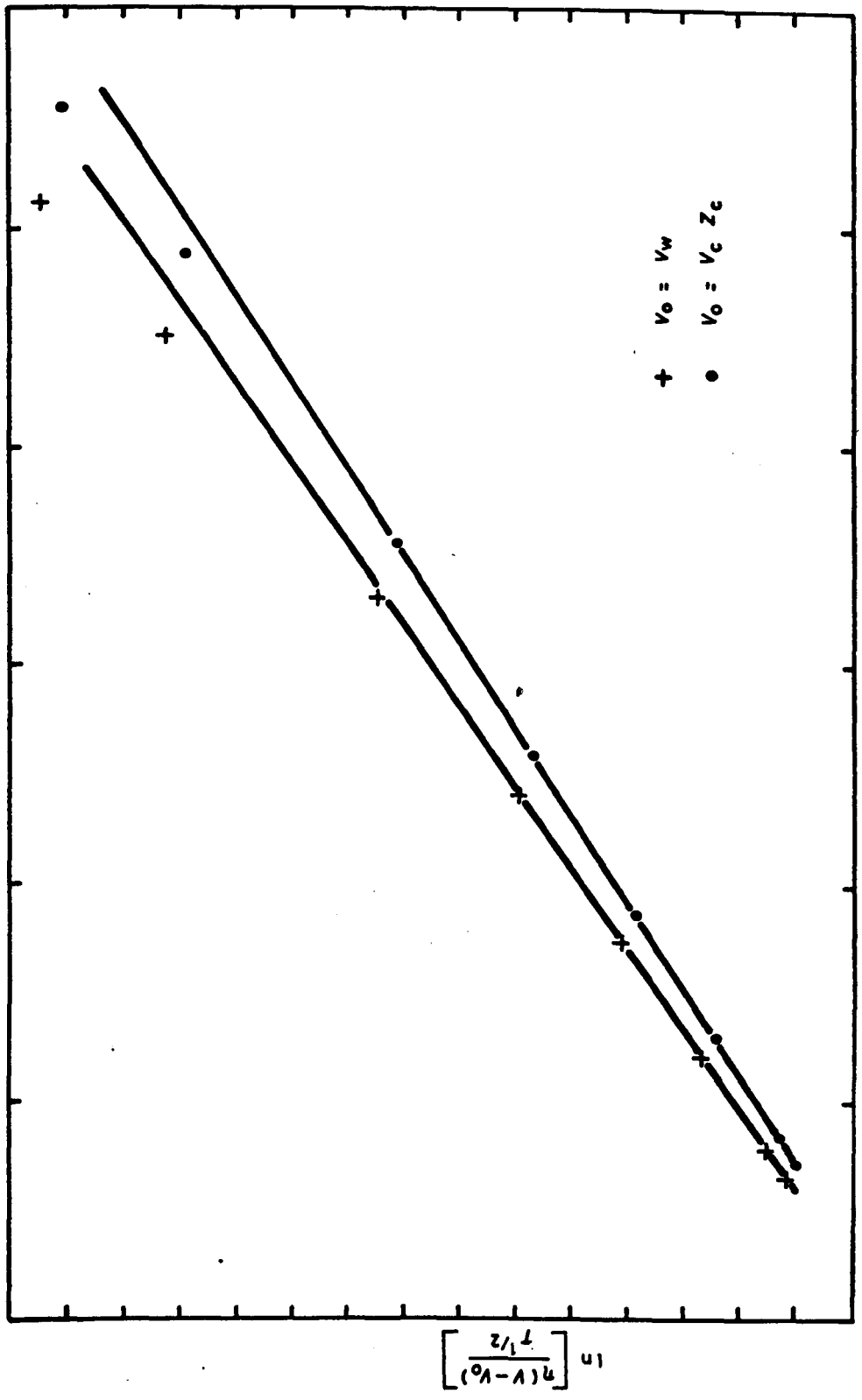

FIG 3.6 TEST OF SIGNIFICANT STRUCTURE EQUATION WITH OCTADECANE DATA

C H A P T E R 4

EXAMINATION OF SIGNIFICANT STRUCTURE EQUATION

SUMMARY OF CHAPTER 4

4 EXAMINATION OF SIGNIFICANT STRUCTURE EQUATION

Using limiting volumes calculated from critical properties and two values of viscosity at atmospheric pressure, the two remaining constants which occur in the significant structure theory have been calculated for over sixty liquids. These two constants, the transmission coefficient and the energy constant, have been correlated graphically with limiting volume, and correlation with other easily obtained properties has been attempted. The transmission coefficient varies regularly with structure and may be predicted from a structure count. The energy constant may also be predicted from a correlation with critical compressibility factor.

Values for the change of limiting volume with pressure, expressed as a compressibility, have been obtained for several liquids using high pressure data. The results have a wide scatter and the compressibility decreases as the temperature rises. Any pattern which may be present is obscured by the roughness of the results which may be caused either by experimental inaccuracies or by limitations of the theory.

CHAPTER 4 - EXAMINATION OF SIGNIFICANT STRUCTURE EQUATION

LIST OF TABLES

LIST OF FIGURES

4 EXAMINATION OF SIGNIFICANT STRUCTURE EQUATION

The work described in this chapter was carried out to find out if methods could be devised for predicting the unknown constants of the significant structure theory for non-spherical molecules. The viscosity equation was used in the form derived by Ree, Ree, and Eyring and later extended by Jhon, Klotz and Eyring as described in Appendix I. The limiting volume at absolute zero, v_o, discussed in Chapter 3 has been used throughout in place of the solid-like volume, v_s.

With the volumes expressed in molar units and m the mass of the molecule the equation is:

$$\eta = \frac{N(\pi mkT)^{1/2}}{(v - v_o)K}\left[\left(\sqrt{2}\frac{v_o}{N}\right)^{1/3} - \left(\frac{v_c}{12N}\right)^{1/3}\right] \exp\left[\frac{-a\epsilon_o Z\, v_o}{(v - v_o)2kT}\left\{\left\{1.0109\left(\frac{v_c}{12v_o}\right)^4 - 2.409\left(\frac{v_c}{12v_o}\right)^2\right\}\right] + \left(\frac{v - v_o}{v}\right)\frac{5}{16}\left(\frac{v_c}{12N}\right)^{-2/3}\left(\left(\frac{mkT}{\pi}\right)^{1/2}\right.\right.$$

All of the parameters in the equation are known or can be deduced with the exception of the transmission coefficient, K, the product $a\epsilon_o Z$ which is in effect an energy constant and the limiting volume v_o. These parameters refer to spherical molecules, and, if calculable without a prior knowledge of viscosity, have 'true' values according to their definitions. If they are determined by fitting viscosity data, however, the values obtained are no longer necessarily true to the definition since they may be influenced by factors not dealt with by the theory. They are therefore essentially empirical constants if significant additional influences are present which

cannot be predicted. Such influences in the present work can obviously be caused by the non spherical shape and in some cases flexibility of the molecules.

The following sections examine the effects of structure on constants derived by fitting to viscosity data. To differentiate between values obtained in this way and those from molecular information the former are given dashed symbols. The symbol K' therefore represents a pseudo transmission coefficient containing structural influences. Similarly the energy constant K" represents the group of constants $a\epsilon_o Z$, and also contains structural influences.

The viscosity and density data used for the paraffins and alkyl benzenes were taken from API44. For the complex hydrocarbons the data of Hogenboom, Webb and Dixon were used and for the halogenated compounds the sources identified in Chapter 7.

4.1 Determination of Constants

To examine the significant structure equation for real liquids at atmospheric or saturation pressure it is necessary to obtain values for three unknown constants: the transmission coefficient, K', the energy constant, K", and the solid-like specific volume v_o. Since values for these constants cannot at present be determined independently they are usually obtained by fitting the equation to viscosity and density data. Values calculated in this way, however, may vary widely depending on the temperature range of the data selected. In fact Hogenboom Webb and Dixon (1967) have observed that the solid-like specific volume would require a negative coefficient of thermal expansion, since they found that v_o obtained from high temperature data was less than that obtained from low temperature data for the same liquids. If this point of view is accepted then it is necessary to introduce yet another unknown constant, the coefficient of thermal expansion, into the equation. Clearly this procedure will produce better fits to experimental data, since the constants have to be treated as disposable, but at the same time the physical significance of all the constants occurring in the equation is diminished if they are determined by fitting. Consequently values obtained in this way are less likely to demonstrate true relationships with the structure of the molecules involved. Since the object of this examination was to discover possible relationships between the necessary constants and structure the introduction of additional parameters has been resisted.

For this reason possible variations of v_o with temperature have been excluded from this investigation, and values of v_o have been calculated from the critical data only. This method eliminates the need for an arbitrary reference temperature at which to determine v_o, provides a

positive link to chemical structure, and allows one of the unknowns to be calculated for many liquids since most critical properties are either known or can be estimated.

Since very little is known about K' or K", values for these have been obtained by fitting to experimental data at two temperatures. The results are given in Table 4.1 together with the critical data used and the standard deviation of the differences between viscosities calculated from the resulting equation and experimental viscosities at other temperatures.

The success of the predicted value of v_o, and the two point fitting described, in representing the data may be judged from Figs 4.1 and 4.2, and from the deviations in Table 4.1. For decane, shown in Fig. 4.1, between temperatures of 250 and 400 K the deviations are less than 0.5 per cent with a maximum deviation of 1.55 per cent at 243 K. For benzene, shown in Fig. 4.2, the deviations are less than 0.27 per cent between 280 and 350 K.

For most of the 65 liquids examined the deviations obtained were less than the accuracy of the data over quite wide temperature ranges. For 11 of the liquids only two viscosity values were available at different temperatures so that it was not possible to check in this way. Of the remaining liquids only four, octadecane, 1,1-diphenylheptane, 9(2-phenylethyl)heptadecane and 1α naphthylpentadecane, gave deviations consistently larger than the estimated experimental accuracy. Constants obtained for these four liquids were given less weight in the following analysis.

4.2 Examination of Transmission Coefficient

The transmission coefficient K is defined as the fraction of molecules which have sufficient activative energy to overcome the potential barrier and which proceed only from initial state, on one side of the barrier, to final state on the other. A value of unity therefore means that all molecular translations contribute directly to the flow. There is a probability, however, that a molecule which has just completed such a translation will immediately translate back to the position it has just vacated. When this occurs the transmission coefficient will be less than unity. Classically these are the only two possible mechanisms and they lead to the conclusion that the maximum value of K is unity. However, it can be shown quantum mechanically that there is a small probability that molecules with energy less than the activation energy can succeed in crossing the potential barrier. This effect is known as 'tunnelling' or 'leakage', and, when present will lead to values of K slightly greater than unity. High values of K' are not interpreted quantum mechanically in this work but are assumed to be caused by the shape and structure of the molecules.

For non-spherical molecules the possible modes of transmission are more varied, and it is difficult to generalise about expected behaviour in a meaningful way. For long flexible molecules for example one might predict that the transmission coefficient would tend to be low because a reverse translation may occur even if the shape of the vacated position had changed slightly. However the activation energy for such segmented flow would be lower than that calculated for a molecular unit and it is difficult to say whether the net result would be a higher or lower value of K'.

In practice the determination of the constants from data provides a method of averaging transmission coefficients and activation energies over the various modes of flow which occur.

The calculated values of K' lie between 0.9 and 1.5 for most of the liquids studied. Values of less than unity were obtained only for the longer normal paraffins (ie those with 12 or more carbon atoms), 1-bromooctane, spiro4,5decane, and 4-methylhexane. All of the liquids with aromatic or partly aromatic molecules gave values greater than 1.1 as did the halogenated liquids with the exception of bromooctane which gave the lowest value obtained.

The broad conclusions resulting from the calculated transmission coefficients are therefore that for aromatic or partly aromatic liquids, a form of tunnelling is taking place and is responsible for a significant part of the flow process. It is interesting to note that the saturated paraffinic ring molecules have K' values slightly less than the equivalent aromatic rings, and are therefore less prone to tunnelling. From the low values of the longer chain paraffins one may conclude that a higher proportion of reflection or reverse translation is taking place. For the longest chain paraffins examined, however, the transmission coefficient tends to increase, indicating that a form of tunnelling is becoming predominant.

When plotted against limiting specific volume as shown on Fig. 4.3, the transmission coefficients fall into quite distinct groups of molecular types. With the exception of the straight chain paraffins these groups all show a similar type of variation with molecular structure represented by v_o. In the aromatic group for example, the highest coefficient is that of benzene, 1.476, and the addition of paraffinic side chains reduces this to 1.260 for propylbenzene. The most dramatic variation is shown by the bromoparaffins which vary from 1.437 for bromopropane down to 0.636 for bromooctane.

The grouping of the liquids on Fig. 4.3 shows clearly that the transmission coefficients which have been calculated vary in a regular manner with structure, and in principle Fig. 4.3 could be used to estimate coefficients from limiting volumes. In practice, however, this would give poor accuracy since the transmission coefficient may vary by 100 per cent or more for a change of only 10 per cent in limiting volume.

The observed values of K' are best represented by means of a structure count, where K' is obtained by summing the contributions from the number and types of molecular groups present. That is

$$K' = \sum_i N_i B_i \qquad (4.1)$$

The groups used are shown in Table 4.2 with the names and values of B obtained. For the normal paraffins, for example, K' is given by

$$K' = 2B(CH3) + (N - 2)\, B(CH2)$$

where N is the number of carbon atoms. Values of +0.613 for B(CH3) and -0.023 for B(CH2) were obtained from the paraffins between ethane and pentadecane. Benzene gave B(C//H) directly and a mean value of B(C//O) was obtained from the other aromatic molecules up to 1-methyl 4-ethyl benzene, using the values of B(CH3) and B(CH2) already determined. Similarly B(CH2R) was taken as the mean of two values obtained from cyclopentane and cyclohexane, and B(CH1R) as the mean of values calculated from the rest of the cycloparaffins using B(CH3) and B(CH2) as before. B(CHOR) was obtained from spiro5,5undecane.

Values of transmission coefficients calculated from this structure count and from the experimental data for these liquids are shown in Fig. 4.4. For all of these liquids, that is normal paraffins from

ethane to pentadecane and the aromatics and cycloparaffins listed, the structure count reproduces the transmission coefficient with a standard deviation of 5.5 per cent. Propane and tridecane have experimental values which deviate widely from the other paraffins, and if these are omitted the standard deviation drops to 4.4 per cent using the same values of B.

The four branched paraffins from 2-methylbutane to 2,4-dimethylpentane gave a mean value of B(CH1).

The bromoparaffins and bromobenzene, while they show a trend similar to the branched paraffins, are more erratic; however a value of B(Br) corresponding to the contribution of the bromine atom has been calculated. In fact the group contributions calculated from data for branched paraffins and bromine containing compounds should be regarded as rough approximations, since the temperature range of the viscosity data used was too short to give reliable values of K'.

The data for chlorobenzene and the three dichlorobenzenes covered a wide temperature range and gave a consistent value for B(Cl). Estimated and observed values of K' for the halogenated liquids and the branched paraffins are shown on Fig. 4.5.

The variation of the group contributions with the number of attached hydrogen atoms is plotted in Fig. 4.6. The trends shown by the different groups are quite similar and it is interesting to note that the straight chain paraffinic line, if extrapolated to CH4, would give a reasonable approximation to the transmission coefficient of methane.

4.3 Examination of Energy Constant

The energy constant K" is a composite one which cannot be separated, and interpretation of the values obtained is therefore more difficult. It is given by

$$K'' = -a\, Z \epsilon_o$$

The constant a is the constant of proportionality between the activation energy and the energy of vaporisation. The theory assumes that the activation energy for viscous flow is a constant fraction of the energy of vaporisation since the flow process and the vaporisation process are similar and involve the extraction of a molecule from the bulk liquid into a free volume. The values of a should be less than unity. For hexagonal packing Z, the number of nearest neighbours, takes the value 12. Values of the minimum energy of the potential function, ϵ_o, are available for a number of substances and are usually expressed in degrees Kelvin by means of the expression ϵ_o/k where k is Boltzmann's constant. For some of the normal paraffins values of ϵ_o/k from Reid and Sherwood (1966) are compared with the ratio K"/k on Fig. 4.7. The agreement is surprisingly good and suggests that for the lower members of the series aZ is approximately equal to one. Since a, ϵ_o and probably Z vary from liquid to liquid nothing further can be deduced from the calculated values of K".

The variation of K" with limiting specific volume is shown on Fig. 4.8. The behaviour of the paraffins is very consistent and the correlation is approximately linear for those members of the series above decane. Also plotted is the value for 9-n-octylheptadecane, an isomer of a paraffin having twenty-five carbon atoms with only one branch. The other groups of liquids also form discrete sets similar to those obtained for the transmission coefficient and can be used to predict

K" from limiting volume; however the slope of the graphs makes the accuracy of prediction rather poor in this case also.

Fig. 4.9 shows the variation of K" with the reciprocal of the critical compressibility factor Z_c, for molecules composed of rigid rings and for the paraffins. Eight of the nine rigid ring compounds give values which lie close to a straight line which also passes through the value for methane, while the paraffins show a regular variation which is linear above octane. Fig. 4.10 shows a similar plot for all of the liquids listed in Table 4.1. Most of the points lie between the two lines already described which appear to define approximately the limits of the effect of molecular flexibility on the effective energy constant.

The correlation with Z_c may be used to estimate the energy constant by means of the following equations.

For rigid rings both saturated and unsaturated, the energy constant is given by

$$10^{20} \times K''_R = + 4.0692/Z_c - 13.8068 , \qquad (4.1a)$$

and for paraffinic chains of more than about eight carbon atoms by

$$10^{20} \times K''_c = + 3.6304/Z_c - 13.1422 . \qquad (4.1b)$$

Combining these two equations gives

$$10^{20} \times K'' = - 7.6432 + A\left[\frac{1}{Z_c} - 1.5147\right]$$

where $A = 3.6304$ for chains, and

$A = 4.0692$ for rings.

Taking as an expression for A

$$A = 4.0692 - f(4.0692 - 3.6304)$$

and solving for f gives

$$f = 9.2742 - 2.2791 \left[\frac{10^{20} \times K'' + 7.6432}{\frac{1}{Z_c} - 1.5147} \right],$$

which allows f to be calculated from the experimental values of K".

The flexibility, f, must be defined in such a way that it is zero for rigid molecules and tends to one for molecules as flexible as octane. Unfortunately the observed values of f calculated from K" are not sufficiently regular to allow accurate expressions to be deduced. The lower members of the paraffin series and the alkyl benzenes gave the most consistent results and could be represented approximately by

$$f = \frac{n - 1}{n} \qquad (4.2)$$

for the paraffins below octane, where n is the number of carbon atoms, and

$$f = \left(\frac{n_c}{n} \right)^{\frac{1}{4}} \qquad (4.3)$$

for the aromatic hydrocarbons, where n is the total number of carbon atoms and n_c is the number of carbon atoms on side chains. Observed and calculated values of f for these two groups are shown in Fig. 4.11.

The final expression for K" in joules is then

$$K'' \times 10^{20} = -7.6432 + \left[4.0692 - f(0.4388) \right] \left[1/Z_c - 1.5147 \right] . \qquad (4.4)$$

Observed and calculated values of K" for the normal paraffins and the nine rigid ring compounds are compared on Fig. 4.12 and for all of the liquids on Fig. 4.13. For the halogenated liquids the halogen atom was treated as an additional carbon atom except in the case of carbon tetrachloride which was assumed to be rigid. For example the flexibility, f, for 1-bromopentane was taken as 5/6.

4.4 Examination of the Effect of Pressure

The significant structure equation has been extended to high pressures by Jhon, Klotz and Eyring (1969) essentially by allowing v_o to vary with pressure by means of a linear compressibility coefficient β. Apart from its influence on v_o, pressure might be expected to affect three other parameters in the equation; the transmission coefficient, the energy constant, and the free length between nearest neighbours, l_f. Since the approximation used for l_f is derived from v_o, the theory therefore does allow for a reduction in free length with pressure. Similarly the inclusion of v_o in the potential function allows for the increase in intermolecular forces with pressure as v_o decreases. The composite energy constant, K", includes Z, the number of nearest neighbours which may vary with pressure in disordered solids; however the solid-like state is considered to be highly ordered so that Z should be independent of pressure. The values of v_o used are consistent with this concept since they are slightly lower than the specific volumes of the corresponding crystalline solids at the melting point. The theory assumes that the transmission coefficient does not vary with pressure, but when shape and flexibility are factors which influence the effective value of K' (and K"), the validity of this assumption must be questioned. Since the effective values of K' are averages over the different modes of flow for asymmetric molecules, a constant value of K' implies that each mode is contributing a constant fraction of the total flow irrespective of pressure. It seems more probable that the most difficult translations, for example in the direction of the axis of symmetry of a disc-shaped molecule, will be almost completely excluded at higher pressures as the volume available for translation decreases. As the precise way in which this behaviour influences the parameters is not understood the total effect of pressure cannot be

deduced.

Nevertheless the results of Jhon, Klotz and Eyring have shown that the significant structure equation, with a single solid-like compressibility term, may be used to describe viscosity over a range of temperatures and for pressures up to 360 MN m^{-2}. Compressibilities have therefore been calculated here for thirteen liquids so that an assessment can be made of the range of values which occur in different types of liquids.

The solid-like compressibility, β, is defined by

$$v_{op} = v_o(1 - \beta P)$$

where v_{op} is the solid-like volume at pressure P, and v_o is the volume obtained from the critical properties as before. Values were obtained using the two constants K' and K", from the previous work at atmospheric pressure, by calculating the optimum (Powell (1965)) value of β for each isotherm of high pressure viscosities. The ratio of the viscosity at pressure to that at atmospheric pressure and the same temperature was used to avoid errors arising from the differences between the accurate viscosities at atmospheric pressure (used to obtain K' and K") and the values quoted for atmospheric pressure in the high pressure data sources. Values at pressures above 500 MN m^{-2} were excluded.

The results are illustrated in Figs 4.14 and 4.15 for cis-decalin and dodecane respectively. The equation is seen to fit the data reasonably well over the full pressure and temperature range, though the deviations along each isotherm are clearly systematic indicating that a slightly different form of equation is required to describe the effect of pressure fully. Numerical results are given in Table 4.3. The effect of accuracy of viscosity data on the values obtained is well

illustrated by the results for benzene where Bridgman's data at 30 and 75°C gave higher compressibilities than those of Kuss at the other temperatures listed. The accuracy of the viscosity data for benzene is discussed in Chapter 7. Quite wide variations in the results are evident, probably because of comparatively small errors in viscosity, and it is difficult to discern a clear cut pattern. However two conclusions may be drawn:

1 Most of the liquids show a consistent decrease in compressibility with increase in temperature. This is contrary to experience for solid materials and is probably caused by the apparent decrease in v_o with temperature discussed in section 4.1

2 The cis structures examined are less compressible at all temperatures than the corresponding trans structures, a characteristic which has also been noted by Hogenboom, Webb and Dixon (1967) for the corresponding liquid properties.

TABLE 4.1

SIGNIFICANT STRUCTURE CONSTANTS FROM VISCOSITY DATA

Liquid	Molecular weight	Critical volume (cc/mol)	Critical compressibility factor	Limiting volume (cc/gm)	Transmission coefficient	Energy constant (10^{-20}J)	Standard deviation (%)
methane	16.04	99.50	0.290	1.7989	1.7203	0.2329	1.21
ethane	30.07	148.00	0.285	1.4027	1.3008	0.1664	2.34
propane	44.09	200.00	0.277	1.2565	1.0453	0.3455	4.05
butane	58.12	255.00	0.274	1.2022	1.1661	0.5139	3.44
pentane	72.15	304.00	0.262	1.1039	1.1312	0.8987	0.07
hexane	86.18	370.00	0.264	1.1335	1.1455	0.7661	0.08
heptane	100.21	432.00	0.263	1.1338	1.1229	0.7934	0.39
octane	114.23	492.00	0.259	1.1155	1.0974	0.9319	0.72
nonane	128.26	548.00	0.254	1.0852	1.0650	1.1856	0.56
decane	142.29	603.00	0.247	1.0468	1.0429	1.5436	0.33
undecane	156.31	657.00	0.243	1.0214	1.0359	1.8540	0.36
dodecane	170.34	713.00	0.237	0.9920	1.0023	2.1880	1.03
tridecane	184.31	770.00	0.210	0.8774	1.0968	3.3790	2.38
tetradecane	198.40	820.00	0.230	0.9506	0.9518	2.7314	0.79
pentadecane	212.42	880.00	0.230	0.9528	0.9348	2.8438	4.65
hexadecane	226.45	930.00	0.220	0.9035	0.8966	3.4002	5.13
heptadecane	240.48	980.00	0.210	0.8558	0.9453	4.0251	1.15
octadecane	254.50	1000.00	0.200	0.7858	0.7983	4.8868	8.30
nonadecane	268.53	1100.00	0.200	0.8193	0.9609	4.6038	2.58
eicosane	282.56	1100.00	0.190	0.7397	1.0094	5.9933	3.16
cyclopentane	70.14	260.00	0.276	1.0232	1.1795	0.9523	0.68
methylcyclopentane	84.16	319.00	0.273	1.0347	1.2358	1.0375	1.97
ethylcyclopentane	98.19	375.00	0.269	1.0273	1.1466	0.9328	1.30

TABLE 4.1 (Contd)

Liquid	Molecular weight	Critical volume (cc/mol)	Critical compressibility factor	Limiting volume (cc/gm)	Transmission coefficient	Energy constant (10^{-20}J)	Standard deviation (%)
cyclohexane	84.16	308.00	0.273	0.9990	1.3465	1.7887	0.76
methylcyclohexane	98.19	368.00	0.269	1.0081	1.2645	1.4417	1.23
benzene	78.11	259.00	0.271	0.8985	1.4755	1.1865	0.12
toluene	92.14	316.00	0.264	0.9053	1.4538	1.1192	0.59
ethylbenzene	106.17	374.00	0.263	0.9265	1.2920	0.9557	0.31
o-xylene	106.17	369.00	0.263	0.9141	1.3703	1.1344	0.26
m-xylene	106.17	376.00	0.260	0.9208	1.3691	0.9933	0.31
p-xylene	106.17	379.00	0.260	0.9281	1.3706	0.9967	0.13
n-propylbenzene	120.20	440.00	0.265	0.9701	1.2604	0.7987	0.35
isopropylbenzene	120.20	428.00	0.265	0.9436	1.2999	1.0115	0.37
1-methyl4-ethylbenzene	120.20	430.00	0.261	0.9337	1.3491	0.8737	0.20
1-bromopropane	123.00	275.00	0.267	0.5969	1.4369	0.5564	-
2-bromopropane	123.00	271.00	0.269	0.5927	1.9328	1.1227	-
1-bromobutane	137.03	330.00	0.263	0.6334	1.1913	0.6030	-
2-bromobutane	137.03	326.00	0.264	0.6280	1.3105	0.8319	-
bromopentane	151.05	385.00	0.257	0.6550	1.4067	1.0516	-
bromohexane	165.08	440.00	0.253	0.6743	1.3956	1.3223	-
bromooctane	193.13	550.00	0.244	0.6949	0.6360	1.2419	-
bromobenzene	157.02	324.00	0.263	0.5427	1.2436	1.0085	-
chlorobenzene	112.56	308.00	0.265	0.7251	1.4090	1.0691	1.06
1,2-dibromoethane	187.88	290.00	0.257	0.3967	1.1112	0.5219	-
1,3-dibromopropane	201.91	345.00	0.251	0.4289	1.0837	0.7670	-
m-dichlorobenzene	147.01	358.00	0.250	0.6088	1.3367	1.3345	1.34
o-dichlorobenzene	147.01	358.00	0.249	0.6064	1.3054	1.4216	1.30
p-dichlorobenzene	147.01	358.00	0.250	0.6088	1.3362	1.4158	0.10

T A B L E 4.1 (Contd)

Liquid	Molecular weight	Critical volume (cc/mol)	Critical compressibility factor	Limiting volume (cc/gm)	Transmission coefficient	Energy constant (10^{-20}J)	Standard deviation (%)
1,1-diphenylethane	182.14	588.00	0.256	0.8264	1.1769	1.9098	2.81
1,1-diphenylheptane	247.19	863.00	0.233	0.8135	1.7401	3.8635	10.53
9-n-octylheptadecane	352.70	1411.00	0.205	0.8201	1.5463	5.8753	2.47
9(2-phenylethyl)heptadecane	344.63	1302.00	0.201	0.7594	1.3620	5.8212	7.37
1-alpha-naphthylpentadecane	338.58	1232.00	0.205	0.7459	1.5014	5.8754	5.59
spiro4,5decane	138.20	492.70	0.267	0.9519	0.9485	1.2869	0.92
spiro5,5undecane	152.20	541.30	0.262	0.9318	1.0659	1.6994	1.14
cis-decahydronaphthalene	138.25	484.00	0.265	0.9277	1.0492	1.6829	1.07
trans-decahydronaphthalene	138.25	498.00	0.274	0.9870	1.0436	1.0631	2.77
cis-octahydroindene	124.20	436.40	0.260	0.9136	1.1643	1.8510	0.91
trans-octahydroindene	124.20	445.90	0.271	0.9729	1.1059	1.1694	1.71
2-methylbutane	72.15	308.00	0.268	1.1441	1.3619	0.9595	-
2-methylpentane	86.17	367.00	0.270	1.1499	1.0444	0.6346	-
3-methylhexane	100.20	418.00	0.267	1.1138	0.9078	0.5518	-
2,2-dimethylbutane	86.17	359.00	0.273	1.1374	1.1547	1.1455	-
2,4-dimethylpentane	100.20	425.00	0.270	1.1452	1.0291	0.6268	-
carbon tetrachloride	153.84	276.00	0.272	0.4880	1.4578	1.4549	2.42

TABLE 4.2

STRUCTURAL CONTRIBUTIONS TO TRANSMISSION COEFFICIENT

Chemical group	Name	B
Paraffinic chains		
H H-C- H	CH3	+0.613
H -C- H	CH2	-0.023
H-C-	CH1	-0.690
-C-	CHO	-1.273
Paraffinic rings		
H H-C-	CH2R	+0.230
H-C-	CH1R	-0.387
-C-	CHOR	-1.180
Aromatic rings		
H =C-	C//H	+0.246
=C-	C//O	-0.468
Halogens		
Br-	Br	+0.793
Cl-	Cl	+0.641

T A B L E 4.3

SOLID-LIKE COMPRESSIBILITY

Liquid	Temperature (K)	Solid-like compressibility ($pm^2\ N^{-1}$)	Liquid	Temperature (K)	Solid-like compressibility ($pm^2\ N^{-1}$)
pentane	303	87.9 (1)*	benzene	298	16.7 (3)
	348	59.8 (1)		303	18.2 (1)
	303	85.6		313	11.6 (3)
				333	13.4 (3)
hexane	303	89.4 (1)		348	89.4 (1)
	348	63.7 (1)		353	16.1 (3)
dodecane	310	4.8 (2)	cis-decalin	288	38.2)
	333	17.0 (2)		310	44.1)
	352	13.1 (2)		333	31.5) (2)
				352	34.2)
hexadecane	372	4.4 (4)		372	28.6)
	477	17.9 (4)			
			trans-	288	94.9)
1,1-diphenylheptane	372	13.1 (5)	decalin	310	94.0)
	408	48.9 (5)		333	91.1) (2)
				352	85.6)
9-n-octylheptadecane	477	21.9 (4)		372	78.2)
				388	69.3)

T A B L E 4.3 (Contd)

Liquid	Temperature (K)	Solid-like compressibility ($pm^2\ N^{-1}$)		Liquid	Temperature (K)	Solid-like compressibility ($pm^2\ N^{-1}$)	
spiro4,5decane	288	87.1		cis-	333	10.8	
	310	77.8		octahydro	352	13.2	(2)
	333	65.9	(2)	indene	372	11.1	
	352	55.2			388	7.7	
	388	26.1					
				trans-	288	101.0	
spiro5,5undecane	310	9.4		octahydro	310	97.5	
	333	19.5		indene	333	88.8	(2)
	352	20.2	(2)		352	79.3	
	372	15.5			372	70.6	
	388	10.8			388	62.7	

*Viscosity data from (1) Bridgman (1958)
(2) Hogenboom, Webb and Dixon (1967)
(3) Kuss (1955)
(4) ASME (1953)
(5) Lowitz et al (1959)

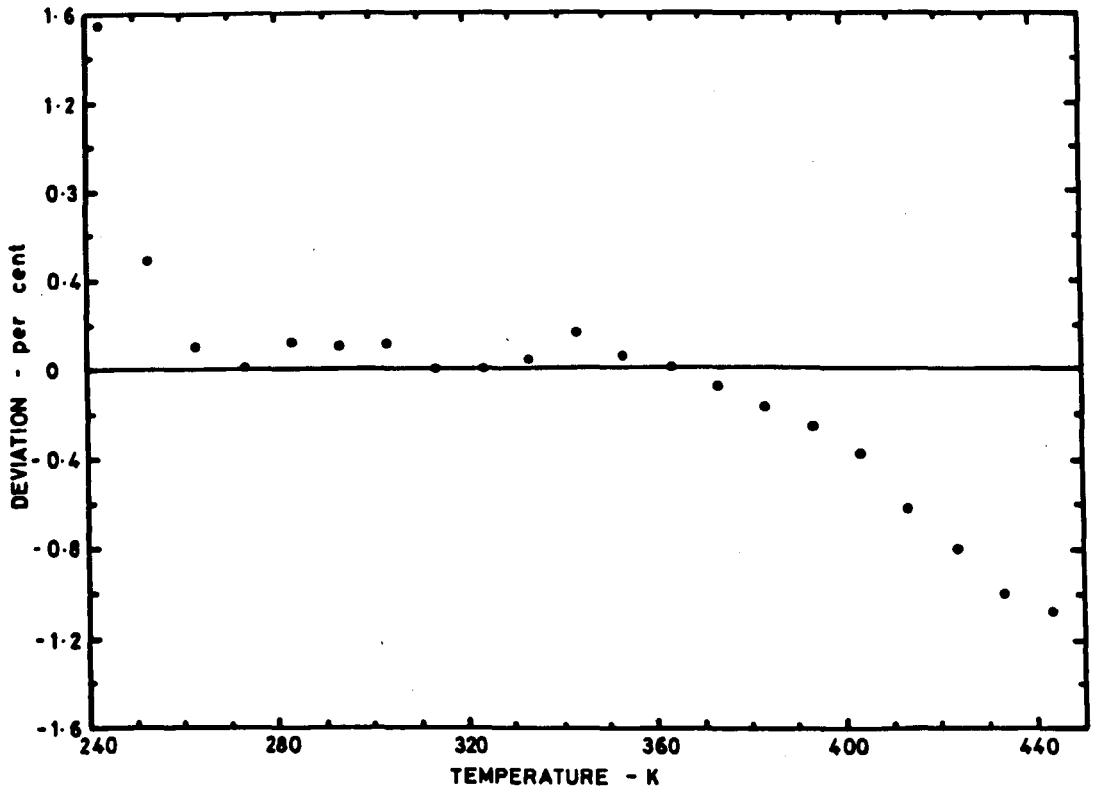

FIG 4·1 FITTING RESULTS FOR DECANE

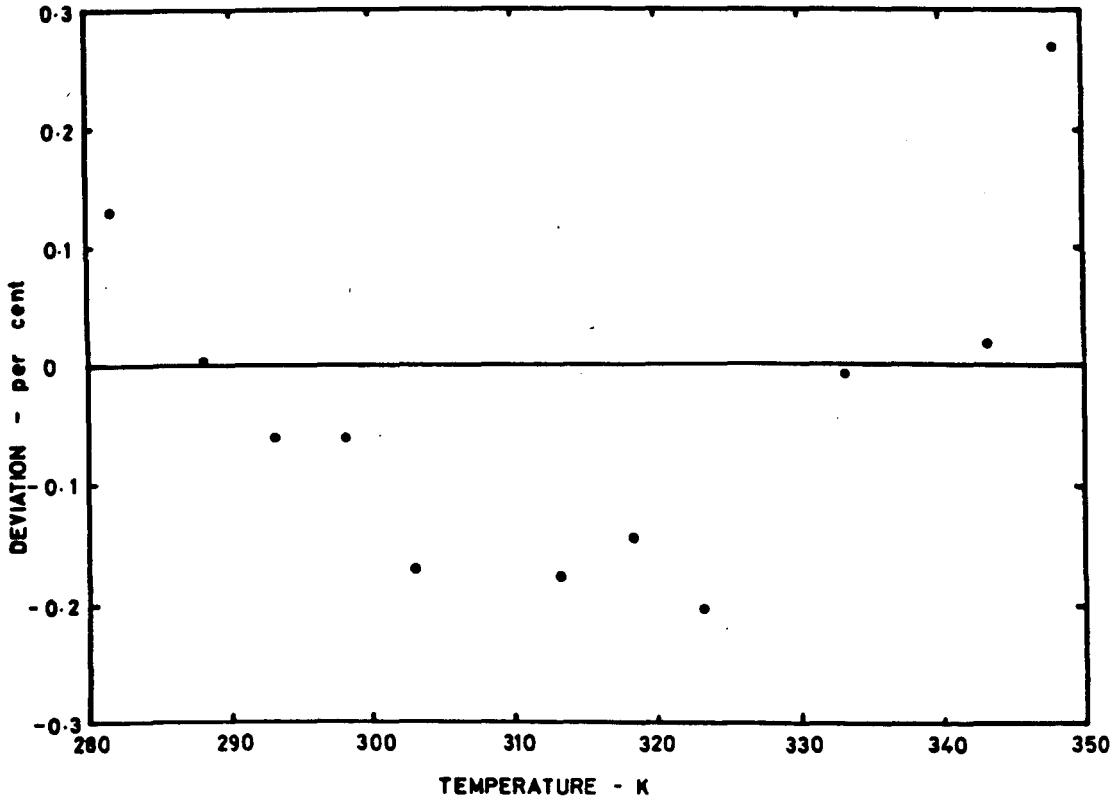

FIG 4·2 FITTING RESULTS FOR BENZENE

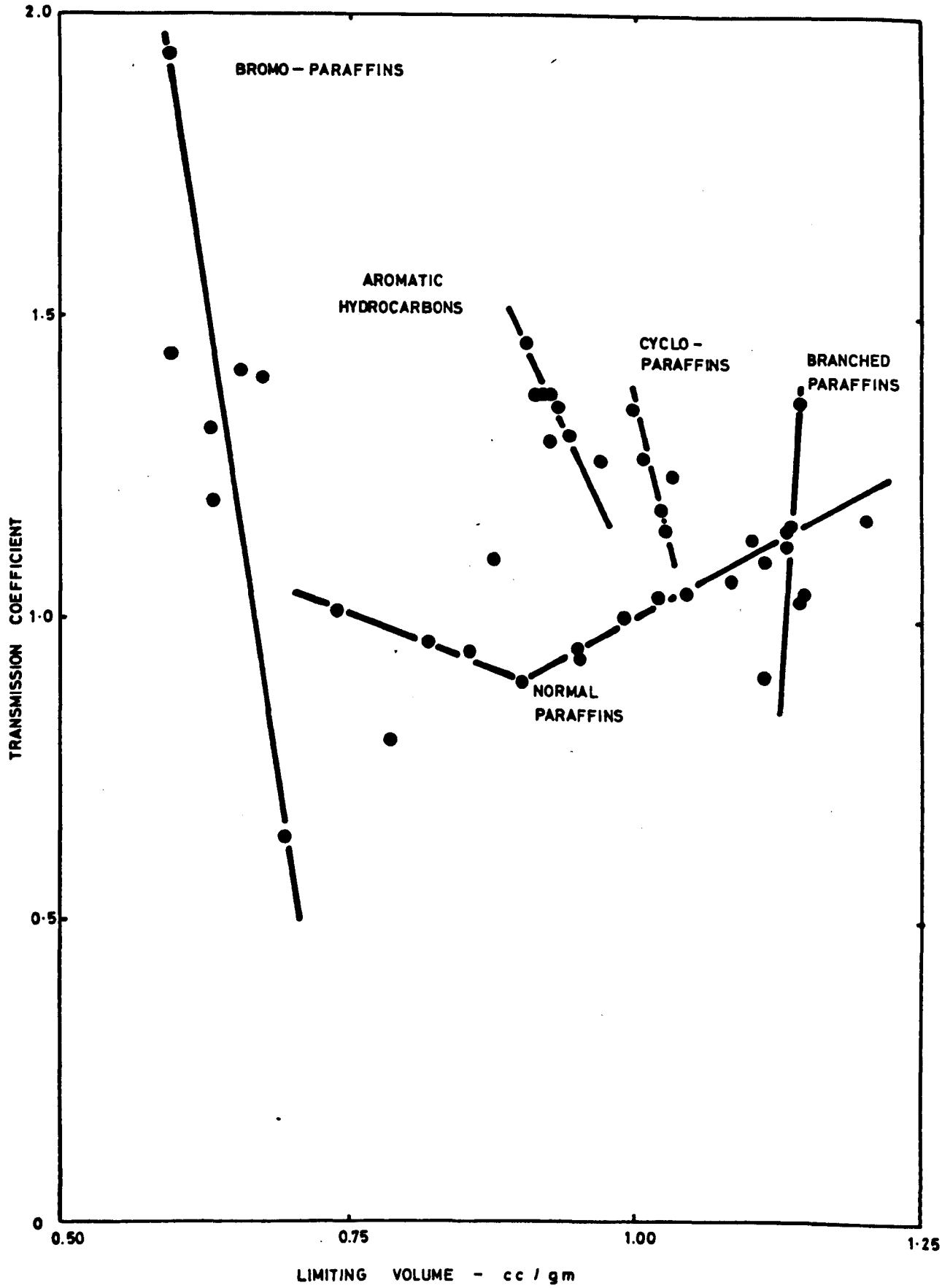

FIG 4.3 TRANSMISSION COEFFICIENT AND LIMITING VOLUME

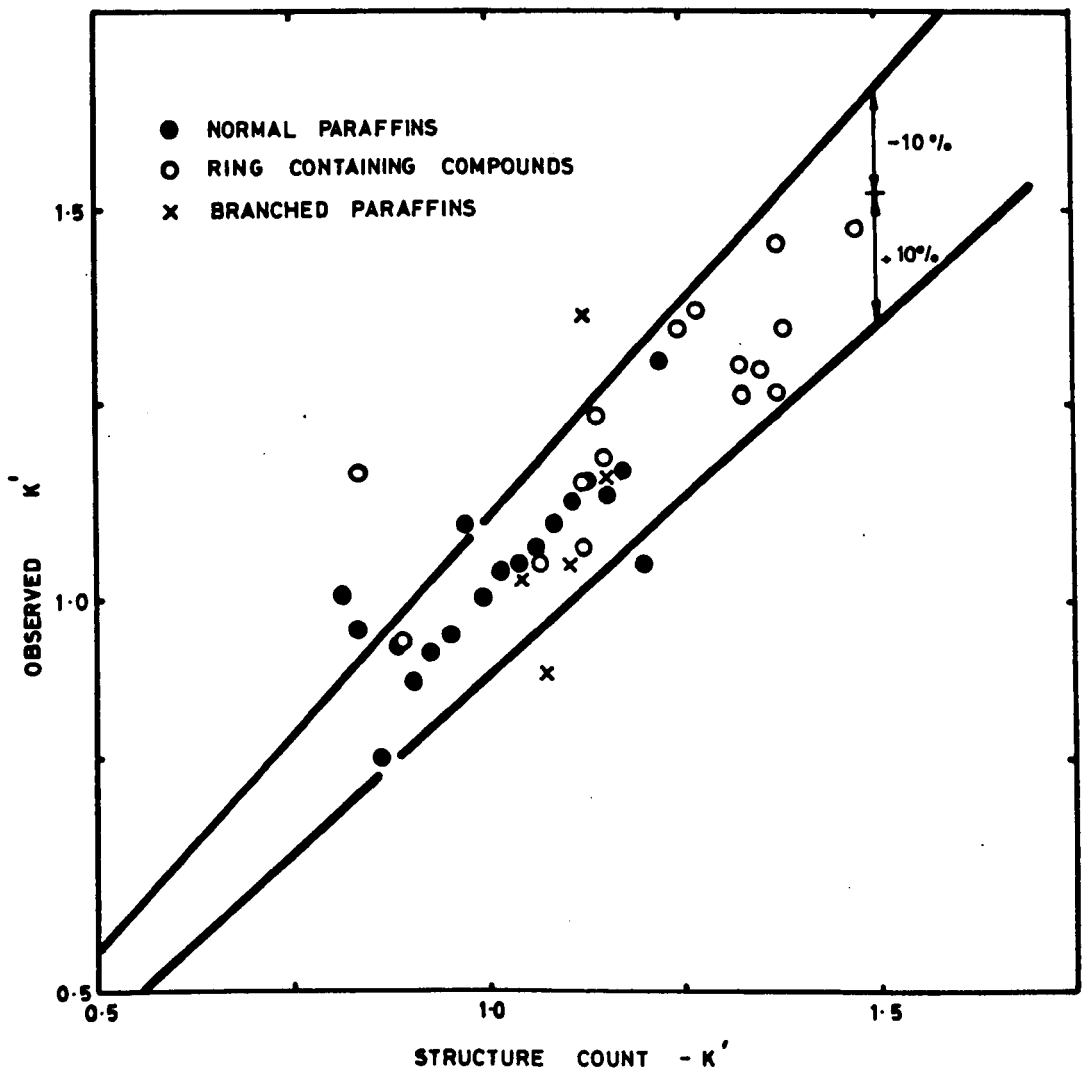

FIG 4.4 CALCULATED AND OBSERVED TRANSMISSION COEFFICIENTS

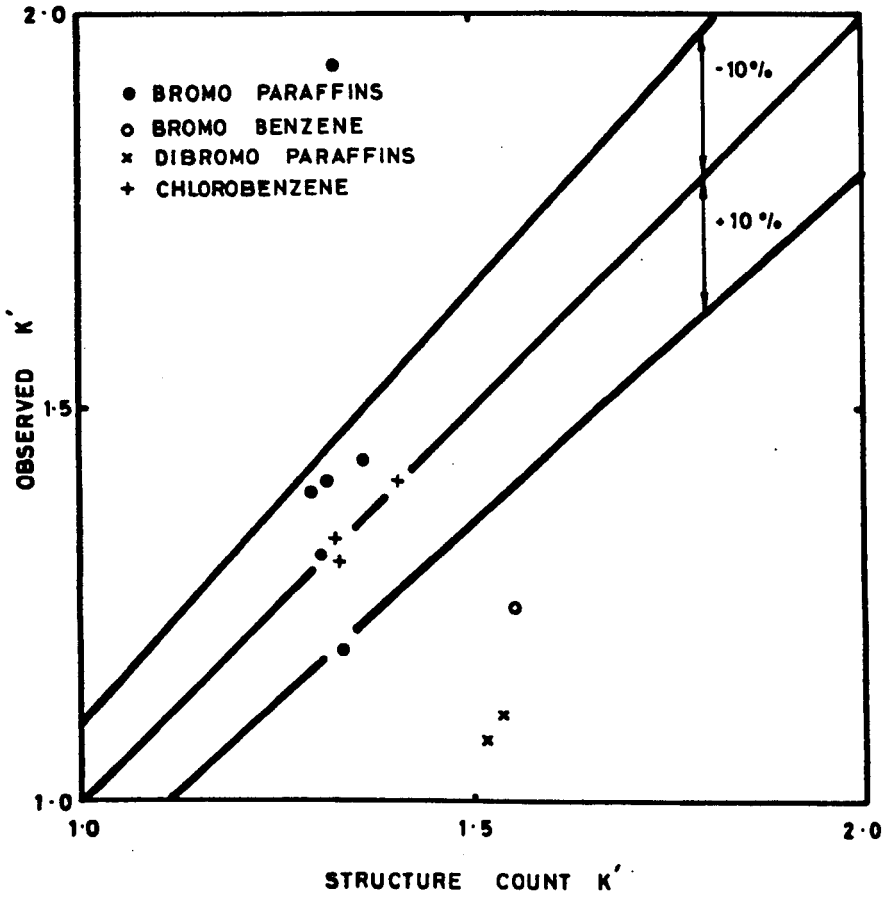

FIG 4.5 CALCULATED AND OBSERVED TRANSMISSION COEFFICIENTS

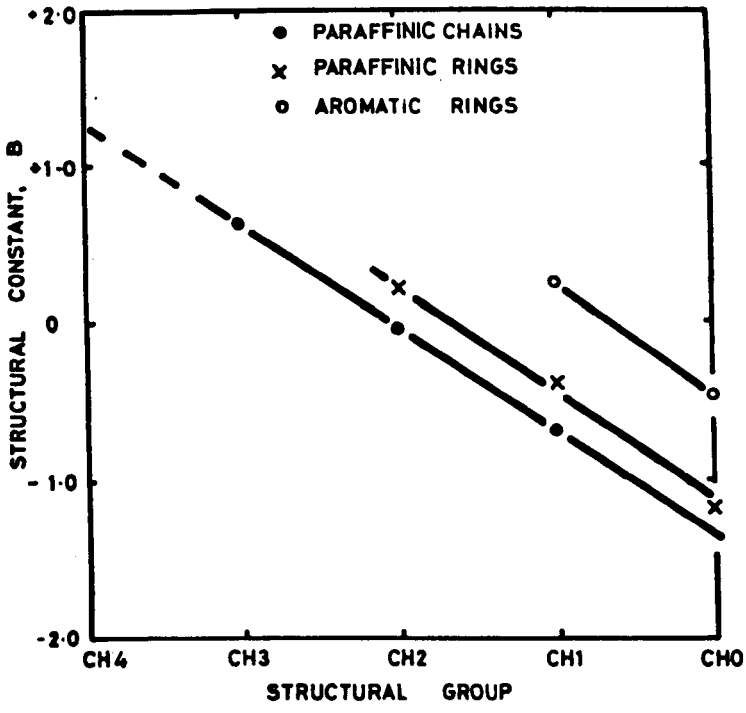

FIG 4.6 STRUCTURE COUNT CONSTANTS

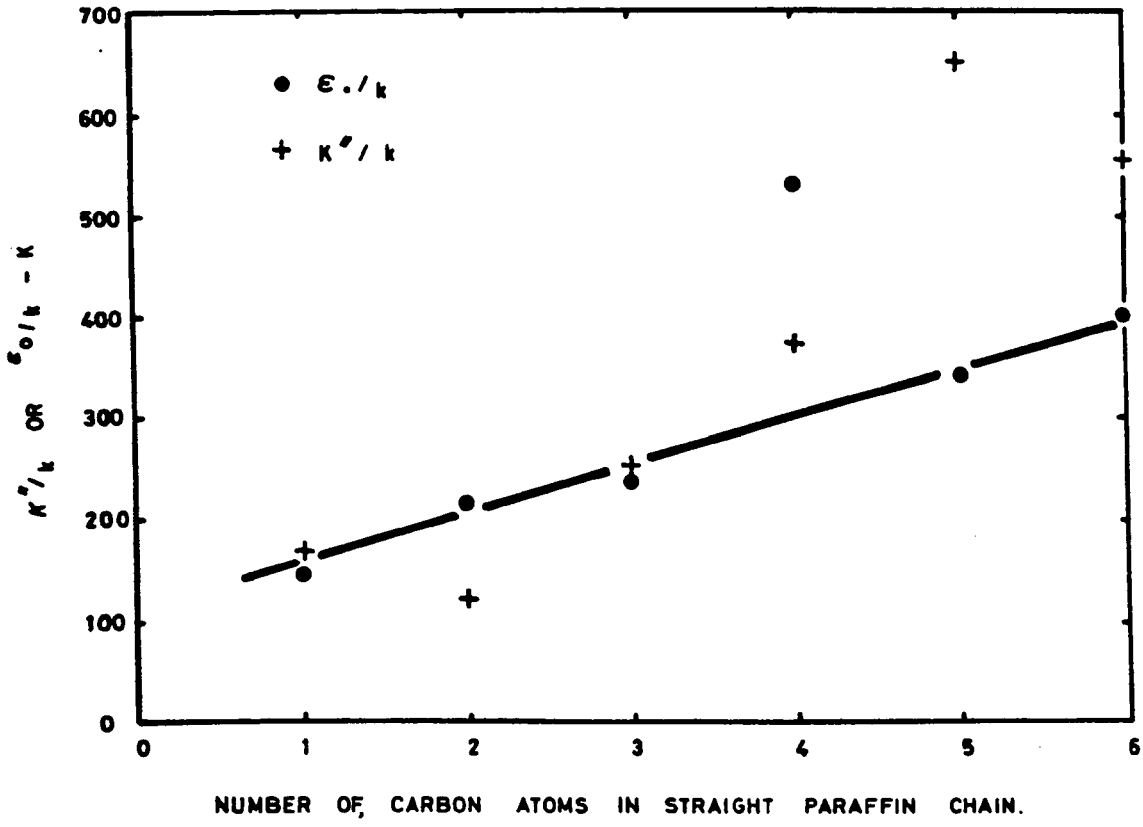

FIG 4.7 ENERGY CONSTANT AND LENNARD - JONES CONSTANT

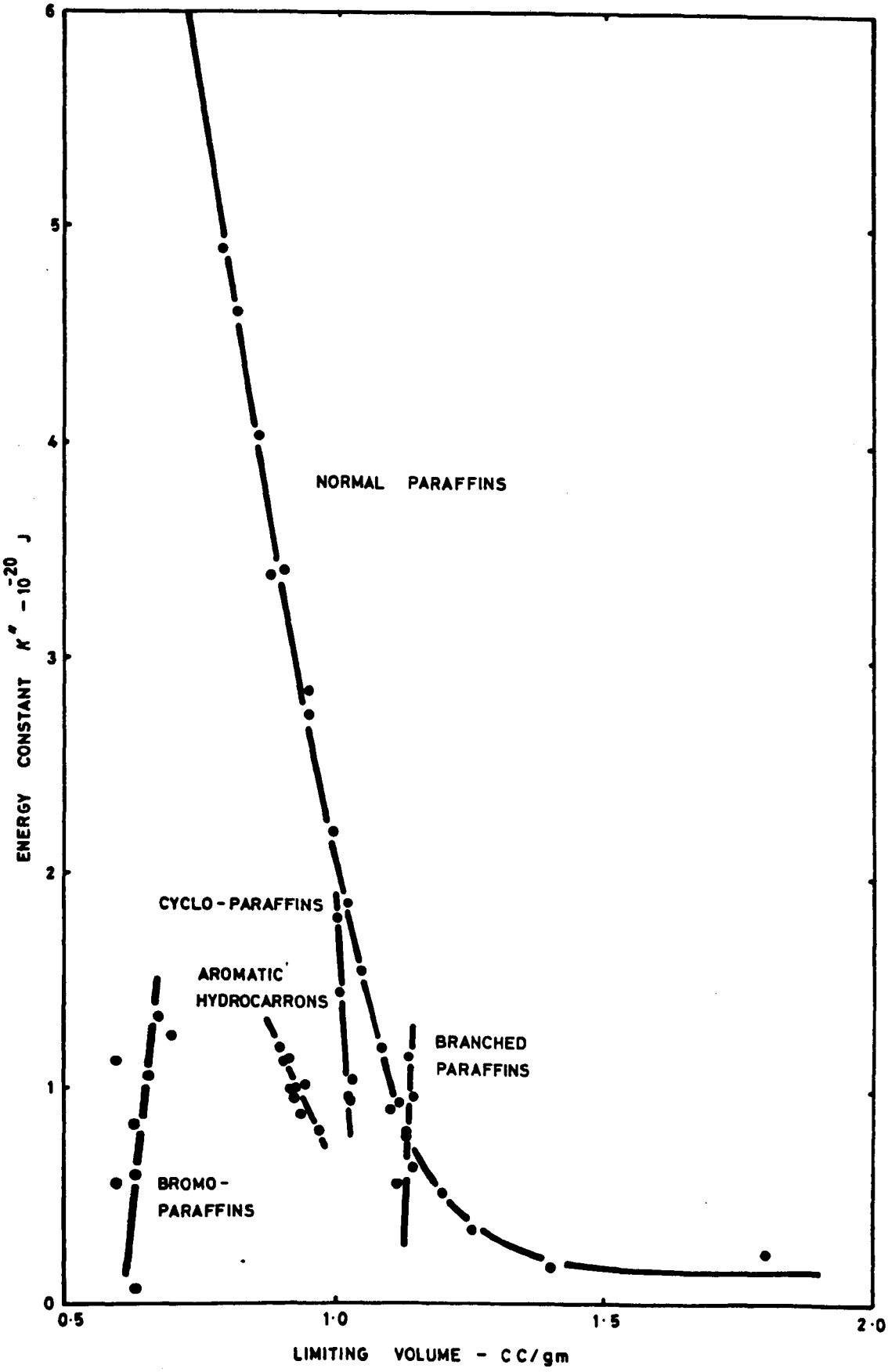

FIG 4.8 ENERGY CONSTANT AND LIMITING VOLUME

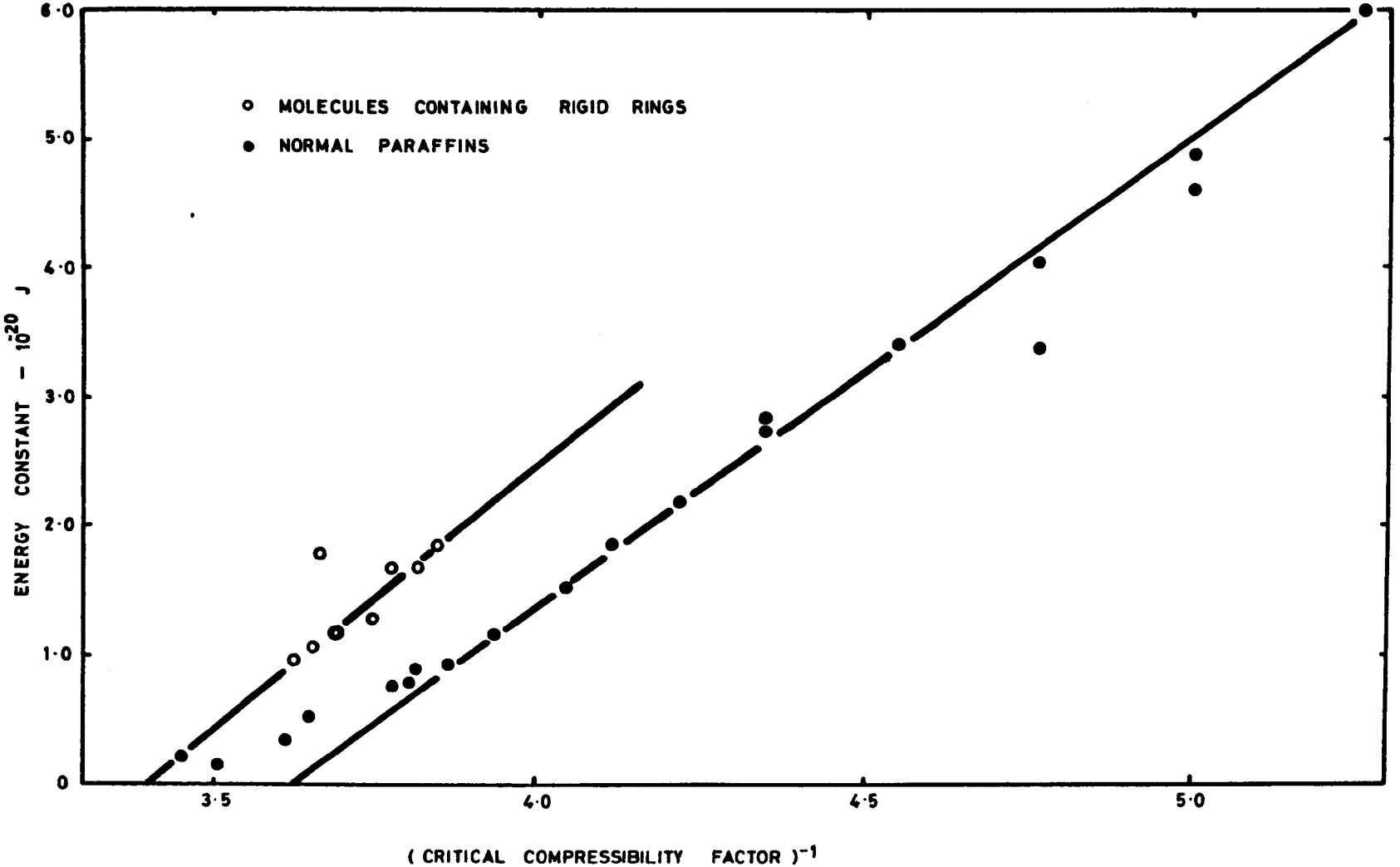

FIG 4.9 ENERGY CONSTANT AND CRITICAL COMPRESSIBILITY FACTOR

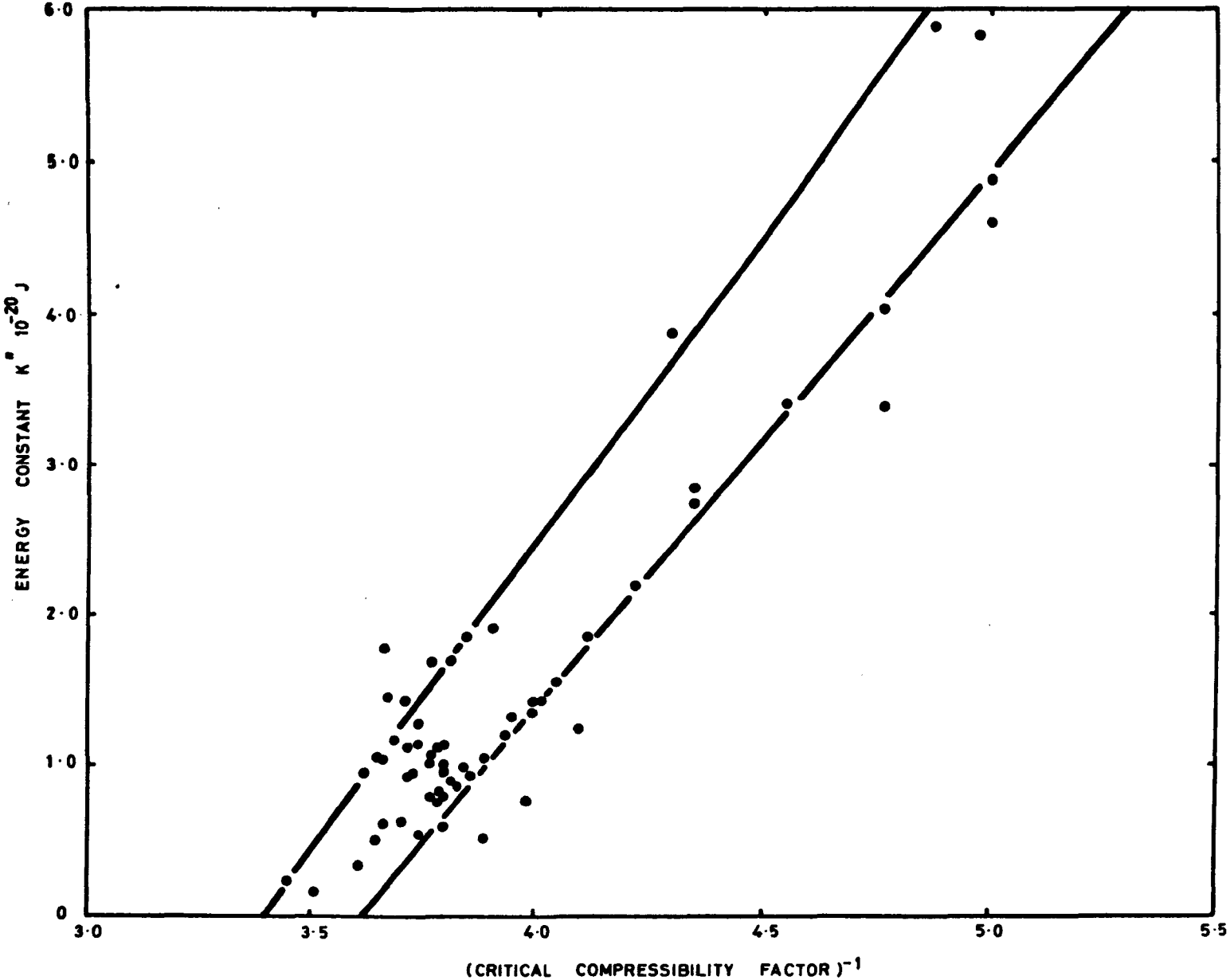

FIG 4.10 ENERGY CONSTANT AND CRITICAL COMPRESSIBILITY FACTOR

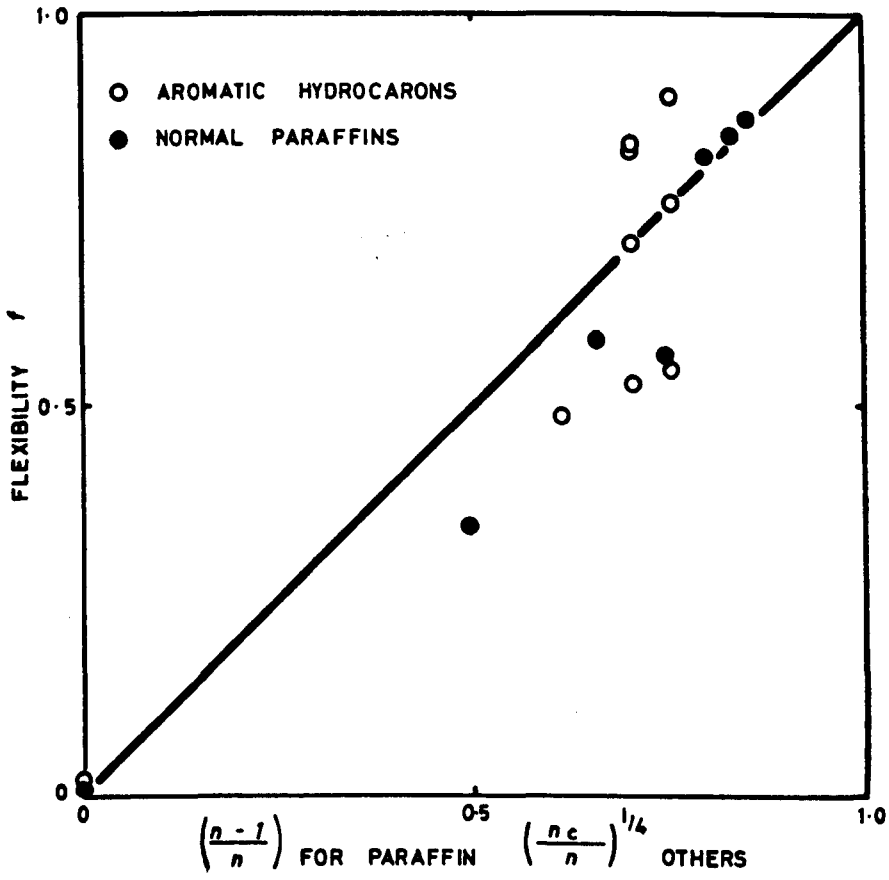

FIG 4.11 FLEXIBILITIES FOR PARAFFINS AND AROMATIC HYDROCARBONS

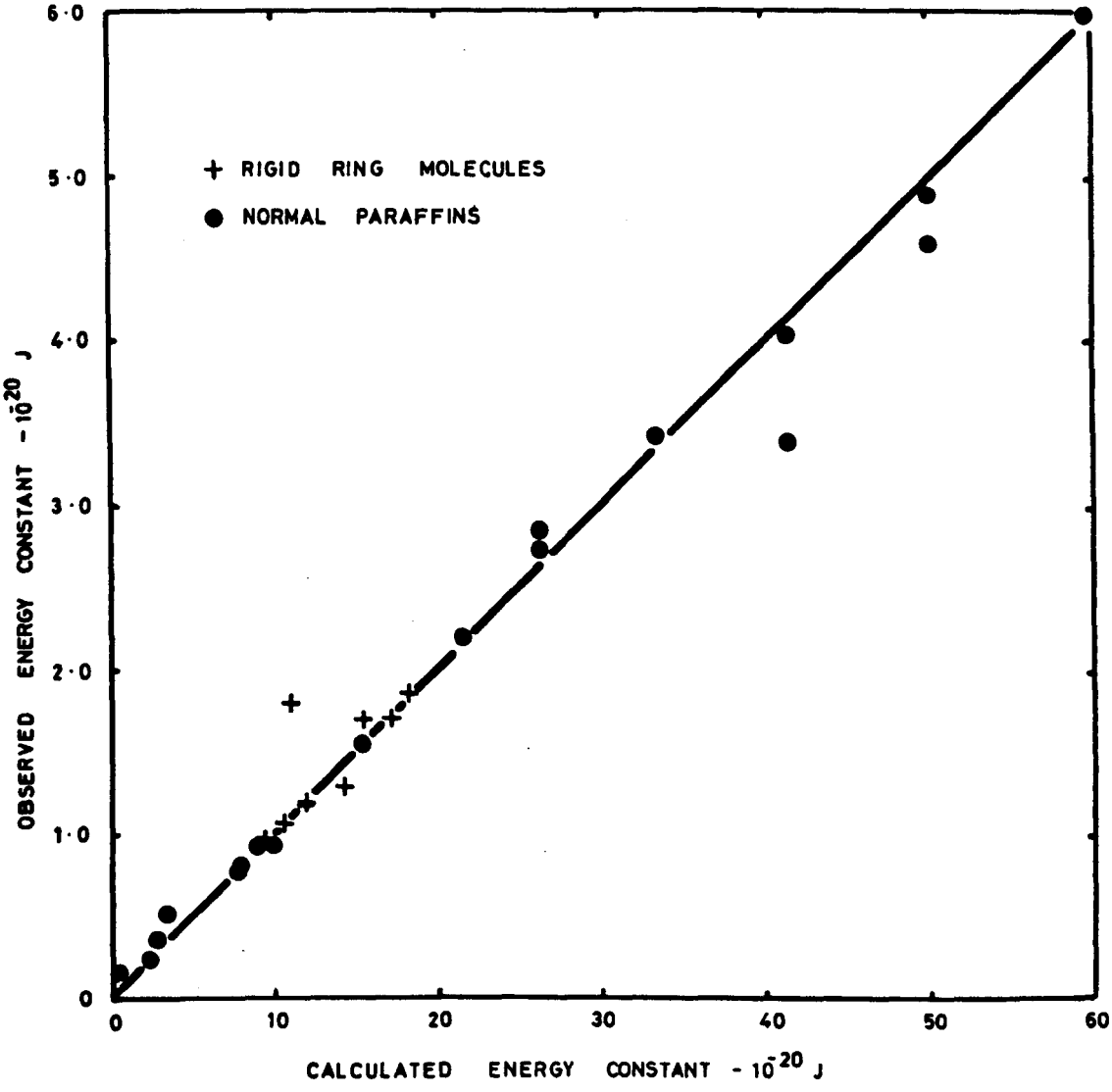

FIG 4.12 CALCULATED AND OBSERVED ENERGY CONSTANTS.

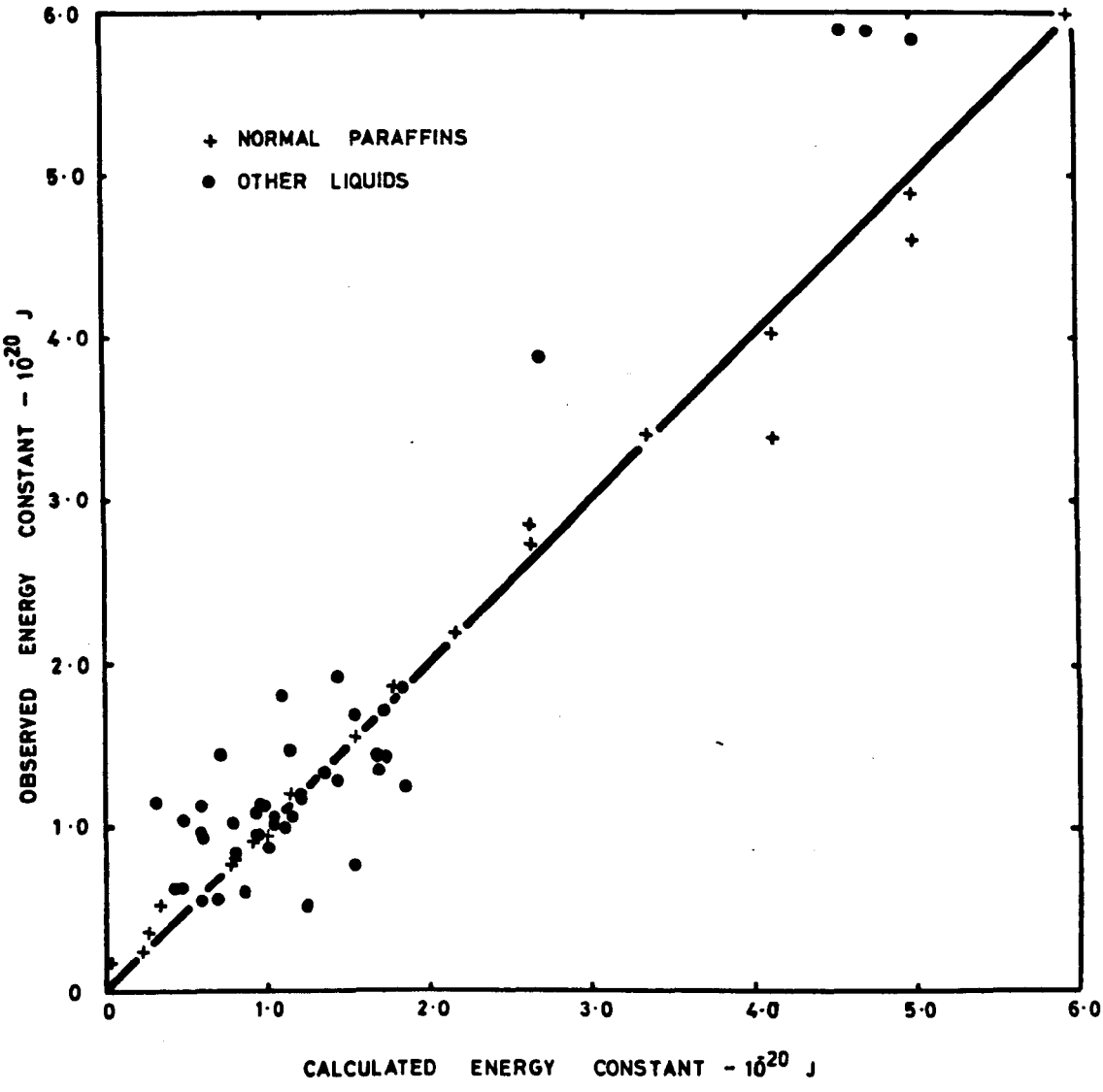

FIG 4.13 CALCULATED AND OBSERVED ENERGY CONSTANTS

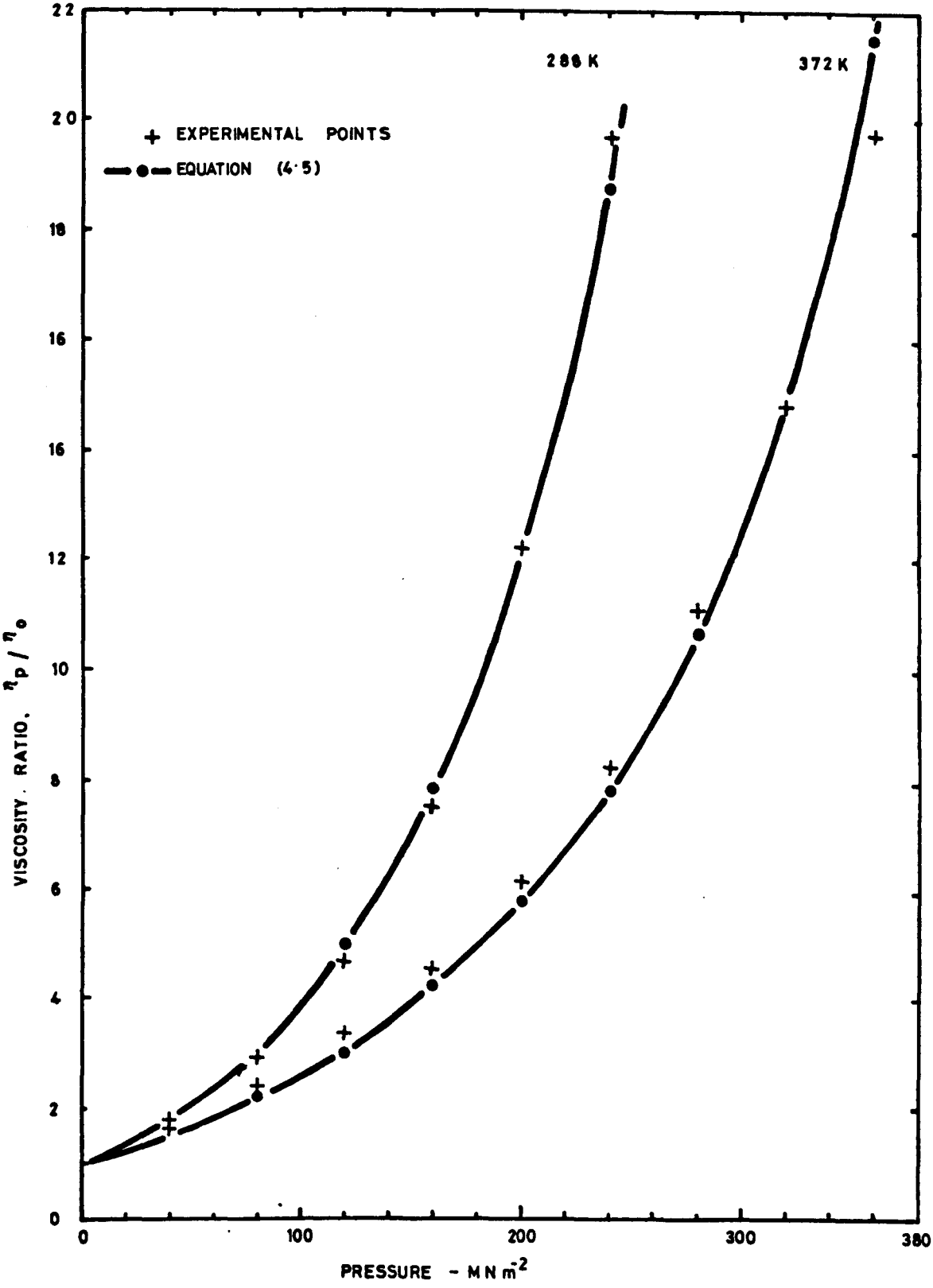

FIG 4.14 VISCOSITY OF CIS-DECALIN UNDER PRESSURE

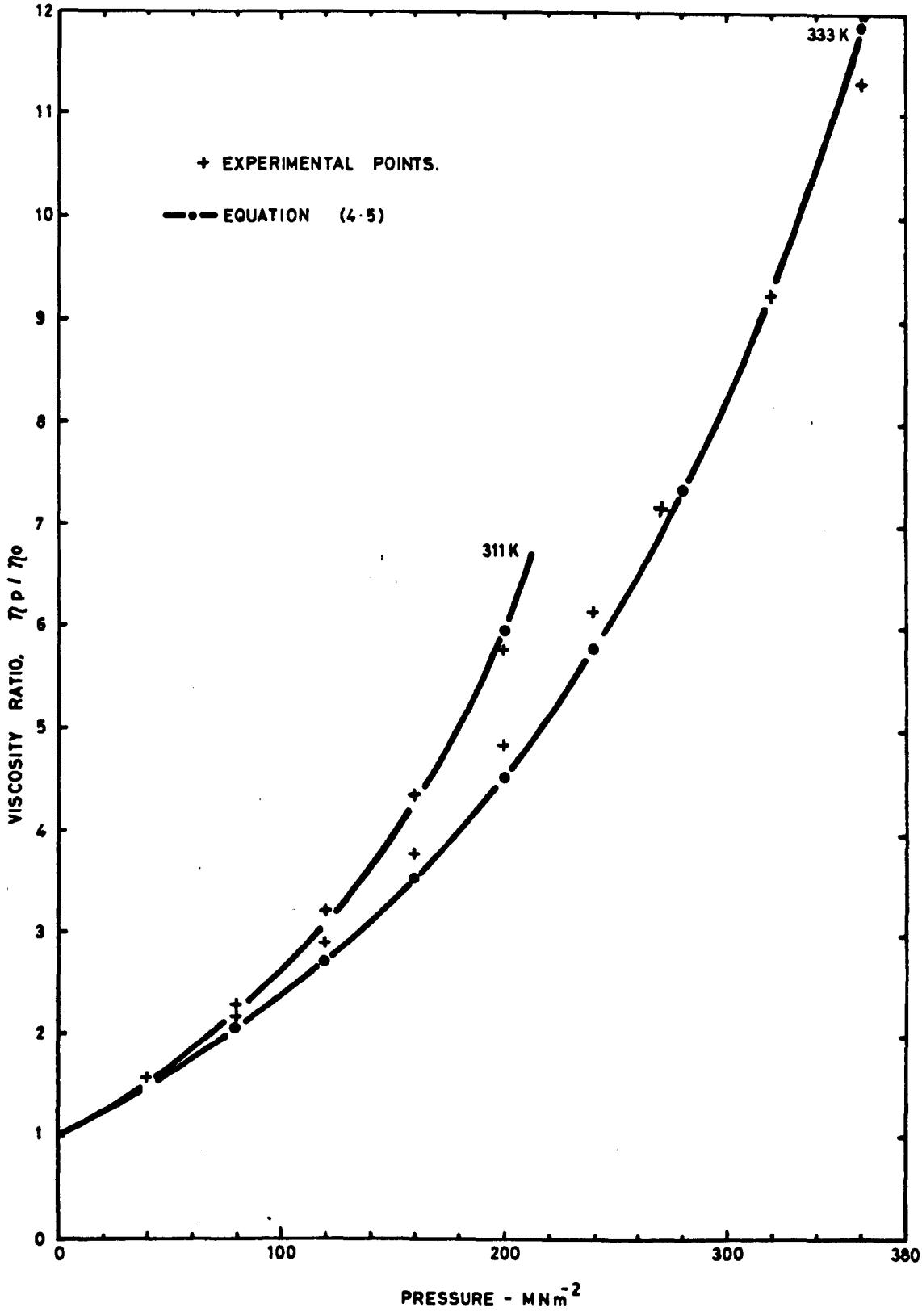

FIG 4.15 VISCOSITY OF DODECANE UNDER PRESSURE

CHAPTER 5

APPARATUS DESIGN AND DEVELOPMENT

SUMMARY OF CHAPTER 5

5 APPARATUS DESIGN AND DEVELOPMENT

Details of design and development are given for the pressurising system, viscometer tube and sinkers, fall time measurement, density measurement and pressure and temperature measurement. The method of filling the viscometer is also described and various aspects of sealing are discussed.

CHAPTER 5 - APPARATUS DESIGN AND DEVELOPMENT

LIST OF TABLES

LIST OF FIGURES

5 APPARATUS DESIGN AND DEVELOPMENT

5.1 Pressurising System and Equipment

5.1.1 System and components

High pressures were generated using the hydraulic system shown diagramatically in Fig. 5.1. The system consisted of a Madan Airhydro Pump supplied by an air line, pressure intensifier, pressure gauge block with pressure release valve, and the pressure vessel enclosed in an oil bath. The pressurising fluid used was kerosene.

Pressures up to 250 MN m^{-2} were obtained directly from the pump. With valves A and C open and valve B closed, pressure was transmitted from the pump to the gauge block and pressure vessel through the two pairs of non-return valves, D and E, on the intensifier body. The pump pressure was monitored by a dial gauge and the final pressure was measured by a resistance gauge in the gauge block. Pumping through this part of the circuit also returned the intensifier piston to its starting position and allowed fluid from the low pressure side of the intensifier to return to the reservoir.

Higher pressures were generated by using the intensifier one or more times. The system was first primed to 250 MN m^{-2} as described above. Then with valves A and C closed and valve B open, the pump pressure was transmitted to the low pressure side of the intensifier. When the pressure generated at the high pressure side of the intensifier (which had an intensification ratio of 18 to 1) exceeded the priming pressure, the non-return valves, E, opened and pressure in the gauge block and main vessel was increased. This process was repeated after repriming if the required pressure was not reached on the first stroke.

The intensifier body, gauge block, and pressure vessel were made from EN26 steel hardened to 1.2 GN m^{-2} (80 tons/in^2). These components

were autofrettaged by applying pressures of about 1.5 GN m^{-2} after manufacture. Autofrettage pressure was generated using the intensifier and during the process the system was filled with brass rod to minimise the fluid volume and the volume change due to pressure. After overstraining the intensifier bore was measured and found to be almost unchanged near the beginning of the piston stroke and about 0.05 mm oversize towards the end. The bore was therefore carefully honed out to a uniform diameter, equal to the maximum value after overstraining, so that effective sealing could be maintained over the full stroke of the piston. A new intensifier piston was made to suit the enlarged bore. The high pressure vessel was also honed out to give a uniform bore. The elastic range of the system after autofrettage is estimated to be 1.35 GN m^{-2}.

The high pressure end of the intensifier piston was made from J37 steel, 10.31 mm diameter by 50 mm long. It is sealed by a square section polyurethane O ring backed by a phosphor bronze anti extrusion ring as shown in Fig. 5.2(A). This sealing arrangement was adopted shortly after autofrettage and has been in operation untouched throughout most of the experimental programme.

The low pressure intensifier piston is of Hecla 108 hardened to 600 DPH, and is sealed by a Bridgman type seal with Neoprene washer. It has not been necessary to remove this component since it was first assembled.

Intensifier, gauge block, and pressure vessel are mounted on self aligning bearings, as shown in Figs 5.3 and 5.4, and can be rotated through 270° by slackening the connection of the priming line.

The pipework and fittings of the primary and intensifier supply circuits

shown in Fig. 5.1 are of standard type made by Aminco. The tube selected had an OD of 6.4 mm (0.25 in), a bore of 1.6 mm (1/16 in) and a working pressure of 700 MN m^{-2}. Between the pressure vessel and gauge block a length of Harwood composite high pressure tube was used. This tube had an OD of 19 mm (0.75 in), a bore of 1.6 mm and a working pressure of 1.4 GN m^{-2}.

5.1.2 Seals

The seals adopted throughout were generally similar to those used by Cappi (1964) and were of the O-ring type supported as shown in Fig. 5.2(C) and on the drawing. For this type of mounting the sealing load must be greater than the load due to the pressure and large enough to compensate for small deformations at the point of sealing. During the autofrettage process and in the earlier experiments various types of O-ring were tried before a successful seal was obtained. Conventional circular section O-rings of butyl rubber, Neoprene and Viton were found to be unreliable in this configuration, and usually limited the maximum pressure to about 300 MN m^{-2}. Most failures on inspection were found to be due either to extrusion of the ring into the sealing gap with consequent tearing of the ring or to complete fracture across a radial plane. The former type of failure was characterised by a slow leak increasing with pressure and the latter by sudden leakage. On one occasion a Viton ring failed suddenly at about 600 MN m^{-2} and on removal was found to be completely powdered. Since the sealing loads could not be increased without risking damage to the seal faces it was clear that the seals would either have to be redesigned or a more suitable seal material would have to be found.

Two seals which persistently gave trouble in the early stages were, in

fact, redesigned successfully. The sealing arrangement of the high pressure piston and the seal between the intensifier bore and the first non-return valve leading to the pressure vessel were converted to anti extrusion ring/O-ring combinations as shown in Fig. 5.2(A). This type of seal may be used either dynamically, as on the piston, or statically, as on the other seal, and does not require any externally applied sealing load. Both of these seals have functioned without attention since they were installed near the beginning of the work.

During autofrettage some difficulty was experienced in obtaining a seal at the high pressure piston. Initially a plain cylindrical piston was used bearing on a separate phosphor bronze seal carrier as shown in Fig. 5.2(B). For the first trial the edge of the carrier was chamfered as suggested by Cappi (1964), but this system failed at quite low pressures and it was clear on inspection that, though the O-rings were providing a seal at low pressures, insufficient load was being produced to deform the phosphor bronze and make it provide a seal at higher pressures. The chamfers were therefore machined off and a slightly raised lip was left at edge of the carrier. This arrangement was much more effective since it encouraged extrusion of the carrier into the gap between the piston and the cylinder at lower pressures. However, it was necessary to carry out the autofrettage in two steps using a slightly larger diameter carrier on the second pressurisation.

The early O-ring failures indicated that two properties of the seal material were important. It was clear that a high resistance to tearing was necessary to avoid destruction on extrusion, and that the material must not reach a brittle vitreous state in the work pressure range to avoid shattering or fracture due to compressive loads. The seals were

therefore replaced by polyurethane rings of square section. Polyurethane has a high resistance to tearing and abrasion and remains flexible at low temperatures. Experience in the use of this material has shown that it also remains flexible at high pressures, since no brittle type failures have been encountered. A large amount of extrusion can also be tolerated without failure as shown in Fig. 5.5. The square section was chosen to minimise ring deformation prior to sealing by extrusion. Polyurethane rings have performed reliabily in the apparatus at pressures up to 700 MN m^{-2}. For higher pressures mild steel anti extrusion rings mounted as shown in Fig. 5.2(D) were necessary at both pressure vessel closures.

Tapered ceramic cone insulators of the type shown in Fig. 5.2(E) were used to seal the electrical leads to the viscometer and pressure gauge. These seals were seated to the closure and the terminal by careful lapping with fine diamond paste, and have been completely trouble free.

5.1.3 Temperature bath

The temperature of the pressure vessel was controlled by keeping it completely immersed in an oil bath as shown in Figs 5.1 and 5.6. The bath was insulated on all sides by 50 mm of fibreglass and heat losses from the free liquid surface were minimised by a double layer of 20 mm Alplas balls. The temperature of the bath fluid, Marlotherm S, was maintained and controlled by a 3 kw Grant Instruments controller with mercury contact thermometer, and additional stirring ensured good circulation. Bath temperature was measured by a quartz crystal thermometer attached to the outside of the vessel at its mid point. Temperatures stable to ±0.02 K were achieved.

5.2 Viscometer and Equipment

5.2.1 High pressure viscometry

To measure viscosity in any situation it is necessary to apply a measured force to the liquid and measure the resultant rate of deformation. From the force and the way in which it is applied it must be possible to calculate the shear stress in the liquid, and from the rate of deformation it must be possible to calculate the shear rate.

The difficulties of designing a mechanical device to either apply a measured shear stress or to measure the resultant shear rate, inside a pressure vessel, have limited this approach to comparatively low pressures. These difficulties are principally caused by the effects of friction at high pressure seals, in the case of external drives, and by heating of the fluid by the motor in the case of internal drives.

For these reasons most high pressure viscosity measurements have been carried out using devices which rely on the effect of gravity to provide the driving force, and obtain shear rate from two internal position measurements and time. The range of shear rates which can be obtained are therefore limited by the physical size and density of the components of the viscometer which determine the magnitude of the force which can be applied to the liquid. With gravity as the driving force, therefore, only modest rates of shear can be obtained since most high pressure vessels have quite small internal capacities.

Several variations of the gravity driven type of high pressure viscometer have been used. Bridgman (1958) carried out extensive measurements using a vertical tube and hemispherically ended sinker,

and detected sinker position by an electrical contact method. Guiding pins were used to keep the sinker in a central position and repeat readings were obtained by inverting the system. By this method measurements up to 1200 MN m^{-2} were made, but the scope of the instrument was limited by the method of timing which would not operate on electrically conducting or polar liquids. Similar apparatus has been used by Cappi (1964), Kleinschmidt (1928) and Dow (1939), though in the case of Cappi an inductive detection method was used which could be applied to conducting liquids. Heiks and Orban (1956), also in similar apparatus, detected the sinker using a radiation detector outside the pressure vessel with a radioactive source embedded in the sinker. The main disadvantage of these methods arises from the use of centring pins. If the pins are a very close fit in the viscometer tube and of accurately equal length then the errors caused by eccentricity are low but the influence of friction between pins and tube is high. If the pins are not a close fit in the tube then the sinker may, or may not, take up an eccentric position depending on its shape, so that erratic timings may be obtained.

Self-centring devices have been used by Boelhower and Toneman (1957), Van Wijh and Van der Veen (1940) and others, and more recently by Harlow (1967) and Irving (1972). Boelhower, Van Wijh and Irving raised the sinker by means of magnetic forces and in those cases it was necessary to have an iron sinker and a non-magnetic tube. This system creates difficulties because of the difference in compressibility and thermal expansion of the two materials. The width of the annulus between sinker and tube varies with temperature and pressure, and though corrections may be applied, these can be quite large. In addition the heating effect of the coils used to raise the sinker disturbes

the thermal equilibrium of the tube and prevents further measurements being made until the temperature stabilises.

Though the equations describing the flow in falling body viscometers have been known for some time they are not normally used as absolute instruments. This is because the sinker velocity is very strongly dependent on the width of the annulus, and the slight variations which always occur over the length of the viscometer tube and sinker therefore have a relatively large effect on the viscometer constant. In addition no accurate method is known for calculating the effect of radial flow at the nose and tail of the sinker. Quite wide variations between calculated and experimental viscometer constants are common, for example the ASME experimental values varied from 0.986 to 1.323 times the calculated value for different sinkers.

If a sphere is used for the falling body as in the instruments of Suge (1937) and Zolotykh (1960), then absolute measurements can be obtained by using Stoke's law and applying the empirical corrections which are available to allow for the influence of the tube walls. However it is necessary to have a relatively large difference between ball and tube diameters so that these corrections are valid. When this is so an inductive method of detecting position of the ball must either be very sensitive, because of the small size of the ball, or of higher magnetic field strength. In the latter case the field is likely to influence the movement of the ball and in the former case the balancing of the detection coils becomes critical and difficult because of the influence of temperature and pressure. Optical detection, as used by Zolotykh for example, is of course limited by the strength of the windows and the opacity of the specimen.

An alternative configuration which has been widely used under pressure is the rolling ball viscometer originated by Flowers (1914). This type of instrument is also used as a relative viscometer by calibrating with liquids of known viscosity. At high viscosities a linear calibration can be obtained with two viscometer constants but at low viscosities, less than 6 mNs m^{-2} for the instrument described by Lowitz, Spencer, Webb and Schiessler (1959), non-linear characteristics are obtained. The main drawbacks with this configuration are the non-linear calibrations and the unknown influence of stick/slip and spin effects during rolling. Though this method has been extensively used at high pressure the present results suggest that values obtained should be treated with caution, especially at low viscosities.

5.2.2 Design of viscometer tube and sinkers

Based on the examination described in the previous section the method chosen for this work was one in which the terminal velocity of a sinker is measured as it falls axially down the centre of a vertical circular tube containing the liquid being measured. The sinker and tube are of the same material, to minimise compressibility and thermal expansion effects, and are non magnetic. Embedded in the sinker is a small ferrite cylinder, 2 mm long and 4 mm diameter. The position of the ferrite is detected by the change in inductance which it causes as it passes through two pairs of coils wound on the outside of the tube. To avoid errors arising from turbulence or friction caused by centring pegs, the sinkers are designed in such a way that they are self centring. Pressure is transmitted to the sample through a flexible bellows.

Two viscometer tubes have been used. The first was designed with a pair of detecting coils near each end of the tube but, during the measurement of 1-bromododecane, it was accidentally damaged by over-pressurisation. At 50°C the test liquid froze at about 350 MN m^{-2} but the pressure was raised to 400 MN m^{-2}. On removal the thin-walled section at the terminal block was found to be partially collapsed and the sections beneath the coil grooves were also deformed. The tube could not be salvaged so a second one, described in the following sections, was designed and made. Normally, if it was suspected that a sample was near its freezing point, the sinker was kept near a pair of detecting coils by tilting the tube. The pressure was then increased slowly and the tube tilted slightly until sinker movement could be detected on the oscilloscope. If the sinker movement became erratic or ceased the pressure was lowered and measurements were limited to a lower round value of pressure.

Both viscometer tubes were made from a solid bar of En58J non-magnetic stainless steel. Fig. 5.7 shows the second tube with three pairs of triggering coils, any two of which can be used to give different working lengths. The diameters of both tubes and sinkers are constant to within ±0.005 mm and deviate from circularity by less than 0.005 mm. The maximum working length is 150 mm.

The triggering coils are wound from 44 SWG insulated copper wire with a resistance of 80 ohms and approximately 550 turns on each coil. They are trimmed to the same resistance within 0.5 ohms and to the same inductance within 0.2 mH. Excess length of wire is wound non-inductively and the ends are soldered to pin connections on Tufnol collars attached to the narrow sections of the viscometer tube. Figs 5.8 and 5.9 show the various parts of the viscometer before and after

assembly. Connecting wires from the collars are then led along axial grooves to a pin/socket connector on the end of the bellows housing. Thin discs of PTFE are used to line the coil grooves before winding. These discs prolong the life of the coils by preventing the lacquer insulation of the wire from being scraped off in repeated use by the corners of the grooves. The grooves are also slotted radially to allow easy access of the pressurising fluid and to avoid setting up excessive pressure gradients during pressurisation.

The pressure transmitting bellows are of 0.1 mm stainless steel seamless tubing with 12 convolutions. Fully compressed the bellows can expel 5.5 μm^3 or 25 per cent of the total sample volume. This amount of contraction is not sufficient for many liquids at pressures much above 500 MN m^{-2}, so the total sample volume may be reduced by enclosing two PTFE fillers, one at the bellows end and the other at the opposite end of the viscometer. It was not possible to use a larger bellows because of lack of space. The bellows end filler rests on the sealed base of the bellows and moves with the bellows as it contracts. It is a push fit in the viscometer tube and so does not move when the vessel is rotated, and a 1 mm diameter axial hole permits easy movement of the test fluid. The length of this filler is adjusted so that, when the bellows are fully compressed, it prevents the sinker from leaving the last of the triggering coils and so provides a useful indication of bellows condition. The other filler is located at the opposite end of the viscometer tube and takes up the volume between the end cap and a point mid way between the two upper pairs of coils. It cannot be included when the upper coils are being used. With both fillers in position the bellows can allow a 38 per cent decrease in specimen volume at the filling temperature. The expansion of most

liquids between 25°C and 100°C is comparatively small and does not result in movements large enough to strain the bellows.

Sealing between the end cap and the viscometer tube and between the tube and the bellows section is effected by 0.1 mm copper washers. These are of small area and are tightly clamped in recesses in the end caps by raised sections of the viscometer tube. While these rings do not have to seal against pressures greater than those generated by the bellows, they do have to remain tight over the full temperature and pressure range. No leaks were traced to the washer seals but the copper disc seal on the vent hole at the top of the viscometer did leak occasionally because it was difficult to ensure that the grub screw was bearing down on it correctly. This difficulty was overcome by pressing the bellows hard by hand for about one minute after the tube had been finally sealed. If no leaks were then visible the tube was loaded into the pressure vessel.

Self-centring sinkers have been employed by several workers. Those used by Nederbragt and others were essentially falling needles with diameter to length ratios of 1 to 10 or less. They had a long tapering nose section to promote a stable flow, a cylindrical body and flat tail. The sinkers used by Irving had a much larger diameter to length ratio, about 1 to 3, a paraboloidal nose, cylindrical body, and flat tail.

The sinkers used in the present investigation were designed after carrying out a series of tests in a perspex model viscometer and in a length of precision bore glass tube. The tube was filled with water, which had been coloured with potassium permanganate, and the behaviour of the sinker under test was observed as it passed down the tube. The

colour of the solution enabled the eccentricity of the sinker to be observed directly. When the sinker was in a central position the liquid in the annular space was of uniform colour around the circumference, and when it was eccentric the variation in depth of colour could be easily seen.

A number of sinker shapes were tried with varying degrees of success. The sinker shape which gave results which led to the final design is shown as the left sinker in Fig. 5.10. When falling down a vertical tube this sinker travelled down the central axis. On tilting the tube it took up an eccentric position but when the tube was restored to the vertical it rapidly recentred itself. It was deduced that for this sinker the centring action occurred because the largest part of the viscous forces act on the upper cylindrical section with the largest diameter. The centre of action of these forces is therefore approximately at the centre of the upper cylinder. The centre of gravity of the whole sinker on the other hand is well below this position. Therefore if the sinker is travelling down the wall of the tube, with the tube vertical, a slight disturbance at the nose, due to the flow of the liquid, will cause it to tilt to a position in which the viscous and gravity forces exert a couple which tends to move it to a central position. The right sinker in Fig. 5.10 is a section of the final design based on these results.

The sinkers are also made from EN58J steel with a solid ferrite core located just below the geometric centre as shown in Fig. 5.10. A number of sinkers with different diameters have been made.

5.2.3 Fall time measurement

The terminal velocity of the sinker is measured by timing its fall over a fixed length. Embedded in the sinker is a small ferrite core which activates the timing device by changing the inductance of a pair of coils at each end of the viscometer tube. The four coils form a bridge which is unbalanced by the passage of the sinker through each coil in turn. When the ferrite core is midway between the first pair of coils the out of balance signal is instantaneously zero and at this point a trigger actuates an electronic timer. The second pair of coils stop the timer in a similar manner.

A block diagram of the circuit is shown in Fig. 5.11. As the sinker with its ferrite core enters the first coil an out of balance signal is produced which is then amplified. The demodulator working in conjunction with the phase shifter then reduce this 300 Hz signal to a DC level which first rises and then falls as the sinker approaches the second coil, reaching zero at the mid point. At this point the DC signal operates a Schmitt trigger which produces a sharp pulse to start or stop the Hewlett Packard Counter Timer type 5223L. The input level at which the trigger operates is offset a little from zero to avoid false triggering caused by background noise in the circuit.

Fall times measured by this method are accurate to less than 0.01 sec, and, when conditions within the viscometer are stable, measurements repeat to within 0.2 per cent.

To check the repeatability of the triggering position the empty viscometer tube was mounted in a small rig as shown in Fig. 5.12. A ferrite core similar to those used in the sinkers was attached to the end of a micrometer head so that it could be brought into the coils and operate

the bridge. The viscometer tube and the micrometer barrel were firmly clamped to a solid base. With the bridge switched on and balanced the ferrite core was brought slowly and smoothly into the coils by the micrometer screw. When the trigger operated a reading was taken and the procedure repeated. After several readings had been obtained the bridge was re-balanced and the procedure repeated again. The maximum difference between any two readings was 0.084 mm. Errors of this magnitude in position detection correspond to expected uncertainties in the length between the pairs of detection coils of ±0.02 per cent for the two centre pairs of coils and ±0.08 per cent for the coils with the smallest separation. These uncertainties contribute directly to variations in the measured values of fall time and therefore to the uncertainty in viscosity. When in use the shortest path length always gave a fall time repeatability less than ±0.2 per cent. The uncertainties measured on the rig are subject to additional errors mainly caused by lack of smoothness in operation, which would cause overshooting of the triggering point, and minor temperature variations not present in the constant temperature bath. The values obtained, though small, are therefore probably larger than the actual contributions from this source.

Changes in position of the coils due to pressure cannot be measured without cumbersome apparatus. However great care was taken to ensure that the coils were well ventilated so that the pressurising fluid could penetrate to the base of each coil without exerting any pressure on the wires. In addition pressure was always increased slowly. Changes in length of the viscometer tube due to compression and thermal expansion were automatically included by the method used for calculating results.

5.2.4 Filling the viscometer

The filling of the viscometer with a clean pure liquid sample is clearly one of the most important parts of the experimental procedure, and before commencing a fill the viscometer tube was completely dismantled. Each part was then thoroughly rinsed in acetone and petroleum ether and then filled with or immersed in a solution of 0.1 N potassium hydroxide in isopropanol and allowed to stand for at least fifteen minutes. The parts were then rinsed several times in filtered distilled water and assembled.

To dry the assembled tube it was attached to the filling rig shown in Fig. 5.13 and evacuated while slight heating was applied to the outside by means of a hot air dryer. When the tube was dry the pressure in the system dropped quite sharply and the tube was then checked for leaks by sealing off part of the system containing a pressure gauge with the tube.

When it was clear that the tube was leak free and dry, the sample to be measured was allowed to flow from the upper chamber through a 1 μm filter into the evacuated viscometer under the action of atmospheric pressure. When the tube was full the filling rig was detached, the sinker introduced and the end cap firmly tightened. Finally the tube was topped up by syringe (with a filter attachment) through the small vent at the top of the end cap. This topping up procedure was necessary because the end cap design did not allow all the air to escape when it was positioned. A later design of end cap made this unnecessary.

In earlier fills and when the effect of dissolved air was being investigated, the sinker was introduced to the tube immediately after

the sample had been allowed in and before the filling rig was removed. This was done by holding the sinker above the tube by means of a magnets, shown in Fig. 5.13, during evacuation and filling, and releasing it when the tube was full. This procedure worked well and cut down the time of exposure to the atmosphere on removing the filling rig but was not necessary when the effect of dissolved air had been established.

5.3 Density Measurement

5.3.1 High pressure density measurement

All liquids increase in density when subjected to an increase in pressure and most experimental measurements have been made using variations of four basic methods.

The simplest method for use under pressure is probably the piston and bottle arrangement, in which pressure is generated by forcing a piston into a closed bottle containing the sample. Pressure may be measured either by an independent gauge or from the force applied to the piston, and volume change can be calculated from the penetration of the piston into the bottle. In the version used by Bridgman (1958) both piston and bottle were enclosed in a separate pressure vessel so that the piston was only subject to small frictional loads. This arrangement is the most accurate for this type of instrument since piston friction is low and the deformations of the materials are limited to those due to compression only. If the bottle is used as the pressure vessel piston friction increases with pressure and the vessel is also subject to elastic deformations. These effects can lead to large corrections at high pressures and limit the use of internally pressurised bottles to comparatively low pressures. Hayward (1964) has, however, used this method to pressures of about 150 MN m^{-2}. Externally pressurised bottles have been used by Kell and Whalley (1965) for very accurate work to pressures of 100 MN m^{-2} and by Bridgman to pressures of about 1200 MN m^{-2}. Both versions of the piston and bottle method clearly rely heavily on the presence of a leak-free seal between piston and bottle.

The most widely used method for high pressures is the bellows or sylphon method also described by Bridgman. The liquid sample is enclosed in

flexible metal bellows, which are placed inside a pressure vessel, and change in length of the bellows is measured as the pressure is increased. Bridgman, Cutler et al (1958), Hogenboom et al (1967), and Lowitz et al (1959) detected change in length using a slide wire device. A high resistance metal wire was attached to the free end of the bellows and a sliding contact was attached to the fixed end. Change in resistance between the sliding contact and one end of the wire was therefore proportional to bellows deflection. In similar apparatus Yazgan (1966) attached the free end of the bellows to the core of a differential transformer mounted inside the pressure vessel. The cross-sectional area of the bellows must be obtained by calibration and corrections for metal compressibility and thermal expansion are small and easily applied.

The main difficulties which arise with this method are likely to arise in the detection of bellows deflection. In all of the methods cited above the detection systems were located inside the pressure vessel and were therefore subject to the high pressure and temperature environment.

In recent years a more sophisticated method based on sound velocity measurement has been used. This method depends upon the integration of the well known equations

$$\beta_T = \beta_S + \frac{T\alpha^2}{C_P}$$

and $$\beta_S = \frac{1}{\rho c^2}$$

By measuring sound velocity under pressure, density and specific heat at atmospheric pressure and integrating with respect to pressure over small increments, it is possible to obtain very accurate densities

within the pressure range of the velocity measurements. No measurements of volume change with pressure are necessary so that this method is clearly of most value at low pressures where direct methods are difficult because of the relatively small movement of the bellows or other sensing device. It has been used by Davis and Gordon (1967) on mercury at pressures up to 1300 MN m^{-2} and by Vedam and Holton (1968) on water up to 1000 MN m^{-2}. In both cases the results are in close agreement with the most accurate values obtained by direct methods. A comparison of the sound velocity method with a bellows method and a bottle method has shown that it may also be used for less simple liquids (Isdale, Brunton and Spence (1975)).

Doolittle, Simon and Cornish (1960) and Grindley and Lind (1971) detected change in volume by measuring the movement along a precision bore tube of a mercury seal used to trap the sample in an enclosed volume. Floating on the mercury seal was a magnetic cylinder and the relative position of this cylinder was detected by a differential transformer outside the pressure vessel. This method is essentially that of the dilatometer often used at atmospheric pressure.

In principle the accuracy of the three direct methods which have been used can be increased to any desired value simply by choosing suitable proportions of container to produce large easily measured deflections. In practice the dimensions of the apparatus are restricted by the size of the pressure vessel or pressurising system. Since there is little difference between the direct methods in respect of accuracy attainable, any choice may be made on the basis of simplicity and ease of operation. The development of a sound velocity method for high pressures is clearly a fairly major task in itself.

5.3.2 Density apparatus

From the examination of the different methods which have been used to measure density under pressure it was decided that a method based on the compression of a bellows would be suitable for the present work. This method was chosen because it is simple and robust and is capable of giving results sufficiently accurate for the viscosity calculations. Since errors of 0.5 per cent in density will give errors of about 0.1 per cent if used to calculate viscosities this was not a very demanding requirement. It also had the advantage that it could be easily fitted in to the existing pressurising system and could be designed to make use of the viscometer bridge circuit by adopting an inductive detection system.

Change in volume is measured by observing the change in length with pressure of sealed bellows containing the liquid to be measured, and initial volume of the sample at atmospheric pressure is obtained from its weight and density. Temperature and pressure are measured as in the viscosity experiments.

The apparatus is shown diagrammatically in Fig.5.14.The bellows housing is mounted on a special end plug closure of the main pressure vessel and is attached to the bellows at its opposite end. The free end of the bellows is attached to one end of a non-magnetic stainless steel rod which projects out of the pressure vessel and temperature bath through a length of non-magnetic high pressure tubing sealed at its extremity. The position of a small ferrite tip attached to the free end of the rod is detected by a pair of coils outside the high pressure tube, and the position of these coils is measured by a micrometer head. A second pair of dummy coils, not shown in the diagram, is mounted in a fixed position remote from unwanted magnetic influences.

The four coils are connected to form a bridge which, with the ferrite tip midway between the sensing coils, is initially balanced. Movement of the ferrite tip, and hence the bellows, unbalances the bridge. The sensing coils are then moved to rebalance the bridge, and their position is measured with the micrometer.

Measurements are easily obtained using the viscometer bridge circuit with the detecting coils connected in place of the viscometer coils. When the temperature and pressure have stabilised and the coils have been balanced, the position of the ferrite tip is located by turning the adjusting screw to move the coils until the Schmitt trigger just operates. A micrometer reading is then taken. The change in length of the bellows due to pressure is then obtained by subtracting from readings taken at atmospheric pressure.

The position of the micrometer is fixed relative to the pressure vessel end cap so that the reading obtained is given by

$$R = l_R + l_B - l_H - \delta l,$$

where δl is the change in length of the bellows due to compression of the liquid only. Since the rod (R), housing (H), and bellows (B) are also subject to changes in length due to pressure, the change in length due to the change in volume of the liquid is given by

$$\delta l = (R_O - R) - \alpha P(l_{RO} + l_{BO} - l_{HO}) ,$$

where α is the linear coefficient of compressibility of the material. A single value of α has been used as the three components were of similar material. The area of the bellows also changes with pressure and is given by

$$A = A_o(1 - 2\alpha P).$$

Specific volume of the sample under pressure is then given by

$$v = v_o - \frac{A_o l}{M}$$

$$\therefore \quad v = v_o - \frac{A_o}{M}\left[(R_o - R) - \alpha P\left\{(R_o - R) + (l_{RO} + l_{BO} - l_{HO})(1 - \beta P)\right\}\right]$$

Typically, at a pressure of 500 MN m^{-2}, the measured deflection was about 20 mm and the emergent length of rod about 150 mm. With a linear coefficient of compressibility of 2.00×10^{-12} m^2 N^{-1}, the change in length due to the compression of the components was 0.17 mm or 0.8 per cent of the change due to liquid compression.

Bellows area was obtained by calibration with water using two different methods. For the first method the bellows were filled at atmospheric pressure and then sealed and weighed. Their length at 25°C was then measured in a small rig using a micrometer screw. Some water was then bled off or added, and the procedure repeated so that the area could be calculated directly from the changes in length and the corresponding changes in volume. The second calibration was carried out under pressure using accurate values for the volume of water. The procedure here was similar to that used for measurement except that area was calculated from the known volume change.

Eight results of the calibrations at atmospheric pressure were discarded as it was suspected that air or vapour bubbles were present in the bellows. The remaining results were averaged, to give an area of $2.255 \times 10^{-4} m^2$, but the scatter was rather high with maximum deviations of ±1.5 per cent.

The second calibration was then carried out in an attempt to obtain a more reliable value for the bellows area. Using the results of Grindley and Lind (1971), seven measurements of bellows area were made at 25°C and at pressures up to 300 MN m^{-2}. The mean area

obtained was 2.207×10^{-4} m^2 with maximum deviations of ±1 per cent.

Further measurements of the density of water were then made at 25°C, 40°C, 60°C and 75°C. The area obtained from the second calibration was used to calculate the results which are compared with the values given by Grindley and Lind in Table 5.1.

Accuracy of the bellows method depends mainly on uncertainties in the measurement of the area of the bellows and the deflection, and, to a lesser extent, on other factors. For a sample of mass 0.03 kg and density 1200 kg m^{-3} with a bellows deflection of 20 mm at 500 kN m^{-2} pressure, the errors are estimated as follows:

1 The bellows area is estimated to be known within ±1 per cent which gives a possible error from this source of $\pm 1.467 \times 10^{-6}$ m^3 kg^{-1} in specific volume.

2 Uncertainty in each micrometer reading was 0.1 mm giving possible errors in deflection of ±0.2 mm. The corresponding error in specific volume is $\pm 1.467 \times 10^{-6}$ m^3 kg^{-1}.

3 Uncertainty in the mass of the sample was about 10^{-5} kg giving possible errors of 0.049×10^{-6} m^3 kg^{-1}.

4 The linear compressibility of the metal components was not measured but a value equal to one third of the suppliers' value of bulk compressibility was used (2.00×10^{-12} m^2 N^{-1}). A ±10 per cent error in this value due to temperature or non linearily with pressures gives an uncertainty of ±0.02 mm in deflection and possible errors in specific volume of $\pm 0.147 \times 10^{-6}$ m^3 kg^{-1}.

5 Errors due to temperature and pressure measurement are estimated

to give possible errors of $\pm 0.50 \times 10^{-6}$ m^3 kg^{-1}.

6 Finally, the specific volume of the sample at atmospheric pressure is subject to an uncertainty of ±0.05 per cent, from pycnometer measurement, or 0.417×10^{-6} m^3 kg^{-1}.

The sum of these errors is 4.047×10^{-6} m^3 kg^{-1} which represents an expected experimental accuracy of ±0.49 per cent. Measured values given in Table 5.1 are all less than this figure probably because a rather large uncertainty (±0.1 mm) was allowed on each micrometer reading. In practice four or more micrometer readings were taken at each point. These always fell within 0.05 mm of each other and in most cases were within 0.02 mm. The additional allowance was made to allow for possible deflection of the pressure vessel and support frame due to pressure, though tests carried out with an open bellows failed to detect any significant deflection. It is therefore concluded that the overall accuracy of the density measurements is ±0.49 per cent.

To avoid unnecessary density measurement a technique of extrapolation and interpolation was devised based on measurements at 25 and 75°C only. Along isobars density itself was interpolated linearly, and along isotherms the density was converted to secant bulk modulus which was then interpolated linearly to be desired pressure and converted back to density. The results of this technique are shown in Table 5.2 which gives interpolated and extrapolated values for water based on the measurements carried out at 25 and 75°C. These results show an apparent increase in accuracy caused by the smoothing effect of the interpolation process and confirm that measurements at 25 and 75°C treated in this way can produce density values sufficiently accurate for the viscosity calculations in the ranges 0 to 500 MN m^{-2} and 25 to 200°C.

5.4 Pressure Measurement

All pressure measurements are derived from the area of a Budenberg Gauge Co Ltd dead weight tester piston and cylinder assembly calibrated at NPL. The effective area was determined, as a function of pressure, by comparing it with a standard NPL pressure balance at pressures up to 800 MN m^{-2}. The NPL certificate gives the area as

$$A = 3.22464 \times 10^{-6}(1 + 3.046 \times 10^{-13}P)\ m^2$$

in a pressurising fluid to DTD 822A at 20°C, and with the piston rotating at about 35 revolutions per minute. The stated accuracy of the area is $\pm 0.36 \times 10^{-9}$ m^2 at 500 MN m^{-2}. A series of weights, weight lifting system and rotation system were then made by Budenberg to provide pressures up to 700 MN m^{-2} in steps of 100 MN m^{-2}. The maximum combined uncertainty in pressure due to area, weights, and the weight lifting and rotation system is estimated to be 0.08 MN m^{-2}.

The dead weight tester was not connected to the high pressure system during viscosity measurement but was used as an intermediate standard. Dead weight testers have a slow leakage of fluid past the piston, and, to maintain constant pressure for a long period of time, it is essential to replace the lost fluid by means of the pressurising system. The principal reason for excluding the dead weight tester from the system was therefore to avoid the need for continuous adjustment of pressure during viscosity measurement, but it was also important to keep the system volume as low as possible and to avoid having too many couplings.

During viscosity determinations pressure was measured by observing the change in resistance of a length of manganin wire. The resistance of the pressurised gauge was determined by measuring its ratio to an unpressurised standard resistance (also of manganin) using an REC

Precision Comparison Bridge, type VLF 51A.

The gauge consisted of about three meters of 40 SWG double silk covered wire wound loosely and non-inductively on a PTFE spool. A four lead system of connection was used to eliminate lead resistance effects and the two leads from the gauge were brought out through the gauge block by ceramic cone insulators. Before calibration the gauge was stabilised by subjecting it to temperature and pressure cycles. Three temperature cycles were carried out each of which consisted of a three hour soak in a dewar flask containing solid carbon dioxide, following by a three hour soak in an oven at 120°C. The gauge was then held at a pressure of about 1 GN m^{-2} for several hours and then allowed to stand overnight at atmospheric pressure. The pressure cycle was also carried out three times.

Calibration was carried out using the dead weight tester and the results of six calibrations are given in Table 5.3. Individual calibrations were similar and showed that the gauge characteristic was essentially linear for pressures of 100 MN m^{-2} and above, with a slight non-linearity (about 2 MN m^{-2}) between atmospheric pressure and 100 MN m^{-2}. Fig. 5.15 shows the results of two calibrations. The slope of the gauge characteristic did not show any systematic variation over the six tests but the gauge resistance at atmospheric pressure (R_o) was clearly subject to a regular increase of 0.033 ohms per month as shown in Fig. 5.16. Since R_o was measured before and after each pressurisation this was not a serious defect. The reason for the drift is not known but it is probably due to the constant immersion of the gauge in the pressurising fluid. The standard resistance remained unchanged throughout the tests.

Two equations were used to calculate pressures in the course of the work. The first equation,

$$P = 403.01 \times 10^6 (R - R_o - 0.0059) \qquad (5.1)$$

was derived from calibration number four only, and was used to obtain the calculated pressures in Table 5.4 for calibrations four and five. The maximum deviation over both calibrations is 0.77 MN m^{-2}, with the rest of the deviations 0.55 MN m^{-2} or less. This equation was used to calculate pressures during the measurements of 1-bromopentane, benzene, carbon tetrachloride, bromododecane, bromooctane, 1,3-dichlorobenzene, and 1,2-dichlorobenzene. The second equation,

$$P = 402.6098 \times 10^6 (R - R_o - 0.0054) \qquad (5.2)$$

was used for all other pressure measurements and was derived from the mean change in resistance at each pressure over all six calibrations. Pressure calculations by the second equation are given in Table 5.3; in this case the maximum deviation is 0.61 MN m^{-2} with the rest 0.46 MN m^{-2} or less.

Accuracy of pressure measurement is assessed as follows:

1 The largest source of error is due to random deviations which occur in the measurement of resistance change. The origin of these has not been positively identified but they appear at all pressures and in each calibration with a standard deviation from the mean of 0.0013 ohms. The corresponding errors in pressure are 0.52 MN m^{-2}.

2 Accuracy of the equations in representing the true gauge characteristic is difficult to assess without a large number of data (because of the superimposed random errors), but the standard deviation in pressure between 100 and 500 MN m^{-2} is 0.33 MN m^{-2}, and

between 100 and 700 MN m^{-2} it is 0.37 MN m^{-2}. While errors due to the form of the equation will clearly be systematic, these values, which are derived from the calculated values given in Table 5.3, provide an overestimate of probable errors from this source.

3 Instrumental and temperature errors are comparatively low. The stated accuracy of the bridge measurement of resistance ratio is 1 in 10^5 for resistance ratios up to 1.1, but for the low ratios used in these experiments, 1.0125, the accuracy is estimated to be 2 in 10^6. Resistance errors, therefore, amount to 0.0002 ohms giving 0.08 MN m^{-2} in pressure. Both gauge and standard resistance were kept as close together as possible and were isolated from stray temperature fluctuations of the room. The maximum temperature difference between the two was less than 0.2°C. Gauge resistance is given by

$$R_G = \frac{X\, R_S(1 + \alpha_E\, T_S)}{(1 + \alpha_E\, T_G)}$$

assuming that the temperature coefficient of resistance does not change with pressure. For pressures up to 500 MN m^{-2} the ratio X

$$1 \leq X \leq 1.0125,$$

and at 25°C the temperature coefficient of resistance of manganin is about 10^{-5} per degree centigrade. The maximum error in resistance is therefore 0.0002 ohms and in pressure 0.08 MN m^{-2}.

4 Uncertainty in dead weight tester pressures was 0.08 MN m^{-2}.

5 If the pressure equation based on all six calibrations is taken to be accurate then the first equation used is subject to systematic errors ranging from -0.10 MN m^{-2} (ie 0.10 MN m^{-2} too low) at 100 MN m^{-2}, to +0.30 MN m^{-2} at 500 MN m^{-2}.

If these errors are applied, however, the errors given in Section 2 should be reduced by a similar amount.

The total errors in pressure from sources 1 to 4 are therefore ± 1.09 MN m^{-2}. This figure is a slight overestimate of the maximum error because the random errors in resistance measurement were observed errors and consequently include the effects of minor temperature differences and probably also the effects of minor bridge balancing errors. The accuracy of measurement from 100 to 500 MN m^{-2} is therefore estimated to be ± 1.00 MN m^{-2}.

For pressures above 700 MN m^{-2} the gauge calibration must be extrapolated. The additional errors incurred then arise from the gauge characteristic which, in the 100 to 700 MN m^{-2} region, is taken to be linear to within ± 0.37 MN m^{2}. Assuming that the non linearity of the gauge does not increase beyond this value, the additional error at 1000 MN m^{-2} is also approximately equal to 0.37 MN m^{-2}. The accuracy of measurement for the higher pressure region therefore ranges from ± 1.00 MN m^{-2} at 500 MN m^{-2} to ± 1.37 MN m^{-2} at 1000 MN m^{-2}. The non-linearity of manganim pressure gauges is discussed by Deaker et al (1972).

T A B L E 5.1

MEASURED DENSITIES OF WATER

Temperature (^{o}C)	Pressure (MN m^{-2})	Density measured (kg m^{-3})	Density from Grindley and Lind (kg m^{-3})	Deviation (%)
25	100	1038.1	1038.0	+0.01
	200	1072.3	1072.1	+0.02
	300	1101.2	1101.4	-0.02
	400	1126.0	1127.1	-0.10
	500	1147.4	1150.1	-0.24
40	100	1030.9	1032.1	-0.12
	200	1064.0	1065.4	-0.13
	300	1092.5	1094.2	-0.16
	400	1117.4	1119.6	-0.20
	500	1139.3	1142.3	-0.26
60	100	1020.6	1022.7	-0.21
	200	1052.8	1055.7	-0.27
	300	1080.8	1084.2	-0.31
	400	1105.4	1109.4	-0.36
	500	1127.1	1132.0	-0.43
75	100	1013.8	1014.7	-0.09
	200	1047.2	1047.8	-0.06
	300	1076.3	1076.3	0.00
	400	1101.8	1101.6	+0.02
	500	1124.3	1124.2	+0.01

TABLE 5.2

INTERPOLATED AND EXTRAPOLATED DENSITIES OF WATER BASED ON MEASUREMENTS AT 25 AND 75°C ONLY

Temperature (°C)	Pressure (MN m^{-2})	Interpolated or extrapolated density (kg m^{-3})	Density from Grindley and Lind (kg m^{-3})	Deviations (%)
50	100	1025.9	1027.5	-0.16
	200	1059.8	1060.7	-0.08
	300	1088.8	1089.3	-0.04
	400	1113.9	1114.5	-0.05
	500	1135.9	1137.2	-0.11
100	100	1001.6	999.9	+0.17
	200	1034.7	1033.8	+0.09
	300	1063.8	1062.8	+0.09
	400	1089.7	1088.4	+0.12
	500	1112.8	1111.2	+0.14

TABLE 5.3

PRESSURE GAUGE CALIBRATION MEASUREMENTS

Pressure ($MN\ m^{-2}$)	Resistance Change, $R - R_o$ (Ω) For calibration number						Mean $R - R_o$ (Ω)	Calculated pressure ($MN\ m^{-2}$)	Difference ($MN\ m^{-2}$)
	1	2	3	4	5	6			
100	0.2532	0.2536	0.2505	0.2535	0.2548	0.2507	0.2527	99.55	-0.45
200	0.5043	0.5034	0.5016	0.5020	0.5018	0.5024	0.5026	200.16	+0.16
300	0.7532	0.7522	0.7505	0.7506	0.7500	0.7521	0.7514	300.33	+0.33
400	1.0014	1.0010	0.9987	0.9998	0.9976	1.0018	1.0001	400.46	+0.46
500	-	-	-	1.2464	1.2461	1.2487	1.2471	499.90	-0.10
600	-	-	-	1.4928	-	1.4956	1.4942	599.39	-0.61
700	-	-	-	-	-	1.7446	1.7446	700.20	+0.20

TABLE 5.4

PRESSURE GAUGE CALIBRATIONS 4 AND 5

Calibration	Pressure ($MN\ m^{-2}$)	Calculated pressure ($MN\ m^{-2}$)	Difference ($MN\ m^{-2}$)
4	100	99.79	-0.21
4	200	199.93	-0.07
4	300	300.12	+0.12
4	400	400.55	+0.55
4	500	499.93	-0.07
4	600	599.23	-0.77
5	100	100.31	+0.31
5	200	199.85	-0.15
5	300	299.88	-0.12
5	400	399.66	-0.34
5	500	499.81	-0.19

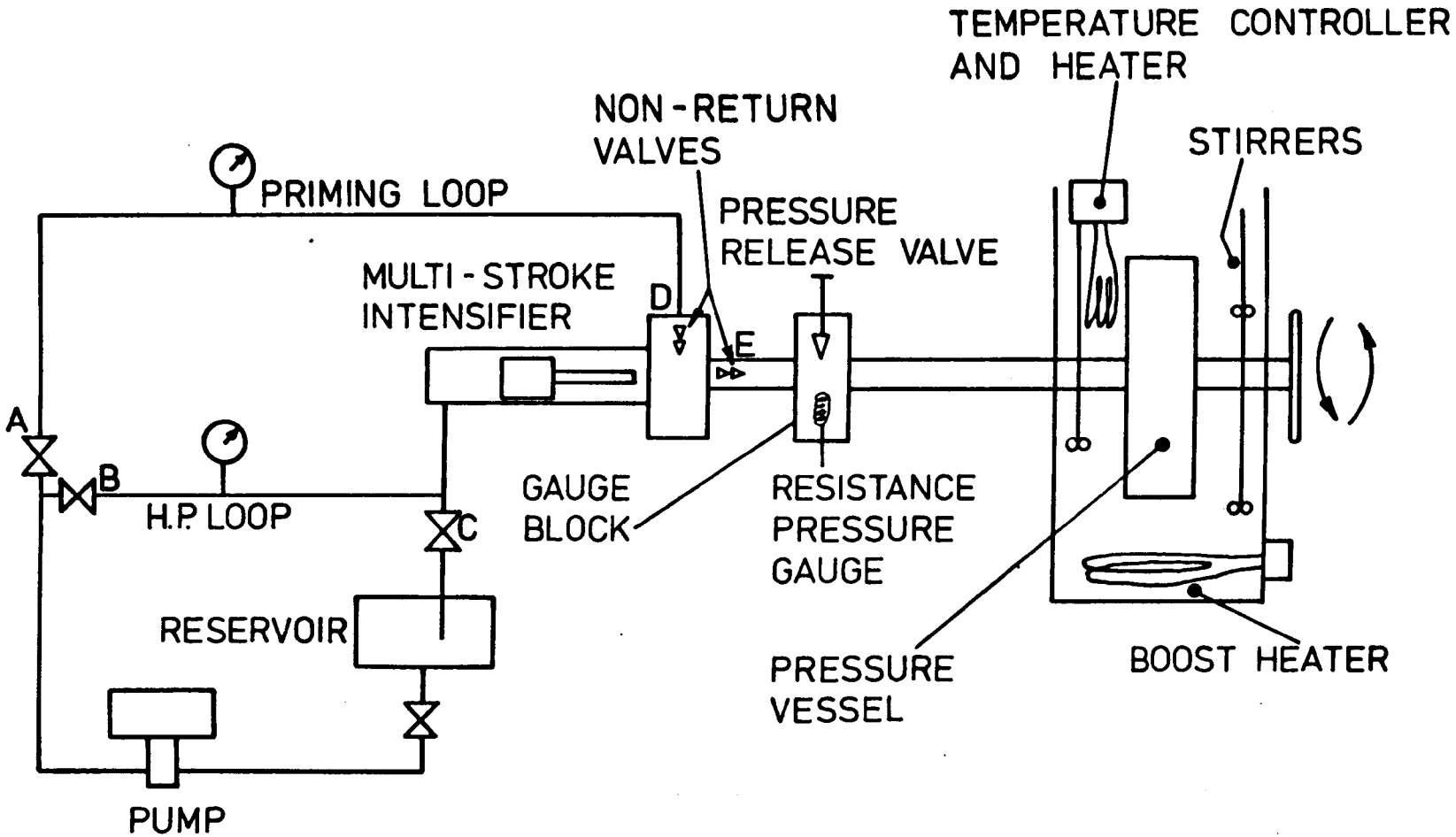

FIG 5.1 PRESSURISING SYSTEM

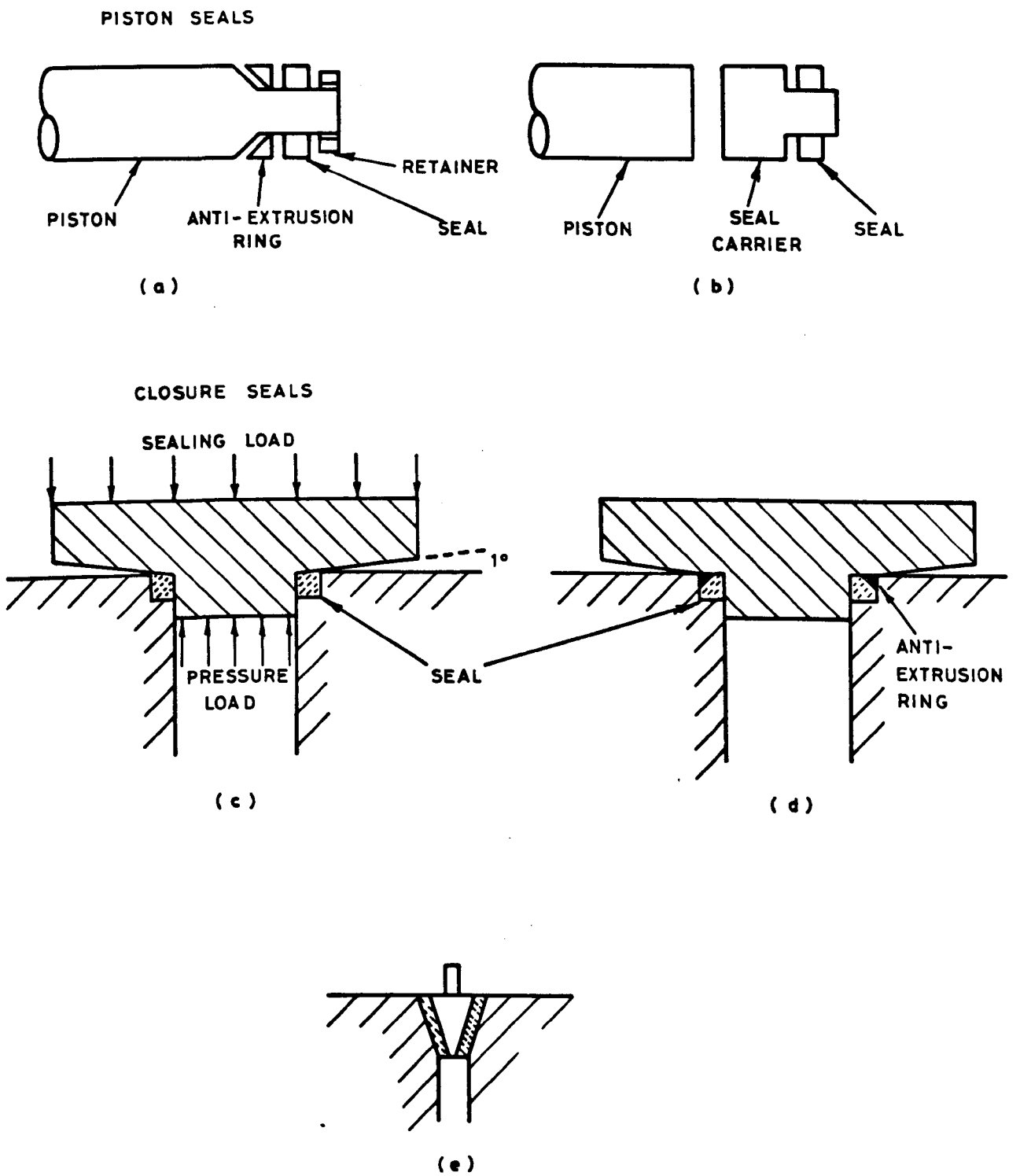
PISTON SEALS
RETAINER
PISTON
ANTI-EXTRUSION RING
SEAL
(a)
PISTON
SEAL CARRIER
SEAL
(b)
CLOSURE SEALS
SEALING LOAD
1°
PRESSURE LOAD
SEAL
(c)
ANTI-EXTRUSION RING
(d)
(e)

FIG 5.2 SEALS

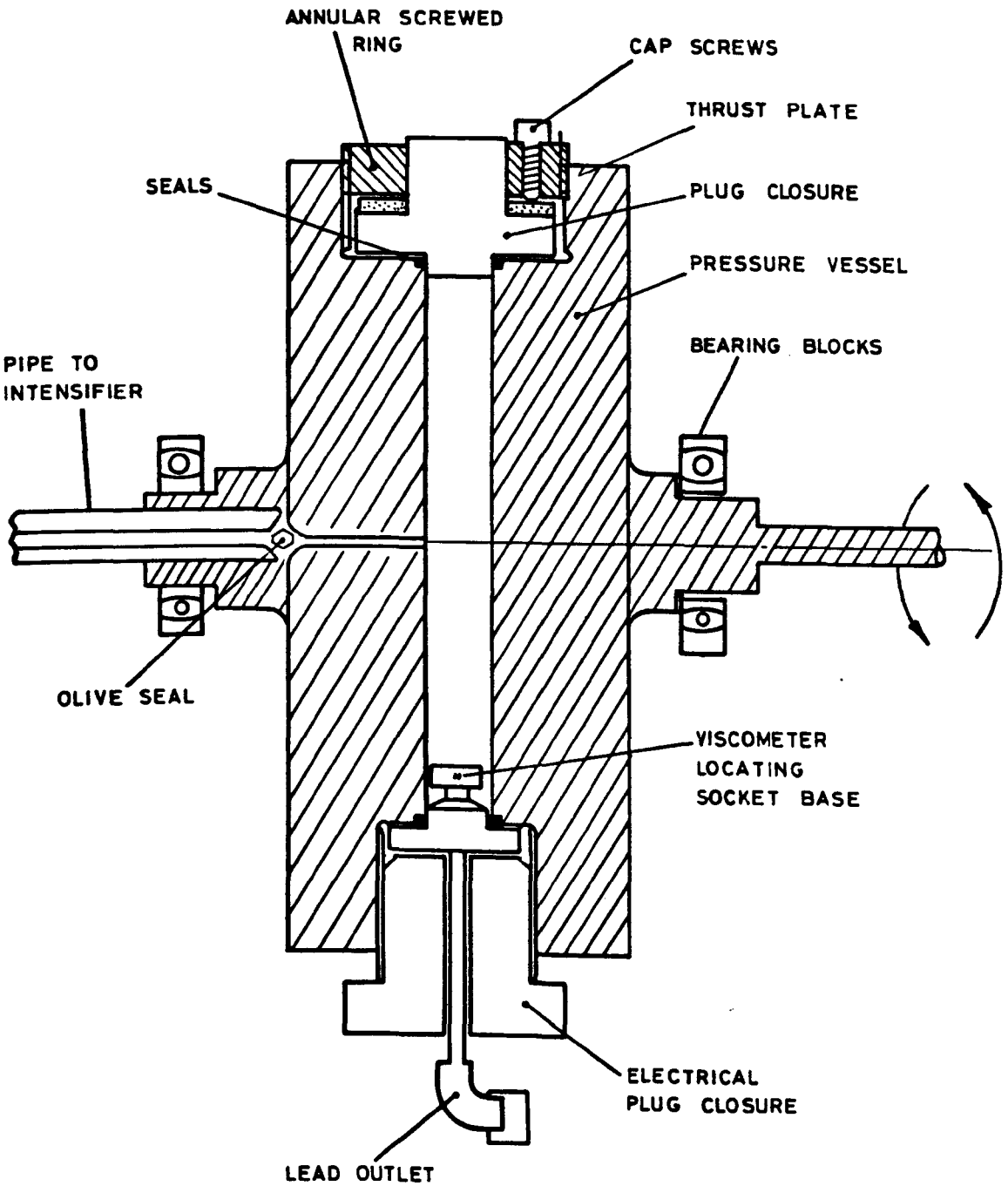

FIG 5.3 HIGH PRESSURE VESSEL

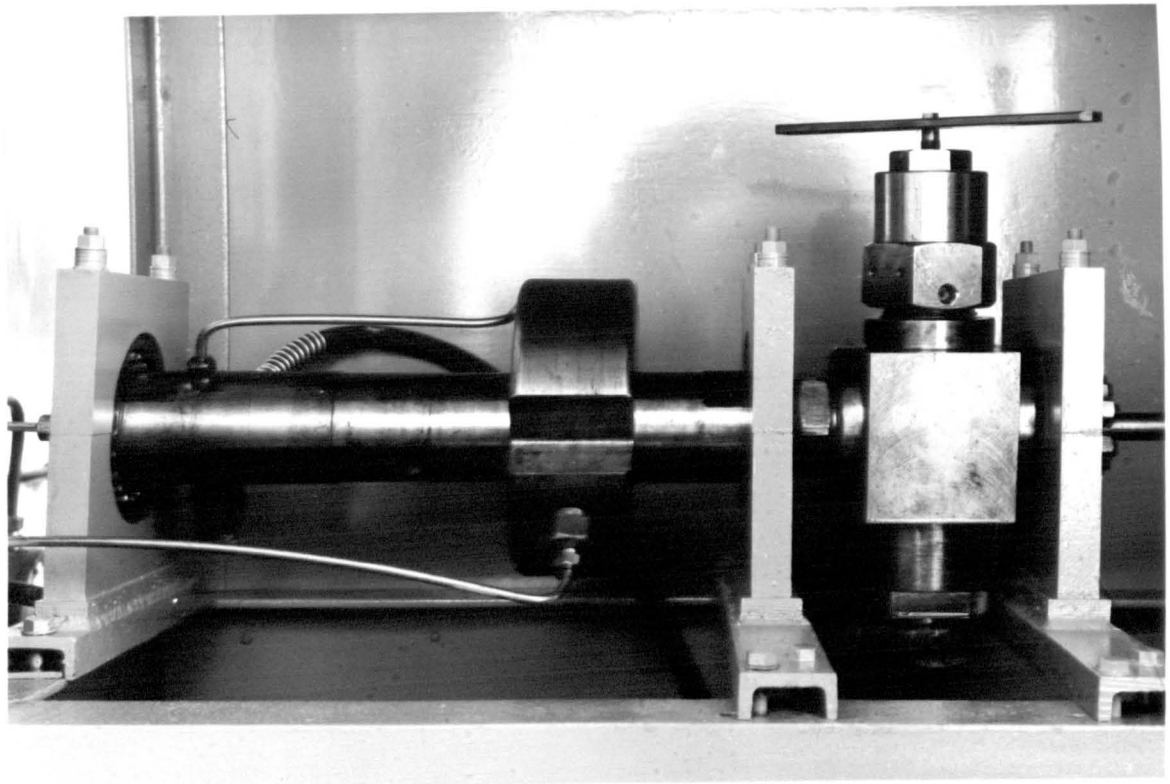

FIG 5.4 INTENSIFIER AND GAUGE BLOCK

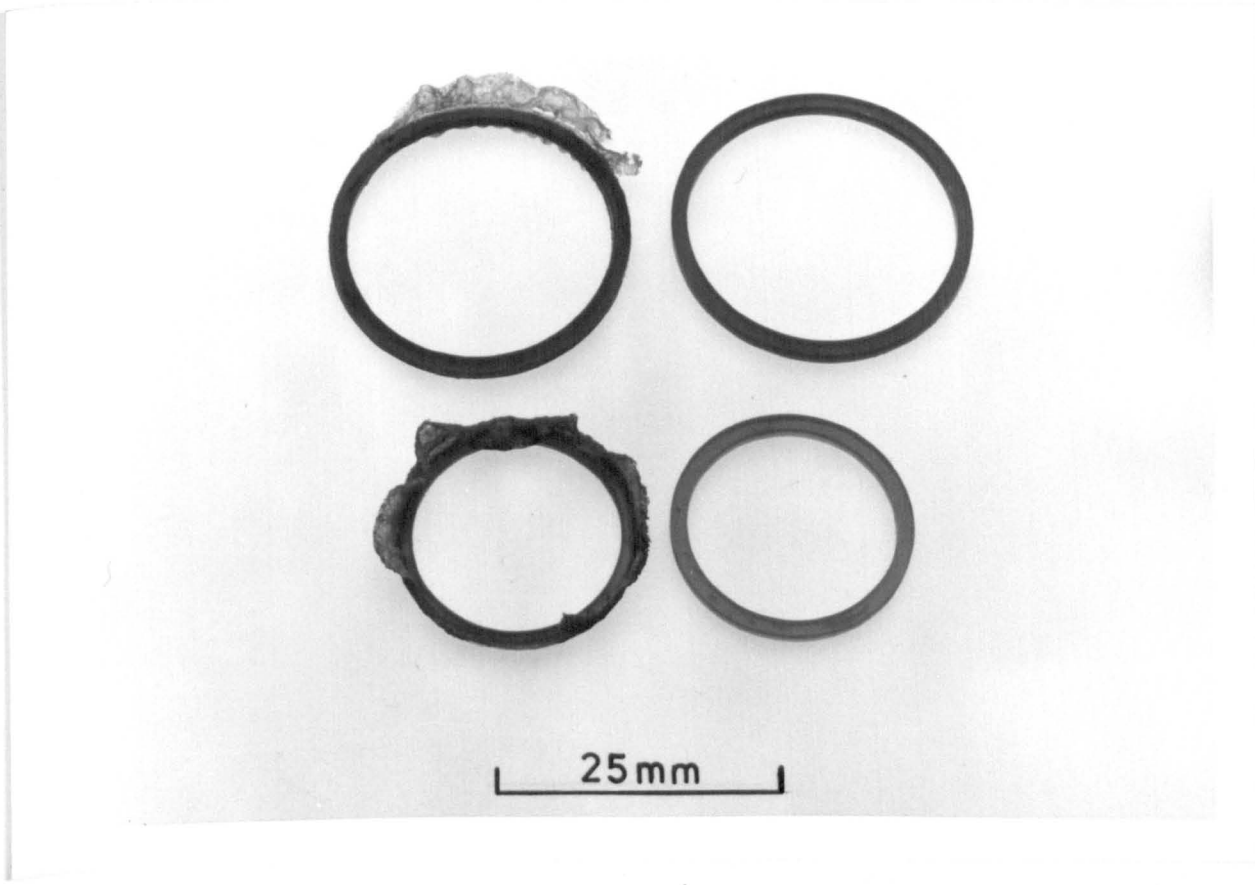

FIG 5-5 EXTRUDED SEALS

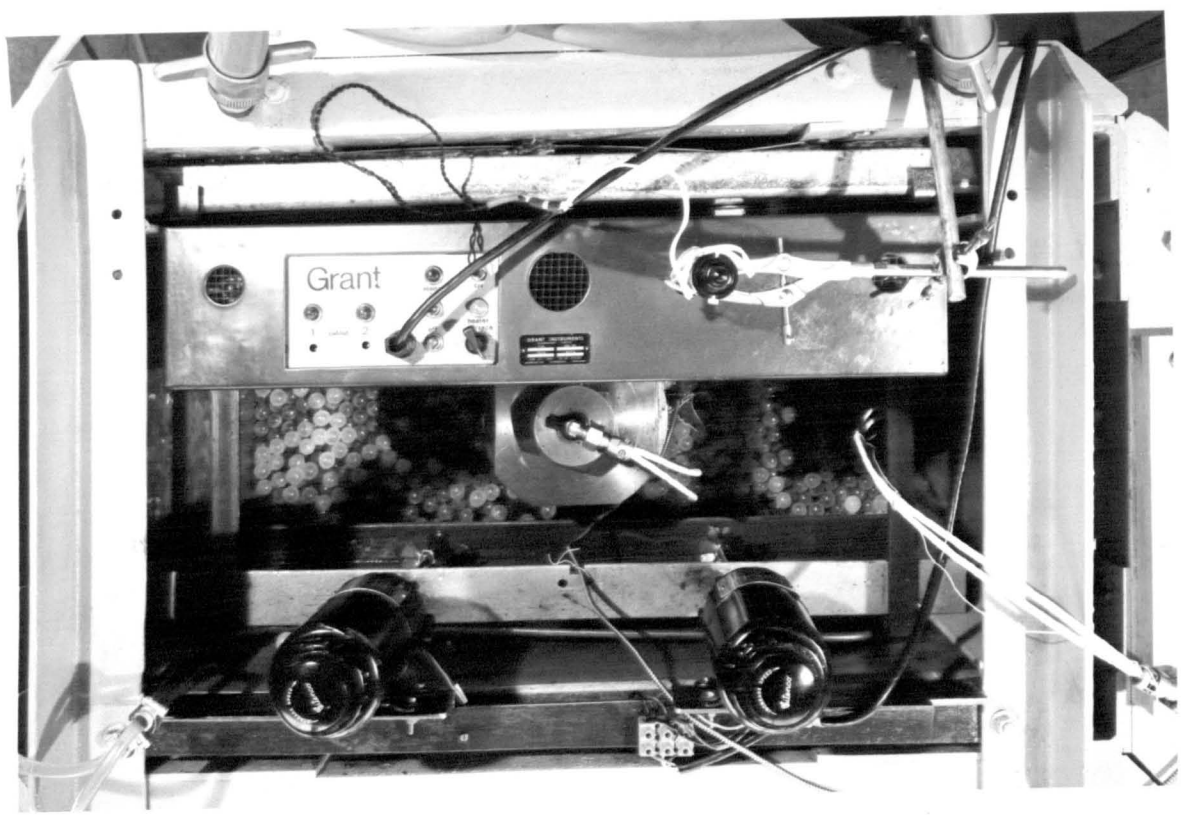

FIG 5·6 TOP VIEW OF TEMPERATURE BATH

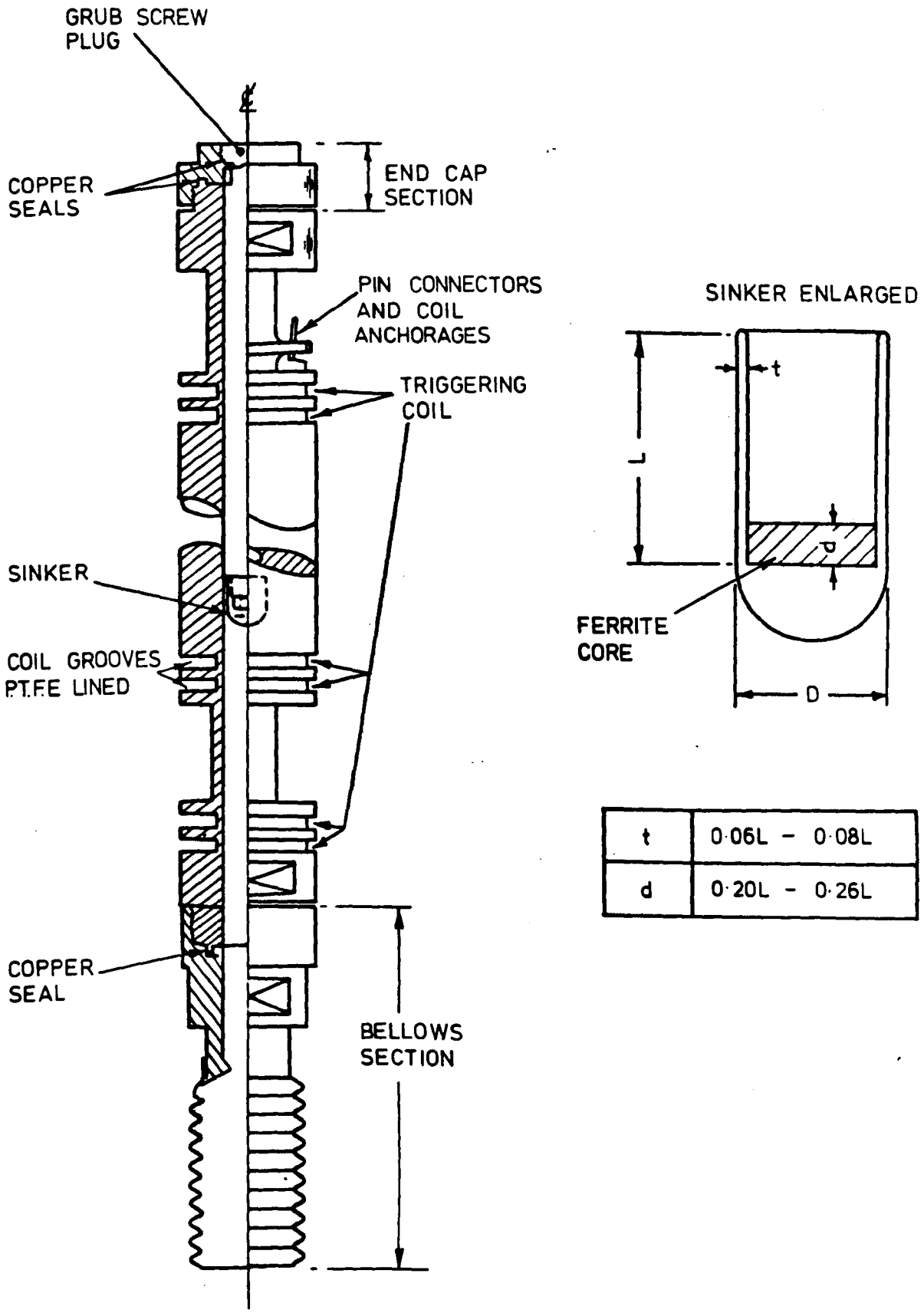

t	0·06L – 0·08L
d	0·20L – 0·26L

FIG 5.7 VISCOMETER TUBE

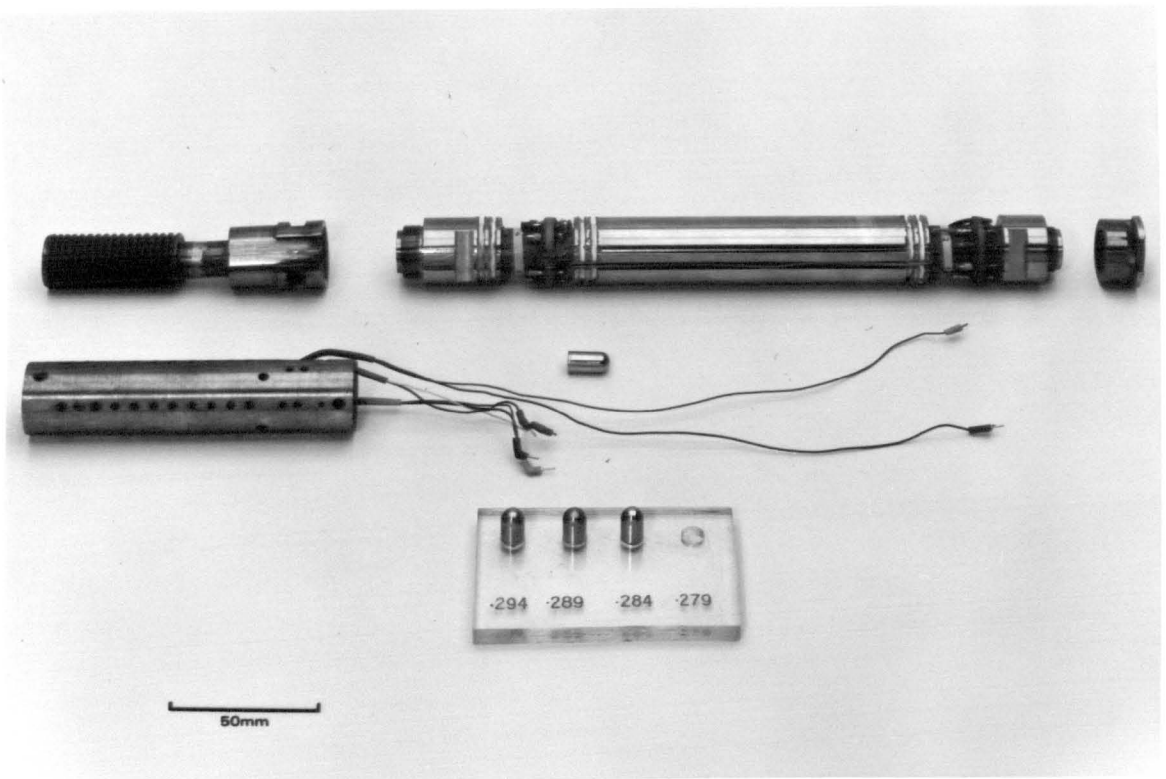

FIG 5·8 VISCOMETER PARTS BEFORE ASSEMBLY

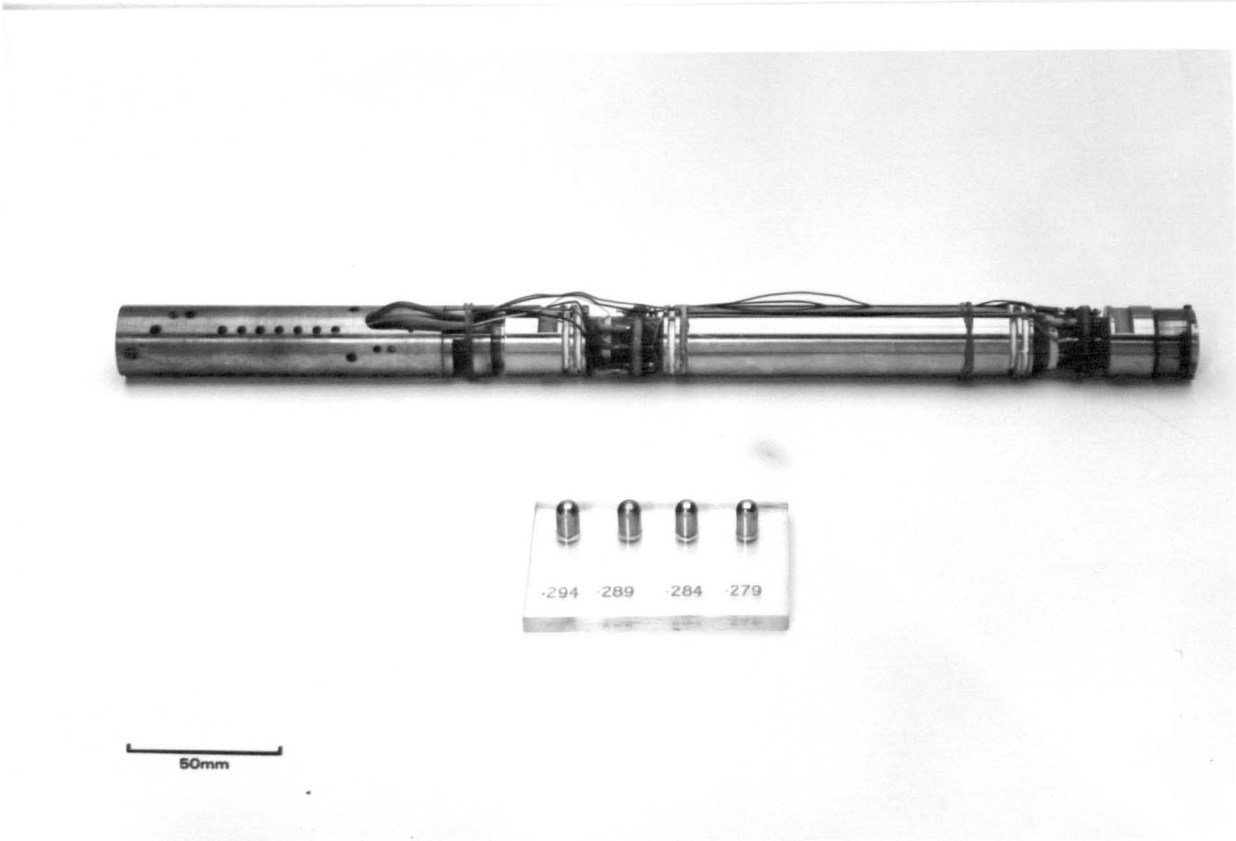

FIG 5·9 ASSEMBLED VISCOMETER

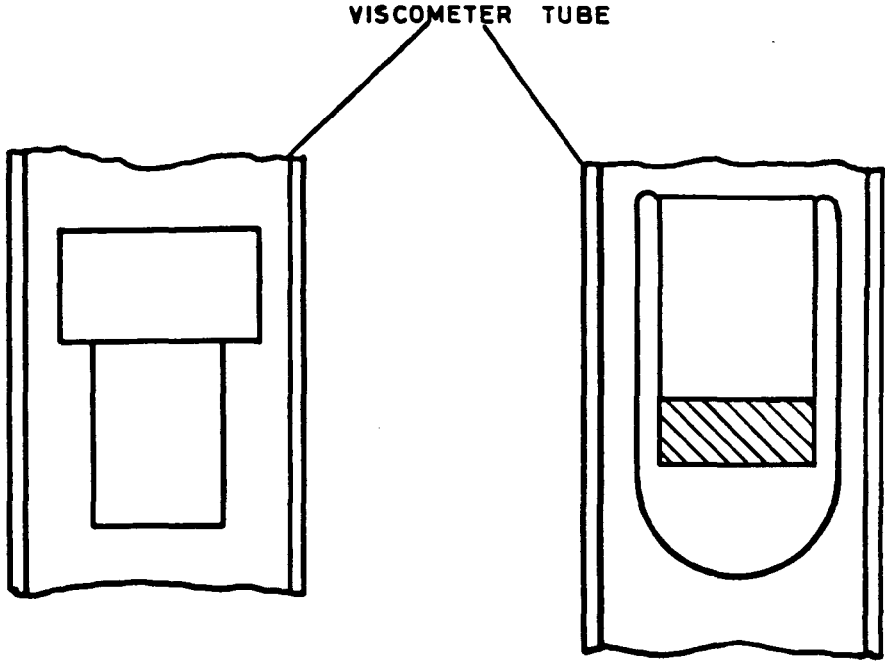

FIG 5.10 SINKERS

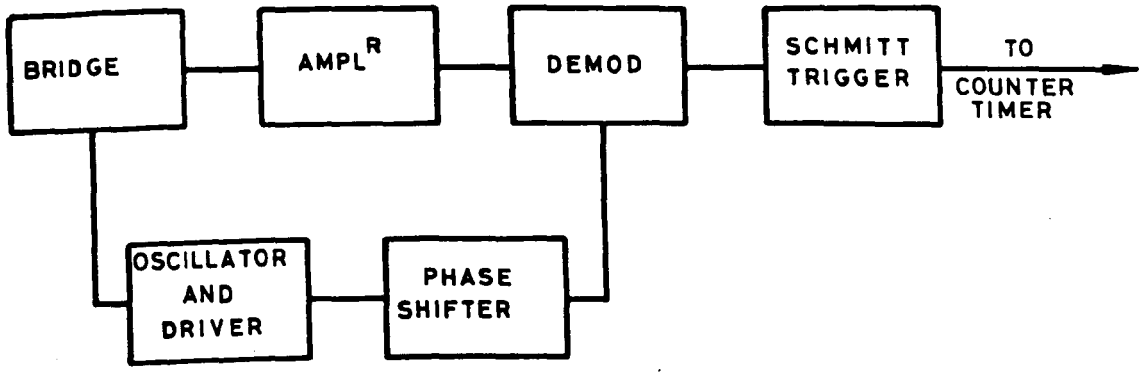

FIG 5.11 BLOCK DIAGRAM OF BRIDGE CIRCUIT

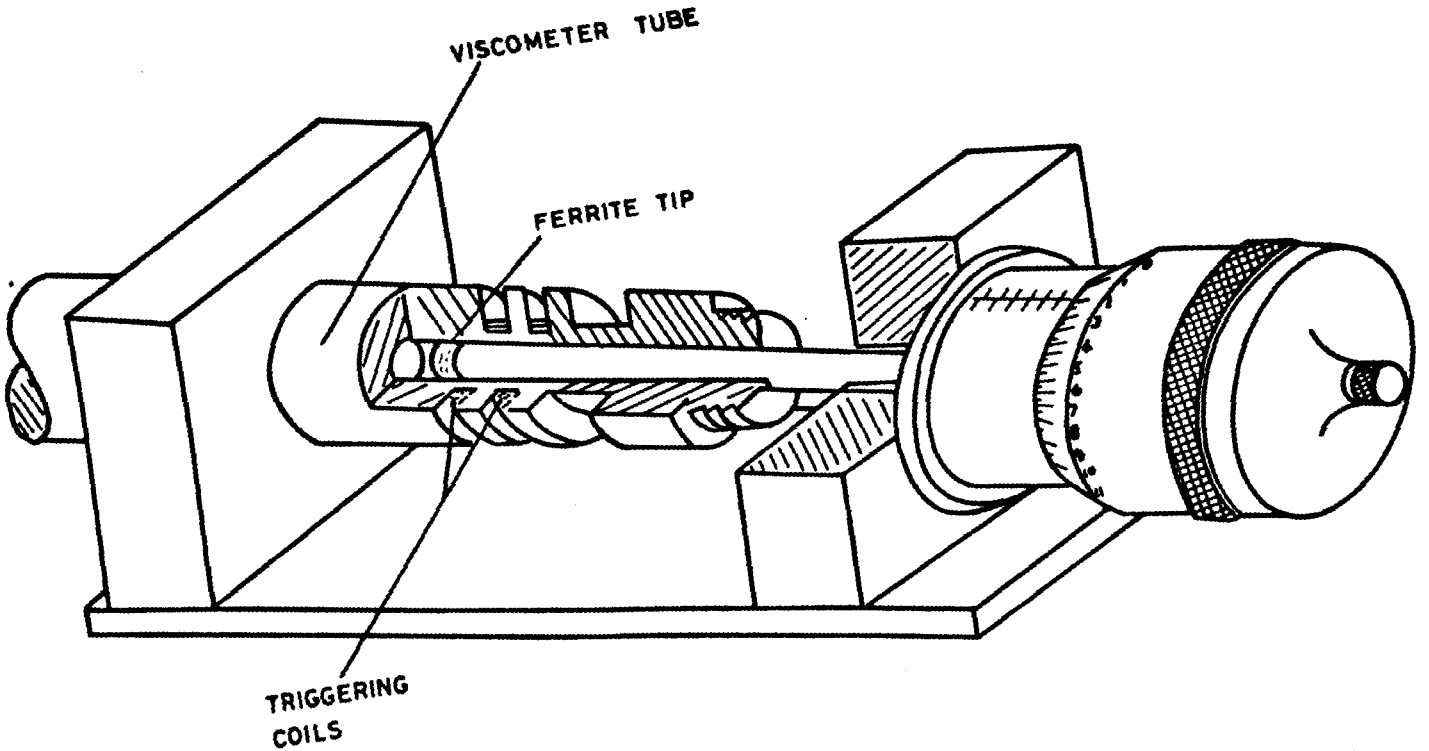

FIG 5.12 COIL TEST RIG

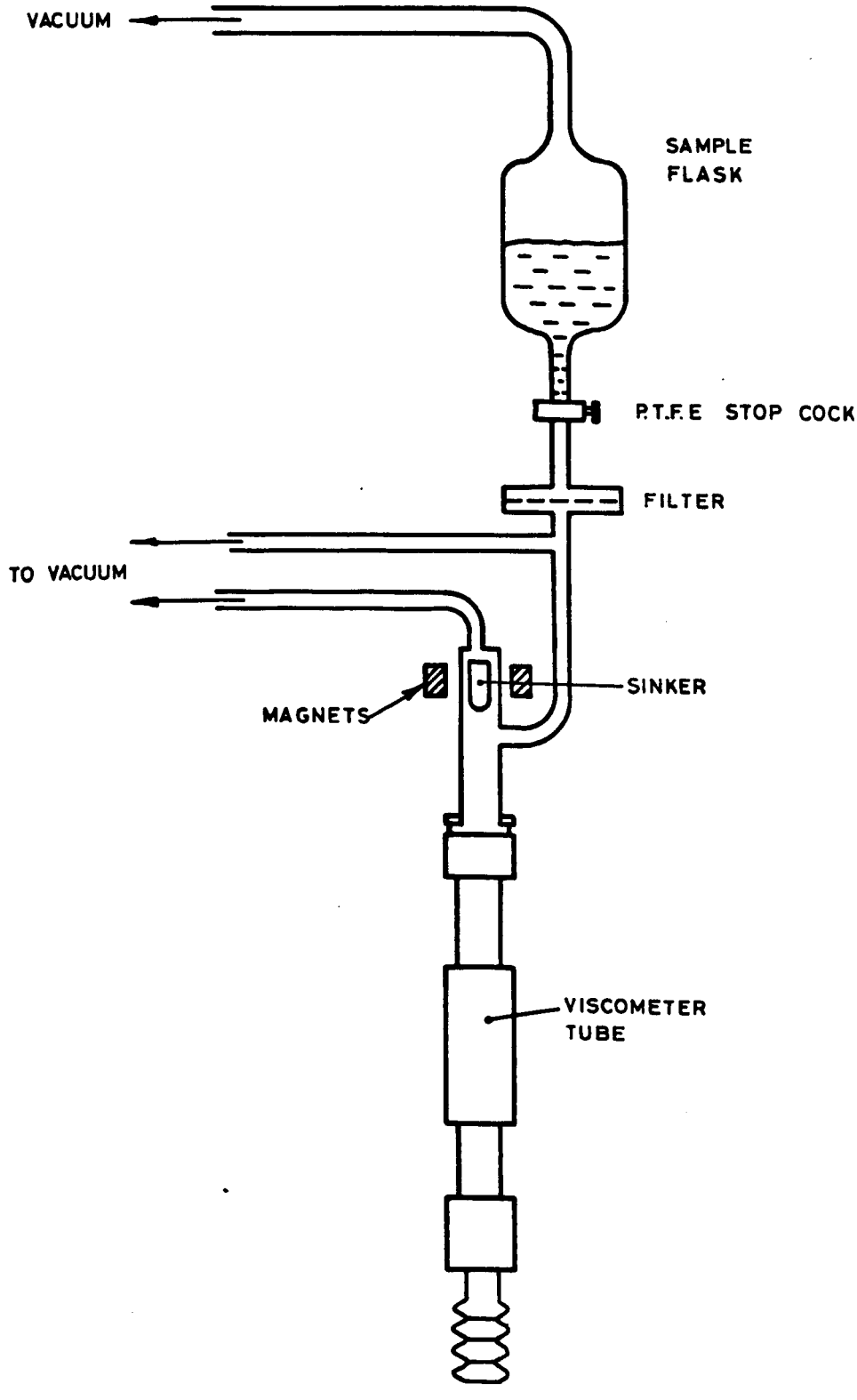

FIG 5.13 FILLING ASSEMBLY

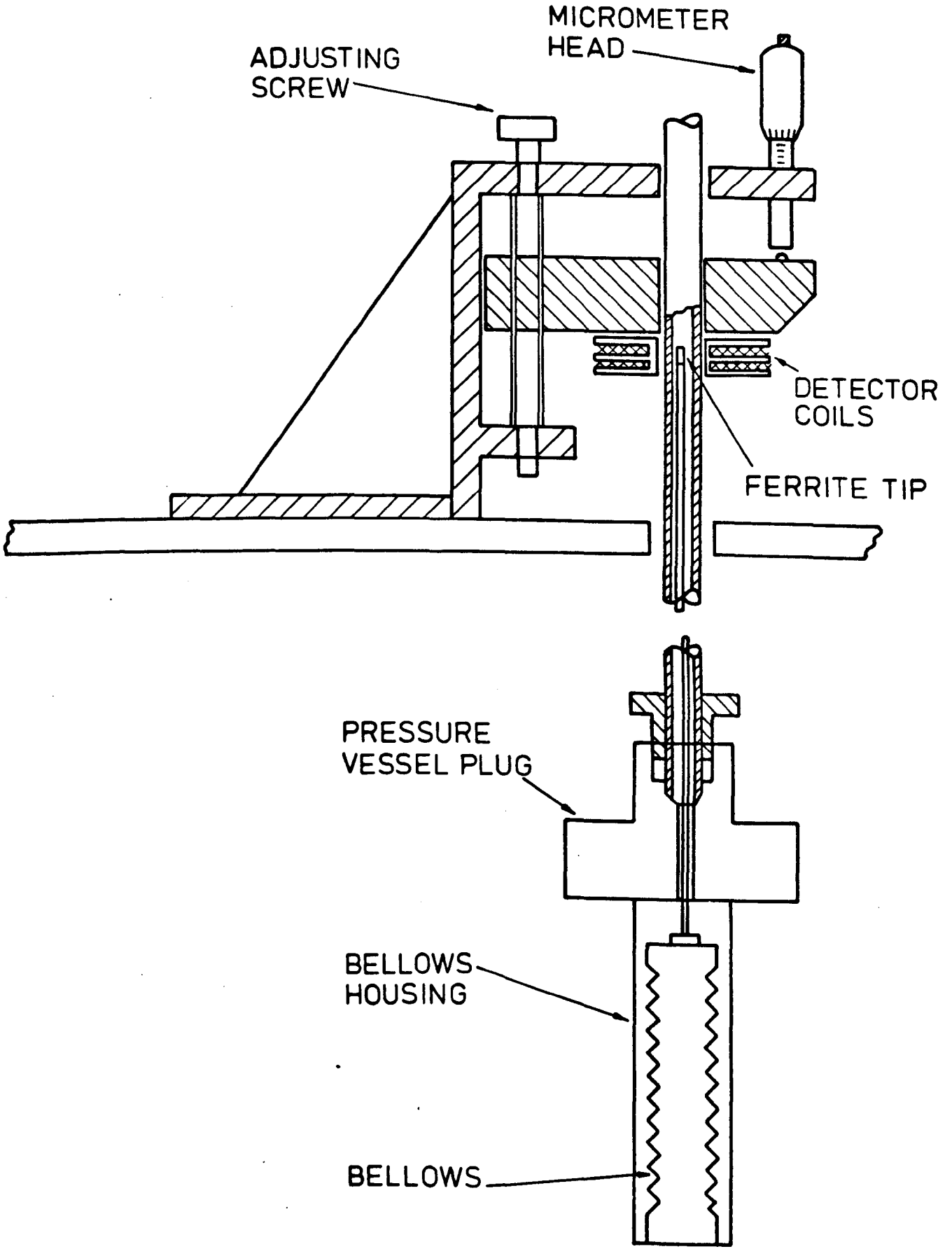

FIG 5.14 DIAGRAM OF BELLOWS APPARATUS

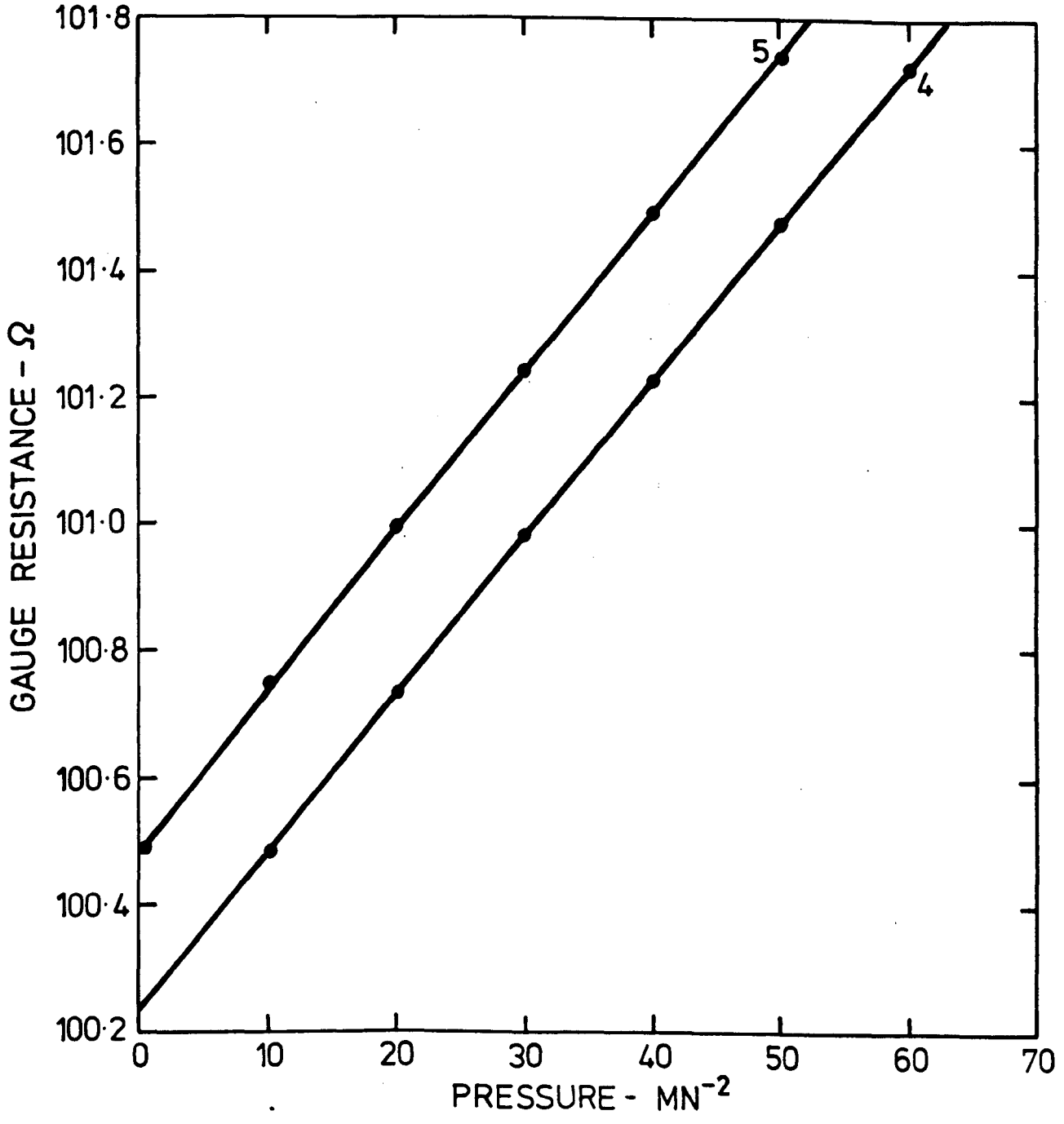

FIG 5.15 PRESSURE GAUGE CALIBRATION

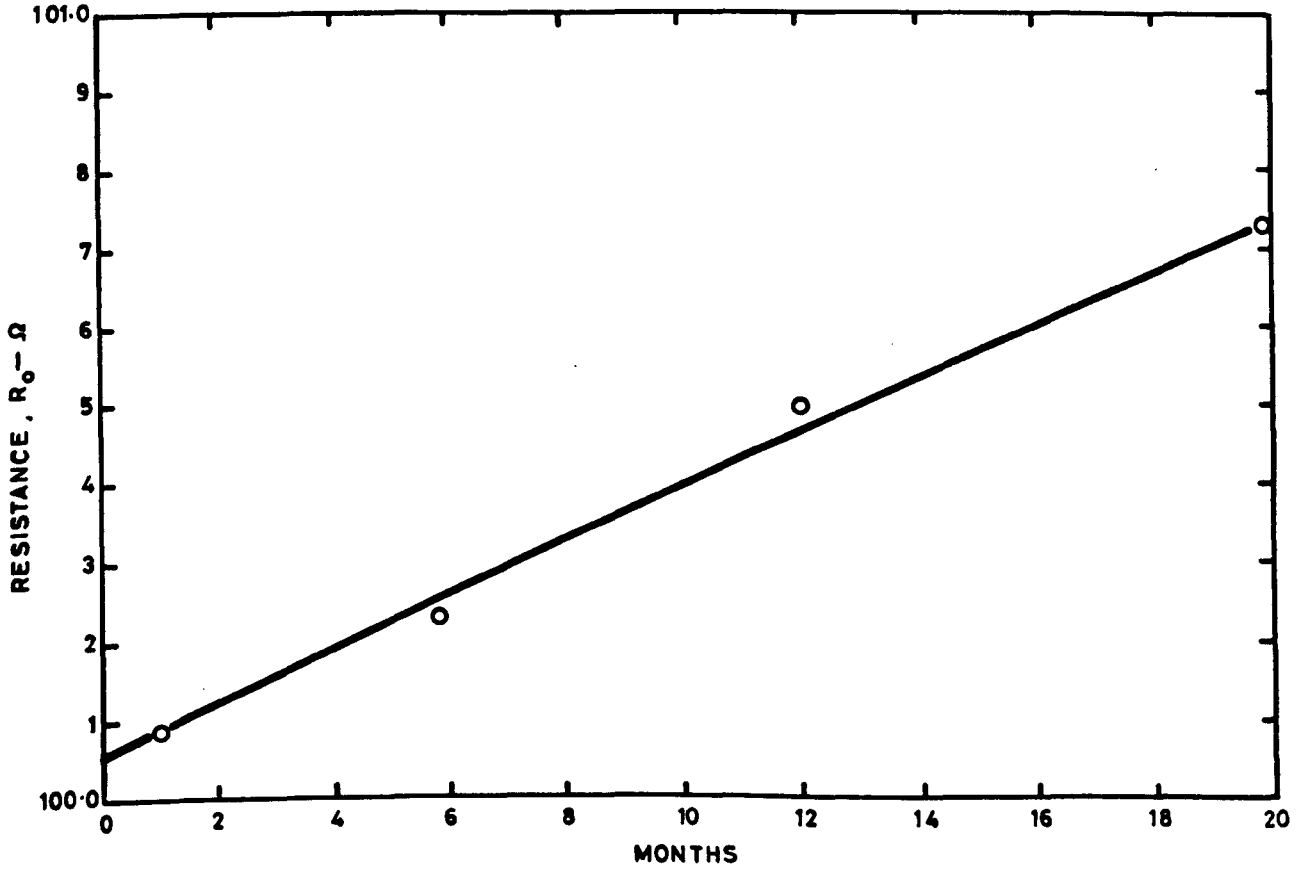

FIG 5.16 PRESSURE GAUGE RESISTANCE

CHAPTER 6

CALIBRATION AND PERFORMANCE OF VISCOMETER

SUMMARY OF CHAPTER 6

6 CALIBRATION AND PERFORMANCE OF VISCOMETER

Details of the calibration of the viscometer are given and the results are compared with theoretical viscometer constants. It is concluded that viscometers of this type could be considered for use as absolute instruments at low Reynolds numbers, since calculated and observed constants agree to within 2 per cent in this region.

The effect of turbulence is also examined and the results show that it does not become significant at the same value of Reynolds number for each sinker/tube combination, probably because of minor differences in surface finish.

Effects due to non-centring of sinkers were also examined but could only be detected for the sinker having the smallest diameter. Measurements indicated that this sinker had to travel a distance of 80 mm before it reached a central position.

CHAPTER 6 - CALIBRATION AND PERFORMANCE OF VISCOMETER

LIST OF TABLES

LIST OF FIGURES

6 CALIBRATION AND PERFORMANCE OF VISCOMETER

6.1 Viscometer Equations and Calibration

For a cylindrical body falling axially down the centre of a vertical circular tube with laminar flow, the equations governing the motion can be solved without much difficulty. However a number of different solutions have been published. The derivation given in Appendix II is believed to be correct and leads to the solution

$$\eta = \frac{Tmg(1 - \rho_L/\rho_S)}{2\pi L_S L_T}\left[\ln(r_2/r_1) - \frac{r_2^2 - r_1^2}{r_2^2 + r_1^2}\right] \qquad (6.1)$$

Equation 6.1 is identical with expressions derived by Lohrenz, Swift and Kurata (1960), and Irving (1972) for corresponding cases. The equation given by Bondi (1951) and attributed to Seeder (1940) is similar but has a factor of 1/2 multiplying the logarithmic terms, and takes the sum of the logarithmic term and the geometric term in parentheses. The equation given by Cappi (1964) is also similar, but additional numerical factors are introduced because of an incorrect transfer of axes occurring in this calculation of flow rate through the annulus.

A different form of equation was used in the ASME Pressure Viscosity Report (1953)

$$\eta = \frac{Tmg\, C_F(1 - \rho_L/\rho_S)}{6\pi L_S L_T}\left(\frac{r_2 - r_1}{r_2}\right)^3\left(\frac{r_2}{r_1}\right)^2\left[1 - \frac{1}{2}\frac{r_2 - r_1}{r_2} - \frac{13}{20}\frac{r_2 - r_1}{r_2}^2 \cdots\right]$$

where C_F is a form factor or calibration constant. The equations given above clearly allow viscosity to be calculated from the physical dimensions of the apparatus and the fall time and therefore the falling cylinder method can in principle be used as an absolute instrument in the same way as the conventional falling ball method. In deriving the equation, however, the influence of entry and exit effects has been neglected. A method of calculating end

effects for flat ended circular cylinders has been developed by Chen and Swift (1972) but this can only be applied to cylinders of length to diameter ratios less than six. Falling cylinder viscometers are therefore usually calibrated with liquids of known viscosity and, even if end effects are assumed to be small, the radii of sinker and tube must be measured to a high degree of accuracy and must be uniform throughout their length.

For a particular instrument with tube and sinker of the same material operating at some temperature t and pressure P, equation (6.1) can be reduced to

$$\eta = \frac{T(1 - \rho_l/\rho_s)}{A[1 + 2\alpha(t - t_o)](1 - 2/3\beta P)} \qquad (6.2)$$

The viscometers used here were calibrated by taking fall time measurements in liquids of accurately known viscosity, at atmospheric pressure and at different temperatures. For low viscosities, water and benzene were used, and in both cases viscosity and density values were taken from API 44 (1969). The water was freshly distilled and the benzene BDH Electronic grade. For higher viscosities a series of mineral oils were measured in U-tube viscometers by the method described in British Standard 188 : 1957. These viscometers were calibrated relative to water by the standard method at NPL, that is by the step up procedure, and gave viscosity values estimated to be accurate to ±0.5 per cent.. The densities of the oils were measured in graduated bicapillary pycnometers and are accurate to ±0.05 per cent. The oil samples were kept in tightly sealed bottles until ready for use. Measured values of the oil properties are given in Table 6.1.

Fig. 6.1 shows the calibration constants obtained plotted against Reynolds number, and illustrates the range of values which were obtained and their relative constancy for different flow conditions. The values were not constant, however, and are more conveniently examined using the theoretical constant, A, calculated from the sinker and tube dimensions using equation 6.2. For these calculations the sinker length was taken to be the length of the parallel section only: no allowance was made for the hemispherical nose. The ratio of theoretical constant to experimental constant is shown on Fig. 6.2, plotted against Reynolds number. The values of this ratio range from 0.95 at high Reynolds numbers to 1.02 at low, a total spread of only 7 per cent. At low Reynolds numbers the experimental constants tend quite closely to the theoretical ones giving values less than 2 per cent low at the highest calibration viscosity in each case.

6.2 Effects of Turbulence

The higher values of calibration constant at high Reynolds numbers encountered in the previous section are due to a transition from laminar to turbulent flow. Several definitions of Reynolds number have been used. Lohrenz (1960) gave the definition

$$Re = De \frac{v\rho}{\eta}$$

where De is an equivalent diameter defined by

$$De = 2\sqrt{2}\, r_1 \left[\ln r_2/r_1 - \frac{r_2^2 - r_1^2}{r_2^2 + r_1^2} \right]^{1/2}$$

Lohrenz, Swift and Kurata (1960) used identical expressions except that the $\sqrt{2}$ was omitted in the definition of equivalent diameter. Chen and Swift (1972) used the expression

$$Re = 2r_2 \frac{V\rho}{\eta}$$

Another definition is given by Prengle and Rothfus (1955) in their study of transition phenomena in annuli. They use for the equivalent diameter a value based on the diameter of the maximum fluid velocity and the tube bore. The equivalent diameter is defined by

$$De = \frac{r_2^2 - r_m^2}{r_2}$$

The expression for the radius of maximum velocity is derived in Appendix II and is given by

$$r_m^2 = \frac{1}{2}(r_2^2 + r_1^2)$$

$$\therefore \quad De = \frac{r_2^2 - r_1^2}{2r_2}$$

The special Reynolds number for annuli is then given by

$$Re = \frac{2De\,\bar{U}\rho}{\eta}$$

$$= \frac{r_2^2 - r_1^2}{r_2} \frac{\bar{U}\rho}{\eta}$$

and substituting for $\bar{U}$ gives

$$Re = \frac{r_1^2}{r_2} \frac{V\rho}{\eta}$$

In all of the above expressions the velocity referred to is expressed in terms of the terminal velocity of the sinker. For pipe flow the velocity term is of course the mean fluid velocity, and Bird, Stewart and Lightfoot (1960) give a definition for annular flow based on this parameter and the simple diametral clearance:

$$Re = \frac{2(r_2 - r_1)\bar{U}\rho}{\eta} \qquad (6.3)$$

Since the best definition is clearly a matter of controversy, equation 6.3 has been used in this work because it is directly related to the pipe flow definition. The mean fluid velocity in the annulus can be converted to the measured quantities as follows:

$$Q = \pi r_1^2 V$$

$$= \pi(r_2^2 - r_1^2)\bar{U}$$

$$\therefore \bar{U} = \frac{V r_1^2}{r_2^2 - r_1^2}$$

$$\therefore Re = \frac{2r_1^2}{(r_2 - r_1)} \frac{V\rho}{\eta} \qquad (6.4)$$

It is worth noting that the various definition may be interconverted by a factor which is related only to the radial dimensions of the instrument. Since Reynolds number is an expression of the relative magnitude of the inertial and viscous forces it is possible to derive, from the Navier Stokes equations, an appropriate ratio based on the geometry of the system. It has been shown by Cole (1957) that for journal and slider bearings the conventional Reynolds number should be multiplied by a modifying factor which takes the form of the ratio of a characteristic film thickness to a characteristic length. In the expressions given above the modifying factors are derived from the radial clearance and the sinker or tube radius. In the present experiments these quantities are of similar magnitude in each viscometer and do not account for the variation in transition Reynolds numbers observed. It is therefore concluded that slight differences in surface finish, circularity, and entry and exit geometry, have been of major importance, and that carefully controlled experiments covering a wide range of clearances, radii, and sinker lengths are necessary to

establish suitable modifying factors for the present design of sinker.

In practice it was convenient to fit the calibration results by equations of the form

$$A = A_o\left[1 + \frac{B}{T(1 - \rho_L/\rho_S)}\right]^N \qquad (6.5)$$

Calculated and experimental values of A are given in Table 6.2 and values of the constants for each viscometer are given in Table 6.3 along with the viscometer dimensions.

6.3 Effects of Eccentricity and Centring

The influence of eccentricity is clearly very important, particularly for viscometers employing self-centring sinkers, and has been investigated by Chen, Lescarboura and Swift (1968), Sabersky and Acosta (1964), Irving (1972) and Cappi (1964). Chen et al produced analytic solutions for cylindrical flat-ended sinkers of sinker to tube diameter ratios 0.8 to 0.99, by using bipolar coordinates. It was shown that shear stress in the annulus varied with angular position and therefore exerted a couple on the sinker. This couple was assumed to be balanced by the action of pins so that the axis of the sinker remained parallel to that of the tube. Approximate solutions for power law fluids were also given, and the theoretical results were later confirmed for Newtonian liquids by Lescarboura and Swift (1968). In his analysis of the eccentric case Cappi made the same incorrect transfer of axes mentioned previously.

The experiments of Irving are the most relevant to the present case since they relate eccentricity and its effect on fall time, to viscometer tube inclination for self-centring sinkers similar to those used in the present experiments. The three theoretical analyses, Chen,

Sabersky and Irving agree very closely, and predict a reduction in fall time of 42 per cent for an eccentricity ratio of 0.7. Irving's experiments show that for a viscometer of diameter ratio 0.928, the maximum reduction in fall time for a tube inclination of 1° is approximately 2 per cent. For viscometers of lower diameter ratio the effect is even less. The inclination of the viscometer tube was measured several times in course of the present work, by placing an inclinometer on the top face of the pressure vessel after carefully cleaning the surface. In all cases the measurements indicated that the tube was within 30 seconds of arc of the vertical, in two planes, and the readings did not vary by more than a few seconds throughout the experiment.

Hemispherically nosed sinkers were found to be self-centring provided the centre of gravity of the sinker was below the centre of action of the viscous forces, that is below the centre of the cylindrical section. The distance they had to travel to become concentric with the tube was investigated in the following tests.

With the sinker initially at the bottom of the tube and the tube oriented in the measuring direction, the vessel was inverted and the sinker allowed to fall backwards, that is with the open and leading, through the two pairs of coils. When it triggered the timing circuit at the second pair of coils, a stopwatch was started and the sinker allowed to continue falling for a preselected delay time. When that time was reached the tube was quickly inverted and a fall time taken with the sinker moving in the forward direction, that is with the spherical end leading. The procedure was then repeated with longer delay times until fall times in the forward direction were stable within ± 0.2 per cent.

The delay in centring was observed only for the sinker/tube combination of diameter ratio K = 0.9586. For higher values of K centring occurred too rapidly to be observed in the present apparatus.

Delay time was converted to distance using the ratio of sinker velocity in the forward direction to that in the backwards direction, and the stable forward velocity. When the forward fall time was stable the velocity ratio was found experimentally to be 0.46 for all sinkers studied. This value is slightly higher than that predicted by Irving (1972) and by Chen (1968) for the ratio of concentric to eccentric sinker velocity, probably because of tilting of the sinker axis and friction between sinker and tube wall while the sinker was falling in the backwards direction.

The results of these tests are shown in Fig. 6.3 where the ratio of eccentric to concentric fall time in the forward direction is plotted against distance travelled by the sinker before it enters the measuring section of the viscometer tube. Since the eccentricity at the beginning of the sinker's movement is not fixed at any one value, the results are scattered; however the continuous line is a measure of the maximum value of the mean eccentricity, measured over the working section, which the sinker can have after travelling the distance stated. The figure therefore shows that an entry length of between 70 and 80 mm is required to guarantee concentric flow at a diameter ratio of 0.9586. Four liquids with viscosities between 5 and 220 mN s m^{-2} were used to obtain these results, but no significant viscosity effect was observed.

In experiments with unguided sinkers Harlow (1967) was unable to obtain reliable fall times, probably because the sinkers were designed to make measurements in either axial direction. The coincidence of the centres of gravity and of action of the viscous forces therefore inhibited the development of the self-centring action.

6.4 Effects of Temperature and Pressure

The effects of temperature and pressure on the performance of the viscometer can be easily calculated using Equation 6.1. Assuming a linear thermal expansion and compressibility and that these two properties are independent of pressure and temperature respectively, then equation 6.1 can be written

$$\eta = \frac{T\, mg(1 - \rho_l/\rho_s)}{2\pi L_s L_T[1 + 2\alpha(t - t_o)][1 - 2/3\beta(P - P_o)]}\left[\ln(r_2/r_1) - \frac{r_2^2 - r_1^2}{r_2^2 + r_1^2}\right]$$

where the linear dimensions now refer to values at the reference temperature t_o and atmospheric pressure P_o, and the sinker density has also been corrected for expansion and compression. For a reference temperature of 25°C the combined compression and thermal expansion correction factors to present viscometers at 100°C and 1000 MN m^{-2} amount to 0.9985, a correction of 0.15 per cent. At 500 MN m^{-2} and 100°C the temperature correction is 1.0025 and the pressure correction 0.9980 giving a combined correction factor of 1.0005, or 0.05 per cent viscosity. For a viscometer with sinker and tube of different materials the corrections to r_1 and r_2 do not cancel out and can lead to a large total correction. Since the corrections to the present viscometer are comparatively small the linear approximations assumed above will not lead to significant errors (Isdale, Spence, and Tudhope (1972)).

6.5 Accuracy

Errors in viscosity measurements arise partly from instrumental errors associated with the viscometer and partly from errors in temperature and pressure. Referring to equation 6.2 the errors are assessed as follows:

1 Relative errors in fall time appear directly as errors in viscosity.

The Hewlett Packard Counter 5223L used for measurement of time is estimated to be accurate to less than 1 in 10^5 so that errors from this source are very small. Each calculation was based on the mean of at least five consecutive measurements of fall time with a maximum deviation from the mean of 0.10 per cent. Viscosity errors are therefore estimated to be less than ±0.10 per cent.

2 The relative accuracy of the viscometer constant, A, is also translated directly to viscosity and is the largest source of error. Conversely the largest source of error in determining A is the uncertainty in determining the viscosity of the calibrating liquids. Viscometers one and three were calibrated with viscosities measured in U-tube viscometers and estimated to be accurate within ±0.5 per cent. Viscometer number two was calibrated using water and benzene with viscosities known to within 0.25 per cent. Additional errors from sinker density, liquid density, fall time and temperature measurement lead to expected maximum errors in A of ±0.92 per cent for viscometers one and three and ±0.67 per cent for viscometer number two. Most of the observed values of A agree with equation 6.5 to within these limits though there is a tendency for a few deviations to be greater in the transition region. To permit maximum errors to be estimated the accuracy of the viscometer constants are therefore set at ±1.0 per cent.

3 Errors due to liquid density are given by

$$\frac{\delta\eta}{\eta} = \frac{\delta\rho_L}{\rho_L} \frac{1}{1-\rho_S/\rho_L}$$

from equation 6.2. These errors clearly decrease with liquid

density and are greatest for the higher density liquids. The highest liquid density which occurred was 2012.6 kg m^{-3} for 1,5-dibromopentane at 25°C and 300 MN m^{-2}, and the sinker density in this case was 7604.4 kg m^{-3}. Allowing ±0.49 per cent for density measurement by the bellows method, therefore, gives a total maximum error of ±0.18 per cent.

4 Errors due to sinker density are similarly given by

$$\frac{\delta\eta}{\eta} = \frac{\delta\rho_s}{\rho_s} \frac{1}{\rho_s/\rho_L - 1}$$

Sinker densities were measured by water displacement in bubble pycnometers at 25°C, and are estimated to be accurate to ±1.0 per cent. For 1,5-dibromopentane as above the possible error in viscosity is therefore 0.36 per cent; however sinker densities are used in the calculation of the viscometer constants during calibration, and errors from this source are consequently reduced by a factor of about 0.4 or less when the measured constant is used for calculations.

5 Errors arising from temperature and pressure measurement also depend on the liquid being measured. The equation

$$\ln\eta = a + \frac{b}{t},$$

with t in °K, is sufficiently accurate at constant pressure to calculate temperature errors and gives

$$\frac{\delta\eta}{\eta} = -\frac{b}{t^2}\delta t .$$

The ice point of the quartz thermometer used for temperature measurement was checked regularly throughout the tests, and its accuracy over the full temperature range was checked by comparison with a platinum resistance thermometer. The accuracy of

measurement is estimated to be better than 0.01 K. Bath temperatures were stable to within ±0.02 K and the mean observed temperature is estimated to be within 0.01 K of the specimen temperature. The maximum error in temperature is therefore estimated to be ±0.02 K. Corresponding errors in viscosity range from ±0.02 to ±0.04 per cent at atmospheric pressure, and from ±0.04 to ±0.07 per cent at the highest pressures measured.

6 Over short pressure ranges at constant temperature viscosity may be expressed by the equation

$$\eta = \eta_0 e^{\alpha P}$$

which gives

$$\frac{\delta\eta}{\eta} = \alpha \delta P$$

For pressures between 100 and 500 MN m^{-2} δP is 1 MN m^{-2} which gives possible errors in viscosity ranging from 1.04 to 0.73 per cent for 1-bromododecane, bromocyclohexane, and chlorocyclohexane, and from 0.75 to 0.40 per cent for the other liquids except water.

Viscosities quoted at 50 MN m^{-2} are subject to larger errors because pressure gauge non linearity increases δP to about 2 MN m^{-2} and the pressure coefficient, α, is larger at lower pressures. For 1-bromododecane at 50 MN m^{-2} viscosity errors from pressure measurement are 2.70 per cent at 25°C and 2.02 per cent at 50°C; for the other liquids they are less than 1.82 per cent.

Since the viscosity of water varies comparatively little with pressure, the errors from pressure measurement are smaller in this case and reach a maximum of 0.12 per cent at 1000 MN m^{-2} and 25°C.

Clearly each measurement has a separate accuracy. However overall

working values may be obtained by summing the maximum contributions from the sources given above. This leads to expected accuracies of 1.46 per cent for water and less than 2.53 per cent for the other ten liquids at pressures of 100 MN m^{-2} and above.

These values may be significantly reduced by considering viscosity ratios only. Equations 6.1 and 6.2 then give

$$\frac{\eta}{\eta_o} = \left(\frac{T}{T_o}\right)\left[\frac{1 - \rho_L/\rho_S}{1 - \rho_{Lo}/\rho_{So}}\right]\left[\frac{1 + \left\{\frac{B}{T_o(1 - \rho_{Lo}/\rho_{So})}\right\}^N}{1 + \left\{\frac{B}{T(1 - \rho_L/\rho_S)}\right\}^N}\right] \qquad (6.6)$$

The errors in fall time ratio are not reduced significantly because systematic errors are small and the ratio itself is comparatively large. The second ratio in equation 6.6, however, lies between about 1.2 and 1.4, so that systematic errors occurring in this ratio will be reduced by a factor of about 0.4. Similarly the third ratio lies between about 1 and 1.05 so that systematic errors here should be reduced by a factor of 0.05. Errors in sinker density are therefore again reduced by a factor of 0.4. Approximately one-half the error in turbulence correction and one-quarter the error in liquid density are estimated to be systematic which gives expected accuracies in viscosity ratio of ±0.91 per cent for water and ±1.95 per cent for the other ten liquids at pressures of 100 MN m^{-2} and above.

Summaries of the performance of the viscometer and the results have already been published as NEL Reports. These are included in Appendix III.

TABLE 6.1

PROPERTIES OF CALIBRATION OILS

Oil No	Temperature (°C)	Kinematic viscosity		Density		Average dynamic viscosity	Average density
		1* ($m^2 s^{-1}$)	2* ($m^2 s^{-1}$)	1 ($kg\ m^{-3}$)	2 ($kg\ m^{-3}$)	($mNs\ m^{-2}$)	($kg\ m^{-3}$)
11	25	8.748	-	834.4	-	7.300	834.4
11	55	4.096	-	814.7	-	3.337	814.7
11	75	2.814	-	800.7	-	2.254	800.7
21	25	36.29	36.46	862.8	862.0	31.37	862.4
31	25	109.14	108.47	873.1	873.0	95.00	873.1
41	25	242.61	243.09	881.1	881.1	214.0	881.1
72	25	495.62	494.55	887.6	887.6	439.4	887.6
73	25	645.79	644.01	885.3	885.4	571.0	885.4
75	25	807.34	807.58	891.4	891.4	719.8	891.4
79	25	1357.2	1354.1	895.7	895.6	1214.0	895.6
21	75	6.443	6.440	830.1	830.3	5.348	830.2
79	75	76.58	-	866.0	-	66.32	866.0

*Measurements in columns labelled 1 and 2 were made using different U-tube viscometers or pycnometer bottles.

TABLE 6.2

MEASURED AND CALCULATED VISCOMETER CONSTANTS

Viscometer No	Calibration liquid	Temperature (°C)	Fall time (s)	Reynolds Number	Measured viscometer constant ($ms^2k\ g^{-1}$)	Calculated viscometer constant ($ms^2k\ g^{-1}$)	Difference (%)
1	11	25.01	313.50	13.72	38 190	37 900	+0.77
	11	55.99	142.10	64.66	37 930	37 900	+0.08
	11	74.99	96.59	138.5	38 240	37 902	+0.89
	water	25.10	38.52	1095.0	37 610	37 961	-0.92
	water	30.06	34.81	1352.0	37 960	37 991	-0.08
	benzene	25.01	25.92	2114.0	38 210	38 175	+0.09
	water	45.00	26.18	2388.0	38 140	38 183	-0.11
	benzene	45.01	20.76	3349.0	39 890	38 561	+3.45
	water	74.99	17.00	5708.0	39 090	39 480	-0.99
	benzene	70.00	15.82	5609.0	40 230	39 827	+1.01
2	water	24.99	32.10	1162.0	31 120	31 117	+0.01
	water	25.11	32.01	1168.0	31 120	31 118	+0.01
	water	29.99	28.71	1449.0	31 090	31 138	-0.15
	benzene	25.01	21.27	2278.0	31 170	31 258	-0.28
	water	55.00	18.28	3567.0	31 350	31 431	-0.26
	benzene	40.01	17.56	3318.0	31 570	31 460	+0.35
	benzene	60.02	14.07	5095.0	32 010	31 990	+0.06
	water	74.98	14.01	6136.0	32 030	32 089	-0.18

TABLE 6.2 (Contd)

Viscometer No	Calibration liquid	Temperature (°C)	Fall time (s)	Reynolds Number	Measured viscometer constant ($ms^2k\ g^{-1}$)	Calculated viscometer constant ($ms^2k\ g^{-1}$)	Difference (%)
3	72	25.01	1701.0	0.007	3 331	3 376	-1.32
	41	25.01	825.8	0.03	3 326	3 378	-1.52
	31	25.01	371.5	0.15	3 377	3 382	-0.14
	79	75.00	262.0	0.30	3 408	3 385	+0.68
	21	25.01	123.5	1.34	3 406	3 397	+0.25
	11	25.02	29.48	23.39	3 512	3 471	+1.17
	21	74.99	21.57	43.43	3 504	3 507	-0.08
	21	74.99	21.44	43.69	3 484	3 508	-0.68
	11	54.99	13.60	108.2	3 553	3 584	-0.87
	11	75.01	9.14	234.5	3 544	3 686	-3.85

TABLE 6.3

VISCOMETER CONSTANTS AND DIMENSIONS

Viscometer No	Sinker dimensions				Tube dimensions		Theoretical viscometer constant A_r	Constants for equation (6.5)		
	Diameter (mm)	Length (mm)	Mass (g)	Density (kg m^{-3})	Diameter (mm)	Length (mm)	($m\ s^2\ kg^{-1}$)	A_o ($m\ s^2\ kg^{-1}$)	B (s)	N
1	7.559	10.185	2.9788	7 604	7.785	148.84	38 240	37 900	6.6973	4
2	7.341	9.580	2.6719	7 308	7.582	149.00	30 452	31 080	5.1540	4
3	7.463	12.547	3.2860	6 429	7.785	34.90	3 397.7	3 374	0.7402	1

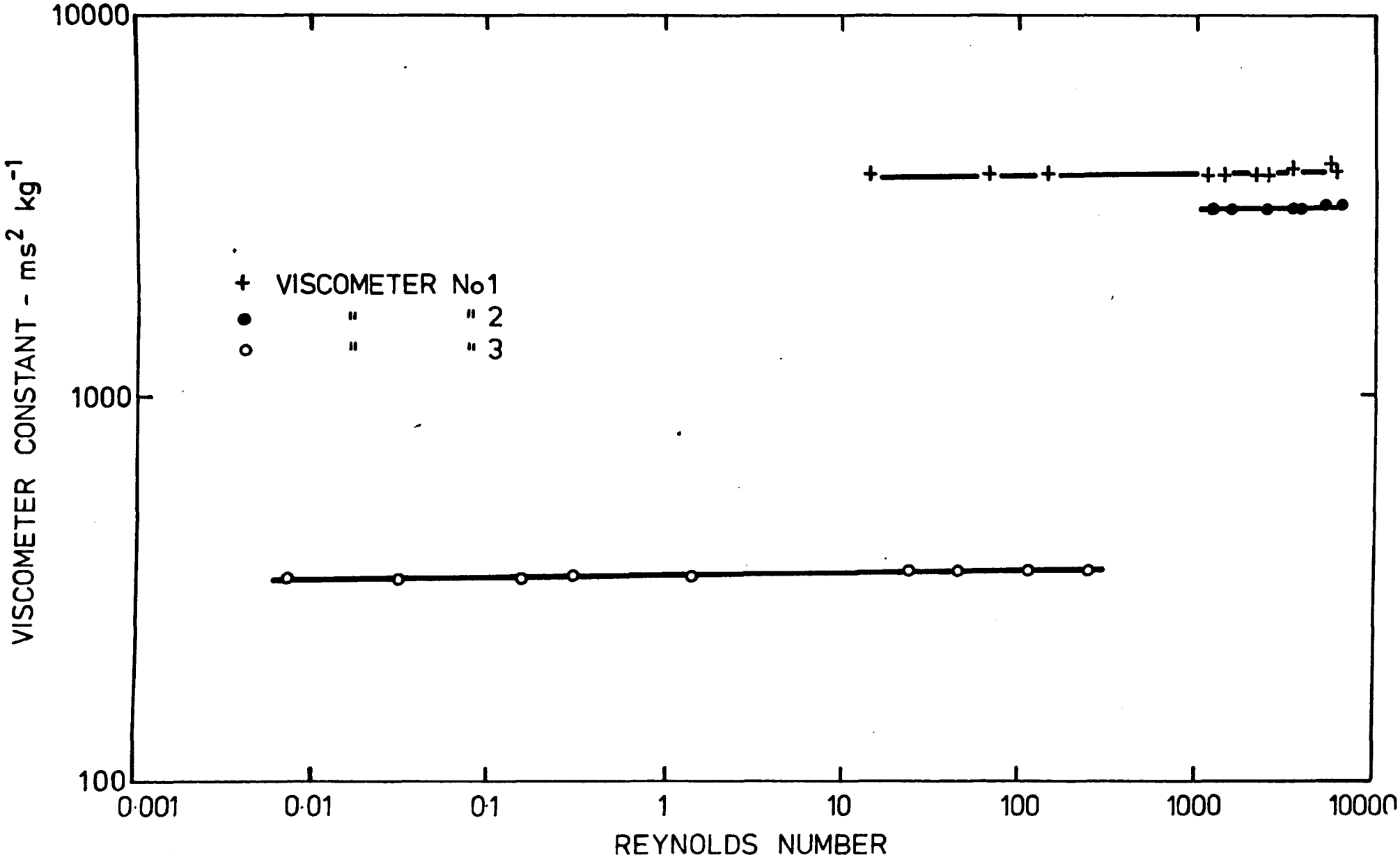

FIG 6.1 MEASURED VISCOMETER CONSTANTS

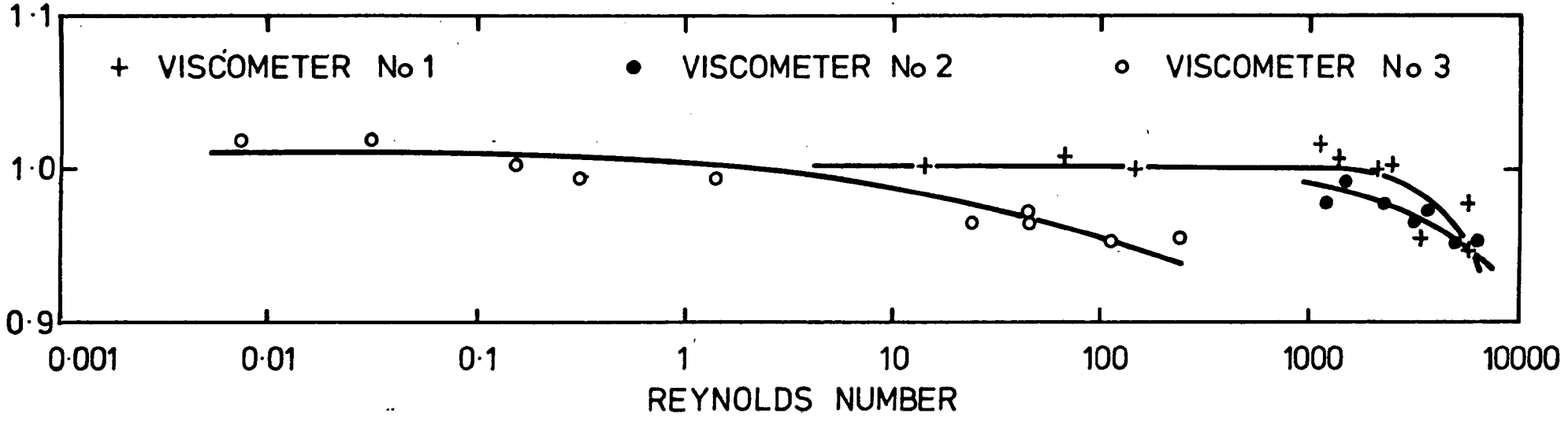

FIG 6.2 THEORETICAL AND MEASURED VISCOMETER CONSTANTS

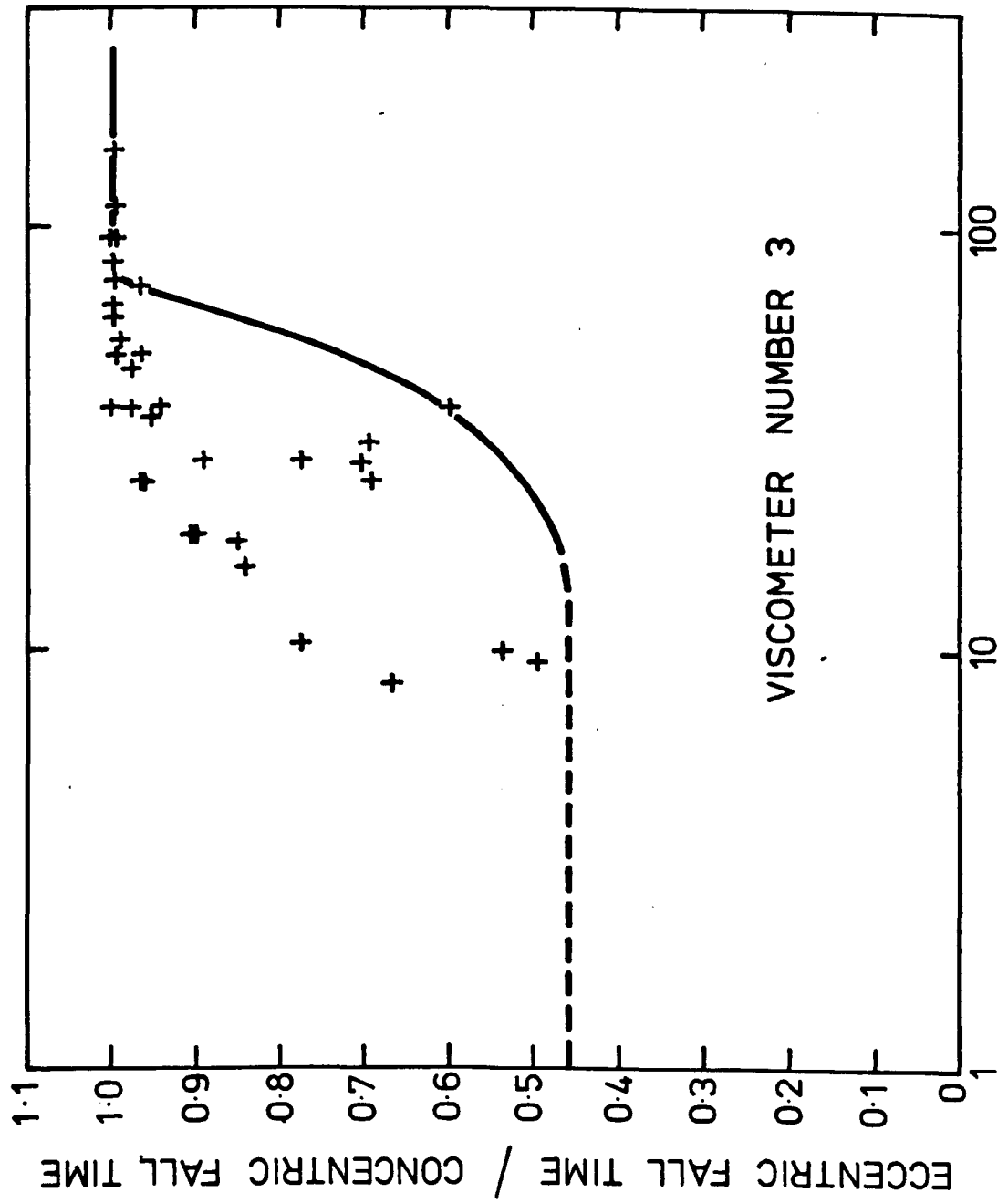

FIG 6.3 CENTRING EFFECTS

CHAPTER 7

EXPERIMENTAL RESULTS

SUMMARY OF CHAPTER 7

7 EXPERIMENTAL RESULTS

Tables of results are given for water, benzene, carbon tetrachloride, 1-bromopentane, 1-bromooctane, 1-bromododecane, 1,2-dichlorobenzene, 1,3 dichlorobenzene, bromocyclohexane, chlorocyclohexane and 1,5-dibromopentane. The results for the first three of these liquids are compared with other data at high pressures and are in good agreement with the most reliable sources available. For the other eight liquids there are no viscosity data under pressure, so comparisons are confined to atmospheric pressure values. These comparisons also show good agreement with the best available data.

The results show that the change in viscosity with pressure is similar to that of other simple liquids and is usually greater for liquids which have higher viscosities at atmospheric pressure. Two exceptions to this generalisation are found in which liquids of similar molecular shape, but having different viscosities at atmospheric pressure, show similar changes in viscosity ratio with pressure over a range of temperature. For these liquids, chlorocyclohexane and bromocyclohexane, and 1,2-dichlorobenzene and 1,3-dichlorobenzene, molecular shape is a major factor controlling the variation of viscosity with pressure.

CHAPTER 7 - EXPERIMENTAL RESULTS

LIST OF TABLES

LIST OF TABLES (contd)

LIST OF FIGURES

LIST OF FIGURES (contd)

7 EXPERIMENTAL RESULTS

7.1 Viscosity Results

The viscosity of eleven liquids has been measured. Between two and six isotherms of each liquid were examined giving a total of forty-four isotherms.

Water, benzene, and carbon tetrachloride were measured partly to test the viscometer and partly to provide new data for these important liquids. The density of these liquids was not measured and values from Bridgman (1958) (benzene and carbon tetrachloride) and Grindley and Lind (1971) (water) were used in equation 6.1 to calculate the results. Freshly distilled water and AR grade benzene and carbon tetrachloride were used.

The other eight liquids measured consisted of four straight chain compounds and four cyclic compounds. Each straight chain compound had a bromine substitution in the first position and one had a second bromine substitution at the opposite end of the chain. The cyclic compounds consisted of two mono-substituted cyclohexanes and two dichlorobenzenes.

The samples were purchased as laboratory grade chemicals and the purity of each was improved by distillation at atmospheric or reduced pressure. After distillation the purified fractions were immediately stored in tightly stoppered glass bottles until required for measurement. The boiling ranges of the samples and the distillation pressures are given in Table 7.1. Sample purity was estimated by gas chromatography and is also given in Table 7.1.

Since it was sometimes difficult to obtain experimental temperature and pressure settings at round numbers, corrections were applied by the following methods.

Corrections to viscosity for temperature settings were all less than 0.2 per cent, and were calculated using

$$\ln\eta = A + \frac{B}{T} \quad . \tag{7.1}$$

For each correction the constants in equation (7.1) were calculated using the point nearest in temperature with the same pressure. If a corresponding pressure was not available the value of B from the nearest pressure and temperature was used. In these cases errors due to the approximate value of B were negligible since the corrections were always small.

For bromocyclohexane, chlorocyclohexane, 1,5-dibromopentane and water pressure settings were accurate and correction to round values was unnecessary. For the other liquids values at round pressures were obtained by fitting each isotherm by the equation

$$\log\left\{\frac{\log\eta + 1.2}{\log\eta_o + 1.2}\right\} = \sum_{i=o}^{n} A_i T_i(P^*) \quad . \tag{7.2}$$

The reduced forms of viscosity and pressure in this equation are similar to those found by Roelands (1966) to be satisfactory for mineral oils and also for some pure liquids.

If more than four points were available N = 3 gave a good fit which was used to calculate values at exact pressures. For smaller numbers of points N was reduced to an appropriate value. Pressure corrections of up to 3.0 MN m^{-2} were applied in this way leading to viscosity corrections of less than 3.5 per cent.

Temperature and pressure corrections are shown in Table 7.2 which gives the complete calculation for 1-bromopentane from experimental observations to viscosity ratios.

The results of measurements made at high pressure are presented in the form of the ratio of the viscosity at pressure to that at atmospheric pressure and the same temperature. These ratios are given in Tables 7.3 to 7.13. Each table is based on measurements made by one falling body viscometer except in the following cases.

For chlorocyclohexane fall time readings at atmospheric pressure were found to be erratic in both viscometers 1 and 3, while at high pressure both viscometers gave consistent fall times which led to calculated viscosities in good agreement. Raising the pressure to a value slightly above atmospheric in this case did not eliminate the erratic fall times and calculation showed that, near atmospheric pressure, the Reynolds number was above that for which the viscometers were calibrated. Viscosities were therefore measured at atmospheric pressure using a master viscometer, and the ratios given in Table 7.13 are based on the mean of the viscosities at pressure, measured by viscometers 1 and 3, and master viscometer values at atmospheric pressure.

Bromocyclohexane was also measured in viscometers 1 and 3, but in this case only viscometer 3 gave unstable fall times at atmospheric pressure due to the high Reynolds number. Table 7.12 is therefore based on the mean of the viscosities at pressure measured by viscometers 1 and 3, and viscosities at atmospheric pressure from viscometer 1.

During measurement of 1,3-dichlorobenzene it was noticed that the calculated viscosities at atmospheric pressure were lower than those expected for this liquid, though the viscometer was functioning well and giving stable and repeatable fall times. On completion of the tests the sample was examined for contamination but none was detected.

However the viscometer tube was found to be slightly deformed in the region outside the measuring section. This probably occurred during loading of the tube into the pressure vessel. Since the results appeared to be consistent they were compared with measurements made in master viscometers at atmospheric pressure by taking the ratio of the viscosity at each temperature to that at 25°C. The maximum difference between the ratio obtained by the master viscometers and the deformed viscometer number 2 was found to be 1.21 per cent, and it was concluded that viscometer number 2 could still be used to measure viscosity ratios with sufficient accuracy. Measurements therefore continued on 1-bromooctane and 1-bromododecane while a new tube was made. Results for these three liquids were therefore calculated using the original calibration, but the viscosity values obtained were discarded while the viscosity ratios were retained. The maximum turbulence correction which occurred was 2.1 per cent for 1,3-dichlorobenzene at 100°C, and, though it was assumed that the turbulence effects in the deformed and undeformed tubes were similar, possible errors from this source are all less than this figure. Viscosity ratios at atmospheric pressure for these three liquids are shown in Fig. 7.1 compared with master viscometer values, and the difference between the ratios is shown in Fig. 7.2. The differences do not vary systematically with viscosity and are consistent with the expected experimental accuracy except for a single value (1-bromooctane at 100°C). It follows that the viscosity ratios given for the 100°C isotherm of 1-bromooctane may be subject to larger errors than the rest of the measurements unless the 5.7 per cent error detected is maintained consistently at all the pressures measured at that temperature. Since the viscometer tube was destroyed during measurements of the next liquid it was not possible to make additional

measurements to check this point.

Viscosities measured at atmospheric pressure are given in Tables 7.14 and 7.15. The values shown for benzene and carbon tetrachloride at 75 and 100°C were calculated using equation 7.2 fitted to all of the points for each isotherm. This procedure was necessary because the Reynolds numbers were high and beyond the calibrated region, and fall times were erratic. Master viscometer measurements were not made in these cases because the temperatures were near or above the boiling points.

Three separate measurements of carbon tetrachloride were made, partly to check the repeatability of the measurement technique and partly to determine the effect of dissolved air. For the first series of measurements the viscometer was filled by syringe at atmospheric pressure and 25°C with air saturated liquid. The other two series of measurements were made on samples which had been deaerated by vigorous agitation at reduced pressure and loaded into the viscometer in the same condition. The results of the three tests are given in Table 7.16.

If Henry's law is obeyed, even approximately, the concentration of air in the solution saturated with air at atmospheric pressure is very small at pressures of the magnitude considered. Consequently any effect on the measured viscosities should also decrease with pressure. The results do not how such a decrease.

The maximum difference between the viscosities of the two air free samples was 1.1 per cent, a satisfactory agreement. While the viscosity of the liquid containing air was consistently lower than the mean viscosity of the air free liquids the maximum difference was only

2.0 per cent at 147.6 MN m^{-2} and 1.4 per cent at atmospheric pressure. It was therefore concluded that the effects of dissolved air fell within the normal experimental scatter. It should be noted that the corresponding maximum difference in viscosity ratio at pressure was 0.7 per cent at 147.6 MN m^{-2}.

The three sets of measurements were averaged to give the results shown in Tables 7.5 and 7.15.

7.2 Comparison of Viscosity Results with Other Data

Of the eleven liquids measured only water, benzene, and carbon tetrachloride are compared with other data under pressure. No data under pressure have been found for the other liquids.

The values given in Table 7.15 are in good agreement with the best available data at atmospheric pressure, though the two values for water at 25 and 50°C are slightly higher, 2.1 per cent and 2.6 per cent respectively, than the values given by API 44. The benzene values are in excellent agreement with data from the same source, the maximum difference being 0.8 per cent at 60°C. However, apart from the benzene values at 75 and 100°C, these viscosities cannot be regarded as new measurements since both liquids were used for calibration. The carbon tetrachloride results are also in good agreement with the values given by Landolt-Bornstein (1969), the maximum difference being 1.9 per cent at 25°C.

Results for water at pressures up to 1000 MN m^{-2} are shown in Fig. 7.3. They are also given numerically in Table 7.17 where they are compared with tabulated values of the Engineering Sciences Data Unit (1963) derived from a correlation of data from several sources by Bruges and

Gibson (1969). The ESDU data are the most reliable available at the present time in this pressure range and are estimated to be accurate to within ±2 per cent. Though the present values tend to be slightly higher than the ESDU values at low pressure and slightly lower at high pressures, the maximum difference between them is only 1.6 per cent.

The benzene results are compared with data from Bridgman (1958) and Kuss (1955) in Figs 7.4 and 7.5 respectively. Bridgman used a falling body viscometer with centring pegs attached to the sinker to obtain his values, while Kuss used a rolling ball viscometer. The present measurements agree well with Bridgman's, the maximum difference being 4.1 per cent at 75°C and 300 MN m^{-2}. At 30°C and 98 MN m^{-2}, however, the benzene froze and measurements at a point corresponding to Bridgman's could not be obtained. The presence of impurities, which in any pure component will tend to raise the freezing pressure at constant temperature, may be the reason for the greater liquid range of Bridgman's sample. Such impurities would not necessarily alter the viscosity significantly. The agreement with Kuss' measurements is poor and the differences tend to increase with pressure and temperature as shown on Fig. 7.5. The rolling ball method is known to be difficult for low viscosity liquids because of non-linear calibration characteristics and the incidence of stick/slip motion or spin instead of pure rolling. These factors may account for the differences observed, which reach a maximum of nearly 13 per cent at 60°C. More recent measurements of benzene by Harlow (1967) at 30, 50 and 75°C are in excellent agreement with the present values. In this case the maximum difference in viscosity is 1.9 per cent at 75°C and 100 MN m^{-2}, though Harlow's values tend to be consistently lower than those given here.

Carbon tetrachloride results are compared with Bridgman's values in Fig. 7.6. The agreement here is also good with a standard deviation of 3.4 per cent, though a maximum difference of 6.0 per cent occurs at 30°C and 147 MN m^{-2}.

Viscosities at atmospheric pressure are compared with data from various sources in Figs 7.7-7.14. For 1-bromopentane, 1-bromooctane, and bromocyclohexane the present measurements agree well with the literature values, the maximum difference being 1.5 per cent. The results for 1-bromododecane agree with those of Cokelet (1969) to within 1 per cent but the values given by Hennelly (1948) are about 6 per cent higher. Similarly the results for 1,3-dichlorobenzene agree with those of Friend (1946) to within 2 per cent but the values given by Griffing (1954) are higher and diverge increasingly with temperature to give a difference of 14 per cent at 100°C. For 1,2-dichlorobenzene on the other hand the agreement with Griffing is good above 40°C while the values of Friend (1946) and Dreisbach (1955) are less than 3 per cent lower. The single point available for 1,5-dibromopentane (Dunstan (1913)) is within 2 per cent of the measured value at 25°C, and for chlorocyclohexane the present measurements are about 3 per cent higher than those tabulated by Landolt-Bornstein (1969).

The estimated accuracy of measurements made by the falling body viscometers is ±2 per cent and by master viscometers ±0.25 per cent. The agreement between the present measurements and the literature values is therefore good when the accuracy of both sources is taken into account. The accuracy of 0.2 per cent claimed by Griffing for the measurements of 1,3-dichlorobenzene is not supported by the present measurements or by those of Friend over a similar temperature range. Hennelly gives values for 1-bromododecane graphically, and numerical values extracted from his diagrams are subject to errors of about 5 per cent.

7.3 Density Results

Densities at atmospheric pressure were measured by the standard bicapillary pycnometer method, and at high pressure using the bellows apparatus described earlier. A complete calculation of the results for bromocyclohexane is given in Table 7.18, and the results for the eight halogenated liquids are given in Tables 7.19-7.26.

Density under pressure is conveniently expressed in terms of the isothermal secant bulk modulus, $\bar{K}$, defined by

$$\bar{K} = \frac{\rho_o P}{\rho - \rho_o} \quad . \tag{7.3}$$

It is found experimentally that for many liquids $\bar{K}$ varies linearly with pressure over quite wide pressure ranges, so that we may write

$$\bar{K} = K_o + mP \quad . \tag{7.4}$$

The bulk modulus values are estimated to be accurate to ±3.0 per cent and, within these limits, equation (7.4) fits the results for all eight liquids at both 25°C and 75°C. Equation constants for the eight halogenated liquids are given in Table 7.27.

Five densities at atmospheric pressure were taken from the literature. These are identified in Table 7.27.

7.4 Comparison of Density Results with Other Data

The maximum difference between the present measurements at atmospheric pressure and those of Dreisbach (1955, 1961), Friend and Hargreaves (1945, 1943), Griffing (1954), Dunstan (1913), and Mumford (1950), is 0.15 per cent, with most differences less than 0.07 per cent. The values given by Heston (1950) for 1-bromopentane, 1-bromododecane, and bromocyclohexane are consistently lower than those given by Dreisbach, and the present measurements, by as much as 0.98 per cent, probably

because of consistent errors in temperature measurement. Values given by Cernyawshaya (1964) range from 0.73 per cent low to 0.19 per cent high when compared with the more accurate values of Dreisbach and the present measurements.

No other sources of data under pressure have been found for these liquids.

7.5 Discussion of Results

Viscosity results for 1-bromopentane are shown in Fig. 7.15 in the form of a plot of the logarithm of viscosity (in mN s m^{-2}) against pressure. The isotherms are concave towards the pressure axis at lower pressures but tend to become linear at higher pressures. Results for the other liquids are similar and this type of variation is common to most pure liquids (see for example Bradley (1963)).

The viscosity results at 25°C are summarised in Fig. 7.16 which shows the variation of viscosity ratio with pressure. Values for a naphthenic and a paraffinic oil from the ASME Pressure Viscosity Report (1953) are included for comparison. Though the relationship between viscosity and structure is not yet understood in detail some useful information may be obtained from comparison of this sort.

The four bromoalkanes conform to the accepted generalisation that the change in viscosity with pressure is greater for liquids which have a high viscosity at atmospheric pressure. This is further illustrated in Fig. 7.17 which shows how the viscosity ratio at 100 MN m^{-2} and 25°C changes with viscosity at atmospheric pressure.

Though the cyclic compounds also conform, since the cyclohexanes with higher viscosities have a greater increase in viscosity ratio with

pressure than the benzenes, they show an additional feature which is of interest. The cyclohexanes, which have molecules of similar shape but viscosities differing by 27-30 per cent at atmospheric pressure, have an almost identical change in viscosity ratio with pressure. The same effect is shown by the dichlorobenzenes, which have slightly different molecular shapes and viscosities differing by 26-28 per cent but similar viscosity ratios. The similarity of the viscosity ratios of the cyclic compounds is shown in Fig. 7.18 and is evident for all the isotherms measured. The slight difference in shape between the two dichlorobenzenes is clearly not of major importance, probably because both molecules have some packing arrangements in common.

Change of density with pressure at 25°C is shown in Fig. 7.19 and is similar for all the liquids measured. It is a consequence of this behaviour that allows equation (7.4) to be used to describe the data, and this is illustrated in Figs 7.20 and 7.21 which show the variation of bulk modulus with pressure for 1-bromododecane and chlorocyclohexane respectively. The results for chlorocyclohexane are not typical since, for this liquid only, the slope of the bulk modulus plot (m in equation (7.4)) was slightly higher at 75°C than at 25°C. This variation, however, is within the expected accuracy of the data when both temperatures are considered and is therefore not due to anomolous behaviour of chlorocyclohexane.

The density results are summarised graphically in Fig. 7.22 in the form of a plot of isothermal secant bulk modulus at atmospheric pressure, K_o, against density at atmospheric pressure. Two distinct trends can be detected and these are evident at both temperatures. The bulk modulus of the straight chain compounds decreases as density

increases while that of the cyclic compounds and 1,5-dibromopentane increases with density. Obviously these trends are only part of a larger pattern which will not become clear without additional data.

The change in bulk modulus with pressure, m, does not vary much within this group of liquids, and is slightly less than that of hydraulic fluids. Chemical structure is therefore not a major factor in determining change in bulk modulus with pressure.

It is concluded that the results show that the change in viscosity with pressure is similar to that of other simple liquids and is usually greater for liquids which have higher viscosities at atmospheric pressure. Two exceptions to this generalisation have been found in which liquids of similar molecular shape, but having different viscosities at atmospheric pressure, show similar changes in viscosity ratio with pressure over a range of temperature. For these liquids, chlorocyclohexane and bromocyclohexane, and 1,2-dichlorobenzene and 1,3-dichlorobenzene, molecular shape is the major factor controlling the variation of viscosity with pressure.

The density results show that, within the accuracy of the present measurements, the linear secant modulus equation (equation (7.4)) may be used to describe the variation of density with pressure in the range examined. The bulk modulus at atmospheric pressure shows a similar relation to chemical structure at different temperatures but the change in bulk modulus with pressure does not vary much within this group of liquids.

TABLE 7.1

LIQUIDS MEASURED

Liquid	Normal boiling temperature (°C)	Boiling range of sample (°C)	Distillation pressure (mmHg)	Purity (%)
1-bromopentane	129.5	37.29-38.25	25	98.9
1-bromooctane	200.0	97.70-98.06	25	96.3
1-bromododecane	275.9	162.53-162.76	25	98.0
1,5-dibromopentane	222.3	114.00-114.46	24	98.7
1,2-dichlorobenzene	180.5	180.33-180.39	760	97.6
1,3-dichlorobenzene	173.5	173.24-173.27	760	99.8
bromocyclohexane	166.8	65.07-65.44	25	98.6
chlorocyclohexane	142.5	48.20-48.80	25	99.3

TABLE 7.2

VISCOSITY CALCULATIONS FOR 1-BROMOPENTANE

Measured						Temperature corrected		Temperature and pressure corrected		
Gauge resistance (Ω)	Pressure (MN m^{-2})	Temperature (^{o}C)	Fall time (s)	Density (g cm^{-3})	Viscosity (mN s m^{-2})	Temperature (^{o}C)	Viscosity (mN s m^{-2})	Pressure (MN m^{-2})	Viscosity (mN s m^{-2})	Viscosity ratio
100.4574	0.1	24.990	28.16	1.212	0.7540	25	0.7539	0.1	0.7558	1.000
100.5815	47.6	25.053	40.78	1.259	1.0857	25	1.0864	50.0	1.0953	1.449
100.7055	97.6	24.983	55.57	1.297	1.4712	25	1.4709	100.0	1.4972	1.981
100.8296	147.6	25.005	73.89	1.328	1.9468	25	1.9471	150.0	1.9745	2.612
100.9536	197.6	25.012	95.48	1.354	2.5055	25	2.5059	200.0	2.5467	3.370
101.2018	297.6	25.031	155.88	1.395	4.0646	25	4.0667	300.0	4.0886	5.409
101.3258	397.6	25.022	246.88	1.427	6.4062	25	6.4089	400.0	6.4440	8.526
101.6981	497.6	25.036	386.72	1.451	9.9995	25	10.0074	500.0	10.1626	13.446
100.4675	0.1	50.027	21.48	1.179	0.5752	50	0.5753	0.1	0.5763	1.000
100.5916	47.6	50.057	30.82	1.233	0.8224	50	0.8228	50.0	0.8316	1.443
100.7156	97.6	50.055	41.59	1.274	1.1038	50	1.1043	100.0	1.1212	1.946
100.9637	197.6	50.037	68.28	1.334	1.7958	50	1.7965	200.0	1.8242	3.165
101.2118	297.6	50.026	105.13	1.376	2.7473	50	2.7481	300.0	2.7726	4.811
101.4599	397.6	50.025	158.09	1.406	4.1126	50	4.1143	400.0	4.1251	7.158
101.7080	497.6	50.022	233.51	1.430	6.0533	50	6.0558	500.0	6.1429	10.659
100.4740	0.1	75.027	17.49	1.148	0.4664	75	0.4666	0.1	0.4670	1.000
100.5981	47.6	75.059	24.77	1.207	0.6617	75	0.6619	50.0	0.6693	1.433
100.7321	101.6	75.039	33.64	1.251	0.8948	75	0.8950	100.0	0.8924	1.911
100.9802	201.6	75.069	54.29	1.313	1.4314	75	1.4322	200.0	1.4172	3.035
101.2283	301.6	75.064	81.15	1.356	2.1256	75	2.1269	300.0	2.1161	4.532

TABLE 7.2 (Contd)

Measured						Temperature corrected		Temperature and pressure corrected		
Gauge resistance (Ω)	Pressure (MN m^{-2})	Temperature (^{o}C)	Fall time (s)	Density (g cm^{-3})	Viscosity (mN s m^{-2})	Temperature (^{o}C)	Viscosity (mN s m^{-2})	Pressure (MN m^{-2})	Viscosity (mN s m^{-2})	Viscosity ratio
100.4961	0.1	100.010	14.34	1.118	0.3774	100	0.3775	0.1	0.3778	1.000
100.6203	47.7	100.010	20.88	1.181	0.5576	100	0.5576	50.0	0.5636	1.492
100.7442	97.6	100.010	27.96	1.228	0.7448	100	0.7449	100.0	0.7596	2.011
100.9923	197.6	100.040	44.59	1.293	1.1781	100	1.1785	200.0	1.1846	3.135
101.2404	297.6	100.030	65.26	1.336	1.7133	100	1.7137	300.0	1.7319	4.584

TABLE 7.3

VISCOSITY RATIOS OF WATER

Temperature (°C)	Pressure (MN m^{-2})	Viscosity ratio
25	0.1	1.000
25	100	1.001
25	200	1.038
25	300	1.099
25	400	1.177
25	500	1.271
25	600	1.385
25	700	1.505
25	800	1.639
25	900	1.794
25	1000	1.967
50	0.1	1.000
50	100	1.042
50	200	1.098
50	300	1.169
50	400	1.248
50	500	1.337
50	600	1.435
50	700	1.539
50	800	1.659
50	900	1.786
50	1000	1.925

TABLE 7.4

VISCOSITY RATIOS OF BENZENE

Temperature (°C)	Pressure (MN m^{-2})	Viscosity ratio
25	0.1	1.000
25	50	1.531
30	0.1	1.000
30	50	1.524
40	0.1	1.000
40	50	1.513
40	100	2.106
60	0.1	1.000
60	50	1.519
60	100	2.085
60	150	2.729
60	200	3.525
75	0.1	1.000
75	50	1.498
75	100	2.071
75	150	2.729
75	200	3.508
75	300	5.692
100	0.1	1.000
100	50	1.560
100	100	2.174
100	150	2.826
100	200	3.546
100	300	5.476

TABLE 7.5

VISCOSITY RATIOS OF CARBON TETRACHLORIDE

Temperature (°C)	Pressure (MN m^{-2})	Viscosity ratio
25	0.1	1.000
25	50	1.558
25	100	2.234
25	150	3.138
30	0.1	1.000
30	50	1.538
30	100	2.173
30	150	3.010
40	0.1	1.000
40	50	1.539
40	100	2.192
40	150	2.995
40	200	4.015
75	0.1	1.000
75	50	1.521
75	100	2.124
75	150	2.822
75	200	3.650
75	300	5.939
100	0.1	1.000
100	100	2.120
100	200	3.571
100	300	5.535

TABLE 7.6

VISCOSITY RATIOS OF 1-BROMOPENTANE

Temperature (°C)	Pressure (MN m^{-2})	Viscosity ratio
25	0.1	1.000
25	50	1.449
25	100	1.981
25	150	2.612
25	200	3.370
25	300	5.409
25	400	8.526
25	500	13.446
50	0.1	1.000
50	50	1.443
50	100	1.946
50	200	3.165
50	300	4.811
50	400	7.158
50	500	10.659
75	0.1	1.000
75	50	1.433
75	100	1.911
75	200	3.035
75	300	4.532
100	0.1	1.000
100	50	1.492
100	100	2.011
100	200	3.135
100	300	4.584

TABLE 7.7

VISCOSITY RATIOS OF 1-BROMOOCTANE

Temperature (°C)	Pressure (MN m^{-2})	Viscosity ratio
25	0.1	1.000
25	50	1.579
25	100	2.360
25	150	3.406
25	200	4.796
25	300	9.089
25	400	16.656
25	500	30.078
50	0.1	1.000
50	50	1.541
50	100	2.229
50	150	3.095
50	200	4.177
50	300	7.232
50	400	12.070
50	500	19.856
75	0.1	1.000
75	50	1.513
75	100	2.141
75	150	2.895
75	200	3.798
75	300	6.190
75	400	9.716
75	500	15.042
100	0.1	1.000
100	50	1.517
100	100	2.120
100	150	2.809
100	200	3.605
100	300	5.665

TABLE 7.8

VISCOSITY RATIOS OF BROMODODECANE

Temperature (°C)	Pressure (MN m^{-2})	Viscosity ratio
25	0.1	1.000
25	50	1.966
25	100	2.823
25	150	4.050
25	200	6.827
50	0.1	1.000
50	50	1.660
50	100	2.553
50	150	3.743
50	200	5.323
50	300	10.237

TABLE 7.9

VISCOSITY RATIOS OF 1,5-DIBROMOPENTANE

Temperature (°C)	Pressure (MN m^{-2})	Viscosity ratio
25	0.1	1.000
25	100	2.198
25	200	4.435
25	300	8.668
50	0.1	1.000
50	100	2.000
50	200	3.640
50	300	6.331
50	400	10.743
50	500	17.977
75	0.1	1.000
75	100	1.922
75	200	3.244
75	300	5.229
75	400	5.647

TABLE 7.10

VISCOSITY RATIOS OF 1,2-DICHLOROBENZENE

Temperature (°C)	Pressure (MN m^{-2})	Viscosity ratio
25	0.1	1.000
25	50	1.424
25	100	1.954
25	150	2.665
25	200	3.671
50	0.1	1.000
50	50	1.386
50	100	1.842
50	150	2.402
50	200	3.116
50	300	5.311
75	0.1	1.000
75	50	1.358
75	100	1.780
75	150	2.286
75	200	2.898
75	300	4.561
75	400	7.105
75	500	11.078
100	0.1	1.000
100	50	1.371
100	100	1.792
100	150	2.274
100	200	2.835
100	300	4.282
100	400	6.373

TABLE 7.11

VISCOSITY RATIOS OF 1,3-DICHLOROBENZENE

Temperature (^{o}C)	Pressure (MN m^{-2})	Viscosity ratio
25	0.1	1.000
25	50	1.468
25	100	1.888
25	150	2.431
25	200	3.358
50	0.1	1.000
50	50	1.367
50	100	1.800
50	150	2.318
50	200	2.947
50	300	4.689
50	400	7.440
75	0.1	1.000
75	50	1.356
75	100	1.753
75	150	2.209
75	200	2.745
75	300	4.179
75	400	6.396
100	0.1	1.000
100	50	1.464
100	100	1.907
100	150	2.410
100	200	3.106

TABLE 7.12

VISCOSITY RATIOS OF BROMOCYCLOHEXANE

Temperature (°C)	Pressure (MN m^{-2})	Viscosity ratio
25	0.1	1.000
25	100	2.709
25	200	6.426
25	300	14.241
25	400	30.694
25	500	66.957
50	0.1	1.000
50	100	2.532
50	200	5.526
50	300	11.322
50	400	22.141
50	500	42.911
50	600	84.991
75	0.1	1.000
75	100	2.414
75	200	4.615

TABLE 7.13

VISCOSITY RATIOS OF CHLOROCYCLOHEXANE

Temperature (°C)	Pressure (MN m^{-2})	Viscosity ratio
25	0.1	1.000
25	100	2.709
25	200	6.535
25	300	14.346
50	0.1	1.000
50	100	2.637
50	200	5.602
50	300	11.283
50	400	22.542
75	0.1	1.000
75	100	2.540
75	200	4.934
75	300	9.431
75	400	17.283
75	500	30.350

TABLE 7.14

VISCOSITIES AT ATMOSPHERIC PRESSURE ($mNs\ m^{-2}$)

Liquid	Temperature (°C)				Viscometer
	25	50	75	100	
1-bromopentane	0.756	0.576	0.467	0.378	2
1-bromooctane	1.4941	1.0265	0.7548	0.5642	MV*
1-bromododecane	3.3547	2.0415	-	-	MV
1,5-dibromopentane	3.099	1.985	1.420	-	1
1,2-dichlorobenzene	1.258	0.965	0.749	0.582	2
1,3-dichlorobenzene	1.0015	0.7529	0.5916	0.4643	MV
bromocyclohexane	1.979	1.356	0.965	-	1
chlorocyclohexane	1.5625	1.0444	0.7480	-	MV

*MV denotes values obtained using master viscometers

TABLE 7.15

VISCOSITIES AT ATMOSPHERIC PRESSURE ($mNs\ m^{-2}$)

Liquid	Temperature (°C)						
	25	30	40	50	60	75	100
Water	0.908	-	-	0.560	-	-	-
Benzene	0.599	0.560	0.493	-	0.386	0.333	0.260
Carbon tetrachloride	0.885	0.835	0.734	-	-	0.502	0.400

TABLE 7.16

VISCOSITIES OF CARBON TETRACHLORIDE AT 40°C

Pressure	Measured viscosities			Mean of deviations		
	(1)*	(2)	(3)	(2) and (3)	(2)-(3)	(1)-mean
(MN m^{-2})	(mNs m^{-2})	(mNs m^{-2})	(mNs m^{-2})	(mNs m^{-2})	(%)	(%)
0.1	0.7274	0.7397	0.7351	0.7374	-0.6	-1.4
47.6	1.1008	1.1231	1.1144	1.1188	-0.8	-1.6
97.6	1.5572	1.5955	1.5777	1.5866	-1.1	-1.9
147.6	2.1419	2.1933	2.1794	2.1864	-0.6	-2.0
172.6	-	2.5467	2.5197	2.5332	-1.1	-
197.6	2.8778	-	-	-	-	-

*(1) Sample saturated with air at atmospheric pressure

(2),(3) Deaerated samples

T A B L E 7.17

COMPARISON OF VISCOSITY RATIOS OF WATER

Pressure ($MN\ m^{-2}$)	Viscosity ratio at 25°C			Viscosity ratio at 50°C		
	ESDU	NEL	Difference (%)	ESDU	NEL	Difference (%)
0.1	1.000	1.000	-	1.000	1.000	-
100	0.993	1.001	0.8	1.032	1.042	1.0
200	1.036	1.038	0.2	1.093	1.098	0.5
300	1.098	1.099	0.1	1.162	1.169	0.6
400	1.176	1.177	0.1	1.240	1.248	0.6
500	1.274	1.271	-0.2	1.328	1.337	0.7
600	1.390	1.385	-0.4	1.428	1.435	0.5
700	1.521	1.505	-1.1	1.540	1.539	-0.1
800	1.666	1.639	-1.6	1.663	1.659	-0.2
900	1.818	1.794	-1.3	1.800	1.786	-0.8
1000	1.972	1.967	-0.3	1.933	1.925	-0.4

TABLE 7.18

DENSITY CALCULATIONS FOR BROMOCYCLOHEXANE

Temperature (^{o}C)	Resistance (Ω)	Pressure (MN m^{-2})	Micrometer reading (mm)	Bellows contraction (mm)	Corrected contraction (mm)	Corrected bellows area (μm^{2})	Volume change (μm^{3})	Density (kg m^{-3})	Bulk modulus (GN m^{-2})
25	100.6372	0.1	19.94	0.0	0.0	220.7	0.0	1329.6	-
	100.8853	97.6	13.59	6.35	6.32	220.6	1.39	1399.0	1.974
	101.1334	197.6	9.20	10.74	10.69	220.5	2.35	1451.0	2.369
	101.3815	297.6	5.96	13.98	13.89	220.4	3.06	1492.0	2.727
	101.6296	397.6	3.39	16.55	16.43	220.4	3.62	1526.0	3.094
	101.8777	497.5	1.28	18.66	18.51	220.3	4.07	1555.0	3.430
75	100.6402	0.1	18.25	0.0	0.0	221.1	0.0	1268.6	-
	100.8883	97.6	10.09	8.16	8.14	221.0	1.80	1351.0	1.600
	101.1364	197.6	4.92	13.33	13.27	220.9	2.93	1409.0	1.984
	101.3845	297.6	1.34	16.91	16.82	220.8	3.72	1452.0	2.358
	101.6326	397.6	-1.57	19.82	19.70	220.7	4.34	1488.0	2.693
	101.8807	497.5	-3.92	22.17	22.03	220.6	4.86	1519.0	3.017

TABLE 7.19

DENSITY AND BULK MODULUS OF 1-BROMOPENTANE

Temperature (°C)	Pressure (MN m^{-2})	Density (kg m^{-3})	Bulk modulus (GN m^{-2})
25	0.1	1211.9	-
	97.6	1293.0	1.552
	197.6	1359.0	1.824
	297.6	1388.0	2.347
	497.5	1451.0	3.021
75	0.1	1148.1	-
	247.6	1333.0	1.783
	297.6	1353.0	1.967

TABLE 7.20

DENSITY AND BULK MODULUS OF 1-BROMOOCTANE

Temperature (°C)	Pressure (MN m^{-2})	Density (kg m^{-3})	Bulk modulus (GN m^{-2})
25	0.1	1107.2	-
	47.7	1145.0	1.456
	97.6	1174.0	1.716
	147.6	1200.0	1.905
	197.6	1222.0	2.101
	247.6	1240.0	2.309
75	0.1	1055.0	-
	97.6	1135.0	1.380
	147.6	1169.0	1.519
	197.6	1192.0	1.722
	247.6	1211.0	1.925
	297.6	1229.0	2.100

TABLE 7.21

DENSITY AND BULK MODULUS OF 1-BROMODODECANE

Temperature (°C)	Pressure (MN m^{-2})	Density (kg m^{-3})	Bulk modulus (GN m^{-2})
25	0.1	1035.7	-
	47.6	1067.0	1.633
	97.6	1095.0	1.801
	147.6	1115.0	2.087
	197.6	1133.0	2.298
	247.6	1147.0	2.549
75	0.1	991.3	-
	97.6	1062.0	1.466
	197.6	1106.0	1.901
	297.6	1141.0	2.271
	397.6	1169.0	2.610
	497.5	1194.0	2.935

TABLE 7.22

DENSITY AND BULK MODULUS OF 1,5-DIBROMOPENTANE

Temperature (°C)	Pressure (MN m^{-2})	Density (kg m^{-3})	Bulk modulus (GN m^{-2})
25	0.1	1692.5	-
	97.6	1770.0	2.225
	197.6	1829.0	2.650
	297.6	1875.0	3.058
	397.6	1918.0	3.382
	497.5	1953.0	3.726
75	0.1	1622.5	-
	97.6	1714.0	1.830
	197.6	1781.0	2.220
	297.6	1837.0	2.551
	397.6	1875.0	2.955
	497.5	1913.0	3.279

TABLE 7.23

DENSITY AND BULK MODULUS OF 1,2-DICHLOROBENZENE

Temperature (°C)	Pressure (MN m^{-2})	Density (kg m^{-3})	Bulk modulus (GN m^{-2})
25	0.1	1300.2	-
	97.6	1362.0	2.142
	197.6	1409.0	2.566
75	0.1	1245.6	-
	97.6	1321.0	1.715
	197.6	1371.0	2.163
	297.6	1411.0	2.538
	397.6	1444.0	2.898

TABLE 7.24

DENSITY AND BULK MODULUS OF 1,3-DICHLOROBENZENE

Temperature (°C)	Pressure (MN m^{-2})	Density (kg m^{-3})	Bulk modulus (GN m^{-2})
25	0.1	1281.9	-
	47.6	1315.0	1.890
	147.6	1370.0	2.296
	197.6	1392.0	2.498
75	0.1	1223.4	-
	97.6	1298.0	1.703
	197.6	1349.0	2.121
	297.6	1388.0	2.509
	397.6	1421.0	2.855

TABLE 7.25

DENSITY AND BULK MODULUS OF BROMOCYCLOHEXANE

Temperature (°C)	Pressure (MN m^{-2})	Density (kg m^{-3})	Bulk modulus (GN m^{-2})
25	0.1	1329.6	-
	97.6	1399.0	1.974
	197.6	1451.0	2.369
	297.6	1492.0	2.727
	397.6	1526.0	3.094
	497.5	1555.0	3.430
75	0.1	1268.6	-
	97.6	1351.0	1.600
	197.6	1409.0	1.984
	297.6	1452.0	2.358
	397.6	1488.0	2.693
	497.5	1519.0	3.017

TABLE 7.26

DENSITY AND BULK MODULUS OF CHLOROCYCLOHEXANE

Temperature (°C)	Pressure (MN m^{-2})	Density (kg m^{-3})	Bulk modulus (GN m^{-2})
25	0.1	993.9	-
	97.6	1052.0	1.770
	197.6	1091.0	2.219
	297.6	1124.0	2.576
	397.6	1159.0	2.790
	497.5	1180.0	3.160
75	0.1	944.8	-
	97.6	1013.0	1.443
	197.6	1057.0	1.865
	297.6	1094.0	2.178
	397.6	1120.0	2.539
	497.5	1143.0	2.868

TABLE 7.27

DENSITY AND BULK MODULUS AT 25 AND 75°C

Liquid	Temperature at 25°C			Temperature at 75°C		
	Density (kg m^{-3})	K_o (GN m^{-2})	m	Density (kg m^{-3})	K_o (GN m^{-3})	m
1-bromopentane	1211.9[1]	1.149	3.772	1148.1	0.860	3.690
1-bromooctane	1107.2[1]	1.270	4.182	1055.0	0.990	3.695
1-bromododecane	1035.7	1.374	4.662	991.3	1.142	3.648
1,5-dibromopentane	1692.5	1.888	3.734	1622.5	1.477	3.633
1,2-dichlorobenzene	1300.2[2]	1.718	4.329	1245.6	1.348	3.923
1,3-dichlorobenzene	1281.9[3]	1.684	4.046	1223.4[3]	1.336	3.842
bromocyclohexane	1329.6	1.628	3.638	1268.6	1.268	3.542
chlorocyclohexane	993.9	1.498	3.351	944.8	1.121	3.526

(1) Values from Dreisbach (1961)

(2) Value from Dreisbach (1955)

(3) Values from Griffing (1954)

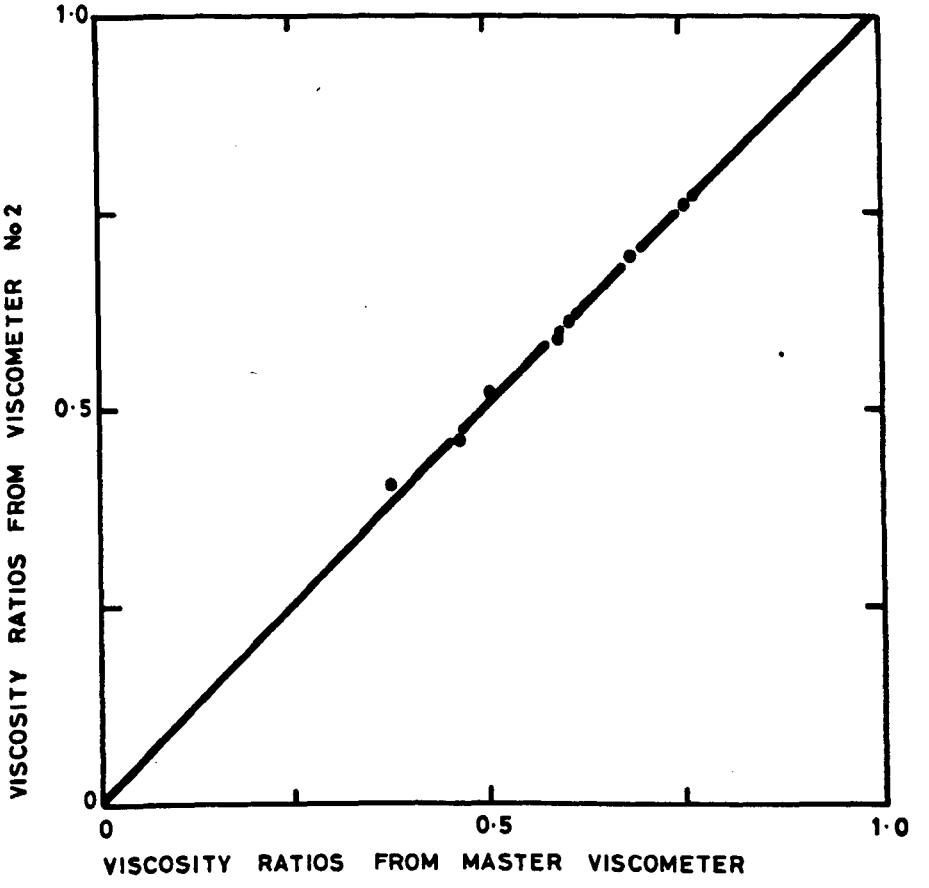

FIG 7.1 VISCOSITY RATIOS AT ATMOSPHERIC PRESSURE FOR 1, 3-DICHLOROBENZENE, 1-BROMOOCTANE AND 1-BROMODODECANE

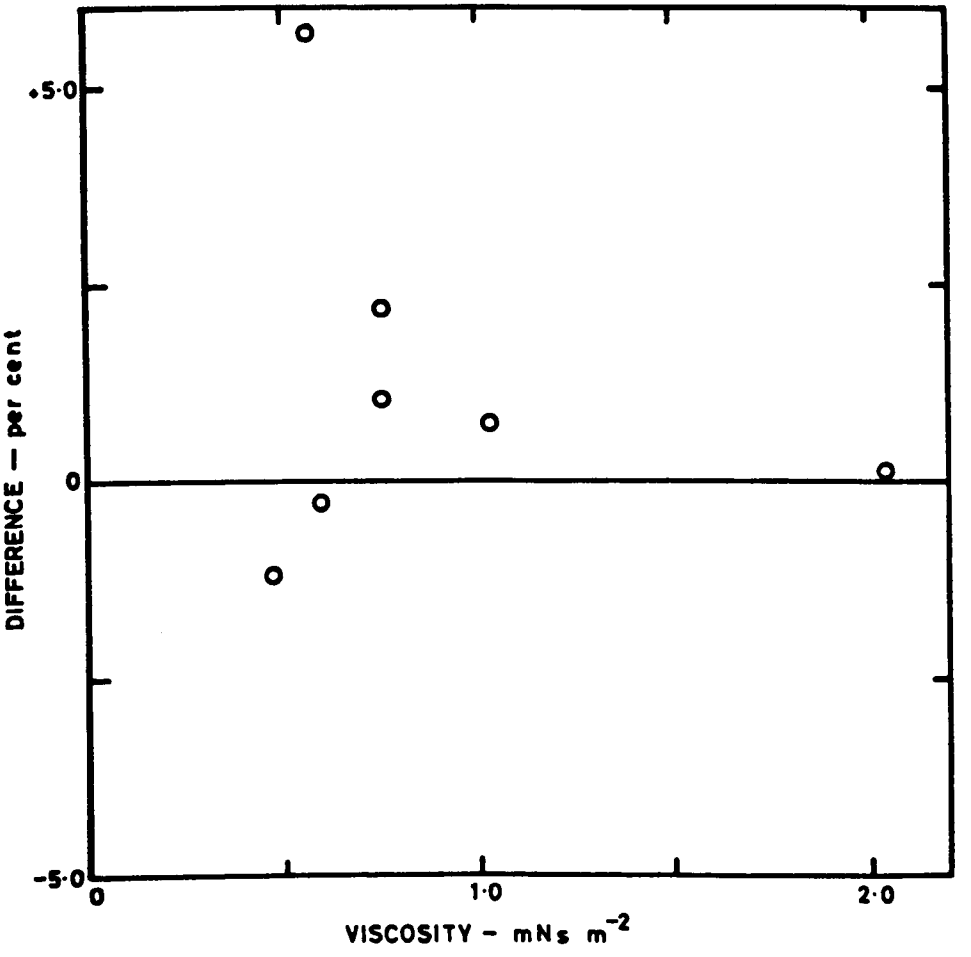

FIG 7.2 DIFFERENCES BETWEEN VISCOSITY RATIOS AT ATMOSPHERIC PRESSURE MEASURED BY VISCOMETER No2 AND BY MASTER VISCOMETER

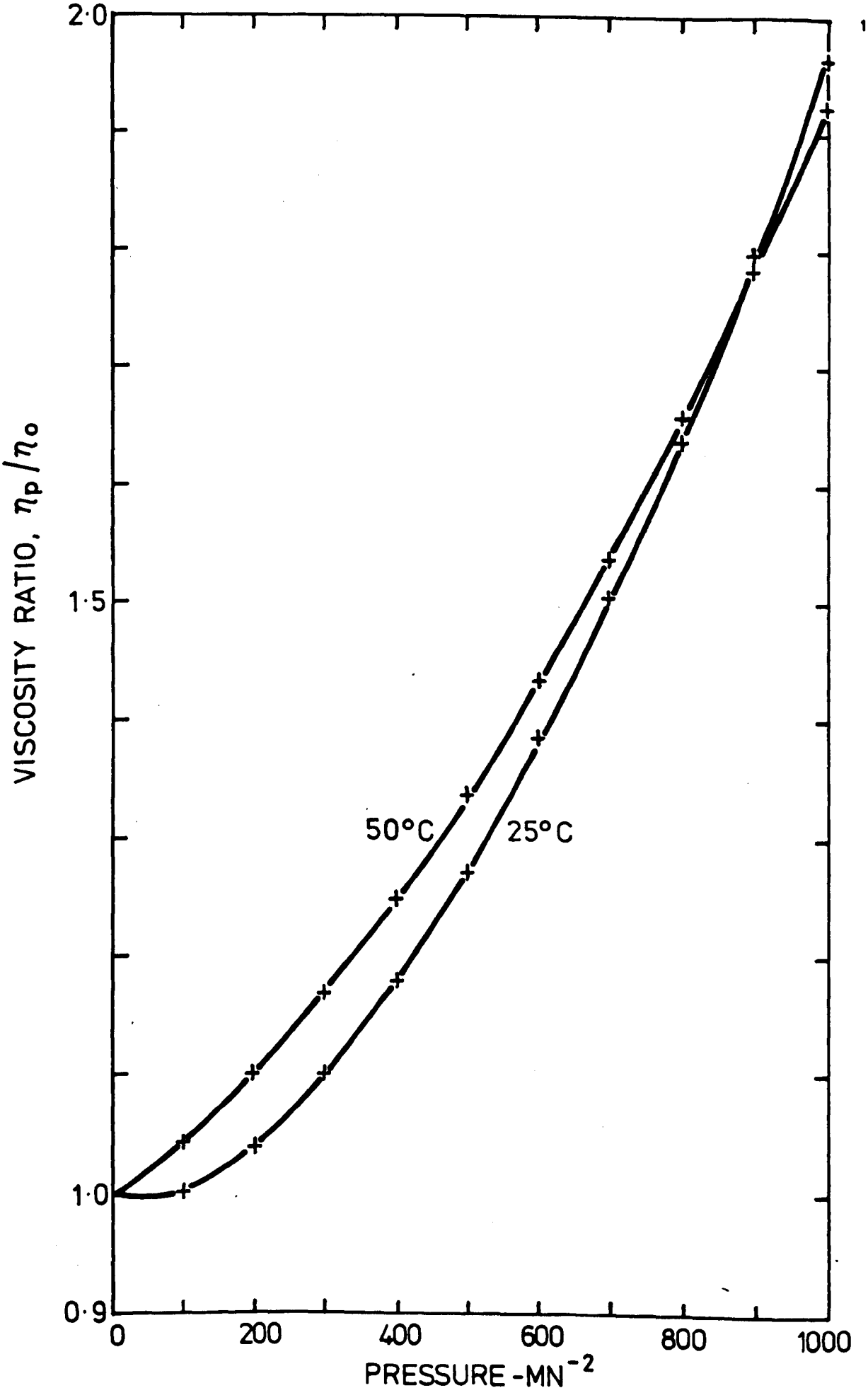

FIG 7.3 VISCOSITY RATIOS OF WATER

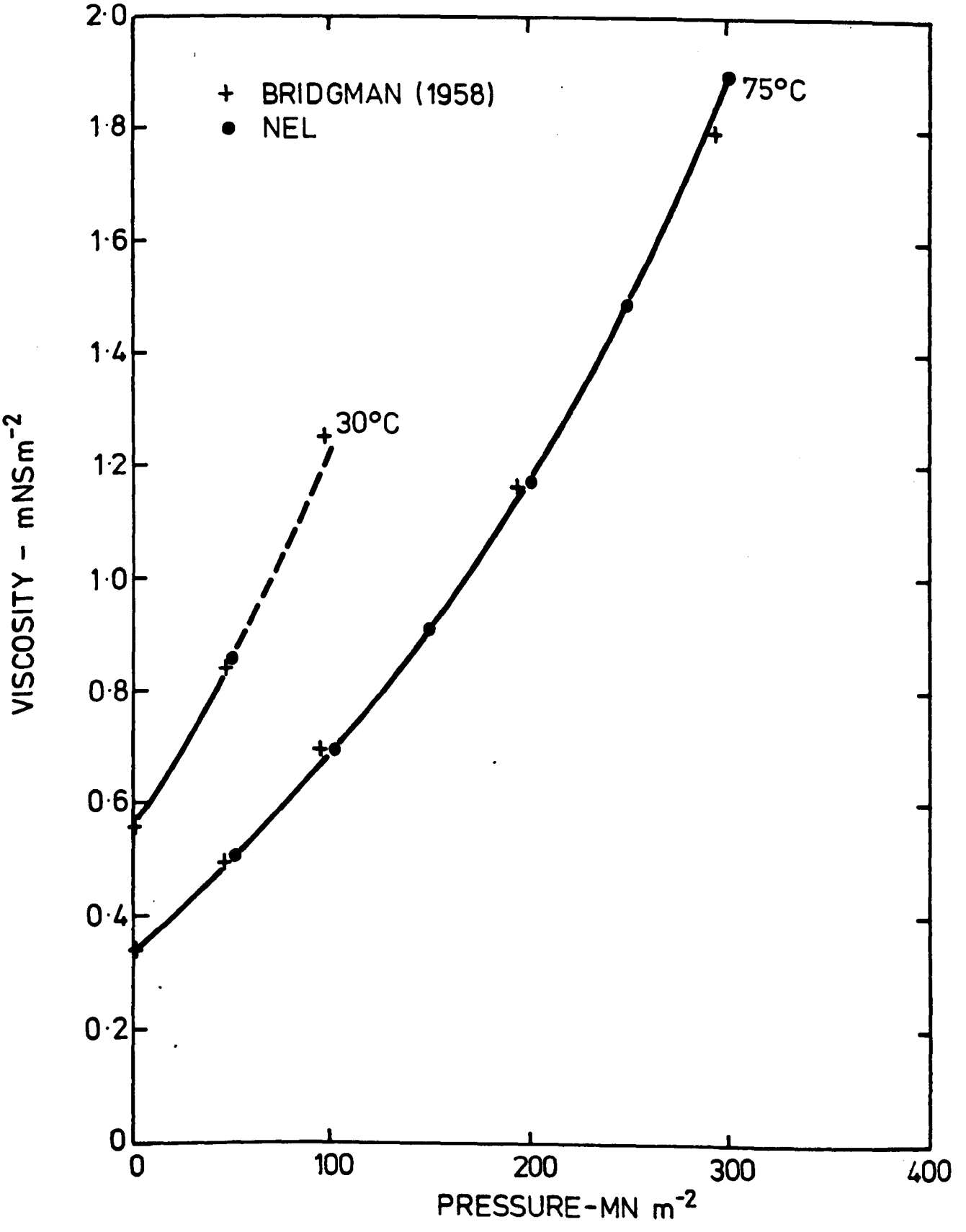

FIG 7.4 VISCOSITY OF BENZENE AT 30° AND 75°C

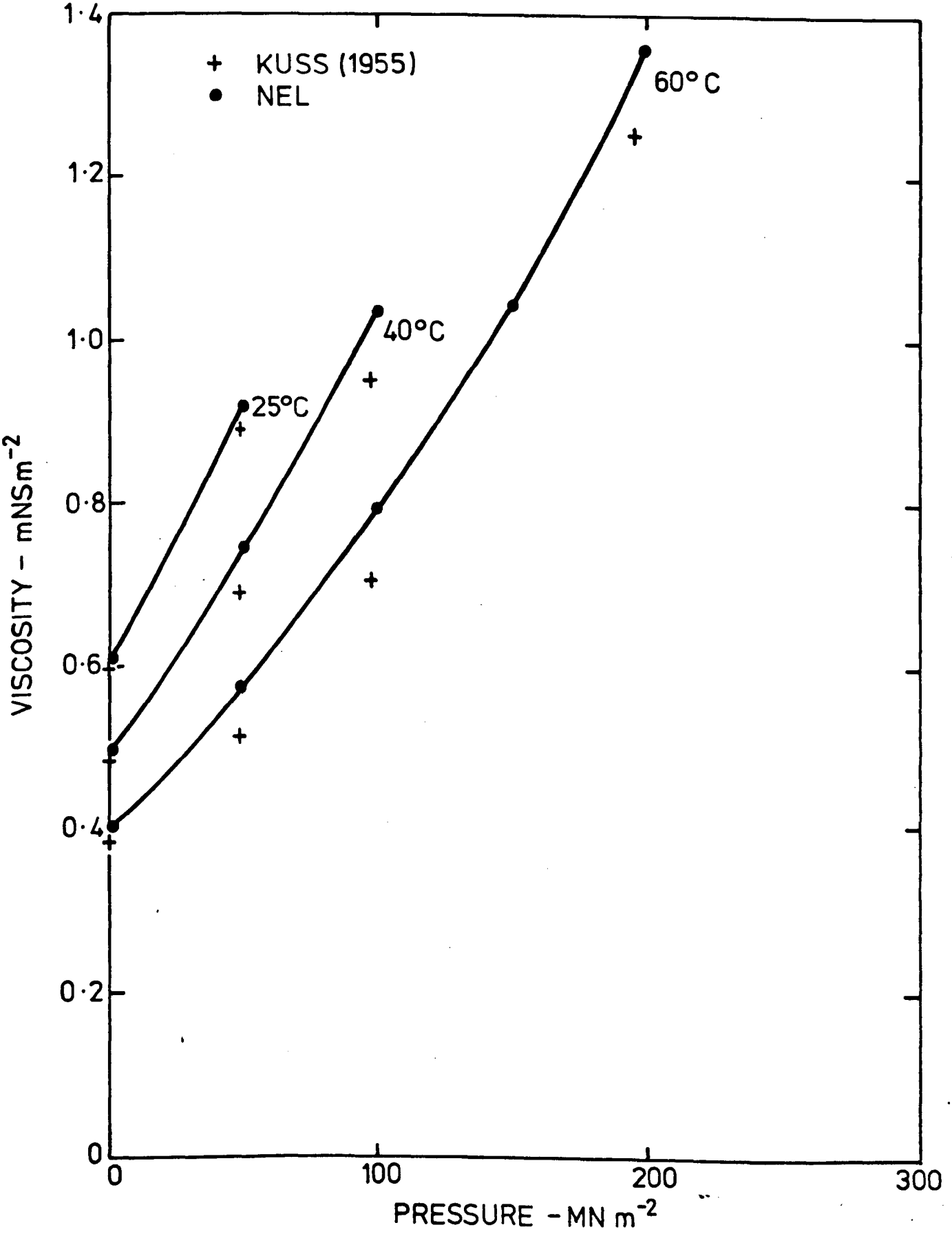

FIG 7.5 VISCOSITY OF BENZENE AT 25, 40, AND 60° C

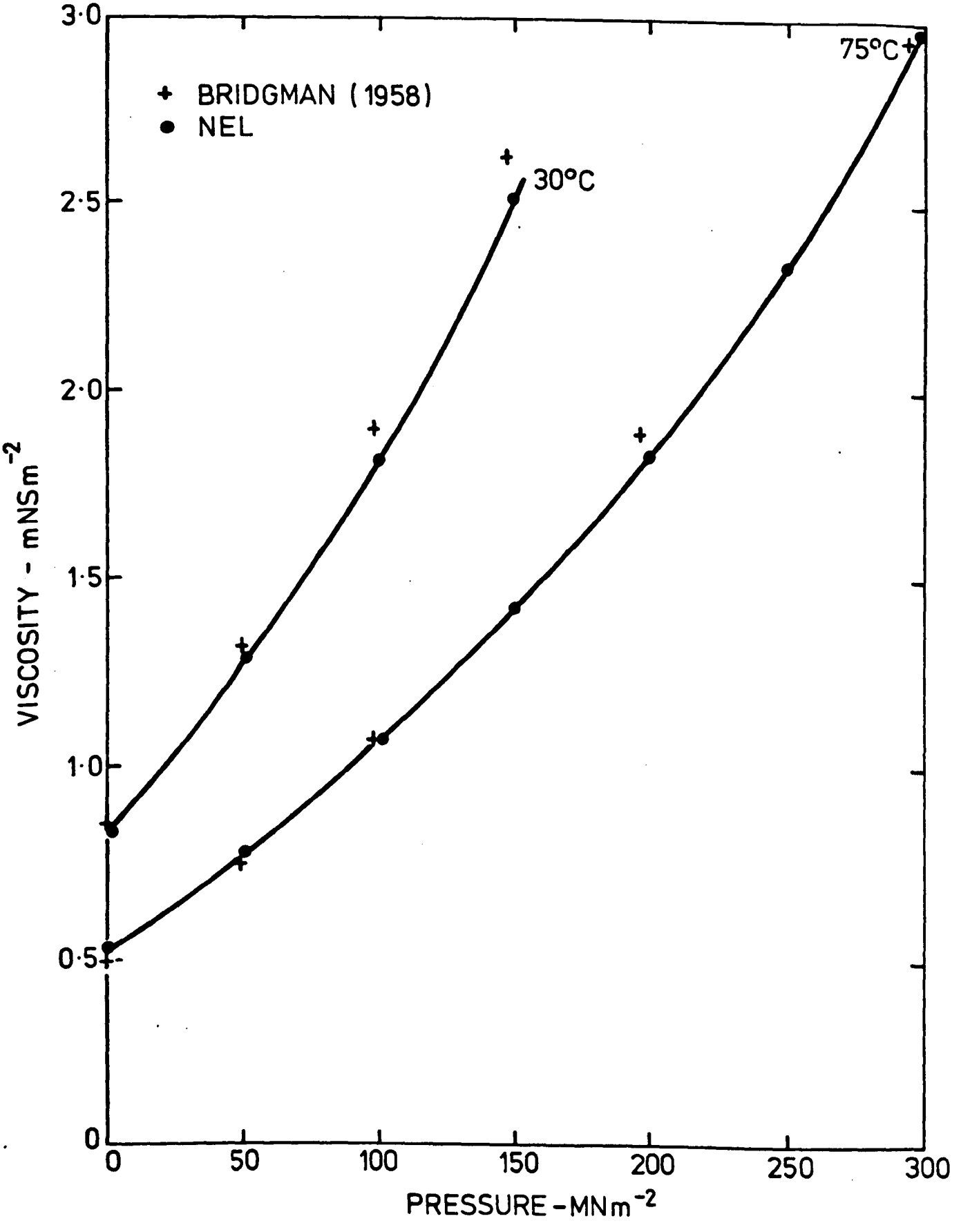

FIG 7.6 VISCOSITY OF CARBON TETRACHLORIDE

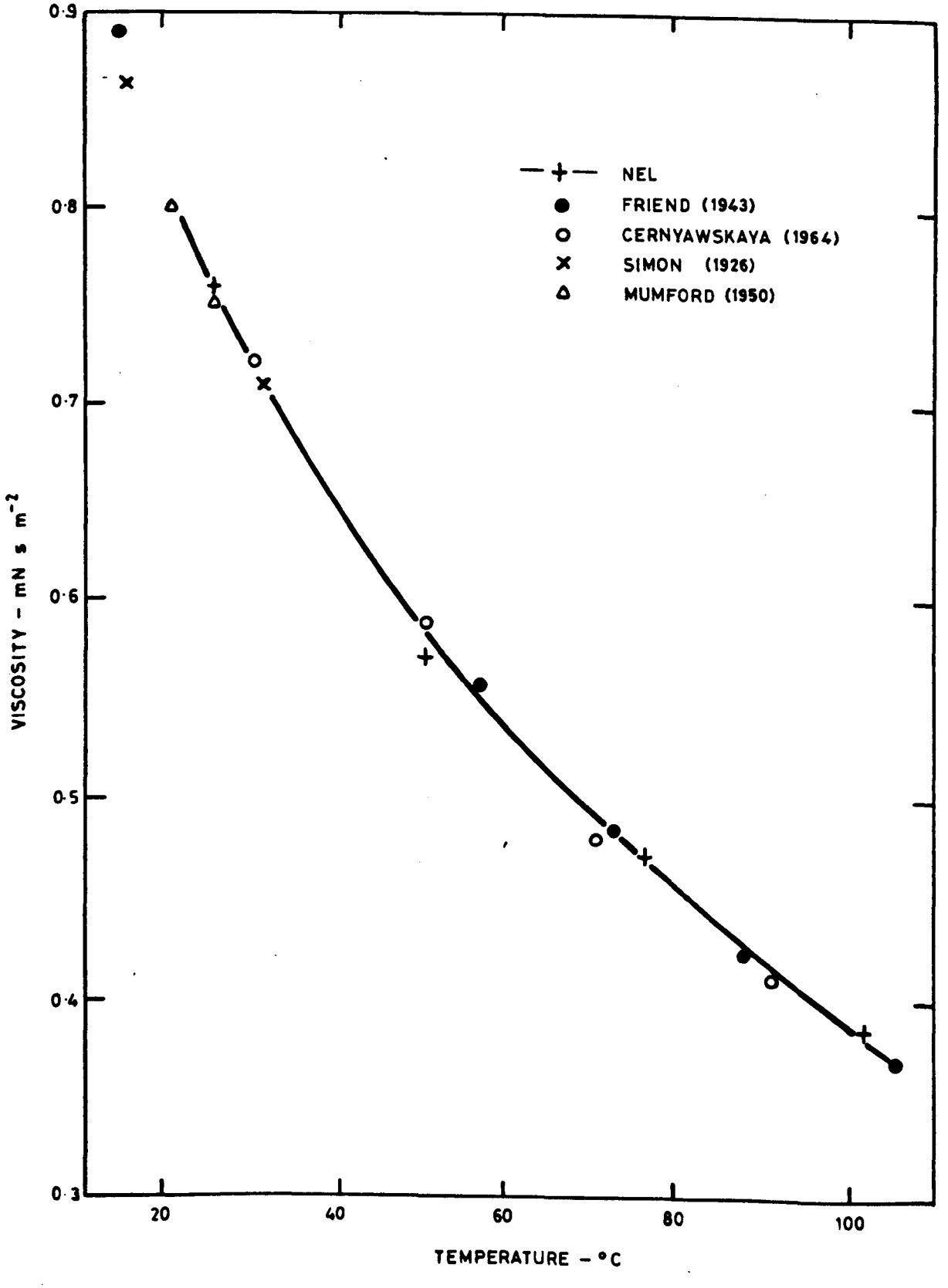

FIG 7.7 VISCOSITY OF 1-BROMOPENTANE

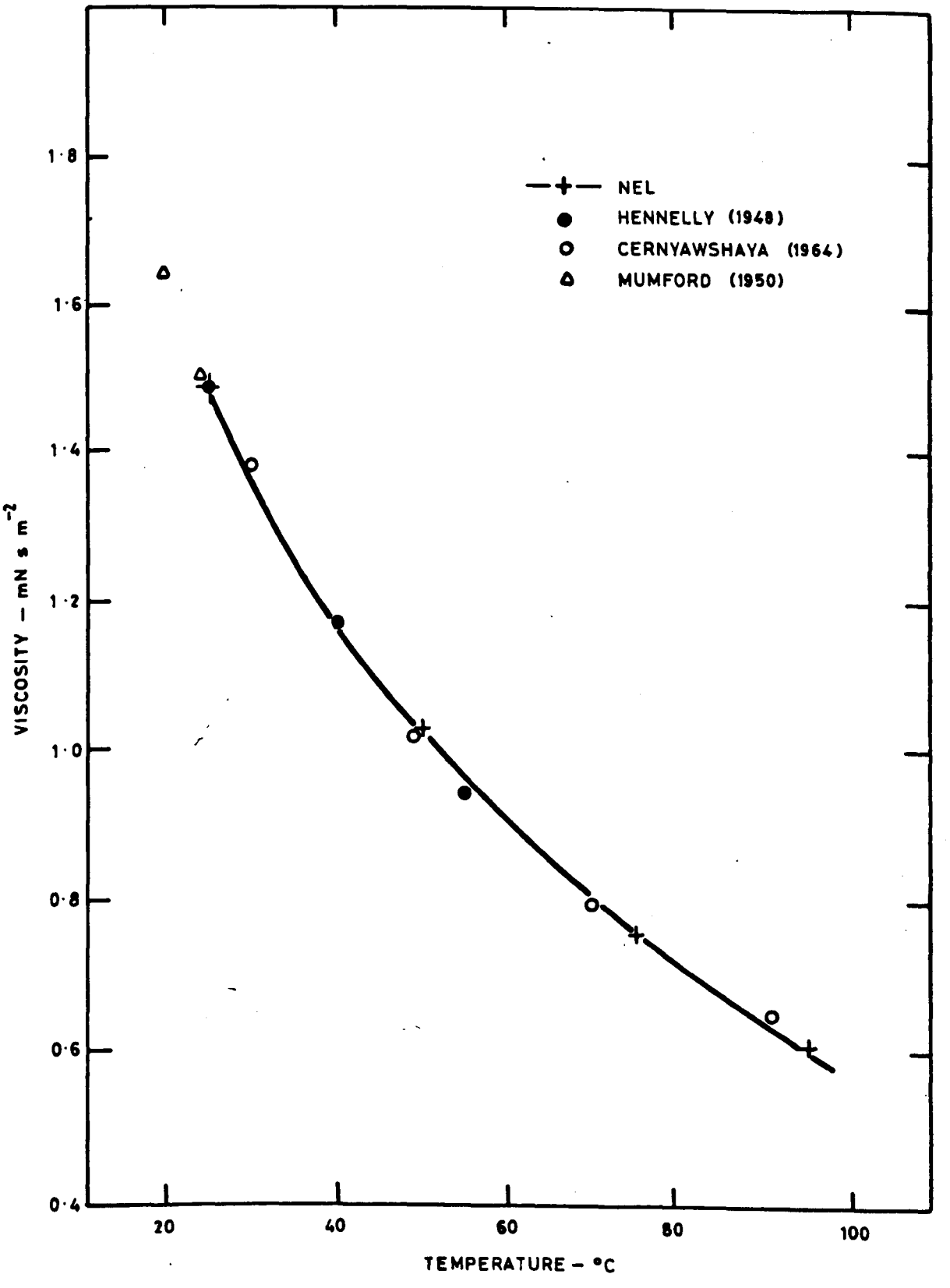

FIG 7.8 VISCOSITY OF 1-BROMOOCTANE

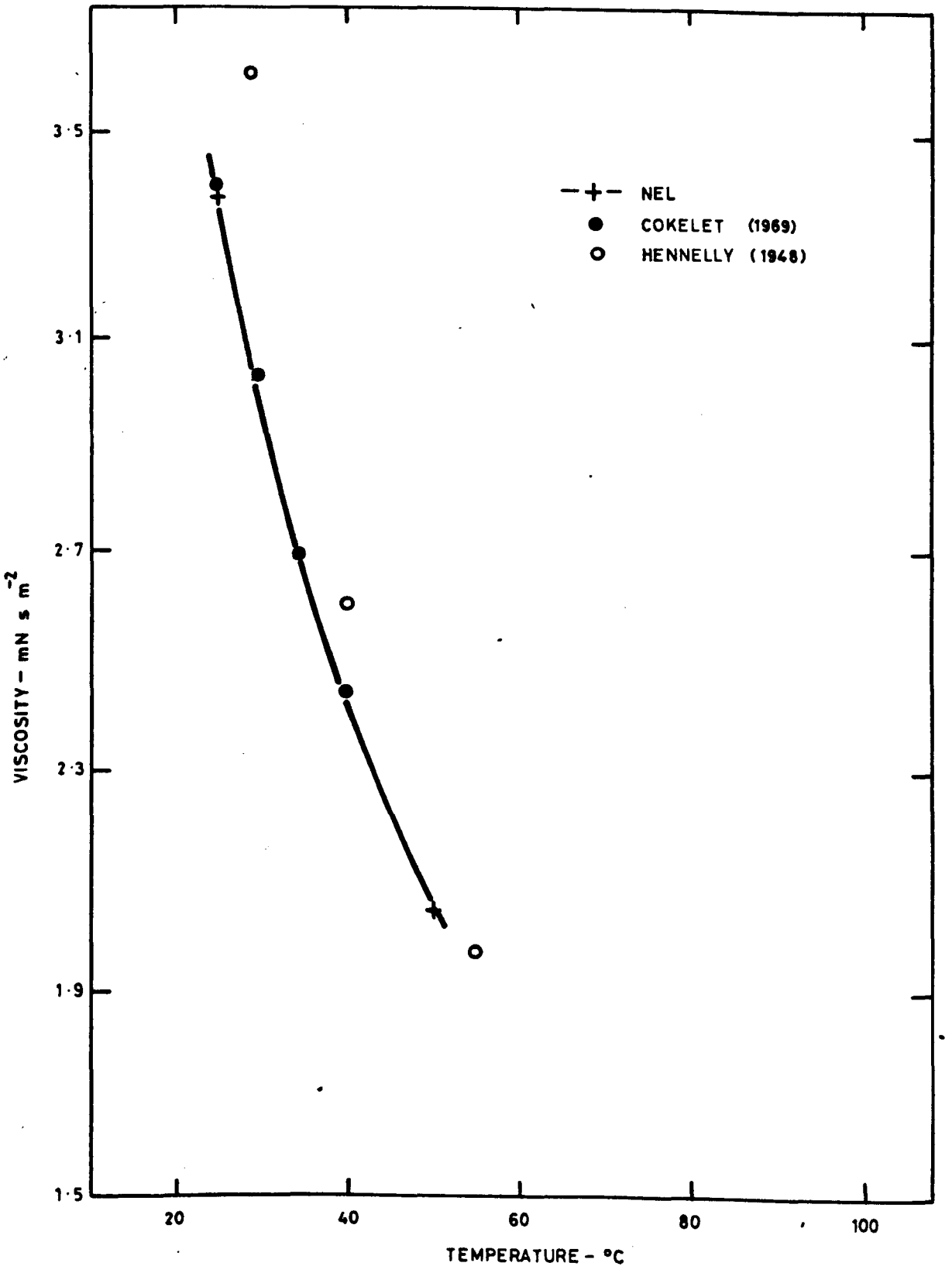

FIG 7.9 VISCOSITY OF 1-BROMODODECANE

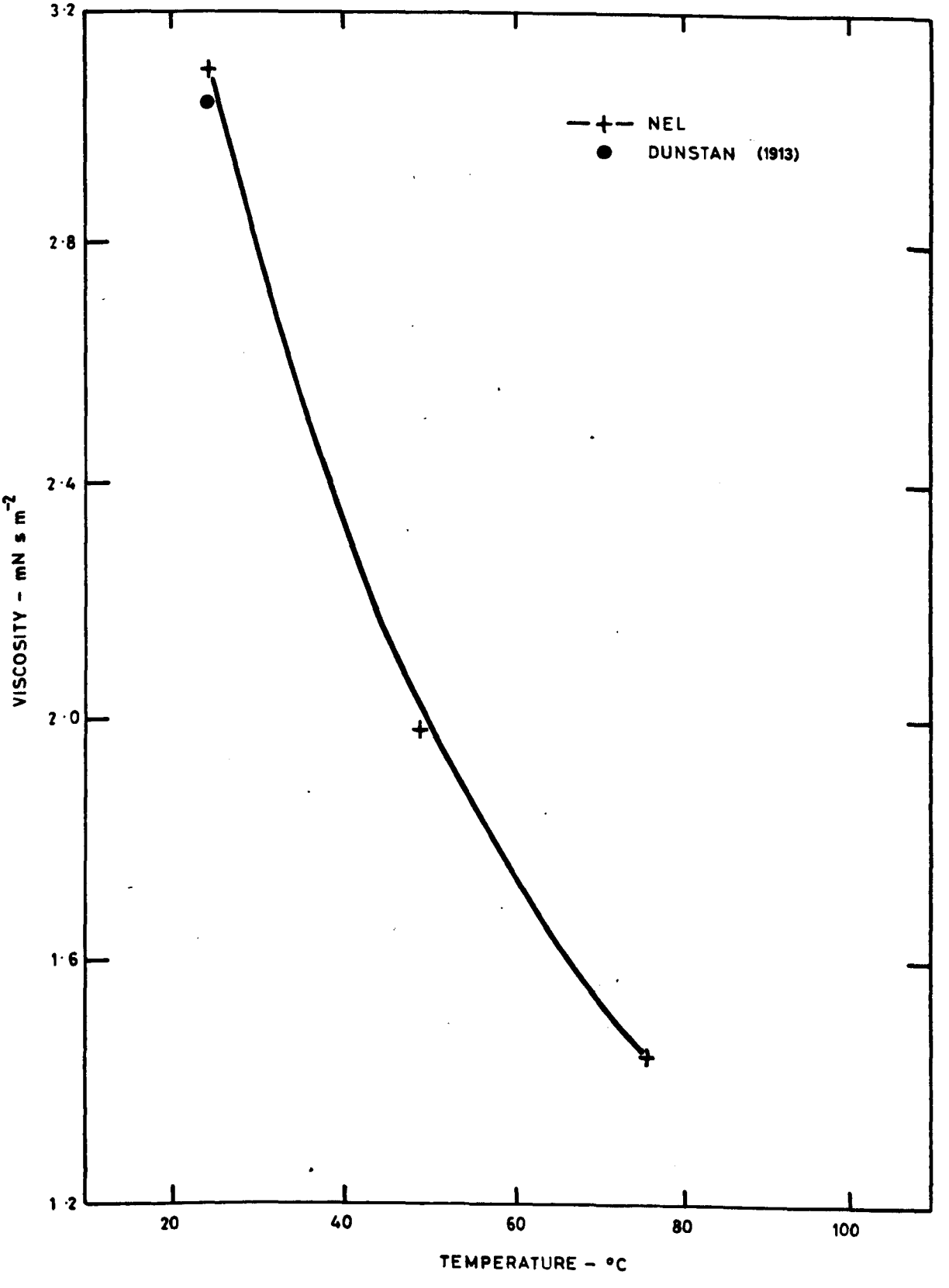

FIG 7.10 VISCOSITY OF 1,5-DIBROMOPENTANE

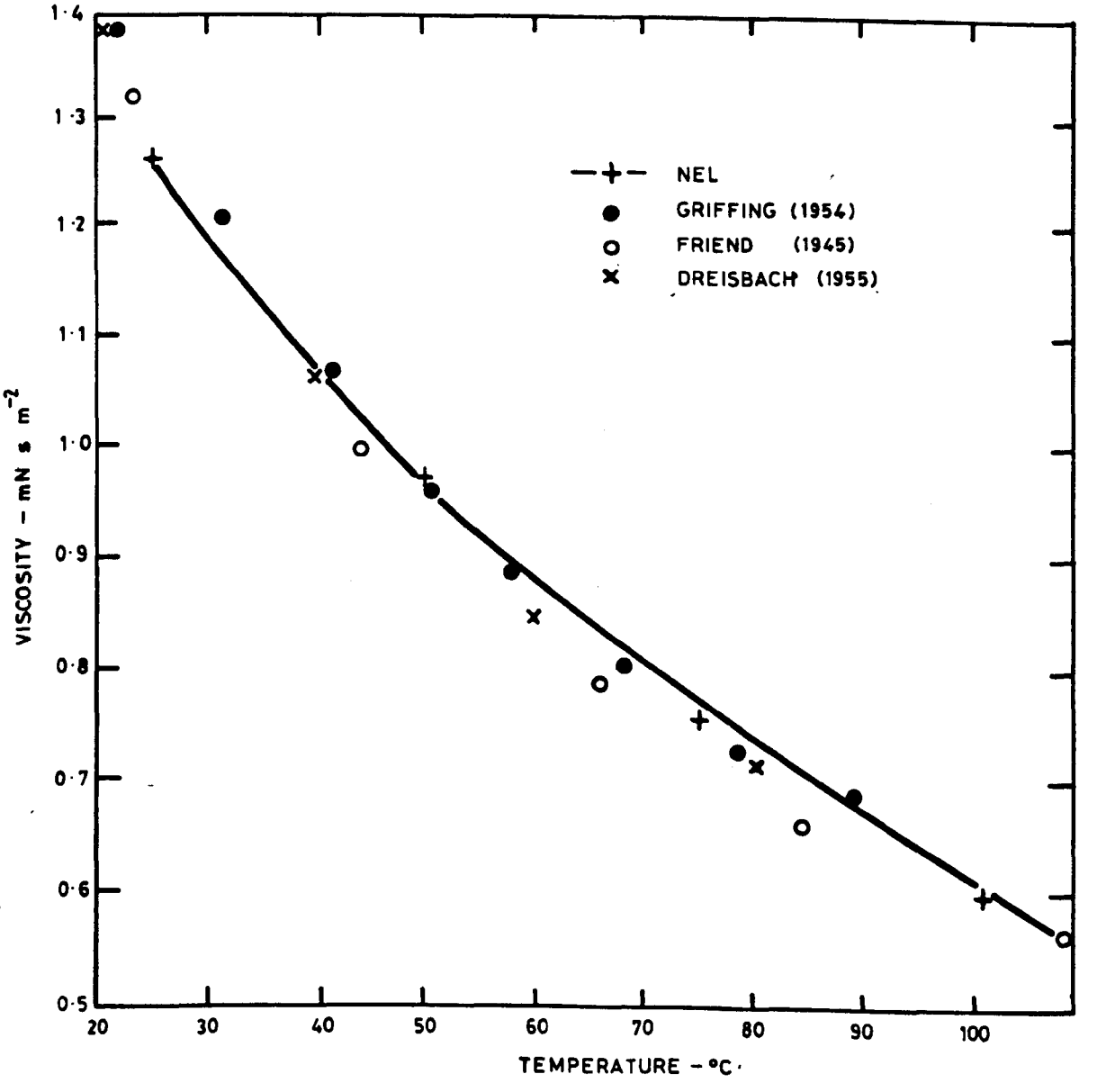

FIG 7.11 VISCOSITY OF 1,2— DICHLOROBENZENE

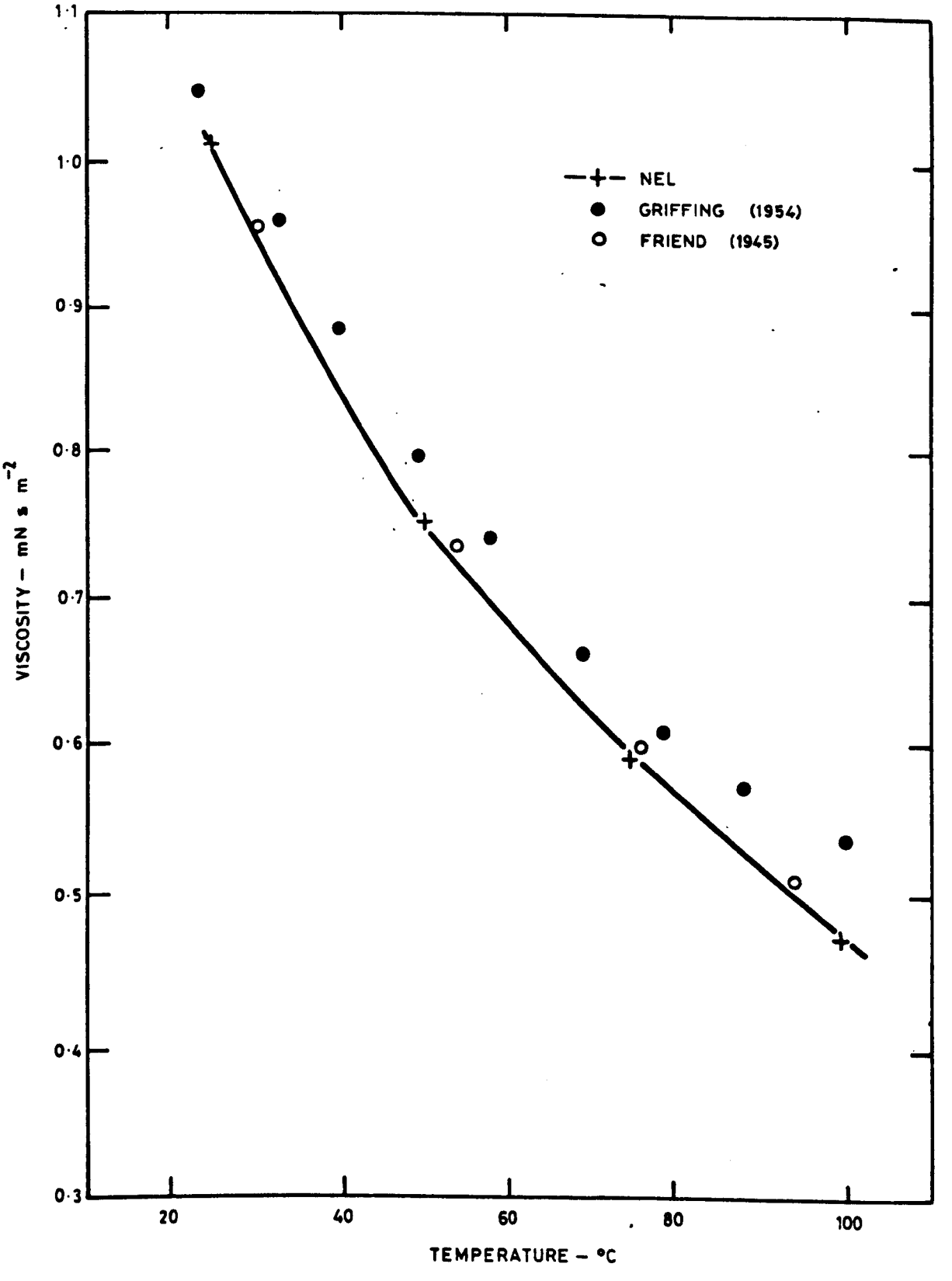

FIG 7.12 VISCOSITY OF 1,3 – DICHLOROBENZENE

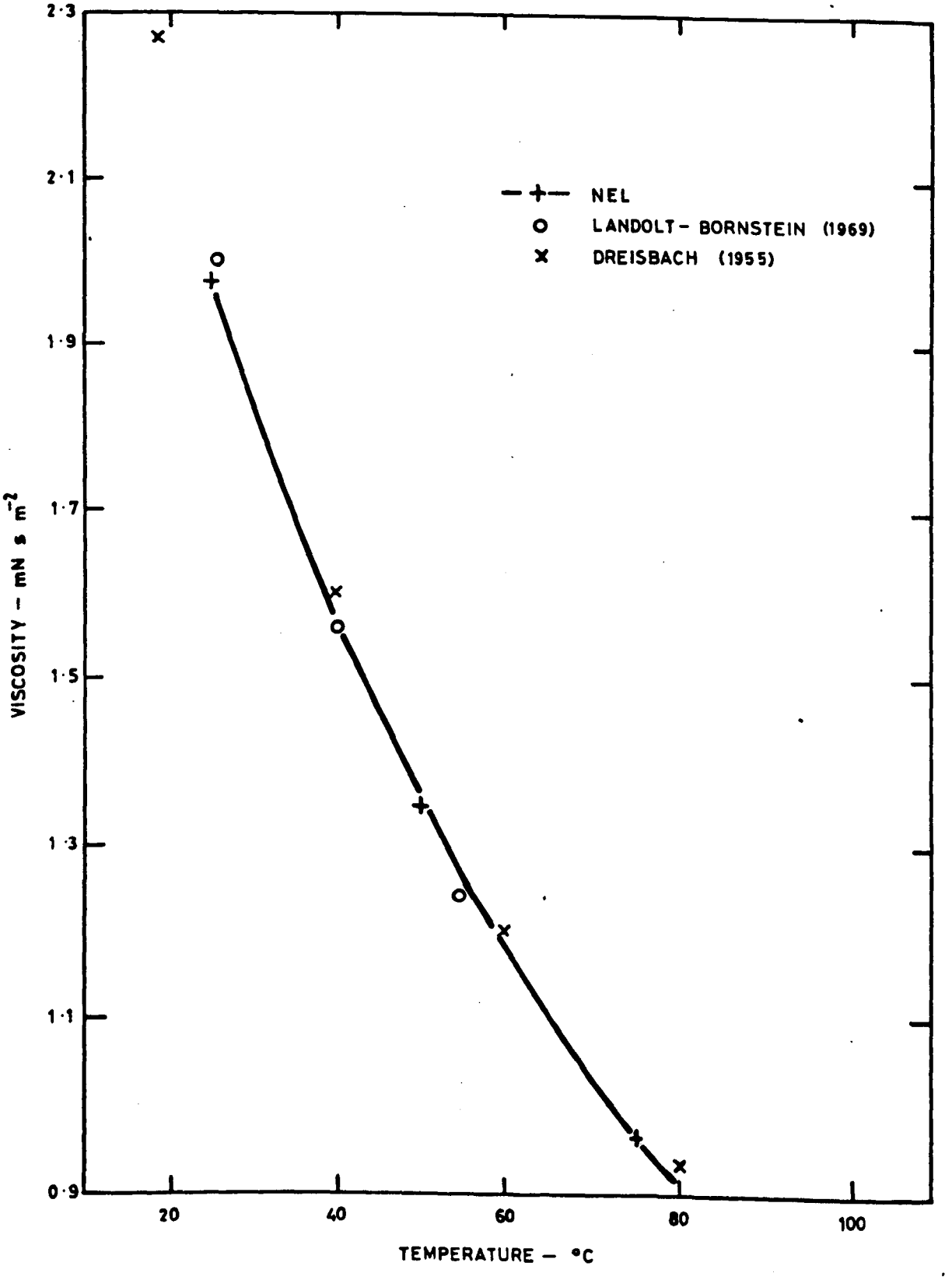

FIG 7.13 VISCOSITY OF BROMOCYCLOHEXANE

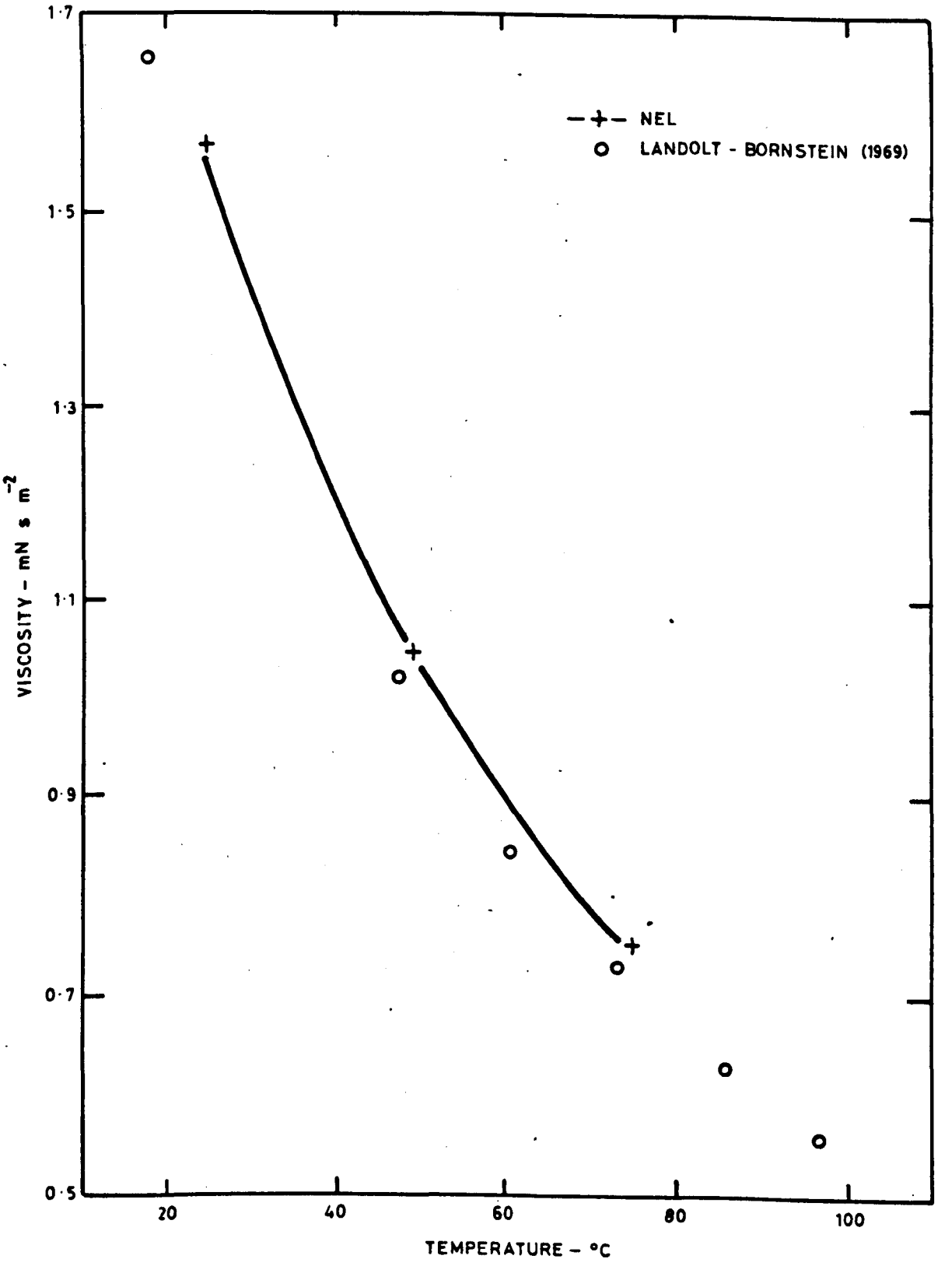

FIG 7.14 VISCOSITY OF CHLOROCYCLOHEXANE

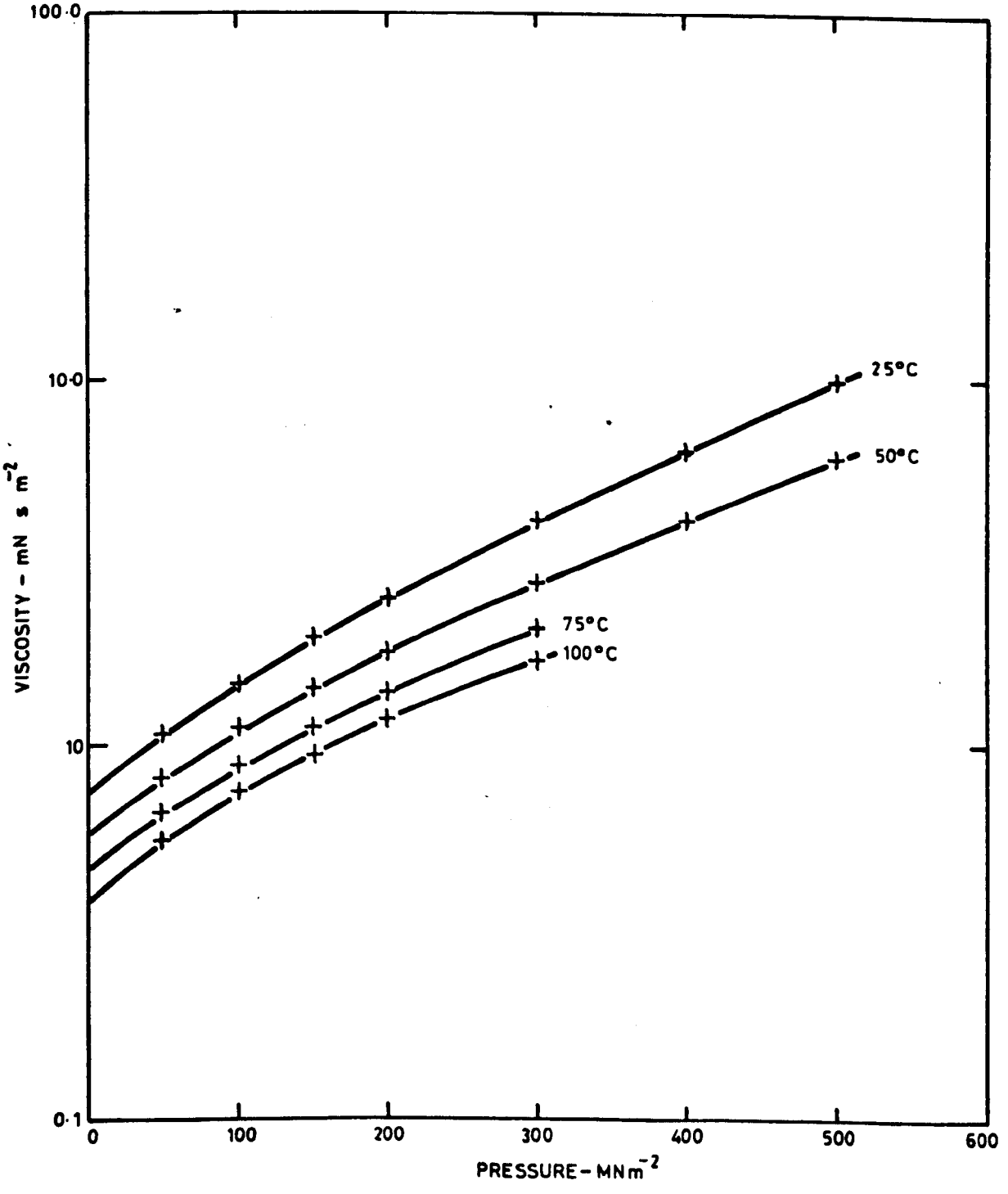

FIG 7.15 VISCOSITY OF 1-BROMOPENTANE UNDER PRESSURE

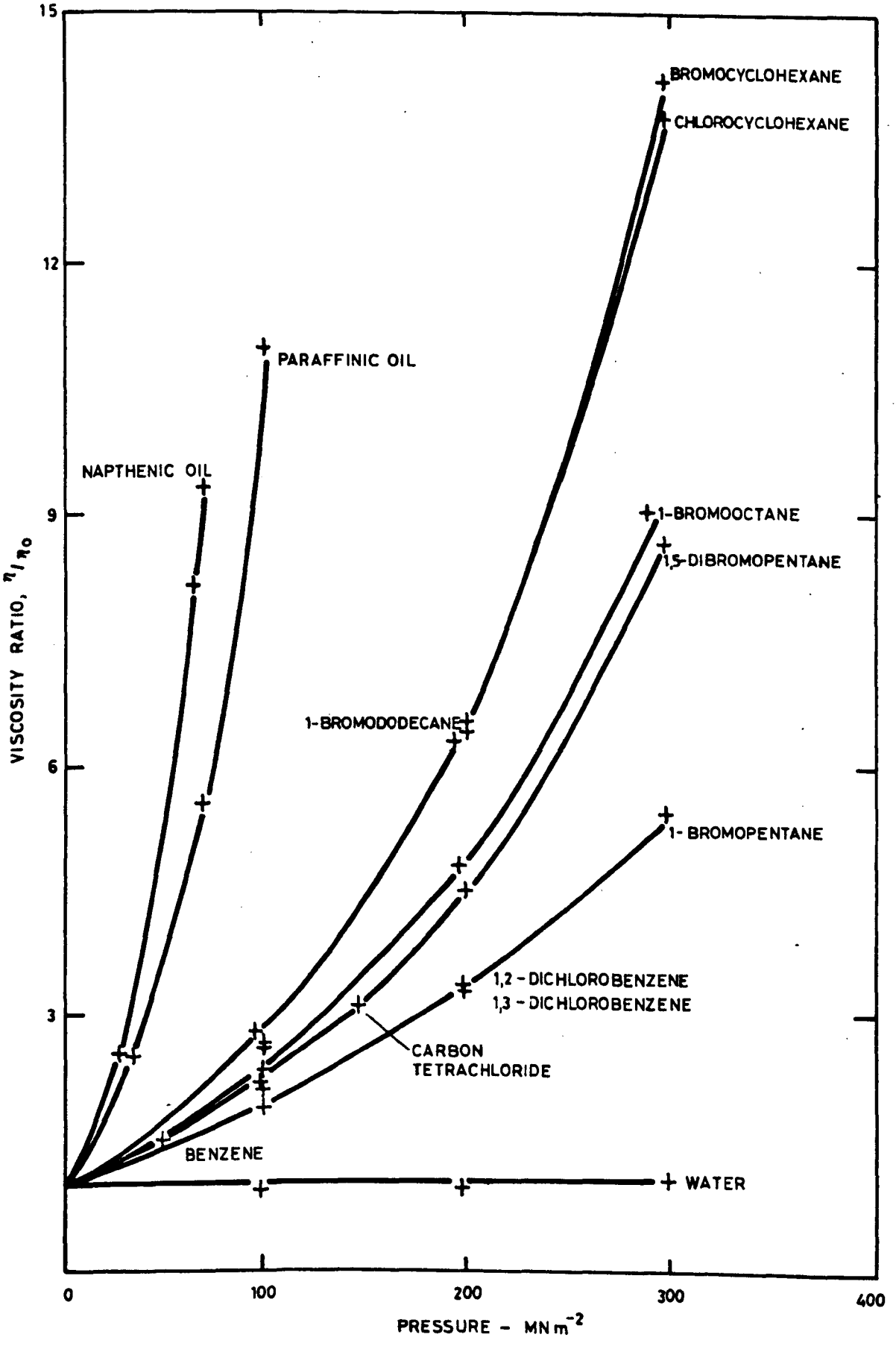

FIG 7.16 VISCOSITY RATIOS AT 25°C

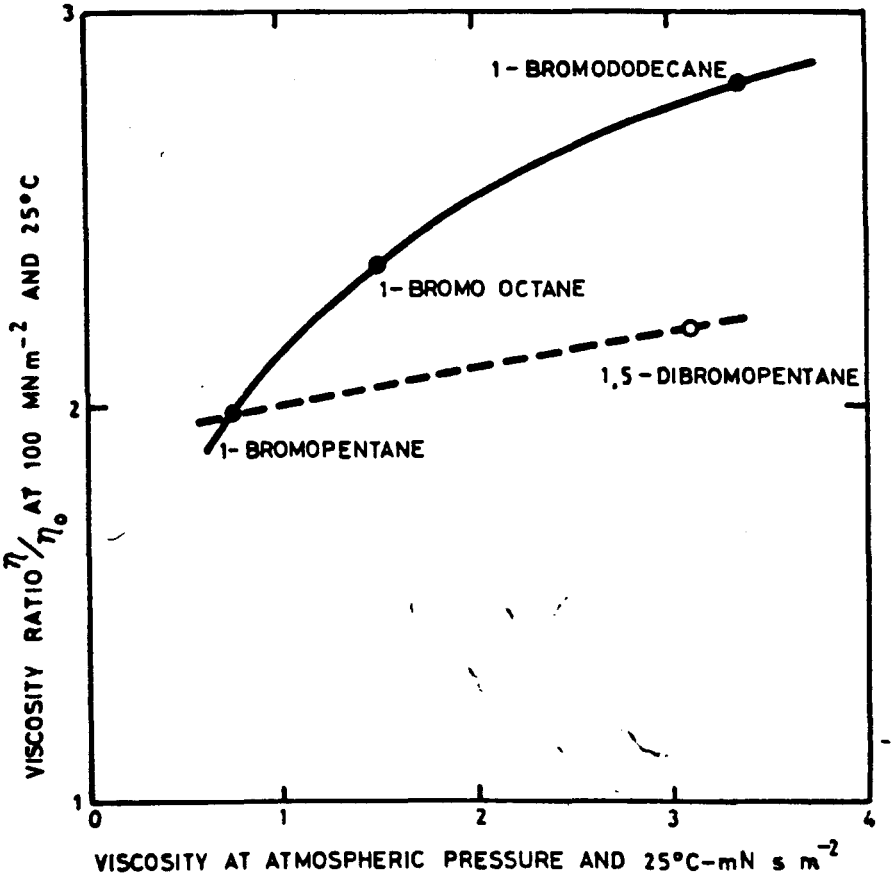

FIG 7.17 VISCOSITY RATIOS OF BROMOALKANES

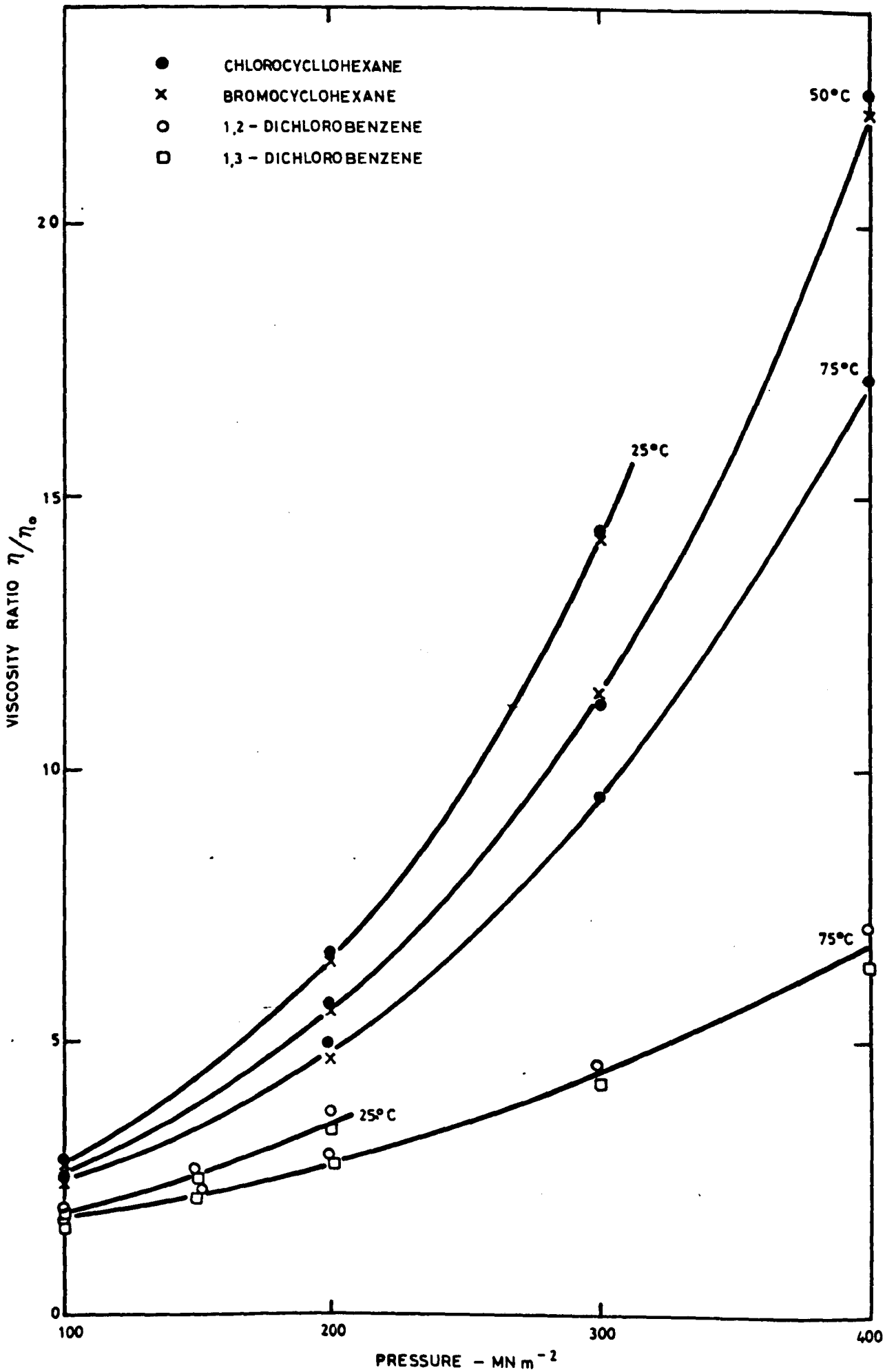

FIG 7.18 VISCOSITY RATIOS OF LIQUIDS HAVING SIMILAR MOLECULES

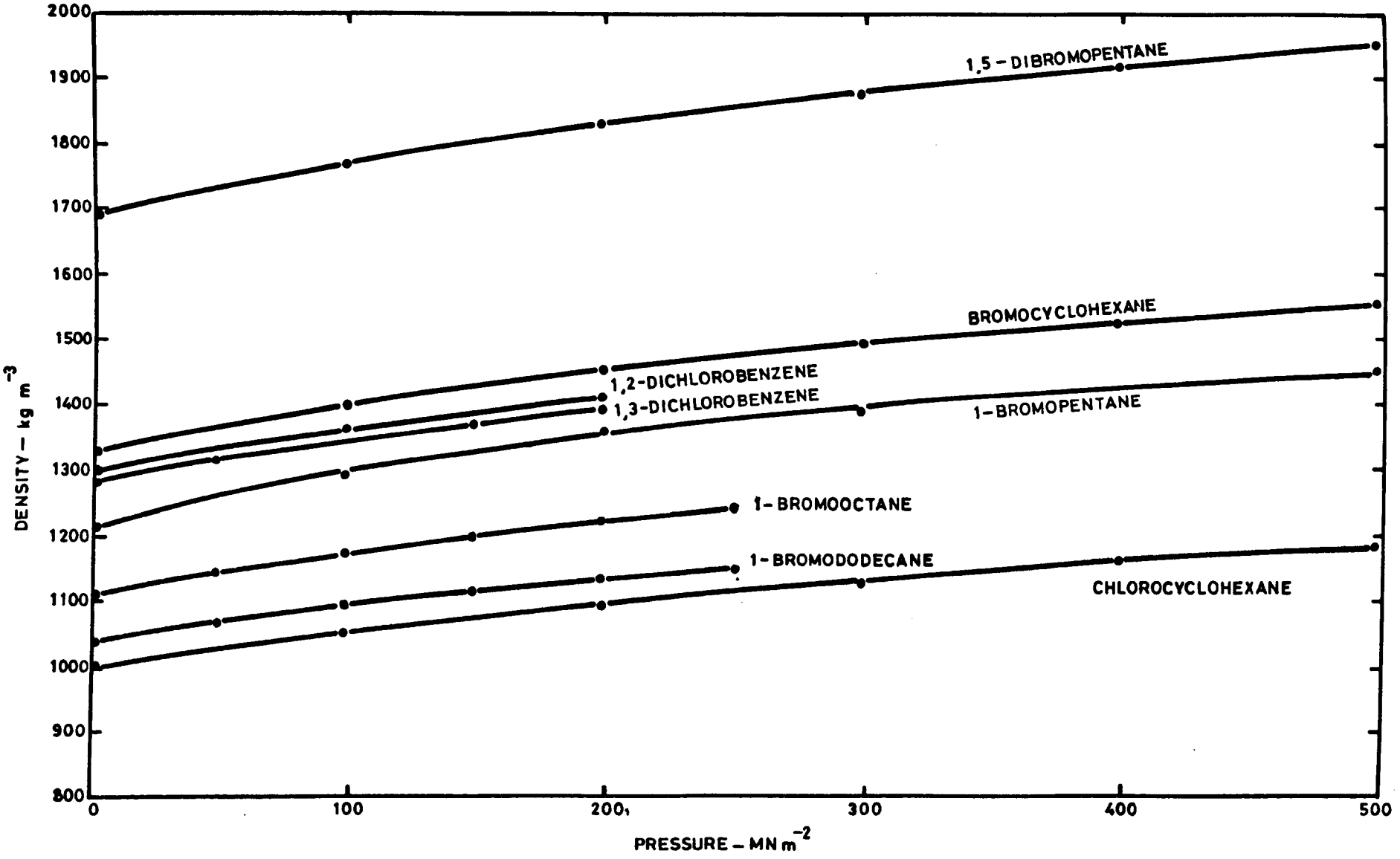

FIG 7.19 DENSITIES AT 25°C

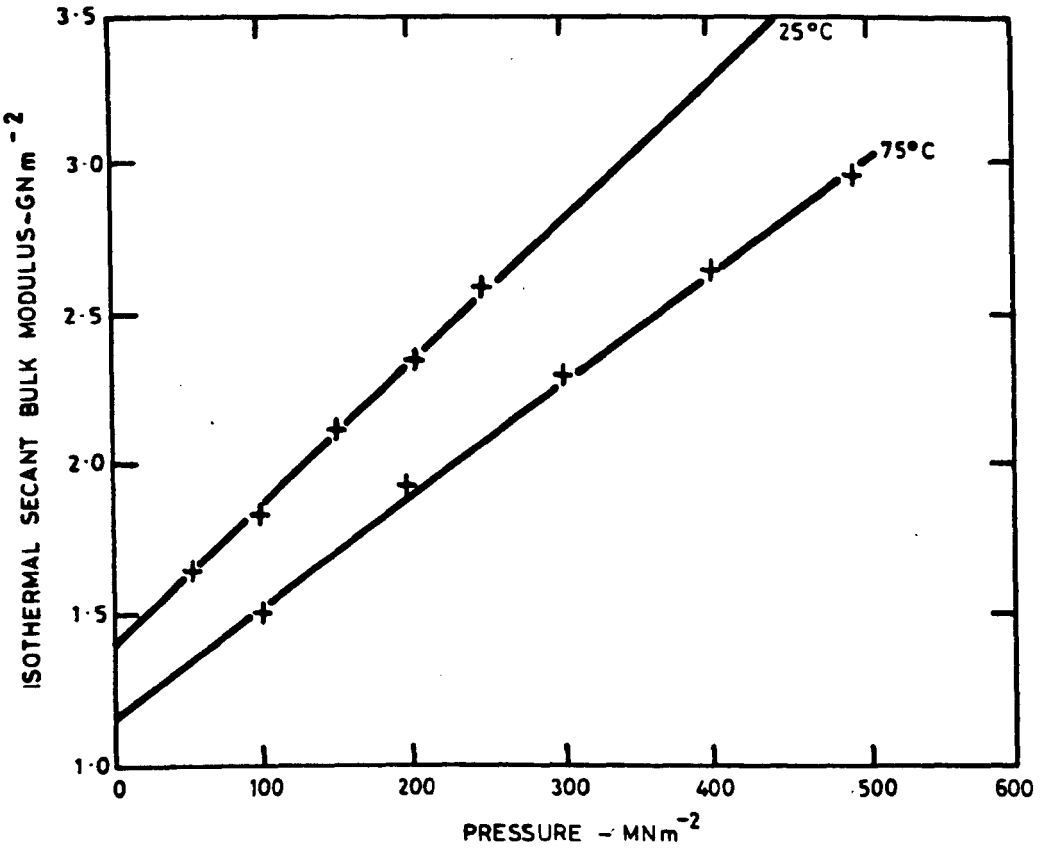

FIG 7.20 BULK MODULUS OF 1-BROMODODECANE

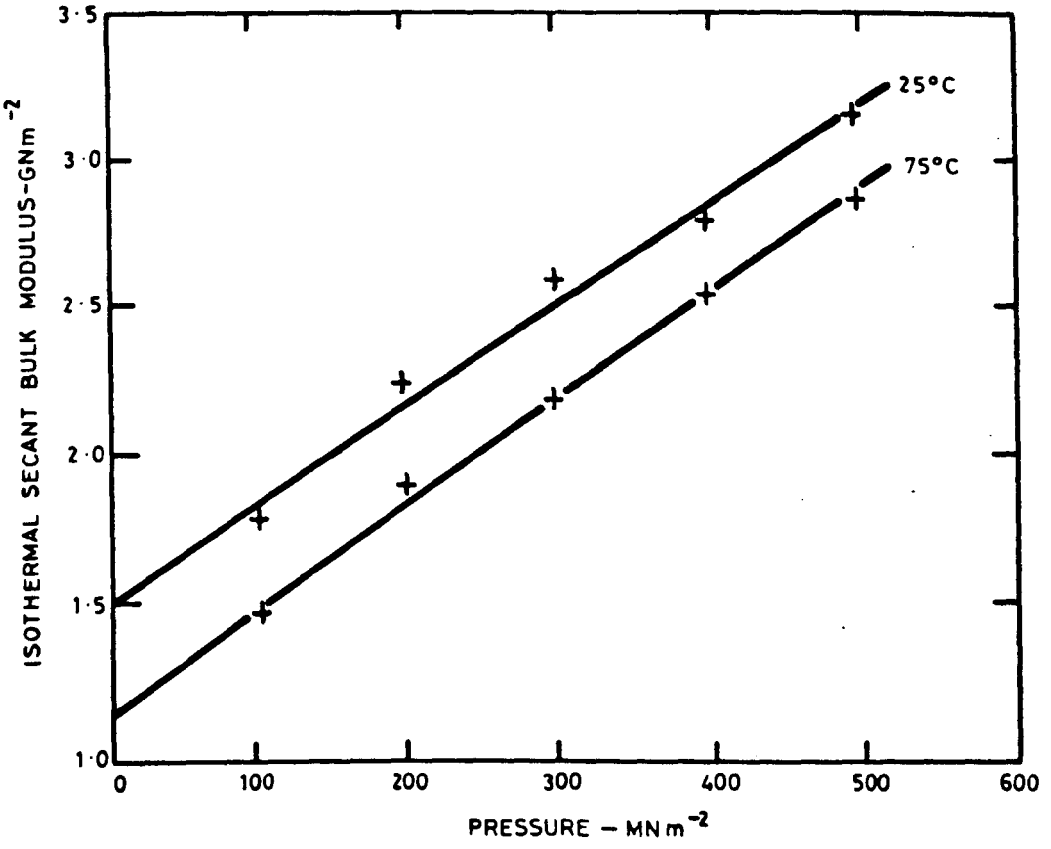

FIG 7.21 BULK MODULUS OF CHLOROCYCLOHEXANE

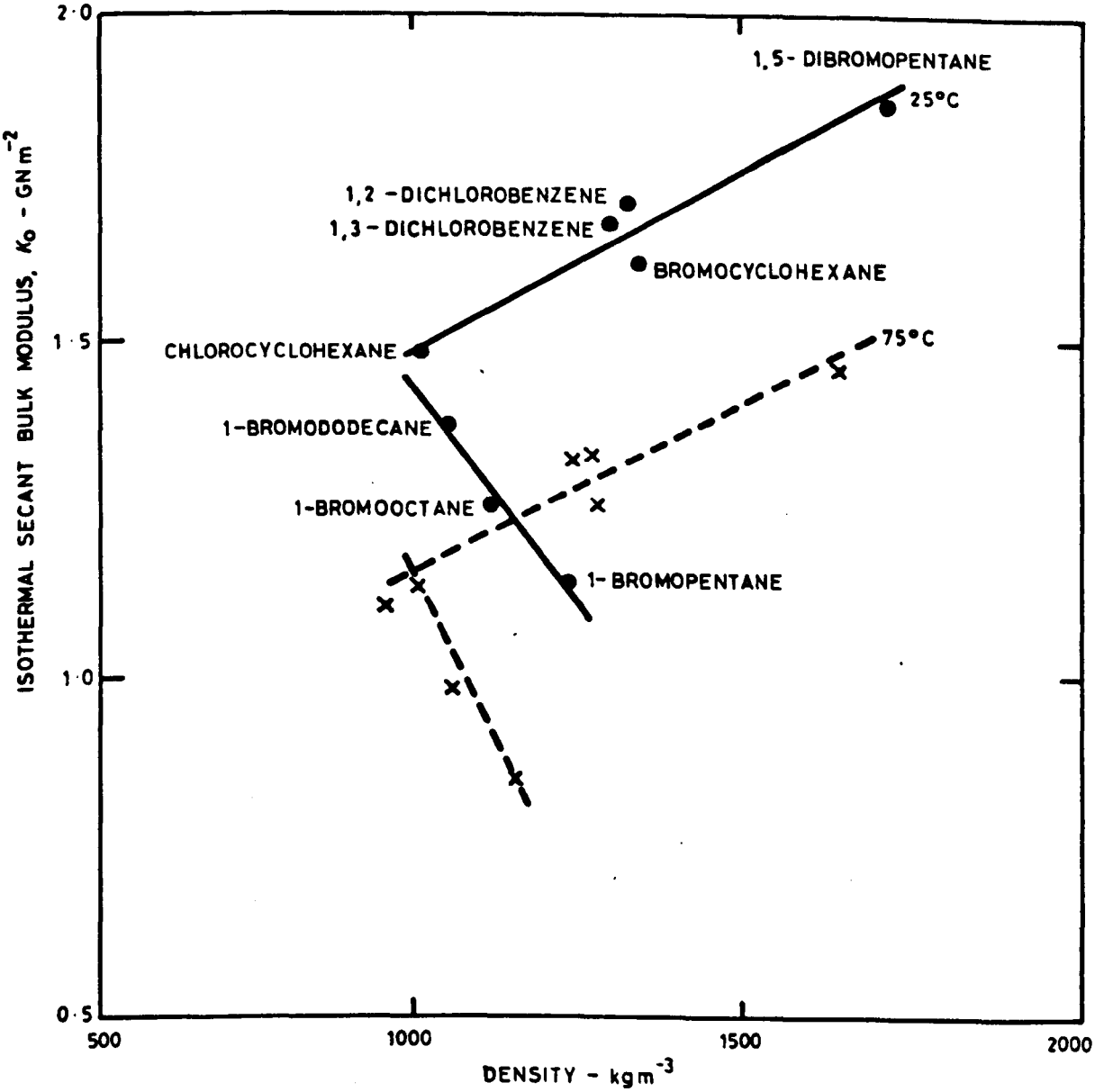

FIG 7.22 RELATIONS BETWEEN BULK MODULUS AND DENSITY AT ATMOSPHERIC PRESSURE

CHAPTER 8

PREDICTION RESULTS

SUMMARY OF CHAPTER 8

8 PREDICTION RESULTS

The methods and correlations derived in Chapter 4 are tested by using them to predict the viscosity of the liquids measured as part of this investigation and of the liquids used in the derivation of the correlations. Predictions have been carried out using only structural or critical data, using one viscosity at atmospheric pressure and critical data, and using two viscosities at atmospheric pressure.

For the sixty-five liquids at atmospheric pressure with two viscosities available the significant structure equation estimates viscosity at other temperatures with an average deviation of about 2 per cent - a values comparable with the accuracy of many of the data. If only one viscosity at atmospheric pressure is available and the energy constant correlation is used, the average deviation rises to 10 per cent; if the structure count and energy constant correlation are used it rises to 23 per cent. Similar values are obtained for the halogenated liquids.

At elevated pressures viscosities are estimated using the mean compressibility given in Chapter 4 and two viscosities at atmospheric pressure. Predictions carried out in this way deviate from experimental measurements by up to about 100 per cent at 500 MN m^{-2}. However corresponding predictions by Roeland's method deviate by up to 500 per cent.

CHAPTER 8 - PREDICTION RESULTS

LIST OF TABLES

LIST OF FIGURES

8 PREDICTION RESULTS

The significant structure theory was tested as a prediction method using the correlations derived in Chapter 4. The atmospheric pressure data used to derive the correlations were used in the first tests with two viscosities to obtain the transmission coefficient and the energy constant; with only one viscosity and the energy constant correlation; and finally with the energy constant correlation and the structure count. A similar series of tests was carried out using the new data at atmospheric and high pressure. In all cases densities at the required temperatures and pressures were known.

8.1 Predictions Using Atmospheric Pressure Data

Table 8.1 summarises the results of tests using the same data as in Chapter 4. Column (1) of the table lists, for comparison, the standard deviation of the differences between observed and calculated viscosities when two values are available to calculate K' and K". The values given in column (2) were observed for the same data when the energy constant, K", was calculated from equations 4.2, 4.3, and 4.4, and the transmission coefficient, K', from a single viscosity at the lowest temperature available in each case. The values given in column (3) were obtained using both the energy constant correlation and the structure count to obtain the transmission coefficient.

While the estimates given in Table 8.1 are not predictions in the strict sense of the word, since the same data were used to develop the correlations, they provide a useful indication of the ability of the significant structure equation and the correlations to deal with a variety of molecular types.

The average value of the standard deviations given in column (1) is 1.9 per cent. If two viscosities are available, therefore, the significant structure equation can provide reasonably good estimate of viscosity over quite wide temperature ranges as already shown in Figs 4.1 and 4.2.

The corresponding average in column (2) is 9.9 per cent. Clearly the expected accuracy for this procedure is less. For ethane, propane, and hexane the flexibility calculated by equation 4.2 is rather high. This leads to low predicted values of the energy constant which result in large deviations, particularly for ethane which has a predicted viscosity 78.8 per cent high at -110°C. Predicted viscosities for 1,1-diphenylheptane are also high for the same reason. In general it is clear that the influence of flexibility is more complex than suggested by equations 4.2 and 4.3. In many cases, however, it may be better to use the energy constant correlation than to rely on two viscosities at temperatures within say 25°C of each other.

When both energy constant and transmission coefficient are calculated without using viscosity, the deviations increase markedly as shown in column (3). In this case the average of the standard deviations is 23.3 per cent. Some of the larger deviations are clearly caused by poor critical data. This is particularly obvious for tridecane which has a value of Z_c 10 per cent lower than the mean of dodecane and tetradecane.

8.2 Predictions Using the New Measurements

Tests similar to those described in the previous section were carried out using the new experimental measurements of the eight halogenated hydrocarbons. For these liquids critical volume and critical compressibility factor were estimated by the methods of Lydersen (1955) and Garcia-Barcena (1958) respectively, and the values obtained are given in Table 8.2. The maximum differences between measured and calculated viscosities at atmospheric pressure are given in Table 8.3. Results for bromopentane are also shown in Fig. 8.1.

For predictions at elevated pressure two viscosities at atmospheric pressure were used in each case to calculate K' and K" while the critical properties were used to obtain v_o as before. Since the values of the solid-like compressibility obtained in Chapter 4 were not sufficiently reliable and did not exhibit regular behaviour, a mean value was used with a negative temperature coefficient:

$$\beta = (13.9 - 0.024T)10^{-11} \ m^2N^{-1} \qquad (8.1).$$

The resulting predictions for those liquids were poor at all temperatures when compared with the present data, as shown in Table 8.4, though the predictions for 1,3-dichlorobenzene were comparatively good. The results for bromopentane are shown on Fig. 8.2.

8.3 Discussion

While the correlations developed here do not provide accurate estimates of viscosity at atmospheric pressure unless one or more experimental values are available, they nevertheless give estimates comparable with those of other recommended methods. Reid and Sherwood (1966) recommend the methods of Souders (1938) and Thomas (1946) with the qualifications: "Neither method is very reliable, ... Usually errors do not exceed

30 per cent, but not infrequently the methods fail to yield a reasonable value." The present results could be described in similar terms though the largest deviations can usually be attributed to poor critical data as in the case of tridecane mentioned earlier.

The results of all the tests are summarised in Table 8.4 for the original liquids and for the eight halogenated liquids. In this case the standard deviations are calculated for all of the points in each group instead of for each liquid. The two groups show similar deviations in each type of test and the comparison confirms that the correlations may be applied to liquids other than those used in derivations, though clearly further testing is necessary to establish the method for unsaturated chains, highly polar liquids etc.

The predictions at high pressure produced by the mean solid-like compressibility are compared with predictions by Roelands' (1966) method in Fig. 8.2. Roelands' method was developed for mineral oils and may be applied to pure liquids of high viscosity. The pressure effect is calculated from a parameter which may be calculated from viscosity and density at atmospheric pressure and 40°C. For the liquids examined here Roelands' method is clearly of little value since it predicts increases in viscosity similar to those observed for mineral oils and much greater than those of simple liquids.

Predictions by the significant structure method were always more accurate than by Roelands' method and gave a standard deviation of 28 per cent when compared with the experimental measurements under pressure. Predicted viscosities for the cyclic compounds and bromo-dodecane were lower than the measured values while those for the

other liquids were either higher or both higher and lower.

The high pressure tests show that while the significant structure method as used above can produce reasonable estimate of viscosity the accuracy is poor and decreases with pressure, probably because the correlations developed do not describe sufficiently well the effects of molecular shape and structure. In fact quite accurate predictions can probably be made using plots of viscosity ratio against pressure (as in Fig. 7.16) for a variety of liquids at the required temperature, by choosing a ratio based on a subjective judgement of molecular structure.

TABLE 8.1

RESULTS OF PREDICTIONS AT ATMOSPHERIC PRESSURE FOR ORIGINAL LIQUIDS

Liquid	Standard deviations (%)		
	(1)	(2)	(3)
methane	1.21	1.78	-
ethane	2.34	60.26	28.84
propane	4.05	49.65	30.42
butane	3.44	11.82	23.55
pentane	0.07	0.21	1.08
hexane	0.08	0.28	1.70
heptane	0.39	0.83	1.63
octane	0.72	3.79	6.57
nonane	0.56	4.04	6.95
decane	0.33	4.66	11.39
undecane	0.36	1.59	6.11
dodecane	1.03	5.26	6.26
tridecane	2.38	19.38	121.29
tetradecane	0.79	0.80	0.75
pentadecane	4.65	12.83	3.15
hexadecane	5.13	5.81	5.93
heptadecane	1.15	2.77	22.91
octadecane	8.30	4.57	9.57
nonadecane	2.58	5.69	60.08
eicosane	3.16	2.57	31.47
cyclopentane	0.68	0.46	0.51
methylcyclopentane	1.97	18.43	30.80
ethylcyclopentane	1.30	11.35	23.77
cyclohexane	0.76	22.20	42.68
methylcyclohexane	1.23	22.04	47.94
benzene	0.12	0.67	1.91
toluene	0.59	3.49	5.67
ethylbenzene	0.31	0.31	4.66
o-xylene	0.26	6.23	9.90
m-xylene	0.31	4.43	21.19
p-xylene	0.13	3.30	20.81
n-propylbenzene	0.35	0.24	5.82
isopropylbenzene	0.37	5.55	23.27
1-methyl4-ethylbenzene	0.20	5.09	25.60
chlorobenzene	1.06	4.87	9.81
m-dichlorobenzene	1.34	15.53	25.97
o-dichlorobenzene	1.30	16.35	23.36
p-dichlorobenzene	0.10	8.11	18.28

TABLE 8.1 (Contd)

Liquid	Standard deviations (%)		
	(1)	(2)	(3)
1,1-diphenylethane	2.81	12.07	64.41
1,1-diphenylheptane	10.53	49.43	63.14
9-n-octylheptadecane	2.47	21.40	50.79
9(2-phenylethyl)heptadecane	7.37	25.48	42.38
1-alpha-naphthylpentadecane	5.59	23.85	24.69
spiro4,5decane	0.92	7.24	22.91
spiro5,5undecane	1.14	2.16	3.68
cis-decahydronaphthalene	1.07	5.32	15.41
trans-decahydronaphthalene	2.77	1.92	7.01
cis-octahydroindene	0.91	0.68	37.00
trans-octahydroindene	1.71	3.48	35.20
2-methylbutane	-	5.96	18.06
2-methylpentane	-	5.57	27.81
3-methylhexane	-	0.37	22.94
2,2-dimethylbutane	-	19.94	50.91
2,4-dimethylpentane	-	1.28	26.86
carbon tetrachloride	2.42	2.38	-

T A B L E 8.2

ESTIMATED CRITICAL PROPERTIES

Liquid	Critical volume* (cc/gm mole)	Critical compressibility factor†
1-bromopentane	385.0	0.258
1-bromooctane	550.0	0.244
1-bromododecane	770.0	0.227
1,5-dibromopentane	453.0	0.240
1,2-dichlorobenzene	358.0	0.248
1,3-dichlorobenzene	358.0	0.250
bromocyclohexane	378.5	0.251
chlorocyclohexane	357.5	0.256

*Estimated by the method of Lydersen (1955)

†Estimated by the method of Garcia-Barcena (1958)

T A B L E 8.3

PREDICTIONS FOR 8 HALOGENATED LIQUIDS AT ATMOSPHERIC PRESSURE

Liquid	Maximum deviations (%)		
	(1)	(2)	(3)
bromopentane	-2.9	- 9.3	+15.5
bromooctane	-2.5	- 2.8	- 2.9
bromododecane	-	+ 3.6	-14.4
1,5-dibromopentane	+1.8	-17.4	+45.2
1,2-dichlorobenzene	-4.0	-18.9	+52.7
1,3-dichlorobenzene	-3.1	-18.6	+76.7
bromocyclohexane	-1.7	+ 6.3	-38.8
chlorocyclohexane	-0.3	+21.1	-52.8

T A B L E 8.4

PREDICTIONS FOR 8 HALOGENATED LIQUIDS AT ELEVATED PRESSURE

Liquid	Standard deviations (%) (1)
bromopentane	50.8
bromooctane	15.4
bromododecane	13.6
1,5-dibromopentane	14.6
1,2-dichlorobenzene	11.5
1,3-dichlorobenzene	5.5
bromocyclohexane	37.7
chlorocyclohexane	27.4

TABLE 8.5

PREDICTION RESULTS FOR ORIGINAL AND NEW DATA AT ATMOSPHERIC PRESSURE

Test method	Original data			New data		
	Standard deviation (%)	No of points	No of liquids	Standard deviation (%)	No of points	No of liquids
1 Using two viscosities	2.8	145	50	2.5	11	8
2 Using one viscosity with energy constant correlation	16.6	150	55	12.0	19	8
3 Using energy constant correlation and structure count	30.9	146	53	35.5	27	8

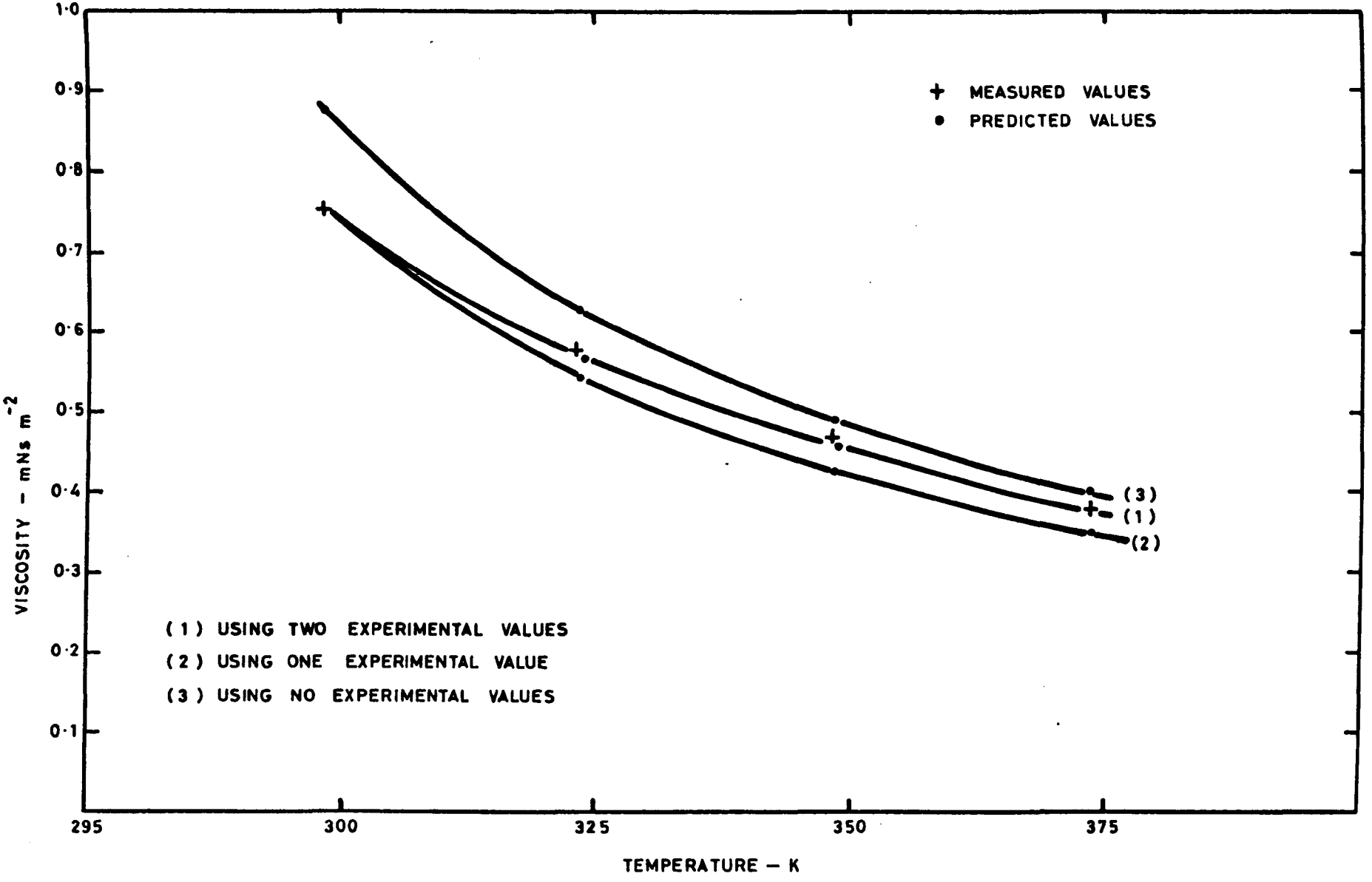

FIG 8·1 PREDICTED VISCOSITIES OF 1 – BROMOPENTANE AT ATMOSPHERIC PRESSURE

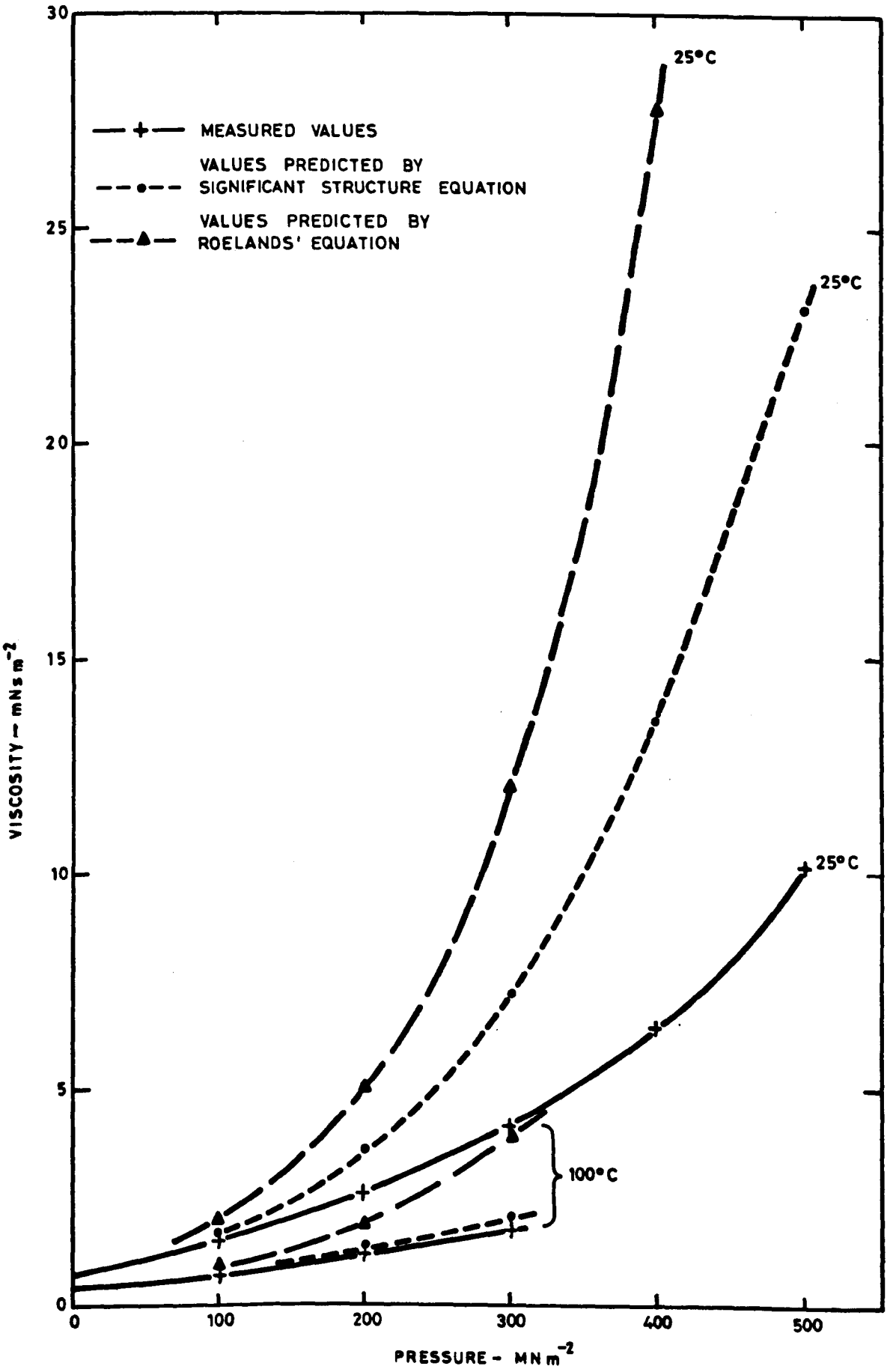

FIG 8.2 PREDICTED VISCOSITIES OF 1-BROMOPENTANE AT ELEVATED PRESSURE

C H A P T E R 9

CONCLUSIONS

9 CONCLUSIONS

1 Viscosity and density data are provided for eight halogenated hydrocarbons. These data show that change in viscosity with pressure is similar for molecules of similar shape. The measurements of benzene and carbon tetrachloride extend the temperature and pressure ranges of existing data for these liquids, while the results for water confirm the reliability of the experimental procedure to high pressure.

2 The self-centring sinkers which have been developed for this work approach the theoretical performance for falling cylinders and do not require pegs or other mechanical centring devices.

3 The limiting volume at absolute zero, which may be calculated from critical properties, has been found to be a useful approximation to the volume of the solid-like state in the significant structure theory of viscosity.

4 For non-spherical molecules the other constants in significant structure theory vary in a regular manner with structure, if determined by fitting to viscosity data. They do not, however, retain their original meaning but become average values over the various modes of flow which occur, and depend on the shape of the molecule.

5 The solid-like compressibility has not been obtained with sufficient accuracy to allow it to be related to structure, though it does have a magnitude characteristic of a solid-like state.

6 Viscosity predictions carried out using the correlations developed here are comparable with those by other methods but are cumbersome

and would be difficult to apply except by computer. They also require volume data.

The performance of the falling body viscometer has conformed quite closely to the theoretical performance expected subject to the assumptions made. This suggests that it should be possible to develop an absolute method based on the present design. However three important factors need further investigation:

i Entry and exit effects. While the present measurements have confirmed that these are small for the apparatus used a method is required to calculate the magnitude of the effects for different geometries.

ii Centring effects. These have been dealt with experimentally in this work but for more general use analytical or numerical relations derived from solutions to the equations of motion for transient non-coaxial flow are required.

iii Effects of turbulence. The results show that the influence of surface finish and probably entry and exit geometry can be critical. Carefully controlled experiments with viscometers of different diameters and surface finishes are required for a general study of transitions in this type of instrument.

This work shows that structure and shape play an important role in determining liquid viscosity and that the constants which occur in the significant structure theory are strongly influenced by the types of structure which are present. Though the magnitude of the constants which have been derived are in some cases unrealistic in terms of the theory for spherical molecules, they are of a similar magnitude. From the theoretical point of view the situation is

clearly unsatisfactory, since theories can only be properly tested in a strictly predictive way. From the practical point of view, however, the methods developed here provide means of quantifying shape and structure which are appropriate to the significant structure equation. Empirical relations derived by van Velzer et al (1972) and based on the Andrade equation also show the influence of structure on viscosity.

The main factor which has limited the present work has been the need to obtain values for three constants for saturation pressure viscosities, and a fourth for high pressure. When such constants are derived by fitting to data, slight errors in the values of one constant, say v_o, produce apparent variations in the others which tend to obscure the underlying relationships which are sought. The independently derived values of v_o were used here in an attempt to minimise this effect and were partially successful. However the form of the equation and the number of constants which had to be obtained by fitting made it difficult to produce the wide ranging and accurate correlations which are necessary for a practical prediction method.

The apparent decrease in v_o at higher temperatures discussed in Chapter 4 illustrates this type of problem. The observed decrease in compressibility of the solid-like state with increasing temperature could be reduced or perhaps eliminated, by allowing a negative thermal expansion coefficient for v_o, but it would then be necessary to specify two parameters to describe small temperature and pressure variations of v_o, a parameter which is itself difficult to obtain accurately. While measured van der Waals' volumes decrease with temperature due to molecular deformation (Bondi (1968)) such

behaviour in a solid-like state must be due to the failure of the assumptions inherent in the theory.

Further development of the significant structure equation for non-spherical molecules must lead to a reduction in the number of unknown constants, either by defining the effects of shape on existing or modified parameters or by simplifying the equation in some way (say by setting $K' = 1$) and empirically examining the effects of structure on the remaining unknowns.

REFERENCES

1 A.I.Ch.E. Physical property estimation system. American Institute of Chemical Engineers, New York, 1965.

2 AMERICAN PETROLEUM INSTITUTE. Selected values of properties of hydrocarbons and related compounds. Research Project 44. New York: American Petroleum Institute, 1969.

3 AMERICAN SOCIETY OF MECHANICAL ENGINEERS. Viscosity and density of over forty lubricating fluids of known composition at pressures to 150 000 psi and temperatures to 425 F. New York: American Society of Mechanical Engineers, 1953.

4 ANDRADE, E. N. da C. The viscosity of liquids. Nature, 1930, 125(3148), 309-310.

5 BARLOW, A. J., LAMB, J., and MATHESON, A. J. Viscous behaviour of supercooled liquids. Proc. Roy. Soc.A, 1966, 292, 322-342.

6 BIRD, R. B., STEWART, W. L., and LIGHTFOOT, E. N. Transport phenomena. New York, London: John Wiley and Sons, Inc., 1960.

7 BOELHOWER, J. W. M. and TONEMAN, L. H. The viscosity pressure dependence of some organic liquids. Inst. Mech. Eng. Conference on Lubrication and Wear, 1-3 October 1957, pp 214-218.

8 BONDI, A. Physical chemistry of lubricating oils. New York, Reinhold Publishing Corp., 1951.

9 BONDI, A. Physical properties of molecular crystals, liquids and glasses. New York, London, Sydney: John Wiley and Sons, Inc., 1968.

10 BORN, M. and GREEN, H. S. A general kinetic theory of liquids. I. The molecular distribution functions. Proc. Roy. Soc. A, 1946, 188, 10-18.

11 BRADLEY, R. S. (Ed) High pressure physics and chemistry. Volume 1. London: Academic Press, 1963.

12 BRETSZNAJDER, S. Prediction of transport and other physical properties of fluids. Oxford, Pergamon Press, 1971.

13 BRIDGMAN, P. W. The physics of high pressure. London: Bell, 1958.

14 BRITISH STANDARDS INSTITUTION. Determination of the viscosity of liquids in c.g.s. units. BS 188 : 1957.

15 BRUGES, E. A. and GIBSON, M. R. Dynamic viscosity of compressed water to 10 kilobar and steam to 1500°C. J. mech. Engng Sci., 1969, 11(2), 189-205.

16 BRUSH, S. G. Theories of liquid viscosity. Chem. Revs., 1962, 62, 513-548.

17 CAPPI, J. B. The viscosity of water at high pressure. PhD thesis. London: Imperial College, University of London, 1964.

18 CERNYAWSKAYA, I. A. Absolute viscosities of alkyl chloride and alkyl bromide series at elevated temperatures (in Russian). Leningradski Universitet. Vestnik. Seriya Fiz. Chem., 1964, (16), 35-37.

19 CHEN, M. C. S., LESCARBOURA, J. A. and SWIFT, G. W. The effect of eccentricity on the terminal velocity of the cylinder in a falling cylinder viscometer. A.I.Ch.E. Jl, 1968, 14(1), 123-127.

20 CHEN, M. C. S. and SWIFT, G. W. Analysis of entrance and exit effects in a falling cylinder viscometer. A.I.Ch.E. Jl, 1972, 18(1), 146-149.

21 COHEN, M. H. and TURNBULL, D. Molecular transport in liquids and glasses. J. Chem. Phys., 1959, 31(5), 1164-1169.

22 COKELET, G. R., HOLLANDER, F. J. and SMITH, J. H. Density and viscosity of mixtures of 1,1,2,2-tetrabromoethane and 1-bromododecane. J. chem. Engng Data, 1969, 14(4), 470-473.

23 COLE, J. A. Experiments on the flow in rotating annular clearances: proceedings of the conference on lubrication and wear held in London on 1 to 3 October 1957. London: Institution of Mechanical Engineers, 1957.

24 CUTLER, W. G., McMICKLE, R. H., WEBB, W., and SCHIESSLER, R. W. Study of the compressions of several high molecular weight hydrocarbons. J. Chem. Phys., 1958, 29(4), 727-740.

25 DAVIS, L. A. and GORDON, R. B. Compression of mercury at high pressure. J. Chem. Phys., 1967, 46(7), 2650-2660.

26 DEAKER, D. L., BASSETT, W. A., MERRILL, L., HALL, H. T., and BARNETT, J. D. High pressure calibration a critical review. J. Phys. Chem. Ref. Data, 1972, 1(3), 773-835.

27 DOOLITTLE, A. K. Studies in Newtonian flow. II. The dependence of the viscosity of liquids on free-space. J. Appl. Phys., 1951, 22(12), 1471-1475.

28 DOOLITTLE, A. K. and DOOLITTLE, D. B. Studies in Newtonian flow. V. Further verification of the free-space viscosity equation. J. Appl. Phys., 1957, 28(8), 901-905.

29 DOOLITTLE, A. K., SIMON, I., and CORNISH, R. H. Compression of liquids. A.I.Ch.E. Jl, 1960, 6, 150-162.

30 DOW, R. B. Viscosity of liquids at high hydrostatic pressures. Phil. Mag., 1939, 28, 403.

31 DREISBACH, R. R. Physical properties of chemical compounds. Advances in Chemistry Series No 15. Washington: American Chemical Society, 1955.

32 DREISBACH, R. R. Physical properties of chemical compounds III. Advances in Chemistry Series No 29. Washington: American Chemical Society, 1961.

33 DUNSTAN, A. E., HILDITCH, T. P. and THOLE, F. B. The relation between viscosity and chemical constitution. VII. The effect of the relative position of two unsaturated groups on viscosity. Das Elbst:., 1913, 103, 133-144.

34 DYMOND, J. H. Transport properties in dense fluids. Proc. Symp. Thermophys. Prop. 6th. New York: A.S.M.E., 1973, pp 143-157.

35 ENGINEERING SCIENCES DATA UNIT. Dynamic viscosity of water substance. Engineering Sciences Data Item No 68009. London: Engineering Sciences Data Unit, 1968.

36 ENSKOG, D. Kinetic theory of processes in moderately low pressure gases. Inaugural Dissertation, Uppsala, Sweden, 1917.

37 EYRING, H. and JHON, M. S. Significant liquid structures. New York, London, Sydney, Toronto: John Wiley and Sons, Inc., 1969.

38 EYRING, H. Viscosity, plasticity, and diffusion as examples of absolute reaction rates. J. Chem. Phys., 1936, 4, 283-291.

39 FRENKEL, J. Kinetic theory of liquids. New York: Dover Publications Inc., 1955.

40 FLOWERS, A. E. Viscosity measurement and a new viscosimeter. Proc. Amer. Soc. Test. Mat., 1914, 14(2), 565-616.

41 FRIEND, J. N. and HARGREAVES, W. D. Viscosity and the boiling point - the rheochor. Phil. Mag., 1943, 34(236), 643-650.

42 FRIEND, J. N. and HARGREAVES, W. D. Viscosity and the hydrogen bond. Hydroxyl and ortho effects. Phil. Mag., 1945, 36(262), 731-756.

43 GARCIA-BARCENA, G. J. S.B. thesis in chemical engineering, Massachusetts Institute of Technology, 1958 (as given by Reid and Sherwood (1966)).

44 GLASSTONE, S., LAIDLER, K. L., and EYRING, H. The theory of rate processes. New York and London: McGraw-Hill, 1941.

45 GREEN, H. S. The molecular theory of fluids. Amsterdam: North Holland Publishing Co., 1952.

46 GRIFFING, V., CARGYLE, M. A., CORVESE, L., and EBY, D. Temperature coefficients of viscosity of some halogen substituted organic compounds. J. phys. Chem., Ithaca, 1954, 58, 1054-1056.

47 GRINDLEY, T. and LIND, J. E. PVT properties of water and mercury. J. Chem. Phys., 1971, 54(9), 3983-3989,

48 GRUNBERG, L. The viscosity of liquid hydrocarbons. J. Inst. Pet., 1955, 41(380), 249-258.

49 HARLOW, A. Further investigations into the effect of high pressure on the viscosity of liquids. PhD thesis. London: Imperial College, University of London, 1967.

50 HAYWARD, A. T. J. The truth about liquids under pressure. Engineering, 1964, 198(5133), 314-316.

51 HEIKS, J. R., and ORBAN, E. Liquid viscosities at elevated temperatures and pressures - viscosity of benzene from 90°C to its critical temperature. J. Phys. Chem., 1956, 60, 1025-1027.

52 HENNELLY, E. J., HESTON, W. M. and SMYTH, C. P. Microwave absorbtion and molecular structure in liquids: III dielectric relaxation and structure in organic halides. J. Amer. Chem. Soc., 1948, 70, 4102-4111.

53 HESTON, W. M., HENNELLY, E. J., and SMYTH, C. P. Dielectric constants, viscosities, densities, refractive indices and dipole moment calculations for some organic halides. J. Amer. Chem. Soc., 1950, 72, 2071-2075.

54 HIRSCHFELDER, J. O., CURTISS, C. F., and BIRD, R. B. Molecular theory of gases and liquids. New York: John Wiley and Sons, Inc., 1954.

55 HOGENBOOM, D. L., WEBB, W., and DIXON, J. A. Viscosity of several liquid hydrocarbons as a function of temperature, pressure, and free volume. J. Chem. Phys., 1967, 46(7), 2586-2598.

56 IRVING, J. B. The effect of non-vertical alignment on the performance of a falling-cylinder viscometer. J. Phys. D: Appl. Phys., 1972, 5(1), 214-224.

57 IRVING, J. B. and BARLOW, A. J. An automatic high pressure viscometer. Journal of Physics E: Scientific Instruments, 1971, 4, 232-236.

58 ISDALE, J. D., BRUNTON, W. C. and SPENCE, C. M. Bulk modulus measurement and prediction. NEL Report No 591. East Kilbride, Glasgow: National Engineering Laboratory, 1975.

59 ISDALE, J. D., SPENCE, C. M. and TUDHOPE, J. S. Physical properties of sea water solutions: viscosity. Desalination, 1972, 10, 319-28.

60 ISDALE, J. D. and SPENCE, C. M. A self-centring falling body viscometer for high pressures. NEL Report No 592. East Kilbride, Glasgow: National Engineering Laboratory, 1975.

61 ISDALE, J. D. and SPENCE, C. M. High pressure viscosities and densities of eight halogenated hydrocarbons. NEL Report No 604. East Kilbride, Glasgow: National Engineering Laboratory, 1975.

62 JHON, M. S., KLOTZ, W. L., and EYRING, H. Theoretical calculation of the pressure dependence of liquid hydrocarbon viscosities. J. Chem. Phys., 1969, 51(9), 3692-3694.

63 KELL, G. S. and WHALLEY, E. The PVT properties of water. 1 - liquid water in the temperature range 0-150°C and at pressures up to 1 Kb. Phil. Trans., A, 1965, 258(1094), 565-614.

64 KIRKWOOD, J. G. Statistical mechanics of fluid mixtures. J. Chem. Phys., 1935, 3, 300-313.

65 KIRKWOOD, J. G., BUFF, F. P., and GREEN, M. S. The statistical mechanical theory of transport processes. III. The coefficients of shear and bulk viscosity of liquids. J. Chem. Phys., 1949, 17, 988-994.

66 KUSS, E. High pressure studies, III. The viscosity of compressed liquids (in German). Z. angew. Phys., 1955, 7(8), 372-378.

67 KLEINSCHMIDT, R. V. Progress in lubrication research. Fourth report of the A.S.M.E. Special Research Committee on Lubrication. Appendix I. T.A.S.M.E., 1928, 50 (APM-50-4), 1-7.

68 LANDOLT-BORNSTEIN (SCHAFER, K., Ed). Numerical data and functional relationships in science and technology (in German). 6th edn.

Group II. vol 5a, p 203. Berlin: Springer, 1969.

69 LESCARBOURA, J. A. and SWIFT, G. W. The effect of eccentricity on the terminal velocity of the cylinder in a falling cylinder viscometer: experimental verification for Newtonian fluids. A.I.Ch.E. Jl, 1968, 14(4), 651-652.

70 LOHRENZ, J. An experimentally verified theoretical analysis of the falling cylinder viscometer. PhD Thesis. Univ. of Kansas, 1960.

71 LOHRENZ, J., SWIFT, G. W. and KURATA, F. An experimentally verified theoretical study of the falling cylinder viscometer. A.I.ChE. Jl, 1960, 6(4), 547-550.

72 LOWITZ, D. A., SPENCER, J. W., WEBB, W., and SCHIESSLER, R. W. Temperature-pressure-structure effects on the viscosity of several higher hydrocarbons. J. Chem., Phys., 1959, 30(1), 73-83.

73 LYDERSEN, A. L. Estimation of critical properties of organic compounds. College of Engineering, Univ. Wisconsin, Eng. Expt. Sta. Rept 3, Madison, Wisconsin, 1955.

74 MATHEWS, A. P. The relation of molecular cohesion to surface tension and gravitation: with a method of determining "a" of van der Waals' equation without assumptions; and the meaning of the constants in the surface tension law of Eotvos, and the latent heat formulas of Dieterici and Mills. J. Phys. Chem., 1961, 20, 554-596.

75 MOONEY, M. A theory of the viscosity of a Maxwellian elastic liquid. Trans. Soc. Rheol., 1957, 1, 63-94.

76 MUMFORD, S. A. and PHILLIPS, J. W. C. The physical properties of some aliphatic compounds. J. Chem. Soc., 1950, 75-84.

77 PARTINGTON, J. R. An advanced treatise on physical chemistry. Volume II. The properties of liquids. London: Longmans, Green and Co., 1951.

78 POWELL, M. A method of minimizing a sum of squares of non-linear functions without calculating derivitives. Comp. J., 1965, 7(4), 303-307.

79 PRENGLE, R. S. and ROTHFUS, R. R. Transition phenomena in pipes and annular cross sections. Ind. and Eng. Chem., 1955, 47(3), 379-386.

80 REE, T. S., REE, T., and EYRING, H. Significant structure theory of transport phenomena. J. Phys. Chem., 1964, 68(11), 3262-3267.

81 REID, R. C. and SHERWOOD, T. K. The properties of liquids and gases. New York: McGraw-Hill, 1966.

82 ROELANDS, C. J. A. Correlational aspects of the viscosity-temperature-pressure relationship of lubricating oils. PhD Thesis. Delft: University of Delft, 1966.

83 SABERSKY, R. H. and ACOSTA, A. J. Fluid flow. London and New York: Macmillan, 1964.

84 SEEDER, W. A. On the viscosity of liquids. Thesis, Utrecht University; H. Veenman en Zonen, Wageningen, Holland, 1943.

85 SIMON, I. Research on the freezing points of organic compounds (in French). Bull. Soc. chim. Belg., 1929, 38(2), 47-70.

86 SOUDERS, M. Viscosity and chemical constitution. J. Amer. Chem. Soc., 1938, 60, 154-158.

87 SUGE, Y. On lubricants. Part I. Physical properties of lubricants. Scientific papers of the Institute of Physical and Chemical Research, Tokyo, 1938, 34(838), 1244-1261.

88 THOMAS, L. H. The dependence of the viscosities of liquids on reduced temperature, and a relation of viscosity, density, and chemical constitution. J. Chem. Soc., 1946, II, 573-579.

89 VAN VELZEN, D., CARDOZO, R. L., and LANGENKAMP, H. A liquid viscosity-temperature-chemical constitution relation for organic compounds. Ind. Eng. Chem. Fundam., 1972, 11(1), 20-25.

90 VAN WIJK, W. R., van der VEEN, J. H., BRINKMAN, H. C., and SEEDER, W. A. The influence of the temperature and the specific volume on the viscosity of liquids. Physica, 1940, 7(1), 45-56.

91 VEDAM, R. and HOLTON, G. Specific volumes of water at high pressures, obtained from ultrasonic-propagation measurements. J. Acoust. Soc. Amer., 1968, 43(1), 108-116.

92 YAZGAN, E. Precise measurement of the velocity of sound in liquids as a function of temperature and pressure by a new electrical method. PhD Thesis. Glasgow: University of Glasgow, 1966.

93 ZOLOTYKH, E. V. Effect of pressures up to 5000 kg/cm^2 on the viscosity of liquids. Trudy in-tov Kom-ta Vses. n-i in-t fiz-tekh. i radiotekh. izmerenii, 1960, 46(106), 81-95. (in Russian)(RTS Translation No 1992, April 1962.)

A P P E N D I X I

SIGNIFICANT STRUCTURE THEORY OF VISCOSITY

APPENDIX I. SIGNIFICANT STRUCTURE THEORY OF VISCOSITY

The significant structure theory developed by Eyring and others assumes that a liquid is composed of a 'quasi-lattice' which contains a random distribution of mobile vacancies. Each vacancy confers gas-like properties to one molecule and allows deformation of the solid-like structure to occur.

If each shear plane then contains a fraction x_s molecules in the solid-like state and x_g molecules in the gas-like state, then by Newton's law viscosity is given by

$$\eta = \tau/G = (x_s\tau_s + x_g\tau_g)/G$$

where τ and G are shear stress and velocity gradient respectively and the subscripts s and g refer to the solid-like and gas-like 'phases'. Hence liquid viscosity is given by

$$\begin{aligned}\eta &= x_s\eta_s + x_g\eta_g \\ &= \frac{v_s}{v}\eta_s + \frac{v - v_s}{v}\eta_g \end{aligned} \qquad \text{(AI.1)}$$

The gas-like viscosity is assumed to be given by

$$\eta_g = \frac{5}{16d^2}\left(\frac{mkT}{\pi}\right)^{1/2} \qquad \text{(AI.2)}$$

The viscosity of the solid-like state is obtained by considering the mechanism shown in Fig. AI.1. The rate of shear, G, is calculated by dividing the velocity of one layer relative to another by the distance between the layers, l, in Fig. AI.1. The velocity of the layer is then taken to be the product of the distance jumped in the direction of the applied stress, $l\cos\theta_i$, the frequency of jumping, $k_i \exp(l_2 l_3 l\tau_s\cos\theta_i/2kT)$. The rate of shear therefore becomes

$$G = \sum_i (k_i \; l \cos\theta_i / l_1) \exp(l \; l_2 \; l_3 \gamma_s \cos\theta_i / 2kT) \qquad \text{(AI.3)}$$

The Eyring flow mechanism has been criticised for example by Mooney (1957), who argued that a molecule subject to an equal and opposite shear stress on its upper and lower surfaces was not subject to a resultant force which would cause it to jump into an adjacent hole. However, the theory assumes that shear stress is borne by <u>planes</u> of molecules in the assembly, some of which contain vacancies. The resulting shear strain is caused by movement of some molecules into adjacent sites and consequently the shear rate may be obtained by specifying the frequency of jumping. It is, therefore, incorrect, according to the model, to attempt to apply shear stresses to individual molecules.

The solid-like viscosity then becomes

$$\eta_s = \gamma_s / \left[\sum_i \left(\frac{l \cos\theta_i}{l_1} \right) k_i \exp\left(\frac{l_2 l_3 l \gamma_s \cos\theta_i}{2kT} \right) \right] \qquad \text{(AI.4)}$$

Ree, Ree, and Eyring (1964) expand equation AI.4 to give

$$\eta_s = \gamma_s / \left[\frac{k'}{l_1} \sum_i \left(\cos\theta_i + \frac{\gamma_s l_2 l_3 l \cos^2\theta_i}{2kT} \right) \right] \quad , \qquad \text{(AI.5)}$$

where it is assumed that the frequency of jumping, k_i, is equal to k' for each position. They use reaction rate theory (Glasstone, Laidler and Eyring (1941)) to calculate the frequency of jumping and assume hexagonal packing to relate the linear dimensions to the solid-like volume. They also assume that the activation enery required for translation to occur is a constant fraction (a') of the potential function, and inversely proportional to the number of holes. With these assumptions they reduce equation AI.5 to

$$\eta_s = \frac{v}{v_s} \frac{N(\pi mkT)^{1/2} l_f}{2(v - v_s)K} \exp\left[\frac{-a' v_s}{v - v_s} \frac{Z \phi(a)}{2kT}\right] \qquad \text{(AI.6)}$$

where K is a transmission coefficient, a' a constant, Z is the number of nearest neighbours, $\phi(a)$ an intermolecular potential function, and l_f the free length between nearest neighbours. By applying hard sphere conditions and assuming K = 1, Ree, Ree, and Eyring were able to use equation AI.6 to calculate viscosities of five liquids with reasonable success.

To extend this equation for use at high pressure Jhon, Klotz, and Eyring (1969) have assumed that the solid-like volume is given by

$$v_s = v_{so}(1 - \beta P) \qquad \text{(AI.7)}$$

Further, they define the free length l_f in terms of the solid-like volume and a collision diameter by

$$l_f = 2\left[\left(\frac{\sqrt{2}\, v_s}{N}\right)^{1/3} - \sigma\right] \qquad \text{(AI.8)}$$

where the collision diameter is given approximately by

$$\sigma \doteq \left(\frac{v_c}{12N}\right)^{1/3} .$$

The potential function was also defined by

$$\phi(a) = \epsilon\left[1.0109\left(\frac{N\sigma^3}{v_s}\right)^4 - 2.4090\left(\frac{N\sigma^3}{v_s}\right)^2\right] . \qquad \text{(AI.9)}$$

By utilising constants from Hogenboom, Webb, and Dixon, obtained by fitting viscosity data at atmospheric pressure, and by obtaining values for β by least squares fitting of high pressure data, Jhon, Klotz and Eyring were able to describe the viscosity-temperature-pressure behaviour of four liquids to within about 27 per cent.

The equation used in the present work, and given in Chapter 4, is formed by substituting equations, AI.2, AI.6, AI.7, AI.8, and AI.9 into equation AI.1, and using the limiting volume v_o in place of the solid-like volume, v_s, as described in Chapters 3 and 4.

The theory clearly relies on the assumption that the energy required by the flow mechanism, is a constant fraction, a', of the molecular potential energy. Since the rigid sphere condition, $\phi(a) = 0$, eliminates a' from the equation this assumption was redundant in the work of Ree, Ree and Eyring and was consequently not tested. In fact there appears to be no way of testing the constancy of a' alone since it is associated with other factors as discussed in section 4.3.

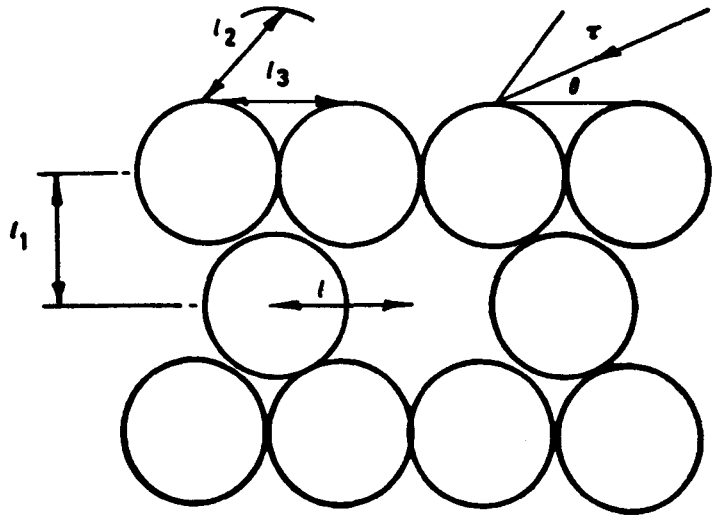

FIG A1.1 SHEAR MECHANISM DIAGRAM

A P P E N D I X II

VISCOMETER THEORY

APPENDIX II. VISCOMETER THEORY

The notation used is given in Fig. AII.1, and the following assumptions are made

1 the liquid is Newtonian

2 flow is laminar and coaxial

3 no slip occurs at liquid/solid boundaries, ie $u(r_1) = V$ and $u(r_2) = 0$

4 the sinker is a uniform right-ended circular cylinder coaxial with a circular tube

5 the velocity profile is fully developed over the length of the sinker though the velocity is zero elsewhere in the liquid.

For radial symmetry the equation of motion reduces to

$$-\frac{\partial p}{\partial z} = \frac{1}{r}\frac{\partial}{\partial r}(r\tau_{rz}).$$

For p independent of r and τ_{rz} ($= \tau$) independent of z

$$\frac{\partial}{\partial r}(r\tau) = -r\frac{\partial p}{\partial z}$$

therefore $$\tau = -\frac{r}{2}\frac{\partial p}{\partial z} + \frac{a}{r}.$$

But $$\tau = -\eta\frac{\partial u}{\partial r}$$

therefore $$\frac{\partial u}{\partial r} = \frac{r}{2\eta}\frac{\partial p}{\partial z} - \frac{a}{\eta r}$$

therefore $$u = \frac{r^2}{4\eta}\frac{\partial p}{\partial z} - \frac{a}{\eta}\ln r + b.$$

But $r = r_1$ at $u = V$

and $r = r_2$ at $u = 0$.

Therefore $$V = \frac{r_1^2}{4\eta}\frac{\partial p}{\partial z} - \frac{a}{\eta}\ln r_1 + b$$

$$0 = \frac{r_2^2}{4\eta}\frac{\partial p}{\partial z} - \frac{a}{\eta}\ln r_2 + b$$

therefore $$a = \frac{\eta V}{\ln \frac{r_2}{r_1}} + \frac{1}{4\eta}\frac{\partial p}{\partial z}\frac{(r_2^2 - r_1^2)}{\ln \frac{r_2}{r_1}}$$

$$b = \frac{a}{\eta}\ln r_2 - \frac{r_2^2}{4\eta}\frac{\partial p}{\partial z}$$

$$= \frac{V \ln r_2}{\ln \frac{r_2}{r_1}} + \frac{1}{4\eta}\frac{\partial p}{\partial z}\frac{(r_2^2 - r_1^2)\ln r_2}{\ln \frac{r_2}{r_1}} - \frac{r_2^2}{4\eta}\frac{\partial p}{\partial z}.$$

Therefore $$\frac{\partial u}{\partial r} = \frac{r}{2\eta}\frac{\partial p}{\partial z} - \frac{V}{r \ln \frac{r_2}{r_1}} - \frac{1}{4\eta r}\frac{\partial p}{\partial z}\frac{(r_2^2 - r_1^2)}{\ln \frac{r_2}{r_1}}$$

$$= \frac{1}{2\eta}\frac{\partial p}{\partial z}\left[r - \frac{1}{2r}\frac{(r_2^2 - r_1^2)}{\ln \frac{r_2}{r_1}}\right] - \frac{V}{r \ln \frac{r_2}{r_1}}.$$

Therefore $$\tau = -\eta\frac{\partial u}{\partial r}$$

$$= -\frac{r}{2}\frac{\partial p}{\partial z} + \frac{\eta V}{r \ln \frac{r_2}{r_1}} + \frac{1}{4r_1}\frac{\partial p}{\partial z}\frac{(r_2^2 - r_1^2)}{\ln \frac{r_2}{r_1}}$$

Therefore $$\tau_1 = -\frac{r_1}{2}\frac{\partial p}{\partial z} + \frac{\eta V}{r_1 \ln \frac{r_2}{r_1}} + \frac{1}{4r_1}\frac{\partial p}{\partial z}\frac{(r_2^2 - r_1^2)}{\ln \frac{r_2}{r_1}}.$$

Now the viscous force at the sinker is given by

$$F_1 = \tau_1 \times (\text{area}) = \tau_1(2\pi r_1 L_s)$$

$$= \pi L_s\left[\frac{2\eta V}{\ln \frac{r_2}{r_1}} + \frac{\partial p}{\partial z}\left\{\frac{1}{2}\frac{(r_2^2 - r_2^2)}{\ln \frac{r_2}{r_1}} - r_1^2\right\}\right].$$

Now volumetric flow is given by

$$Q_z = -\pi r_1^2 V$$

$$= 2\pi\int_{r_1}^{r^2} urdr$$

$$= 2\pi \int_{r_1}^{r_2} \left\{ \frac{r^3}{4\eta} \frac{\partial p}{\partial z} - \frac{ar \ln r}{\eta} + br \right\} dr$$

$$= 2\pi \left\{ \frac{r^4}{16\eta} \frac{\partial p}{\partial z} + \frac{b}{2} r^2 \right\}_{r_1}^{r_2} - \frac{2\pi a}{\eta} \int_{r_1}^{r_2} r \ln r \, dr$$

$$Q_z = 2\pi \left\{ \frac{\partial p}{\partial z} \frac{1}{16\eta} (r_2^4 - r_1^4) + \frac{b}{2} (r_2^2 - r_1^2) \right\} -$$

$$- \frac{2\pi a}{\eta} \left\{ \frac{r^2}{2} \ln r - \frac{1}{4} r^2 \right\}_{r_1}^{r_2}$$

$$= 2\pi \left\{ \frac{\partial p}{\partial z} \frac{1}{16\eta} (r_2^4 - r_1^4) + \frac{b}{2} (r_2^2 - r_1^2) \right\} -$$

$$- \frac{2\pi a}{\eta} \{ \tfrac{1}{2}(r_2^2 \ln r_2 - r_1^2 \ln r_1) - \tfrac{1}{4}(r_2^2 - r_1^2) \}.$$

Substituting a and b gives

$$Q_z = \frac{\pi V}{\ln \frac{r_2}{r_1}} \{ -(r_2^2 \ln r_2 - r_1^2 \ln r_1) + r_2^2 \ln r_2 - r_1^2 \ln r_2 \} +$$

$$+ \frac{\partial p}{\partial z} \frac{\pi}{4\eta} (r_2^2 - r_1^2) \left\{ \frac{1}{2} (r_2^2 + r_1^2) + (r_2^2 - r_1^2) \frac{\ln r_2}{\ln \frac{r_2}{r_1}} - \right.$$

$$\left. - r_2^2 - \frac{r_2^2 \ln r_2 - r_1^2 \ln r_1}{\ln \frac{r_2}{r_1}} + \frac{1}{2} \frac{r_2^2 - r_1^2}{\ln \frac{r_2}{r_1}} \right\}.$$

But $$Q_z = -\pi r_1^2 V.$$

Therefore $$-\pi r_1^2 V = \frac{\pi V}{\ln \frac{r_2}{r_1}} \left\{ \frac{1}{2} (r_2^2 - r_1^2) - r_1 \ln \frac{r_2}{r_1} + \right.$$

$$\left. + \frac{\pi}{8\eta} \frac{\partial p}{\partial z} \left\{ \frac{(r_2^2 - r_1^2)^2}{\ln \frac{r_2}{r_1}} - (r_2^4 - r_1^4) \right\} \right.$$

Therefore $$\frac{\partial p}{\partial z} = \frac{-4\eta V}{(r_2^2 - r_1^2) - \ln \frac{r_2}{r_1} (r_2^2 + r_1^2)}.$$

Balancing forces gives

$$mg\left(1 - \frac{\rho_L}{\rho_s}\right) + F_1 + \pi r_1^2 \frac{\partial p}{\partial z} L_s = 0.$$

Substituting F_1 and $\partial p/\partial z$ gives

$$mg\left(1 - \frac{\rho_L}{\rho_s}\right) = 2\pi\eta V L_s \left\{\frac{r_2^2 + r_1^2}{(r_2^2 - r_1^2) - (r_2^2 + r_1^2) \ln \frac{r_2}{r_1}}\right\}$$

$$\text{therefore} \qquad \eta V = \frac{-mg\left(1 - \frac{\rho_L}{\rho_s}\right)}{2\pi L_s} \left(\ln \frac{r_2}{r_1} - \frac{r_2^2 - r_1^2}{r_2^2 + r_1^2}\right)$$

$$\text{therefore} \qquad \eta = \frac{-mg\left(1 - \frac{\rho_L}{\rho_s}\right)T}{2\pi L_s L_T} \left(\ln \frac{r_2}{r_1} - \frac{r_2^2 - r_1^2}{r_2^2 + r_1^2}\right) \qquad \text{(AII.1)}$$

$$\text{or} \qquad \eta = \frac{T\left(1 - \frac{\rho_L}{\rho_s}\right)}{A(1 + 2\alpha\theta)}$$

$$\text{where} \qquad A = \frac{2\pi L_s L_T}{mg\left(\ln \frac{r_2}{r_1} - \frac{r_2^2 - r_1^2}{r_2^2 + r_1^2}\right)}.$$

To find the radius of maximum velocity, r_m

$$\frac{\partial u}{\partial r} = 0$$

$$\text{therefore} \qquad \frac{r_m}{2\eta} \frac{\partial p}{\partial z} - \frac{V}{r_m \ln \frac{r_2}{r_1}} - \frac{1}{4\eta r_m} \frac{\partial p}{\partial z} \frac{(r_2^2 - r_1^2)}{\ln \frac{r_2}{r_1}} = 0$$

$$\text{therefore} \qquad r_m^2 = \frac{2\eta V}{\frac{\partial p}{\partial z} \ln \frac{r_2}{r_1}} + \frac{1}{2} \frac{(r_2^2 - r_1^2)}{\ln \frac{r_2}{r_1}}.$$

Substituting $\partial p/\partial z$ gives

$$r_m^2 = -\frac{2\eta V\{(r_2^2 - r_1^2) - \ln\frac{r_2}{r_1}(r_2^2 + r_1^2)\}}{\ln\frac{r_2}{r_1}\,4\eta V} +$$

$$+\frac{1}{2}\frac{(r_2^2 - r_1^2)}{\ln\frac{r_2}{r_1}}$$

$$= -\frac{1}{2}\left\{\frac{(r_2^2 - r_1^2)}{\ln\frac{r_2}{r_1}} - (r_2^2 + r_1^2)\right\} + \frac{1}{2}\frac{(r_2^2 - r_1^2)}{\ln\frac{r_2}{r_1}}$$

$$r_m^2 = \tfrac{1}{2}(r_2^2 + r_1^2). \qquad \text{(AII.2)}$$

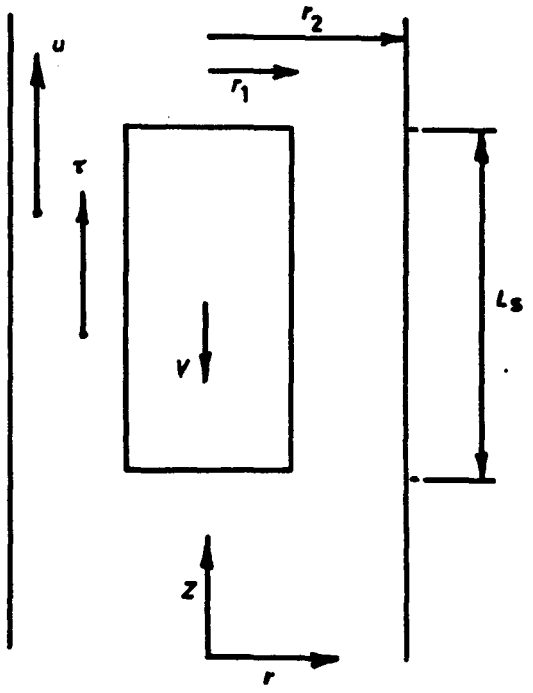

FIG A11.1 NOTATION

APPENDIX III

NEL REPORTS

NEL Report No 592

NATIONAL ENGINEERING LABORATORY

A Self-centring Falling Body Viscometer for High Pressures

J D ISDALE and C M SPENCE

DEPARTMENT OF INDUSTRY
JUNE 1975

Issued by

NATIONAL ENGINEERING LABORATORY,
EAST KILBRIDE, GLASGOW

DEPARTMENT OF INDUSTRY

NATIONAL ENGINEERING LABORATORY

A SELF-CENTRING FALLING BODY VISCOMETER FOR HIGH PRESSURES

by

J D Isdale, B Sc and C M Spence

(Fluids Group: Properties of Fluids Division)

SUMMARY

A self-centring falling body viscometer has been developed and used to measure the viscosity of water, benzene, and carbon tetrachloride in the temperature range 25-100°C and for pressures up to 1000 MN m^{-2}. The effects of turbulence and centring of the sinkers are examined and the possibility of using this type of viscometer in an absolute way is discussed. The experimental results are compared with available data.

BLANK PAGE IN ORIGINAL

CONTENTS

Distribution Group: Fluid properties data

NOTATION

A	Viscometer constant
A_o	Viscometer constant in equation (4)
B	Viscometer constant in equation (4)
g	Gravitational constant
K	Ratio of diameter of sinker to viscometer bore
L_s	Sinker length
m	Sinker mass
N	Constant in equation (4)
P	Liquid pressure
Re	Reynolds number
r_1	Sinker radius
r_2	Tube radius
T	Time for sinker to fall fixed length
t	Liquid temperature
t_o	Temperature at which viscometer is measured
V	Terminal velocity of sinker
α	Linear coefficient of expansion of tube and sinker
β	Coefficient of compressibility of tube and sinker
η	Liquid viscosity
ρ_L	Liquid density
ρ_s	Sinker density

1 INTRODUCTION

Liquid viscosity is a property which shows marked variations with temperature and pressure and is of importance in many fields of engineering. In mechanical engineering, it is an important property of all lubricants, and, since extremely high pressures are generated in many types of bearings, its variation with pressure is a factor of considerable interest. Hydraulic fluids are not often used at pressures above about 500 MN m^{-2}, but since pressures of this magnitude usually cause a large increase in viscosity the effect of pressure is again an important variable. In chemical engineering, pressures similar to those of hydraulic systems are often used and the effect of pressure on the viscosity of heat-transfer liquids, chemical process liquids, and refrigerants can be of importance.

This report describes a viscometer which has been developed at NEL to measure the viscosity of liquids in the temperature range 20-100°C and for pressures up to 1000 MN m^{-2}. The viscometer is of the falling body type in which a sinker falls axially down the centre of a vertical circular tube containing the liquid whose viscosity is to be measured. Sinker velocity is measured using induction coils wound outside the viscometer tube so that measurement is not restricted to non-conducting liquids. The sinker may be returned to its starting position by rotating the pressure vessel so that a complete series of measurements can be made without disturbing the liquid sample.

Viscometers of this type frequently[1] make use of small pegs attached to the sinker to maintain near concentric flow. However these protrusions may introduce additional turbulence in the liquid and frictional effects[2] as they slide down the tube wall. To eliminate these possibilities self-centring sinkers without pegs have been developed and the influence of turbulence and centring effects on their performance is examined. Measurements of water, benzene, and carbon tetrachloride made with the viscometer are presented and its use for absolute measurements is discussed.

2 THEORY OF VISCOMETER

For a plain cylindrical body falling axially down a closed vertical tube with terminal velocity V, at constant temperature t_o and with laminar flow prevailing, the equations governing the motion can be solved to give

$$V = -\frac{mg\left(1-\frac{\rho_L}{\rho_s}\right)}{2\pi L_s \eta}\left\{\ln\left(\frac{r_2}{r_1}\right)-\frac{(r_2^2-r_1^2)}{(r_2^2+r_1^2)}\right\}. \qquad (1)$$

For a particular instrument with tube and sinker of the same material operating at some temperature t and pressure P, equation (1) can be reduced to

$$\eta = \frac{T(1-\rho_L/\rho_s)}{A\{1+2a(t-t_o)\}(1-2/3\beta P)}. \qquad (2)$$

The use of equations (1) and (2) would clearly allow the instrument to be used for absolute measurement; however the calculation of the viscometer constant, A, is strongly dependent on the difference between the two radii r_1 and r_2. This difference must be kept small so that the viscous forces incurred at the entry and exit of the annulus are small compared with the forces acting within the annulus[2], and it follows that small errors in the measurement of r_1 and r_2 can produce large errors in the calculated value of A. The viscometer constant is therefore usually calculated from measurements at atmospheric pressure in liquids whose viscosities are known accurately. It is theoretically independent of temperature, pressure, and viscosity for laminar co-axial flow.

Measurements with a similar instrument have shown[3] that the viscometer constant is independent of temperature in the range 25-180°C. Calibration of the present instruments at 25 and 75°C also confirm this result. The constancy of A with pressure cannot be demonstrated because of

the lack of accurate viscosity data under pressure, however the dimensional changes which occur due to pressure are less than those due to temperature.

3 APPARATUS

3.1 Viscometer Tubes

The viscometer tubes are made from a solid bar of En58J non-magnetic stainless steel. Fig. 1 shows a tube with three pairs of triggering coils, any two of which can be used to give different working lengths. The diameters of both tubes and sinkers are constant to within ±0.005 mm and deviate from circularity by less than 0.005 mm.

The triggering coils are wound from 44 s.w.g. insulated copper wire with a resistance of 80 ohms and approximately 550 turns on each coil. They are trimmed to the same resistance within 0.5 ohms and to the same inductance within 0.2 mH. Connecting wires from the coils pass through ceramic cone insulators in the end closure of the pressure vessel.

Pressure is transmitted from the pressurizing fluid (kerosene) to the sample by stainless steel bellows at one end of the viscometer tube.

The sinkers are also made from En58J steel with a solid ferrite core located as shown in Fig. 1. They are hollow cylinders with one end closed by a solid hemisphere. The edges of the open end of the cylinders are radiussed so that no sharp corners are formed. The sinker lengths given in Table 1 are the lengths of the cylindrical sections only, that is, from the points at which the cylinders are tangent to the hemisphere to those at which they are tangent to the radiussed ends.

In operation, two pairs of coils are connected to form an a.c. bridge circuit which is initially balanced. When the ferrite core of a sinker passes through the first pair of coils, the inductance of each coil increases in turn and the bridge is unbalanced first in one direction and then the other. The out-of-balance signals are modified and used to operate a trigger which starts an electronic timer when the ferrite core is at the mid-point of the first pair of coils. The second pair of coils switches off the timer in a similar manner.

Hemispherically nosed sinkers were found to be self-centring provided the centre of gravity of the sinker was below the centre of action of the viscous forces, that is below the centre of the cylindrical section. The distance they had to travel to become concentric with the tube was investigated in the following tests.

With the sinker initially at the bottom of the tube and the tube oriented in the measuring direction, the vessel was inverted and the sinker allowed to fall backwards, that is with the open end leading, through the two pairs of coils. When it triggered the timing circuit at the second pair of coils, a stopwatch was started and the sinker allowed to continue falling for a preselected delay time. When that time was reached the tube was quickly inverted and a fall time taken with the sinker moving in the forward direction, that is with the spherical end leading. The procedure was then repeated with longer delay times until fall times in the forward direction were stable within ±0.2 per cent.

The delay in centring was observed only for the sinker/tube combination of diameter ratio K = 0.9586. For higher values of K centring occurred too rapidly to be observed in the present apparatus.

Delay time was converted to distance using the ratio of sinker velocity in the forward direction to that in the backwards direction, and the stable forward velocity. When the forward fall time was stable the velocity ratio was found experimentally to be 0.46 for all sinkers studied. This value is slightly higher than that predicted[4,5] for the ratio of concentric to eccentric sinker velocity, probably because of tilting of the sinker axis and friction between sinker and tube wall while the sinker was falling in the backwards direction.

The results of these tests are shown in Fig. 2 where the ratio of eccentric to concentric fall time in the forward direction is plotted against distance travelled by the sinker before it enters the measuring section of the viscometer tube. Since the eccentricity at the beginning of the sinker's movement is not fixed at any one value, the results are scattered; however the continuous line is a measure of the maximum value of the mean eccentricity, measured over the working section, which the sinker can have after travelling the distance stated. The figure therefore shows that an entry length of between 70 and 80 mm is required to guarantee concentric flow at a diameter ratio of 0.9586. Four liquids with viscosities between 5 and 220 mN s m^{-2} were used to obtain these results, but no significant viscosity effect was observed.

3.2 Pressurizing System

Fig. 3 shows a diagram of the pressurizing circuit, which is made up of a hydraulic reservoir containing the pressurizing fluid, a pump driven by compressed air, pressure intensifier, pressure gauge block and let down valve, and the pressure vessel immersed in a constant temperature bath.

Pressures up to 250 MN m^{-2} can be generated directly by the pump through the priming loop. Higher pressures are then obtained using the intensifier loop, which can be reprimed and used as often as necessary to produce the required pressure.

The temperature of the pressure vessel is maintained constant to within ±0.02K by immersion in a constant temperature bath and is measured by a quartz thermometer attached to the outer surface of the vessel at its mid-point. The temperature inside the pressure vessel is not measured but is taken to be equal to the bath temperature when sufficient time has been allowed for equalization and when the viscometer fall-time measurements become constant. Increases in temperature of the sample due to pressurization are also allowed to decay before meaningful fall-time measurements are taken.

3.3 Pressure Measurement

Pressure is measured by a manganin wire resistance gauge in a separate gauge block as shown in Fig. 3. The resistance of the pressurized gauge is determined by comparing it with an unpressurized standard resistance. The resistance of manganin is known[6] to vary linearly with pressure over a wide pressure range and it therefore provides a useful means of calculating pressures above the limit of conventional free piston dead weight pressure balances.

The gauge consists of about 3 m of 40 s.w.g. double silk covered manganin wire wound loosely and non-inductively on a ptfe former. Before calibration it was aged by temperature cycling between −30°C and 120°C and by pressure cycling between one atmosphere and 1000 MN m^{-2}.

Calibration was carried out using a free piston dead weight pressure balance calibrated at NPL. The gauge characteristic is linear in pressure, but its resistance at atmospheric pressure varies with time. Fig. 4 shows the results of two calibrations carried out at an interval of six months. To counteract this drift, the resistance at atmospheric pressure is measured before each pressurization and the pressure calculated using the mean slope. Pressures calculated in this way agree with dead weight tester values to within 1 MN m^{-2}.

4 VISCOMETER CALIBRATION

Distilled water, AR grade benzene, and a series of stable mineral oils were used to calibrate the viscometer at atmospheric pressure. The viscosities of the oils were first measured in U-tube viscometers and the densities in bicapillary pycnometers at 25 and 75°C. Values for water and benzene were taken from API 44[7].

The measured viscometer constants are plotted against Reynolds number in Fig. 5, which shows the wide range of constants that can be obtained for relatively small changes in diameter. Reynolds number used here is defined for annular flow by

$$Re = \frac{2r_1^2 \rho_L V}{(r_2 - r_1)\eta} . \qquad (3)$$

At high Reynolds numbers a turbulent transition is indicated by an increase in the measured value of A. This is shown in Fig. 6 where the ratio of the theoretical value of A (calculated from equations (1) and (2)) to the measured value is plotted against Reynolds number. The transition regions for the different sinkers do not coincide, probably because of small differences in surface finish. However for Reynolds numbers less than 1, theoretical and experimental constants agree to within 2 per cent. These results therefore suggest that it may be possible to make absolute measurements with this type of instrument if the Reynolds number is low. It should also be noted that changes in A due to turbulence are all less than 5 per cent in the ranges examined.

In practice, it was convenient to apply corrections for the turbulence effect by fitting measured viscometer constants to the equation

$$A = A_o \left[1 + \left\{\frac{B}{T(1 - \rho_L/\rho_s)}\right\}^N\right] \qquad (4)$$

where A_o, B, and N are constants for a particular tube and sinker. The values of these constants for the combinations examined are given in Table 1 together with the theoretical viscometer constants, and the curves shown in Fig. 6 are from values calculated from equation (4).

5 EXPERIMENTAL RESULTS

The measurements reported here were made partly to check the performance of the viscometer and partly to provide new data on important liquids. Water, benzene, and carbon tetrachloride have been measured by other workers and the new measurements therefore, in addition to their intrinsic value, allow useful comparisons to be made.

Each viscosity given is based on the mean of at least four consecutive fall-time measurements. When temperature and pressure were stable, the maximum difference between any two measured fall times was 0.2 per cent. The results have not been smoothed, but minor corrections (less than 1 per cent viscosity) have been applied to compensate for experimental temperature or pressure settings which did not coincide with the round values given here.

Liquid densities under pressure are required to calculate viscosity from equation (2), and these can be measured if necessary[8]. For the present measurements, however, water densities from Grindley and Lind[9] and benzene and carbon tetrachloride densities from Bridgman[10] have been used.

Results for water at 25 and 50°C for pressures up to 1000 MN m^{-2} are shown in Fig. 7. They are also given numerically in Table 2 in the form of the ratio of viscosity at pressure to viscosity at atmospheric pressure at the same temperature. They are compared with tabulated values of the Engineering Sciences Data Unit[11], which are derived from a correlation of data from several sources by Bruges and Gibson[12]. The ESDU data are the most reliable available at the present time in this pressure range and are estimated to be accurate to within ±2 per cent. Though the NEL values tend to be slightly higher than the ESDU values at low pressure and slightly lower at high pressures, the maximum difference between them is only 1.6 per cent.

Measurements of benzene viscosity ratios are given in Table 3. For temperatures near or above the normal boiling point, a slight pressure was applied to prevent the formation of vapour bubbles. Though too low to measure with this apparatus, the applied pressures were higher than the saturation pressure but not high enough to produce a significant change in viscosity. This is confirmed by the measured viscosities which are also given in Table 3; however to obtain best values for viscosity under pressure the most accurate atmospheric or saturation pressure data available should be used together with the viscosity ratios given.

The benzene results are compared with data from Bridgman[10] and Kuss[13] in Figs 8 and 9 respectively. Bridgman used a falling body viscometer with centring pegs attached to the sinker to obtain his values, while Kuss used a rolling ball viscometer. The NEL measurements agree well with Bridgman's, the maximum difference being 4.1 per cent at 75°C and 300 MN m^{-2}. At 30°C and 98 MN m^{-2}, however, the benzene froze and measurements at a point corresponding to Bridgman's could not be obtained. The presence of impurities, which in any pure component will tend to raise the freezing pressure at constant temperature, may be the reason for the greater liquid range of Bridgman's sample. Such impurities would not necessarily alter the viscosity significantly. The agreement with Kuss' measurements is poor and the differences tend to increase with pressure and temperature as shown on Fig. 9. The rolling ball method is known to be difficult[14] for low viscosity liquids because of non-linear calibration characteristics and the incidence of stick/slip motion instead of pure rolling. These factors may account for the differences observed, which reach a maximum of nearly 13 per cent at 60°C.

Carbon tetrachloride results are compared with Bridgman's values in Fig. 10 and are given in Table 4. The agreement here is also good with a standard deviation of 3.4 per cent, though a maximum difference of 6.0 per cent occurs at 30°C and 147 MN m^{-2}.

6 CONCLUSIONS

A falling body viscometer has been developed for the measurement of liquid viscosity in the temperature range 25-100°C and for pressures up to 1000 MN m^{-2}. Measurements of the viscosity of water, benzene, and carbon tetrachloride made with the viscometer have shown that the unguided sinkers used can produce accurate data in these temperature and pressure ranges. Measurements of halogenated hydrocarbons will be given in a later report.

The sinkers act in a self-centring manner and are in the form of hemispherically nosed cylinders with their centre of gravity below the centre of action of the viscous forces. For the three sizes examined, centring effects were significant only at a sinker/tube diameter ratio of 0.9586, when the distance required for centring became comparatively large (about ten sinker diameters).

At low Reynolds numbers calculated and measured viscometer constants agreed within 2 per cent and it follows that absolute measurements of comparable accuracy could be undertaken with the present design.

At high Reynolds numbers the influence of surface finish on the onset of turbulence is very marked because of the small annular clearance, and calibration is essential.

REFERENCES

1 CAPPI, J. B. *The viscosity of water at high pressure*. Ph D. Thesis. London: Imperial College, University of London, 1964.

2 CHEN, M. C. S. and SWIFT, G. W. Analysis of entrance and exit effects in a falling cylinder viscometer. *AIChE Jl*, 1972, **18**(1), 146-149.

3 ISDALE, J. D., SPENCE, C. M. and TUDHOPE, J. S. Physical properties of sea water solutions: viscosity. *Desalination*, 1972, **10**, 319-28.

4 CHEN, M. C. S., LESCARBOURA, J. A. and SWIFT, G. W. The effect of eccentricity on the terminal velocity of the cylinder in a falling cylinder viscometer. *AIChE Jl*, 1968, **14**(1), 123-127.

5 IRVING, J. B. The effect of non-vertical alignment on the performance of a falling-cylinder viscometer. *J. Phys. D: Appl. Phys.*, 1972, **5**(1), 214-224.

6 DEAKER, D. L., BASSETT, W. A., MERRILL, L., HALL, H. T. and BARNETT, J. D. High pressure calibration a critical review. *J. Phys. Chem. Ref. Data*, 1972, 1(3), 773-835.

7 AMERICAN PETROLEUM INSTITUTE. Selected values of properties of hydrocarbons and related compounds. *Research Project* 44. New York: American Petroleum Institute, 1969.

8 ISDALE, J. D., BRUNTON, W. C. and SPENCE, C. M. Bulk modulus measurement and prediction. *NEL Report* No 591. East Kilbride, Glasgow: National Engineering Laboratory, 1975.

9 GRINDLEY, T. and LIND, J. E. PVT properties of water and mercury. *J. Chem. Phys.*, 1971, **54**(9), 3983-3989.

10 BRIDGMAN, P. W. *The physics of high pressure*. London: Bell, 1958.

11 ENGINEERING SCIENCES DATA UNIT. Dynamic viscosity of water substance. *Engineering Sciences Data Item* No 68009. London: Engineering Sciences Data Unit, 1968.

12 BRUGES, E. A. and GIBSON, M. R. Dynamic viscosity of compressed water to 10 kilobar and steam to 1500°C. *J. mech. Engng Sci.*, 1969, 11(2), 189-205.

13 KUSS, E. High pressure studies, III. The viscosity of compressed liquids (in German). *Z. angew. Phys.*, 1955, **7**(8), 372-378.

14 LOHRENZ, J., SWIFT, G. W. and KURATA, F. An experimentally verified theoretical study of the falling cylinder viscometer. *AIChE Jl*, 1960, **6**(4), 547-550.

LIST OF TABLES

LIST OF FIGURES

TABLE 4

Viscosity and Viscosity Ratio of Carbon Tetrachloride

Temperature (°C)	Pressure (MN m^{-2})	Viscosity (mN s m^{-2})	Viscosity ratio
25	0.1	0.885	1.000
25	50	1.379	1.558
25	100	1.976	2.234
25	150	2.777	3.138
30	0.1	0.835	1.000
30	50	1.284	1.538
30	100	1.814	2.173
30	150	2.512	3.010
40	0.1	0.734	1.000
40	50	1.130	1.539
40	100	1.609	2.192
40	150	2.199	2.995
40	200	2.949	4.015
75	0.1	0.502	1.000
75	50	0.764	1.521
75	100	1.067	2.124
75	150	1.418	2.822
75	200	1.834	3.650
75	300	2.983	5.939
100	0.1	0.400	1.000
100	100	0.848	2.120
100	200	1.428	3.571
100	300	2.214	5.535

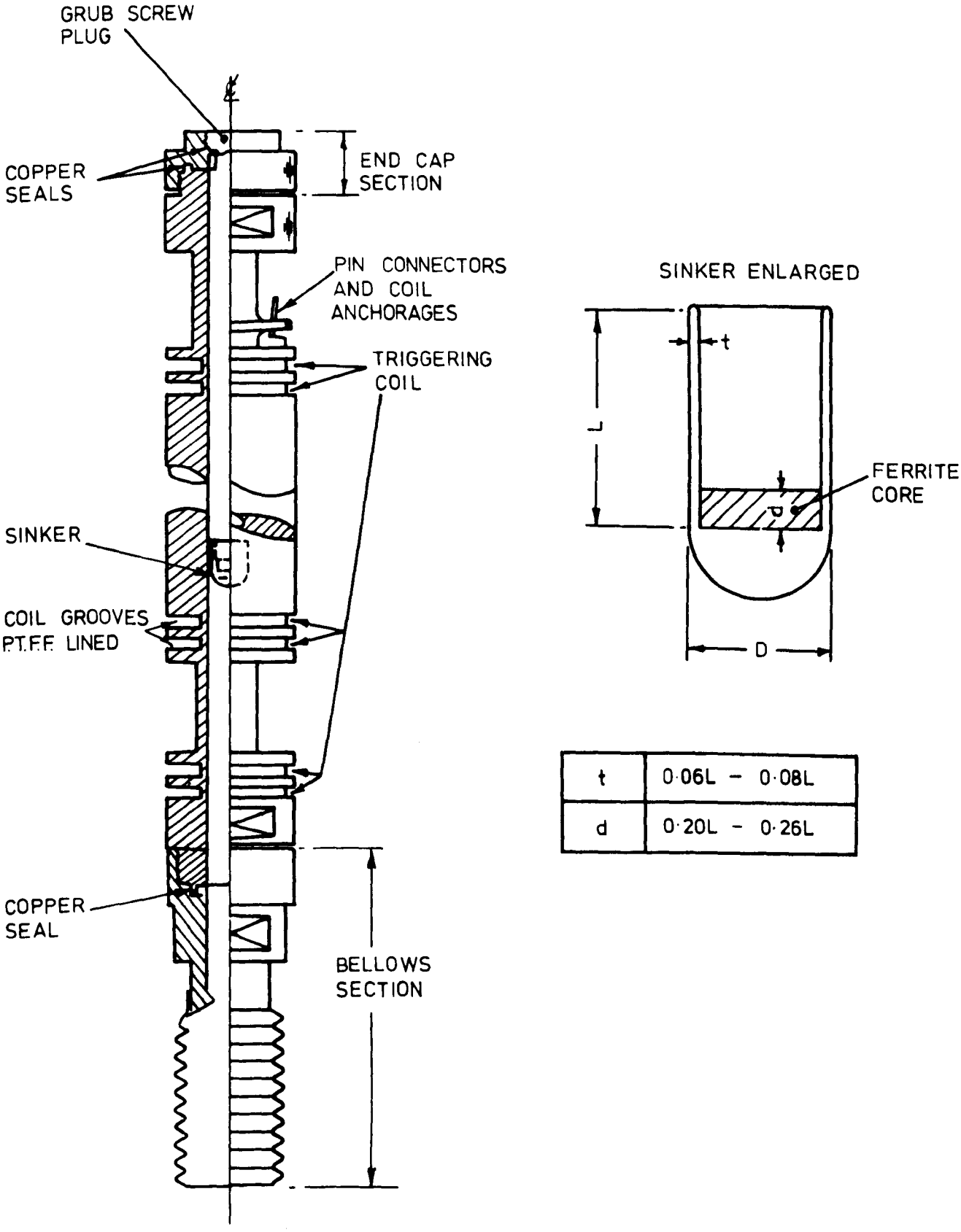

t	0·06L – 0·08L
d	0·20L – 0·26L

Fig. 1 Viscometer Tube

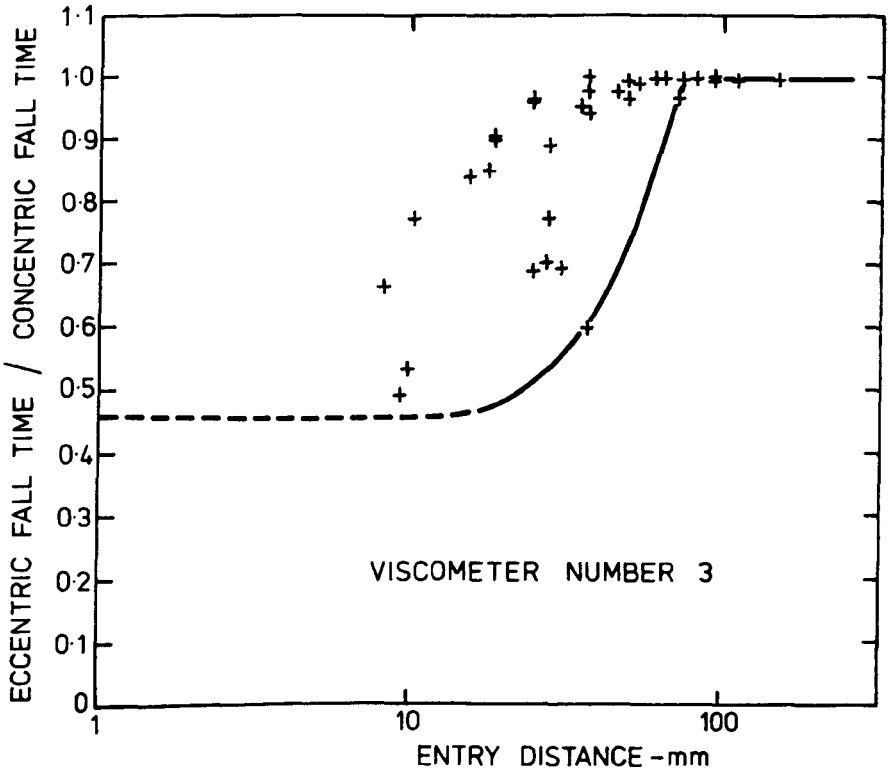

Fig. 2 Centring Effects

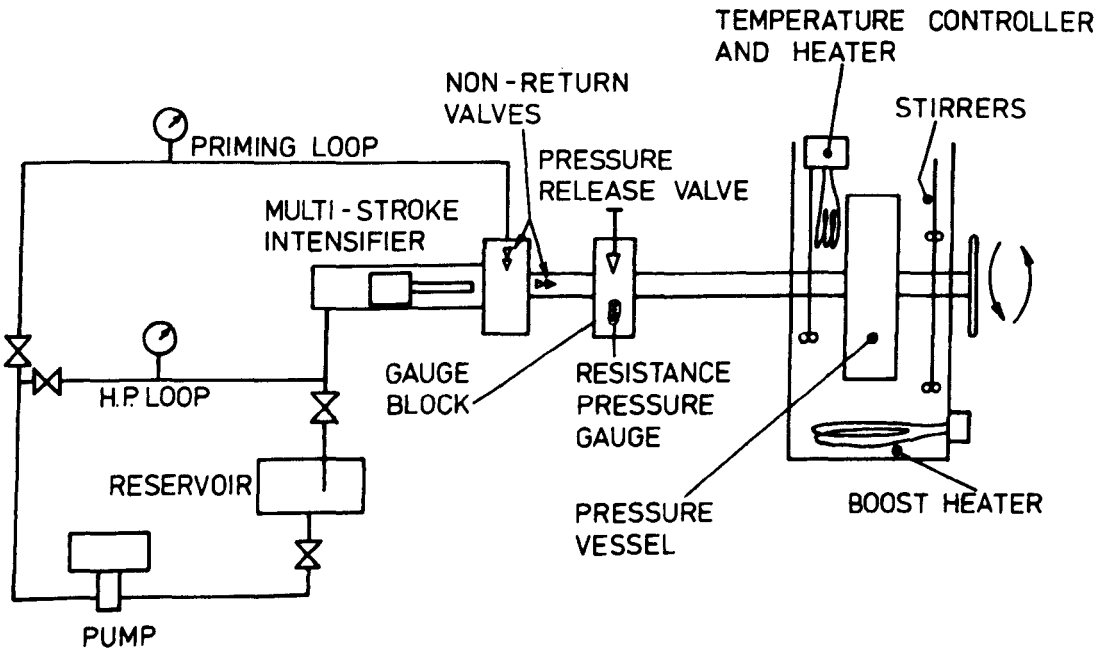

Fig. 3 Pressurizing System

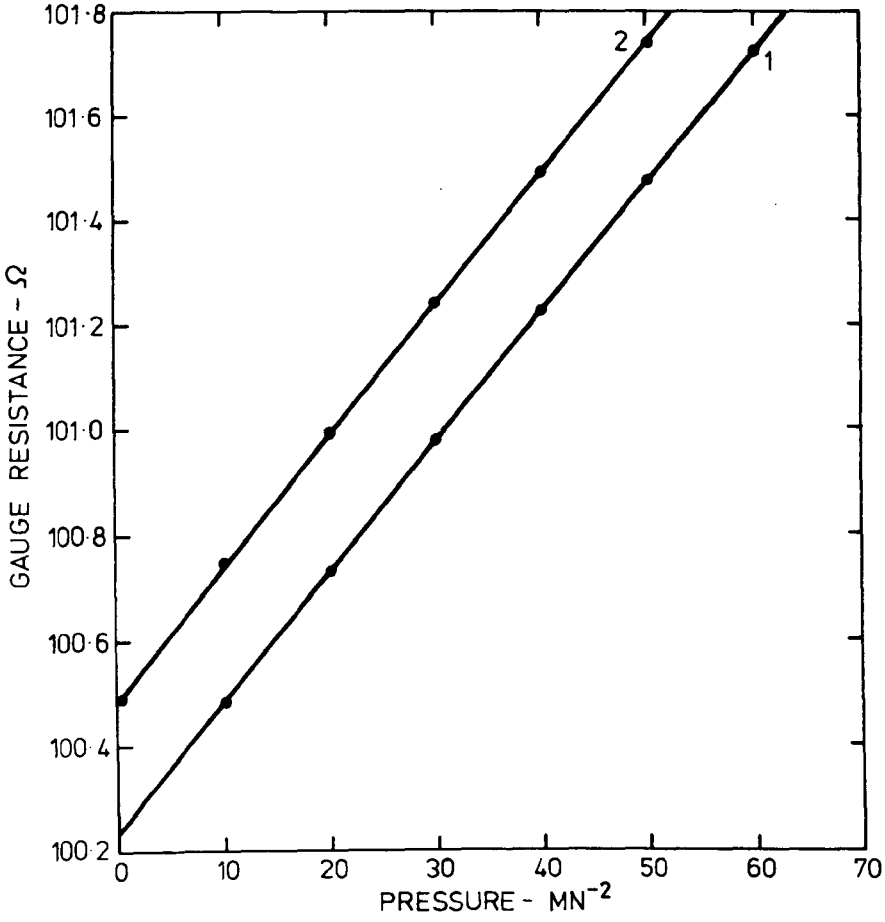

Fig. 4 Pressure Gauge Calibration

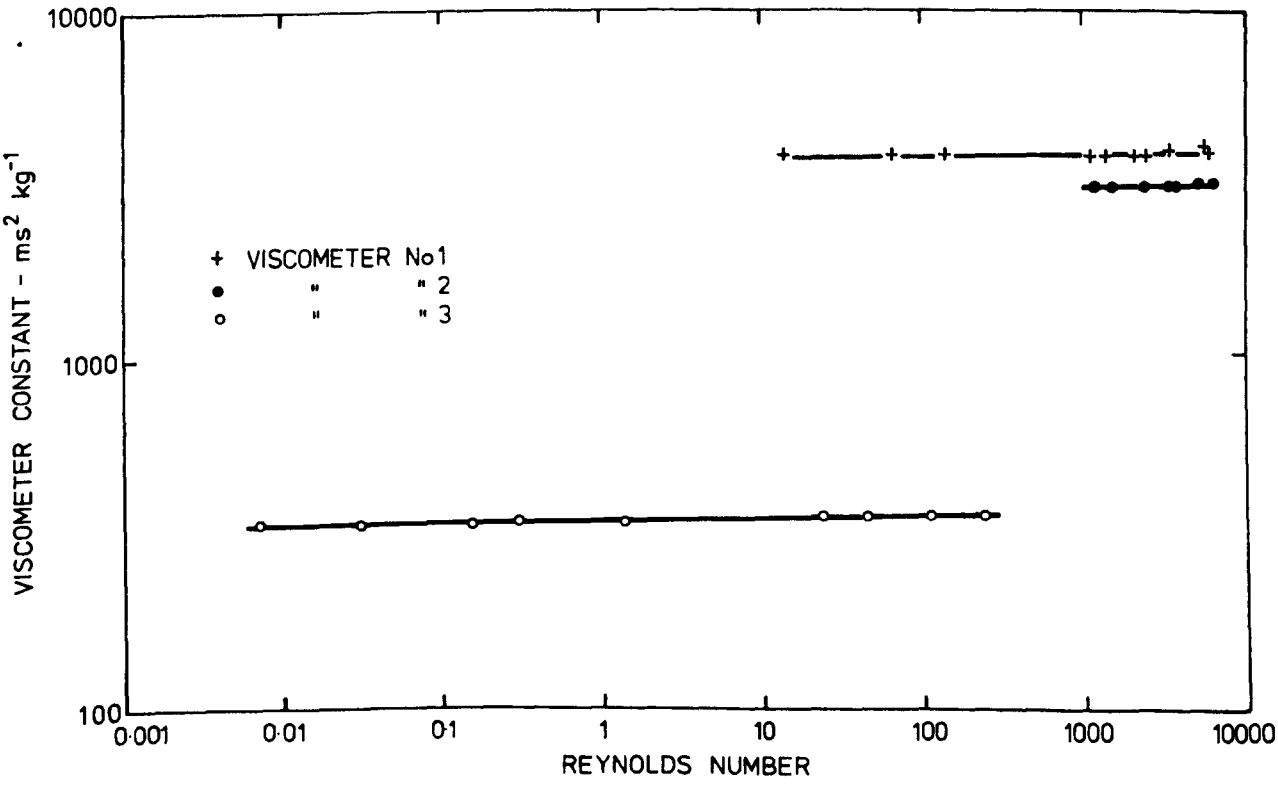

Fig. 5 Measured Viscometer Constants

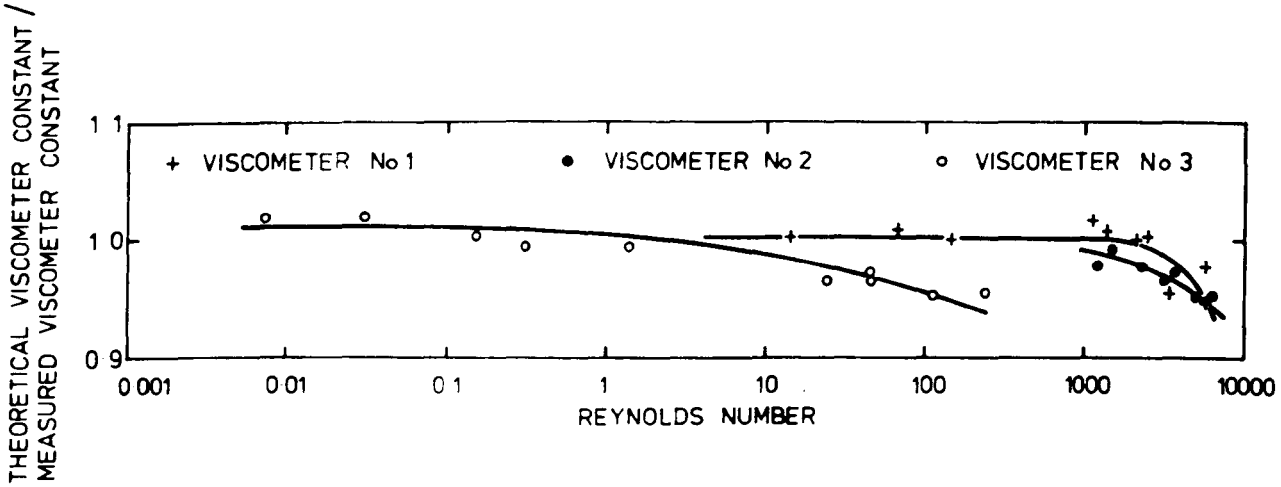

Fig. 6 Theoretical and Measured Viscometer Constants

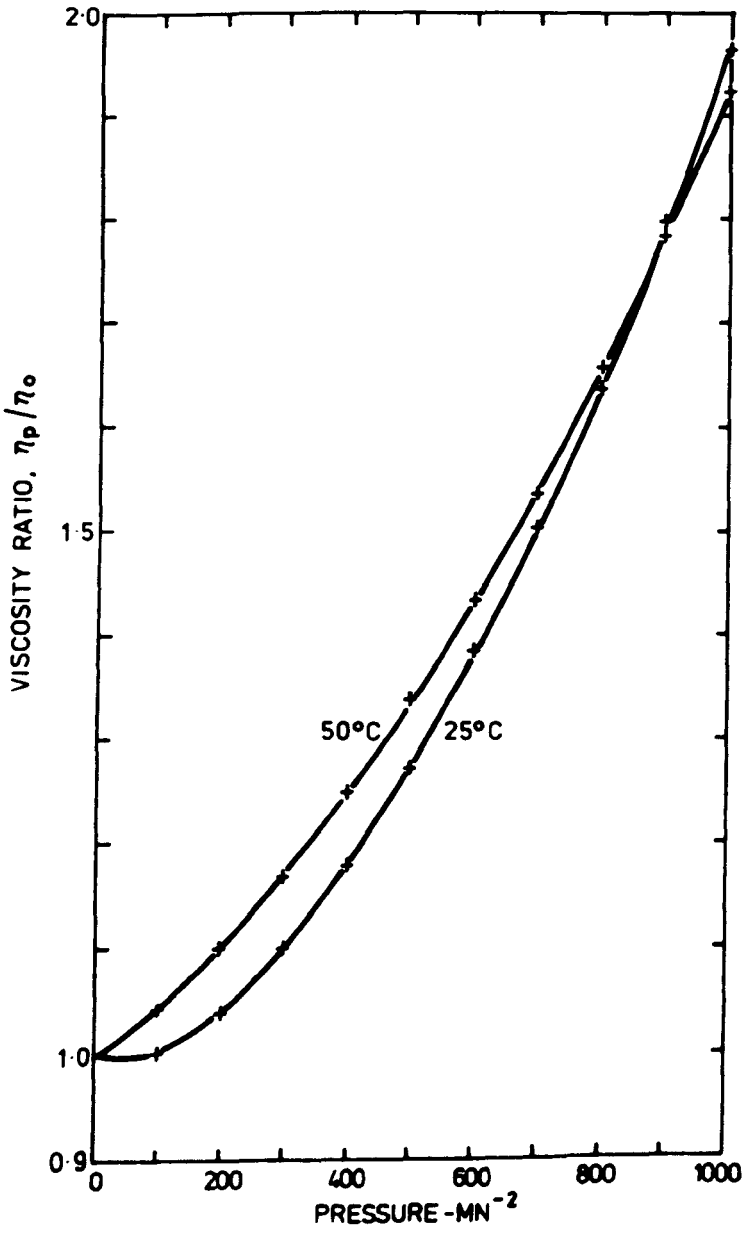

Fig. 7 Viscosity Ratio of Water

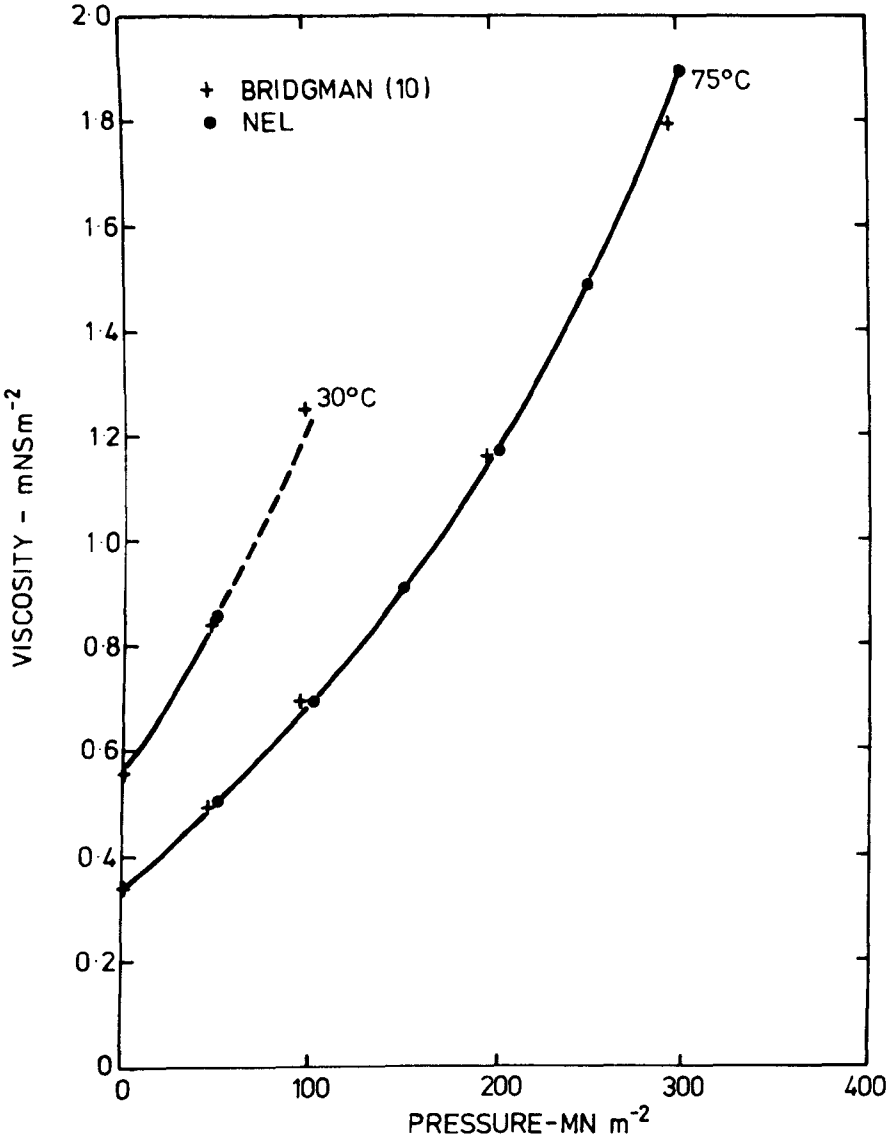

Fig. 8 Viscosity of Benzene (NELand Bridgman)

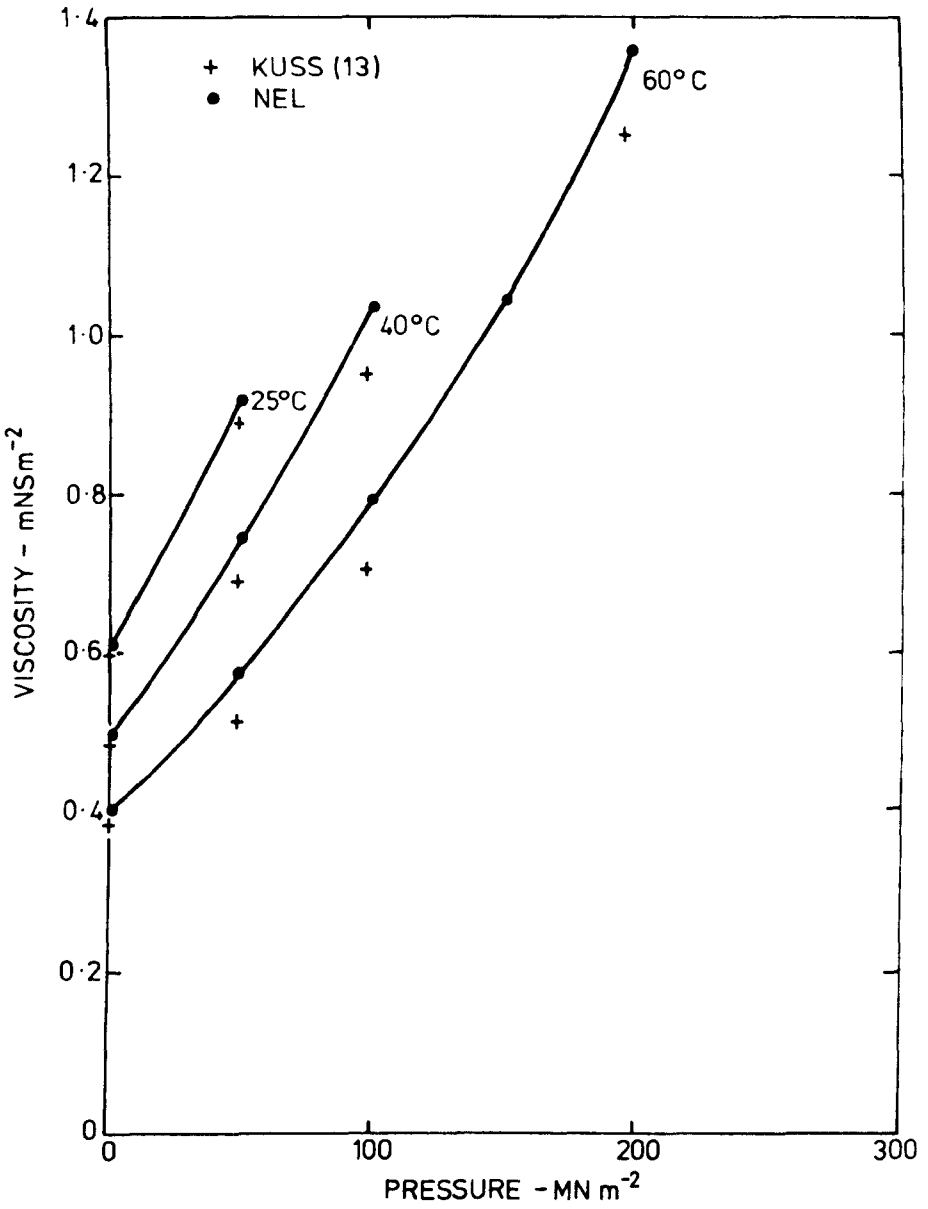

Fig. 9 Viscosity of Benzene (NEL and Kuss)

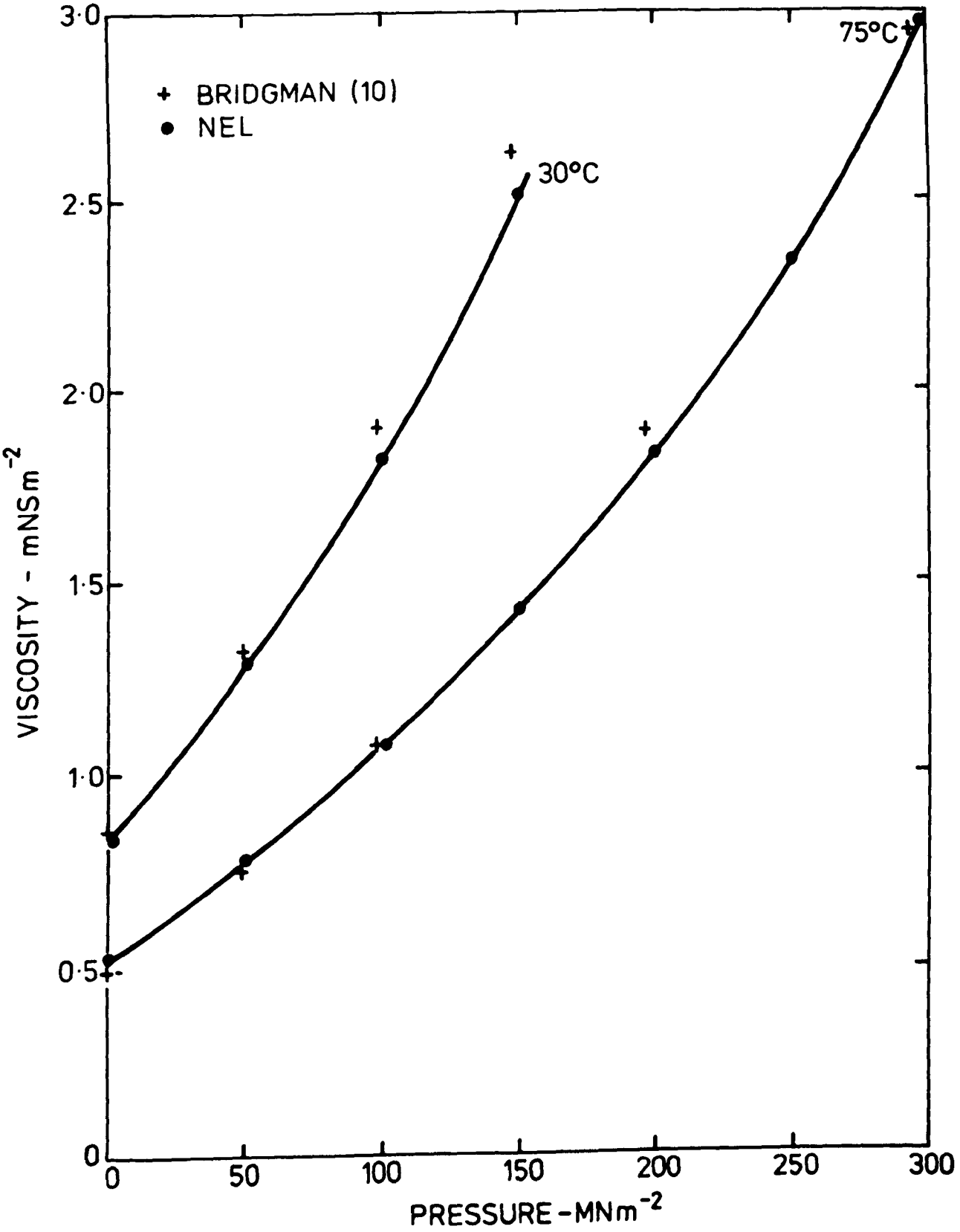

Fig. 10 Viscosity of Carbon Tetrachloride (NEL and Bridgman)

RE 39381/2 400 5/75 NEL 592 CL

ISDALE, J D and SPENCE, C M.

A self-centring falling body viscometer for high pressures.

NEL Report No 592. East Kilbride, Glasgow: National Engineering Laboratory. June 1975.
20 pages (6 figures), 30 cm.

A self-centring falling body viscometer has been developed and used to measure the viscosity of water, benzene, and carbon tetrachloride in the temperature range 25-100°C and for pressures up to 1000 MN m^{-2}. The effects of turbulence and centring of the sinkers are examined and the possibility of using this type of viscometer in an absolute way is discussed. The experimental results are compared with available data.

ISDALE, J D and SPENCE, C M.

A self-centring falling body viscometer for high pressures.

NEL Report No 592. East Kilbride, Glasgow: National Engineering Laboratory. June 1975.
20 pages (6 figures), 30 cm.

A self-centring falling body viscometer has been developed and used to measure the viscosity of water, benzene, and carbon tetrachloride in the temperature range 25-100°C and for pressures up to 1000 MN m^{-2}. The effects of turbulence and centring of the sinkers are examined and the possibility of using this type of viscometer in an absolute way is discussed. The experimental results are compared with available data.

ISDALE, J D and SPENCE, C M.

A self-centring falling body viscometer for high pressures.

NEL Report No 592. East Kilbride, Glasgow: National Engineering Laboratory. June 1975.
20 pages (6 figures), 30 cm.

A self-centring falling body viscometer has been developed and used to measure the viscosity of water, benzene, and carbon tetrachloride in the temperature range 25-100°C and for pressures up to 1000 MN m^{-2}. The effects of turbulence and centring of the sinkers are examined and the possibility of using this type of viscometer in an absolute way is discussed. The experimental results are compared with available data.

ISDALE, J D and SPENCE, C M.

A self-centring falling body viscometer for high pressures.

NEL Report No 592. East Kilbride, Glasgow: National Engineering Laboratory. June 1975.
20 pages (6 figures), 30 cm.

A self-centring falling body viscometer has been developed and used to measure the viscosity of water, benzene, and carbon tetrachloride in the temperature range 25-100°C and for pressures up to 1000 MN m^{-2}. The effects of turbulence and centring of the sinkers are examined and the possibility of using this type of viscometer in an absolute way is discussed. The experimental results are compared with available data.

NEL PUBLICATIONS

The following reports are available on request from NEL

PUGH, H Ll D and CHANDLER, E F. Mechanical properties of materials under pressure. *NEL Report* No 577

Index of NEL Publications 1972-1973. *NEL Report* No 578

HENDRY, J C and MACLEAN, M S. Extrudability of a cast steel. *NEL Report* No 579

COCKCROFT, M G and MACLEAN, M S. Impact properties of cold worked mild steel. *NEL Report* No 580

THOMSON, J F. Performance of high speed steel punches in backward extrusion of cans. *NEL Report* No 581

SCOWEN, G D. Design optimization of externally pressurized gas lubricated thrust bearings for stability. *NEL Report* No 582

HOLMES, R and POOK, L P. Plain fatigue strength of a carbon manganese steel at elevated temperatures. *NEL Report* No 583

FINLAY, I C and GRANT, W D. The accuracy of some simple methods of rating evaporative coolers. *NEL Report* No 584

POOK, L P and GREENAN, A F. Preliminary tests to determine the fatigue strength of defective steel castings. *NEL Report* No 585

CRAIG, J B. Quality of response on the NEL Road Simulator. *NEL Report* No 586

MARSH, K J, MARTIN, T and McGREGOR, J. The effect of random loading and corrosive environment on the fatigue strength of fillet-welded lap joints. *NEL Report* No 587

POOK, L P. Approximate stress intensity factors for spot and similar welds. *NEL Report* No 588

NEAL, A N. A method for the analysis of incompressible flow on an axisymmetric surface through a pump or fan blade row. *NEL Report* No 589

Advances in thermal and mechanical design of shell-and-tube heat exchangers: Report of a meeting at NEL, 28 November 1973. *NEL Report* No 590

ISDALE, J D, BRUNTON, W C and SPENCE, C M. Bulk modulus measurement and prediction. *NEL Report* No 591

NEL Report No 604

NATIONAL ENGINEERING LABORATORY

High Pressure Viscosities and Densities of Eight Halogenated Hydrocarbons

J D ISDALE and C M SPENCE

DEPARTMENT OF INDUSTRY
DECEMBER 1975

Issued by

NATIONAL ENGINEERING LABORATORY,
EAST KILBRIDE, GLASGOW

DEPARTMENT OF INDUSTRY

NATIONAL ENGINEERING LABORATORY

HIGH PRESSURE VISCOSITIES AND DENSITIES OF EIGHT HALOGENATED HYDROCARBONS

by

J D Isdale, B Sc, and C M Spence

(Fluids Group: Properties of Fluids Division)

SUMMARY

Measurements of the viscosity and density of eight halogenated hydrocarbons are presented for temperatures between 25 and 100°C and for pressures up to 500 MN m^{-2}. The new measurements agree well with published data at atmospheric pressure. The influence of chemical structure on the relationships between viscosity and pressure and between bulk modulus and density is examined.

BLANK PAGE IN ORIGINAL

CONTENTS

Distribution Group: Fluid properties data

NOTATION

A	Constant in equation (1)
a_i	Constants in Chebyshev series
B	Constant in equation (1)
$\bar{K}$	Isothermal secant bulk modulus
K_o	Isothermal secant bulk modulus at atmospheric pressure
m	Constant in equation (4)
N	Degree of Chebyshev series
P	Pressure (MN m^{-2})
P^*	Reduced pressure defined by $P^* = \log\left(1 + \frac{P}{200}\right)$
T	Temperature (K)
$T_i(x)$	Chebyshev series of degree i
η	Viscosity (mNs m^{-2})
η_0	Viscosity at atmospheric pressure (mN s m^{-2})
ρ	Density at pressure P
ρ_0	Density at atmospheric pressure P_o
Σ'	Summation, the first term of which is halved.

1 INTRODUCTION

Halogenated hydrocarbons are being used increasingly as hydraulic fluids, lubricants, refrigerants, and in other applications where chemical stability and a range of physical properties may be required. The effect of pressure on viscosity and density is important for many applications, but very few measurements under pressure are available for this group of liquids.

Apparatus has recently been developed at NEL for the measurement of viscosity[1] and density[2] at high pressures, and investigations of these properties can now be carried out at pressures up to 1000 MN m^{-2} and at temperatures up to about 200°C. Viscosity is measured by a falling body method and density by a technique using flexible bellows.

This report gives the results of tests on eight pure halogenated hydrocarbons between 25 and 100°C and for pressures up to 500 MN m^{-2}. Simple straight chain and cyclic compounds with one or two halogen substitutions have been investigated so that the effect of simple structural changes can be examined. A future report will deal in more detail with the effects of structure on viscosity.

2 LIQUIDS MEASURED

Four straight chain compounds and four cyclic compounds have been investigated. Each straight chain compound had a bromine substitution in the first position and one had another bromine substitution at the opposite end of the chain. The cyclic compounds consisted of two monosubstituted cyclohexanes and two dichlorobenzenes.

The samples were purchased as laboratory grade chemicals and the purity of each was improved by distillation at atmospheric or reduced pressure. After distillation, the purified fractions were immediately stored in tightly stoppered glass bottles until required for measurement. The boiling ranges of the samples and the distillation pressures are given in Table 1. Sample purity was estimated by gas chromatography and is also given in Table 1.

3 VISCOSITY MEASUREMENT

Viscosity measurements were made using pressurized falling body viscometers with self-centring sinkers. The viscometers were calibrated at atmospheric pressure with liquids having accurately known viscosities. Viscosity was obtained by measuring the time taken for the sinker to fall vertically down the centre of a fixed length of the viscometer tube containing the liquid. The average of at least four measurements of fall time was taken for each viscosity measurement. Corrections were applied for the effects of temperature and pressure on the viscometer dimensions and liquid density, and for the effect of turbulence on the calibrations. The dimensions of the viscometers are given in Table 2.

The pressure vessel containing a viscometer was immersed in an oil bath, the temperature of which was held constant to within ±0.02 K. Temperature was measured by a quartz thermometer in the bath, and pressure by a manganin wire resistance gauge in a separate pressure vessel at the same pressure as the main vessel but at room temperature. Since it was sometimes difficult to obtain experimental temperature and pressure settings at round numbers, corrections were applied by the following methods.

Corrections to viscosity for temperature settings were all less than 0.2 per cent, and were calculated using

$$\ln \eta = A + \frac{B}{T}. \qquad (1)$$

For each correction the constants in equation (1) were calculated using the point nearest in temperature with the same pressure. If a corresponding pressure was not available the value of

B from the nearest pressure and temperature was used. In these cases errors due to the approximate value of B were negligible since the corrections were always small.

For bromocyclohexane, chlorocyclohexane, and 1,5-dibromopentane pressure settings were accurate and correction to round values was unnecessary. For the other liquids, values at round pressures were obtained by fitting each isotherm by the equation

$$\log\left(\frac{\log \eta + 1.2}{\log \eta_0 + 1.2}\right) = \sum_{i=0}^{N} a_i T_i(P^*). \qquad (2)$$

The reduced forms of viscosity and pressure in this equation are similar to those found by Roelands[3] to be satisfactory for mineral oils and also for some pure liquids.

If more than four points were available $N = 3$ gave a good fit which was used to calculate values at exact pressures. For smaller numbers of points N was reduced to an appropriate value. Pressure corrections of up to 3.0 MN m^{-2} were applied in this way, leading to viscosity corrections of less than 3.5 per cent.

An example of these temperature and pressure corrections is given in Table 3, which shows the experimentally observed viscosities of 1-bromopentane and the corrected values.

Some of the liquids were also measured at atmospheric pressure in master viscometers[4]. The results of these and measurements made by falling body viscometers at atmospheric pressure are given in Table 4.

The results of measurements made at high pressure are presented in the form of the ratio of the viscosity at pressure to that at atmospheric pressure and the same temperature. These ratios are given in Tables 5–12. Each table is based on measurements made by one falling body viscometer except in the following cases.

For chlorocyclohexane, fall time readings at atmospheric pressure were found to be erratic in both viscometers 1 and 3, while at high pressure both viscometers gave consistent fall times which led to calculated viscosities in good agreement. Raising the pressure to a value slightly above atmospheric[1] in this case did not eliminate the erratic fall times, which were probably due to the very high Reynolds numbers. Master viscometer values were therefore used to calculate the ratios given in Table 12, which are based on the mean of the viscosities at pressure, measured by viscometers 1 and 3, and master viscometer values at atmospheric pressure.

Bromocyclohexane was also measured in viscometers 1 and 3, but in this case only viscometer 3 gave unstable fall times at atmospheric pressure. Table 11 is therefore based on the mean of the viscosities at pressure measured by viscometers 1 and 3, and viscosities at atmospheric pressure from viscometer 1.

4 DENSITY MEASUREMENTS

The variation of density with pressure was obtained by measuring the change in length of sealed flexible bellows containing the liquid. The bellows were pressurized in the same pressure vessel as the viscometers but in independent tests. Effective area of the bellows was obtained by calibration with water and the initial volume of the sample from its weight and density at atmospheric pressure. Densities at atmospheric pressure were measured in bicapillary pycnometers except for five values which were taken from the literature. These are indicated in Table 13, which summarizes the complete set of density results.

Density under pressure is expressed in the form of the isothermal secant bulk modulus $\bar{K}$ defined by

$$\bar{K} = \frac{\rho P}{\rho - \rho_0}. \qquad (3)$$

It is found experimentally that for many liquids $\bar{K}$ varies linearly with pressure over quite wide pressure ranges, so that we may write

$$\bar{K} = K_o + mP. \qquad (4)$$

The bulk modulus measurements are estimated to be accurate to ±3.0 per cent and, within these limits, equation (4) fitted the results for all eight liquids at both 25°C and 75°C. Figs 1 and 2 show the results for 1-bromododecane and chlorocyclohexane. Equation constants for all the liquids are also given in Table 13.

Densities at intermediate pressures and other temperatures for the calculation of viscosity were obtained using the constants for equation (4) and by linear interpolation or extrapolation of density at constant pressure. Values obtained in this way are given in Table 3 for 1-bromopentane.

5 COMPARISON WITH OTHER DATA AT ATMOSPHERIC PRESSURE

Viscosities at atmospheric pressure are compared with data from various sources in Figs 3–10. For 1-bromopentane, 1-bromooctane and bromocyclohexane, the NEL measurements agree well with the literature values, the maximum difference being 1.5 per cent. The results for 1-bromododecane agree with those of Cokelet[5] to within 1 per cent, but the values given by Hennelly[6] are about 6 per cent higher. Similarly the results for 1,3-dichlorobenzene agree with those of Friend[7] to within 2 per cent, but the values given by Griffing[8] are higher and diverge increasingly with temperature to give a difference of 14 per cent at 100°C. For 1,2-dichlorobenzene on the other hand the agreement with Griffing is good above 40°C while the values of Friend[7] and Dreisbach[9] are less than 3 per cent lower. The single point[10] available for 1,5-dibromopentane is within 2 per cent of the measured value at 25°C, and for chlorocyclohexane the present measurements are about 3 per cent higher than those tabulated in Landolt-Börnstein[11].

The estimated accuracy of measurements made by the falling body viscometers is ±2 per cent and by master viscometers ±0.25 per cent. The agreement between the present measurements and the literature values is therefore good when the accuracy of both sources is taken into account. The accuracy of 0.2 per cent claimed by Griffing[8] for the measurements of 1,3-dichlorobenzene is not supported by the NEL measurements or by those of Friend[7] over a similar temperature range. Hennelly[5] gives values for 1-bromododecane graphically, and numerical values extracted from his diagrams are subject to errors of about 5 per cent.

6 DISCUSSION OF RESULTS

Viscosity results for 1-bromopentane are shown in Fig. 11 in the form of a plot of the logarithm of viscosity (in mN s m^{-2}) against pressure. The isotherms are concave towards the pressure axis at lower pressures but tend to become linear at higher pressures. Results for the other liquids are similar and this type of variation is common to most pure liquids.

The viscosity results at 25°C are summarized in Fig. 12,which shows the variation with pressure of the ratio of viscosity at pressure to that at atmospheric pressure and the same temperature. Results for water, benzene, and carbon tetrachloride[1] are included for comparison along with a naphthenic and a paraffinic oil[12]. Though the relationship between viscosity and structure is not yet understood in detail some useful information may be obtained from comparison of this sort.

The four bromoalkanes conform to the accepted generalization that the change in viscosity with pressure is greater for liquids which have a high viscosity at atmospheric pressure. This is further illustrated in Fig. 13, which shows how the viscosity ratio at 100 MN m^{-2} and 25°C changes with viscosity at atmospheric pressure.

Though the cyclic compounds also conform, since the cyclohexanes with higher viscosities have a greater increase in viscosity ratio with pressure than the benzenes, they show an additional

feature which is of interest. The cyclohexanes, which have molecules of similar shape but viscosities differing by 27–30 per cent, have an almost identical change in viscosity ratio with pressure. The same effect is shown by the dichlorobenzenes, which have slightly different molecular shapes and viscosities differing by 26–28 per cent but similar viscosity ratios. The similarity of the viscosity ratios of the cyclic compounds is shown in Fig. 14 and is evident for all the isotherms measured. The slight difference in shape between the two dichlorobenzenes is clearly not of major importance, probably because both molecules have some packing arrangements in common.

The density results are shown graphically in Fig .15 in the form of a plot of isothermal secant bulk modulus at atmospheric pressure, K_o, against density at atmospheric pressure. Two distinct trends can be detected and these are evident at both temperatures. The bulk modulus of the straight chain compounds decreases as density increases while that of the cyclic compounds and 1,5-dibromopentane increases with density. Obviously these trends are only part of a larger pattern which will not become clear without additional data.

The change in bulk modulus with pressure m varies by less than 11 per cent within this group of liquids and is slightly less than that of hydraulic fluids. Chemical structure is therefore not a major factor in determining change in bulk modulus with pressure.

7 CONCLUSIONS

Viscosities and densities of eight halogenated hydrocarbons have been measured at temperatures between 25 and 100°C and for pressures up to 500 MN m^{-2}. The measurements are in good agreement with other data at atmospheric pressure.

The results show that the change in viscosity with pressure is similar to that of other simple liquids and is usually greater for liquids which have higher viscosities at atmospheric pressure. Two exceptions to this generalization have been found in which liquids of similar molecular shape, but having different viscosities at atmospheric pressure, show similar changes in viscosity ratio with pressure over a range of temperature. For these liquids, chlorocyclohexane and bromocyclohexane, and 1,2-dichlorobenzene and 1,3-dichlorobenzene, molecular shape is the major factor controlling the variation of viscosity with pressure.

The density results show that, within the accuracy of the present measurements, the linear secant modulus equation (equation (2)) may be used to describe the variation of density with pressure in the range examined. The bulk modulus at atmospheric pressure shows a similar relation to chemical structure at different temperatures, but the change in bulk modulus with pressure does not vary much within this group of liquids.

REFERENCES

1 ISDALE, J. D. and SPENCE, C. M. A self-centring falling body viscometer for high pressures. *NEL Report* No 592. East Kilbride, Glasgow: National Engineering Laboratory, 1975.

2 ISDALE, J. D., BRUNTON, W. C. and SPENCE, C. M. Bulk modulus measurement and prediction. *NEL Report* No 591. East Kilbride, Glasgow: National Engineering Laboratory, 1975.

3 ROELANDS, C. J. A. *Correlational aspects of the viscosity-temperature-pressure relationship of lubricating oils.* PhD Thesis. Delft: University of Delft, 1966.

4 BRITISH STANDARDS INSTITUTION. Determination of the viscosity of liquids in c.g.s. units. *B.S.* 188 : 1957.

5 COKELET, G. R., HOLLANDER, F. J. and SMITH, J. H. Density and viscosity of mixtures of 1,1,2,2-tetrabromoethane and 1-bromododecane. *J. chem. Engng Data*, 1969, **14**(4), 470–473.

6 HENNELLY, E. J., HESTON, W. M. and SMYTH, C. P. Microwave absorbtion and molecular structure in liquids: III dielectric relaxation and structure in organic halides. *J. Amer. Chem. Soc.*, 1948, **70**, 4102–4111.

7 FRIEND, J. N. and HARGREAVES, W. D. Viscosity and the hydrogen bond. Hydroxyl and ortho effects. *Phil. Mag.*, 1945, **36**(262), 731–756.

8 GRIFFING, V., CARGYLE, M. A., CORVESE, L. and EBY, D. Temperature coefficients of viscosity of some halogen substituted organic compounds. *J. phys. Chem., Ithaca*, 1954, **58**, 1054–1056.

9 DREISBACH, R. R. Physical properties of chemical compounds. *Advances in Chemistry Series* No 15. Washington: American Chemical Society, 1955.

10 DUNSTAN, A. E., HILDITCH, T. P. and THOLE, F. B. *The relation between viscosity and chemical constitution. VII. The effect of the relative position of two unsaturated groups on viscosity.* Das Elbst., 1913, 103, 133–144.

11 LANDOLT-BÖRNSTEIN (SCHÄFER, K., Ed). *Numerical data and functional relationships in science and technology* (in German). 6th edn. Group II, vol 5a, p 203. Berlin: Springer, 1969.

12 AMERICAN SOCIETY OF MECHANICAL ENGINEERS. *Viscosity and density of over forty lubricating fluids of known composition at pressures to 150 000 psi and temperatures to 425 F.* New York: American Society of Mechanical Engineers, 1953.

13 FRIEND, J. N. and HARGREAVES, W. D. Viscosity and the boiling point – the rheochor. *Phil. Mag.*, 1943, **34**(236), 643–650.

14 CERNYAWSKAYA, I. A. Absolute viscosities of alkyl chloride and alkyl bromide series at elevated temperatures (in Russian). *Leningradski Universitet. Vestnik. Seriya Fiz. Khem.*, 1964, (16), 35–37.

15 SIMON, I. Research on the freezing points of organic compounds (in French). *Bull. Soc. chim. Belg.*, 1929, **38**(2), 47–70.

16 MUMFORD, S. A. and PHILLIPS, J. W. C. The physical properties of some aliphatic compounds. *J. Chem. Soc.*, 1950, 75–84.

17 DREISBACH, R. R. Physical properties of chemical compounds III. *Advances in Chemistry Series* No 29. Washington: Americal Chemical Society, 1961.

LIST OF TABLES

LIST OF FIGURES

TABLE 1

Liquids Measured

Liquid	Normal boiling temperature °C	Boiling range of sample °C	Distillation pressure mmHg	Purity per cent
1-bromopentane	129.5	37.29– 38.25	25	98.9
1-bromooctane	200.0	97.70– 98.06	25	96.3
1-bromododecane	275.9	162.53–162.76	25	98.0
1,5-dibromopentane	222.3	114.00–114.46	24	98.7
1,2-dichlorobenzene	180.5	180.33–180.39	760	97.6
1,3-dichlorobenzene	173.5	173.24–173.27	760	99.8
bromocyclohexane	166.8	65.07– 65.44	25	98.6
chlorocyclohexane	142.5	48.20– 48.80	25	99.3

TABLE 2

Viscometer Dimensions

Viscometer number	Sinker dimensions		Tube dimensions	
	Diameter mm	Length mm	Diameter mm	Length mm
1	7.559	10.185	7.785	148.84
2	7.341	9.580	7.582	149.00
3	7.463	12.547	7.785	34.90

TABLE 3

Viscosity Calculations for 1-Bromopentane

Measured					Temperature corrected		Temperature and pressure corrected	
Pressure MN m^{-2}	Temperature °C	Fall time s	Density g cm^{-3}	Viscosity mN s m^{-2}	Temperature °C	Viscosity mN s m^{-2}	Pressure MN m^{-2}	Viscosity mN s m^{-2}
0.1	24.990	28.16	1.212	0.7540	25	0.7539	0.1	0.7558
47.6	25.053	40.78	1.259	1.0857	25	1.0864	50.0	1.0953
97.6	24.983	55.57	1.297	1.4712	25	1.4709	100.0	1.4972
147.6	25.005	73.89	1.328	1.9468	25	1.9471	150.0	1.9745
197.6	25.012	95.48	1.354	2.5055	25	2.5059	200.0	2.5467
297.6	25.031	155.88	1.395	4.0646	25	4.0667	300.0	4.0886
397.6	25.022	246.88	1.427	6.4062	25	6.4089	400.0	6.4440
497.6	25.036	386.72	1.451	9.9995	25	10.0074	500.0	10.1626
0.1	50.027	21.48	1.179	0.5752	50	0.5753	0.1	0.5763
47.6	50.057	30.82	1.233	0.8224	50	0.8228	50.0	0.8316
97.6	50.055	41.59	1.274	1.1038	50	1.1043	100.0	1.1212
197.6	50.037	68.28	1.334	1.7958	50	1.7965	200.0	1.8242
297.6	50.026	105.13	1.376	2.7473	50	2.7481	300.0	2.7726
397.6	50.025	158.09	1.406	4.1126	50	4.1143	400.0	4.1251
497.6	50.022	233.51	1.430	6.0533	50	6.0558	500.0	6.1429

TABLE 3 (contd)

0.1	75.027	17.49	1.148	0.4664	75	0.4666	0.1	0.4670
47.6	75.059	24.77	1.207	0.6617	75	0.6619	50.0	0.6693
101.6	75.039	33.64	1.251	0.8948	75	0.8950	100.0	0.8924
201.6	75.069	54.29	1.313	1.4314	75	1.4322	200.0	1.4172
301.6	75.064	81.15	1.356	2.1256	75	2.1269	300.0	2.1161
0.1	100.010	14.34	1.118	0.3774	100	0.3775	0.1	0.3778
47.7	100.010	20.88	1.181	0.5576	100	0.5576	50.0	0.5636
97.6	100.010	27.96	1.228	0.7448	100	0.7449	100.0	0.7596
197.6	100.040	44.59	1.293	1.1781	100	1.1785	200.0	1.1846
297.6	100.030	65.26	1.336	1.7133	100	1.7137	300.0	1.7319

TABLE 4

Viscosities at Atmospheric Pressure – mN s m^{-2}

Liquid	Temperature °C				Viscometer
	25.00	50.00	75.00	100.00	
1-bromopentane	0.756	0.576	0.467	0.378	2
1-bromooctane	1.4941	1.0265	0.7548	0.5642	MV
1-bromododecane	3.3547	2.0415	–	–	MV
1,5-dibromopentane	3.099	1.985	1.420	–	1
1,2-dichlorobenzene	1.258	0.965	0.749	0.582	2
1,3-dichlorobenzene	1.0015	0.7529	0.5916	0.4643	MV
bromocyclohexane	1.979	1.356	0.965	–	1
chlorocyclohexane	1.5625	1.0444	0.7480	–	MV

TABLE 5

Viscosity Ratios of 1-Bromopentane

Temperature °C	Pressure MN m^{-2}	Viscosity ratio
25	0.1	1.000
25	50.0	1.449
25	100.0	1.981
25	150.0	2.612
25	200.0	3.370
25	300.0	5.409
25	400.0	8.526
25	500.0	13.446
50	0.1	1.000
50	50.0	1.443
50	100.0	1.946
50	150.0	2.514
50	200.0	3.165
50	300.0	4.811
50	400.0	7.158
50	500.0	10.659
75	0.1	1.000
75	50.0	1.433
75	100.0	1.911
75	150.0	2.440
75	200.0	3.035
75	300.0	4.532
100	0.1	1.000
100	50.0	1.492
100	100.0	2.011
100	150.0	2.551
100	200.0	3.135
100	300.0	4.584

TABLE 6

Viscosity Ratios of 1-Bromooctane

Temperature °C	Pressure MN m^{-2}	Viscosity ratio
25	0.1	1.000
25	50.0	1.579
25	100.0	2.360
25	150.0	3.406
25	200.0	4.796
25	300.0	9.089
25	400.0	16.656
25	500.0	30.078
50	0.1	1.000
50	50.0	1.541
50	100.0	2.229
50	150.0	3.095
50	200.0	4.177
50	300.0	7.232
50	400.0	12.070
50	500.0	19.856
75	0.1	1.000
75	50.0	1.513
75	100.0	2.141
75	150.0	2.895
75	200.0	3.798
75	300.0	6.190
75	400.0	9.716
75	500.0	15.042
100	0.1	1.000
100	50.0	1.517
100	100.0	2.120
100	150.0	2.809
100	200.0	3.605
100	300.0	5.665

TABLE 7

Viscosity Ratios of 1-Bromododecane

Temperature °C	Pressure MN m^{-2}	Viscosity ratio
25	0.1	1.000
25	50.0	1.966
25	100.0	2.823
25	150.0	4.050
25	200.0	6.827
50	0.1	1.000
50	50.0	1.660
50	100.0	2.553
50	150.0	3.743
50	200.0	5.323
50	300.0	10.237

TABLE 8

Viscosity Ratios of 1,5-Dibromopentane

Temperature °C	Pressure MN m^{-2}	Viscosity ratio
25	0.1	1.000
25	100.0	2.198
25	200.0	4.435
25	300.0	8.668
50	0.1	1.000
50	100.0	2.000
50	200.0	3.640
50	300.0	6.331
50	400.0	10.743
50	500.0	17.977
75	0.1	1.000
75	100.0	1.922
75	200.0	3.244
75	300.0	5.229
75	300.0	5.647

TABLE 9

Viscosity Ratios of 1,2-Dichlorobenzene

Temperature °C	Pressure MN m^{-2}	Viscosity ratio
25	0.1	1.000
25	50.0	1.424
25	100.0	1.954
25	150.0	2.665
25	200.0	3.671
50	0.1	1.000
50	50.0	1.386
50	100.0	1.842
50	150.0	2.402
50	200.0	3.116
50	300.0	5.311
75	0.1	1.000
75	50.0	1.358
75	100.0	1.780
75	150.0	2.286
75	200.0	2.898
75	300.0	4.561
75	400.0	7.105
75	500.0	11.078
100	0.1	1.000
100	50.0	1.371
100	100.0	1.792
100	150.0	2.274
100	200.0	2.835
100	300.0	4.282
100	400.0	6.373

TABLE 10

Viscosity Ratios of 1,3-Dichlorobenzene

Temperature °C	Pressure MN m^{-2}	Viscosity ratio
25	0.1	1.000
25	50.0	1.468
25	100.0	1.888
25	150.0	2.431
25	200.0	3.358
50	0.1	1.000
50	50.0	1.367
50	100.0	1.800
50	150.0	2.318
50	200.0	2.947
50	300.0	4.689
50	400.0	7.440
75	0.1	1.000
75	50.0	1.356
75	100.0	1.753
75	150.0	2.209
75	200.0	2.745
75	300.0	4.179
75	400.0	6.396
100	0.1	1.000
100	50.0	1.464
100	100.0	1.907
100	150.0	2.410
100	200.0	3.106

TABLE 11

Viscosity Ratios of Bromocyclohexane

Temperature °C	Pressure MN m^{-2}	Viscosity ratio
25	0.1	1.000
25	100.0	2.709
25	200.0	6.426
25	300.0	14.241
25	400.0	30.694
25	500.0	66.957
50	0.1	1.000
50	100.0	2.532
50	200.0	5.526
50	300.0	11.322
50	400.0	22.141
50	500.0	42.911
50	600.0	84.991
75	0.1	1.000
75	100.0	2.414
75	200.0	4.615

TABLE 12

Viscosity Ratios of Chlorocyclohexane

Temperature °C	Pressure MN m^{-2}	Viscosity ratio
25	0.1	1.000
25	100.0	2.790
25	200.0	6.535
25	300.0	14.346
50	0.1	1.000
50	100.0	2.637
50	200.0	5.602
50	300.0	11.283
50	400.0	22.542
75	0.1	1.000
75	100.0	2.540
75	200.0	4.934
75	300.0	9.431
75	400.0	17.283
75	500.0	30.350

TABLE 13

Density and Bulk Modulus at 25 and 75°C

Temperature °C	25.00			75.00		
Liquid	Density kg m^{-3}	K_o GN m^{-2}	m	Density kg m^{-3}	K_o GN m^{-2}	m
1-bromopentane	1211.9[17]	1.149	3.772	1148.1	0.860	3.690
1-bromooctane	1107.2[17]	1.270	4.182	1055.0	0.990	3.695
1-bromododecane	1035.7	1.374	4.662	991.3	1.142	3.648
1,5-dibromopentane	1692.5	1.888	3.734	1622.5	1.477	3.633
1,2-dichlorobenzene	1300.2[9]	1.718	4.329	1245.6	1.348	3.923
1,3-dichlorobenzene	1281.9[8]	1.684	4.046	1223.4[8]	1.336	3.842
bromocyclohexane	1329.6	1.628	3.638	1268.6	1.268	3.542
chlorocyclohexane	993.9	1.498	3.351	944.8	1.121	3.526

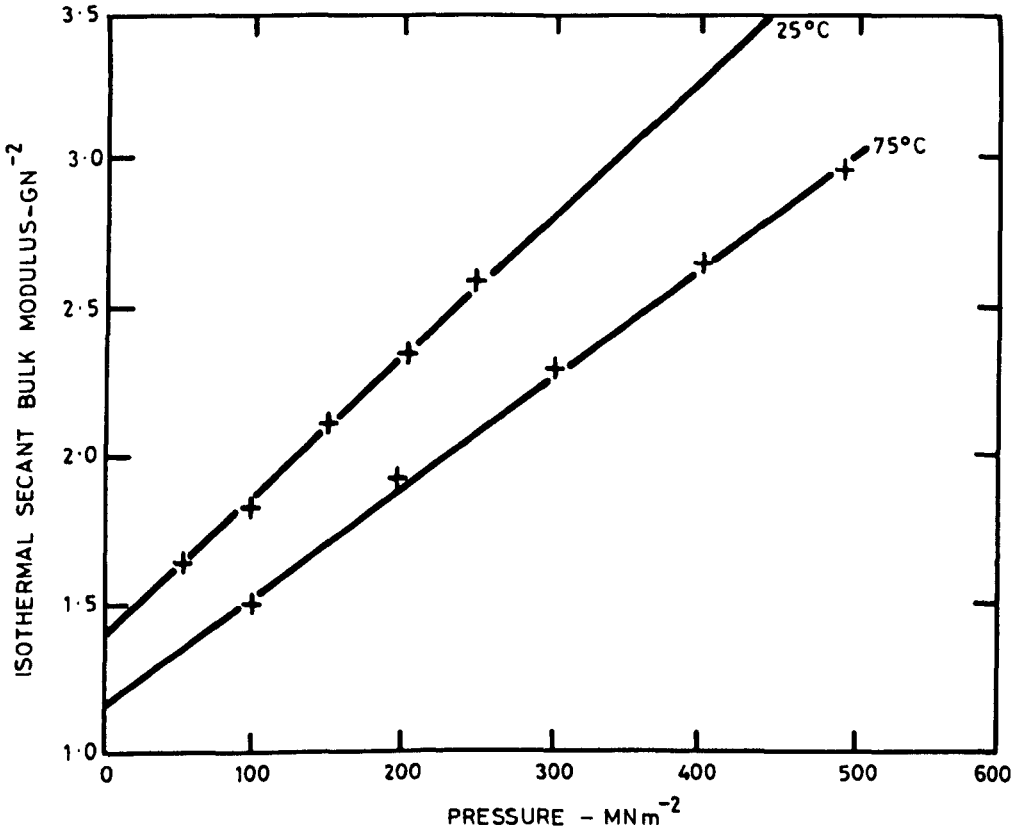

Fig. 1 Bulk Modulus of 1-Bromododecane

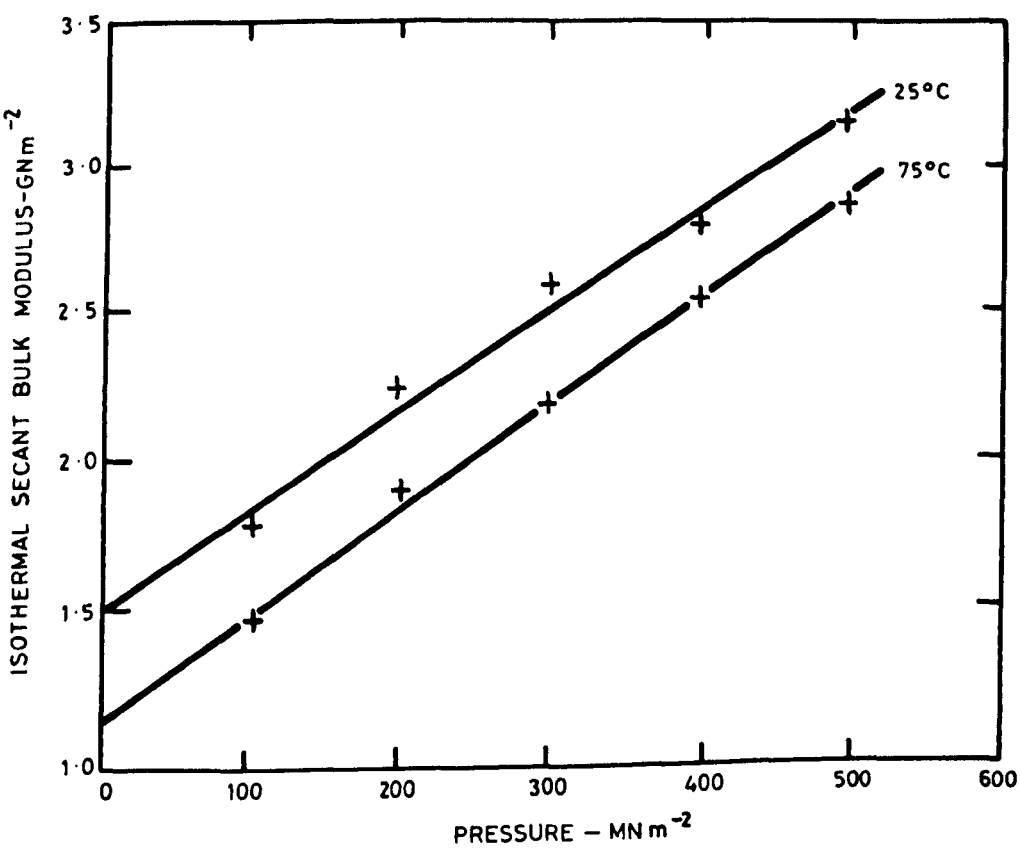

Fig. 2 Bulk Modulus of Chlorocyclohexane

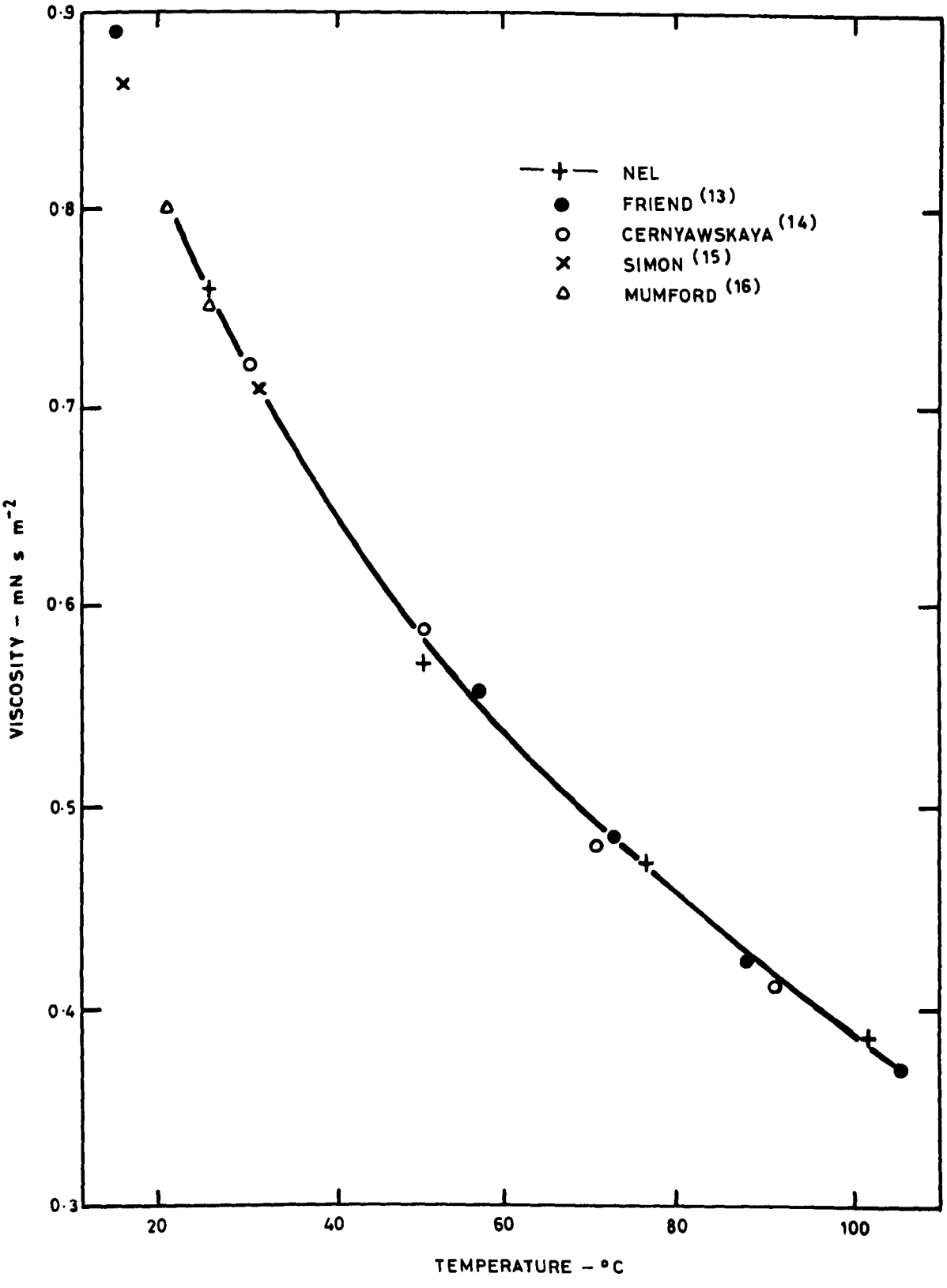

Fig. 3 Viscosity of 1-Bromopentane

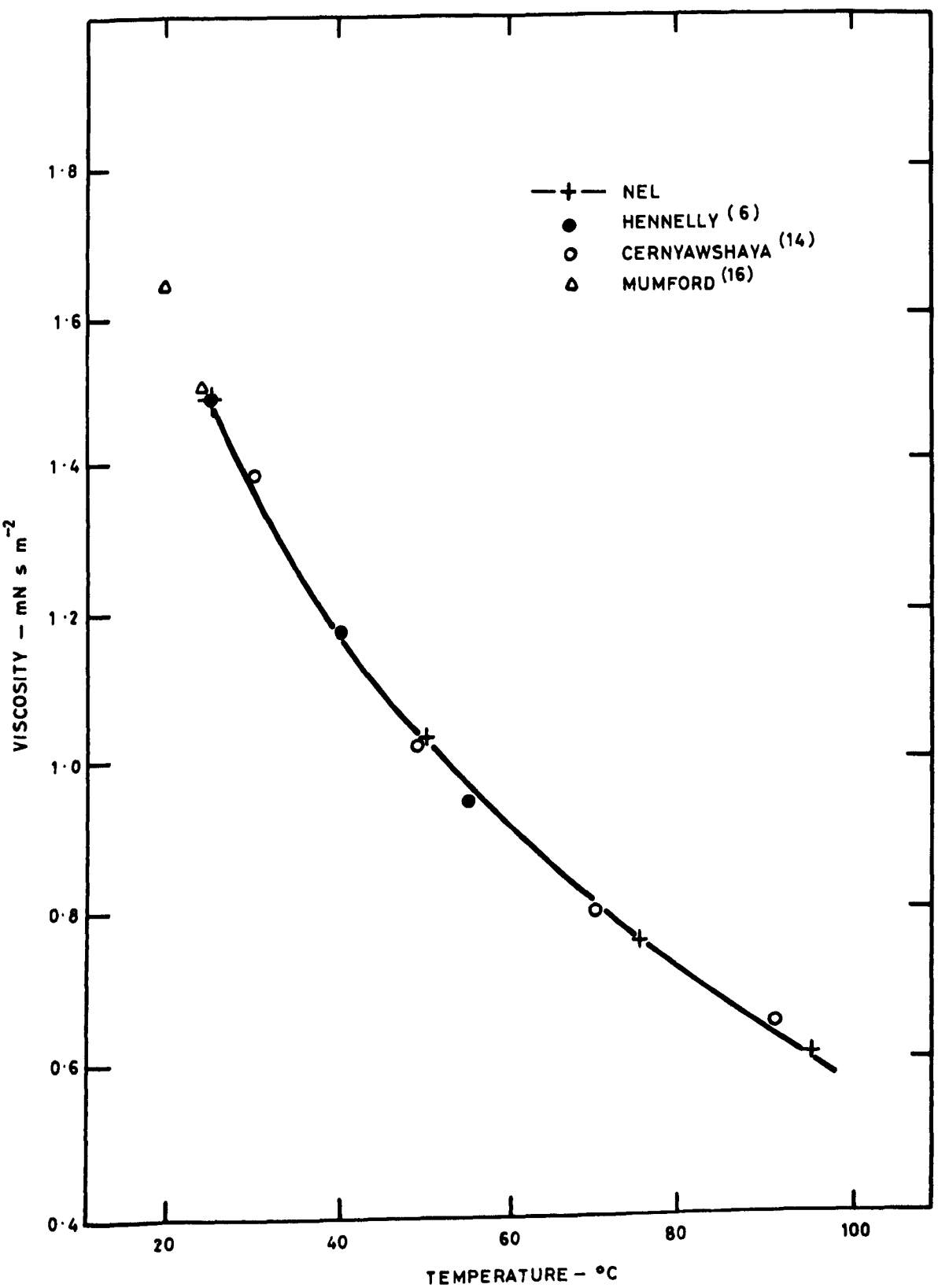

Fig. 4 Viscosity of 1-Bromooctane

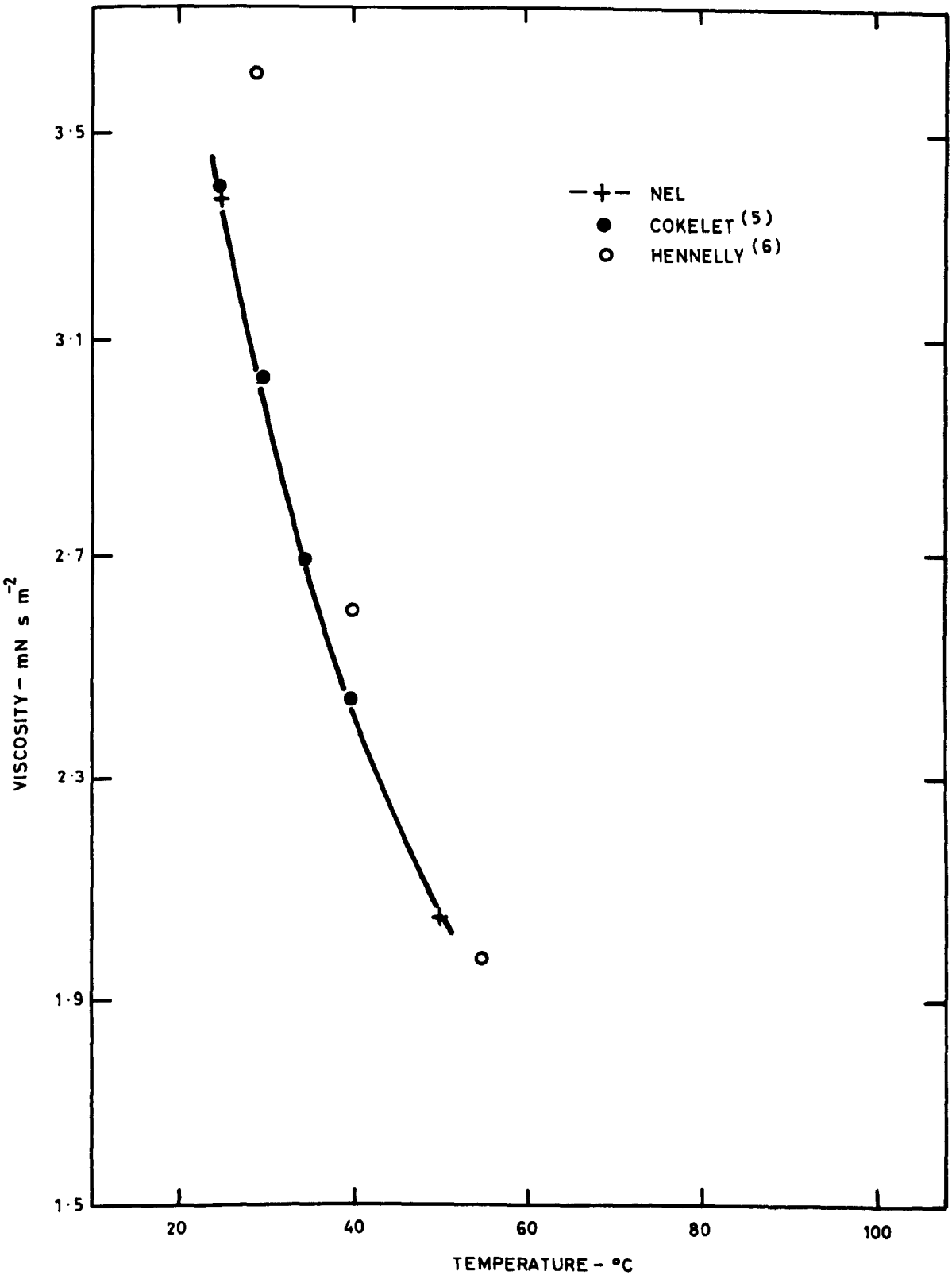

Fig. 5 Viscosity of 1-Bromododecane

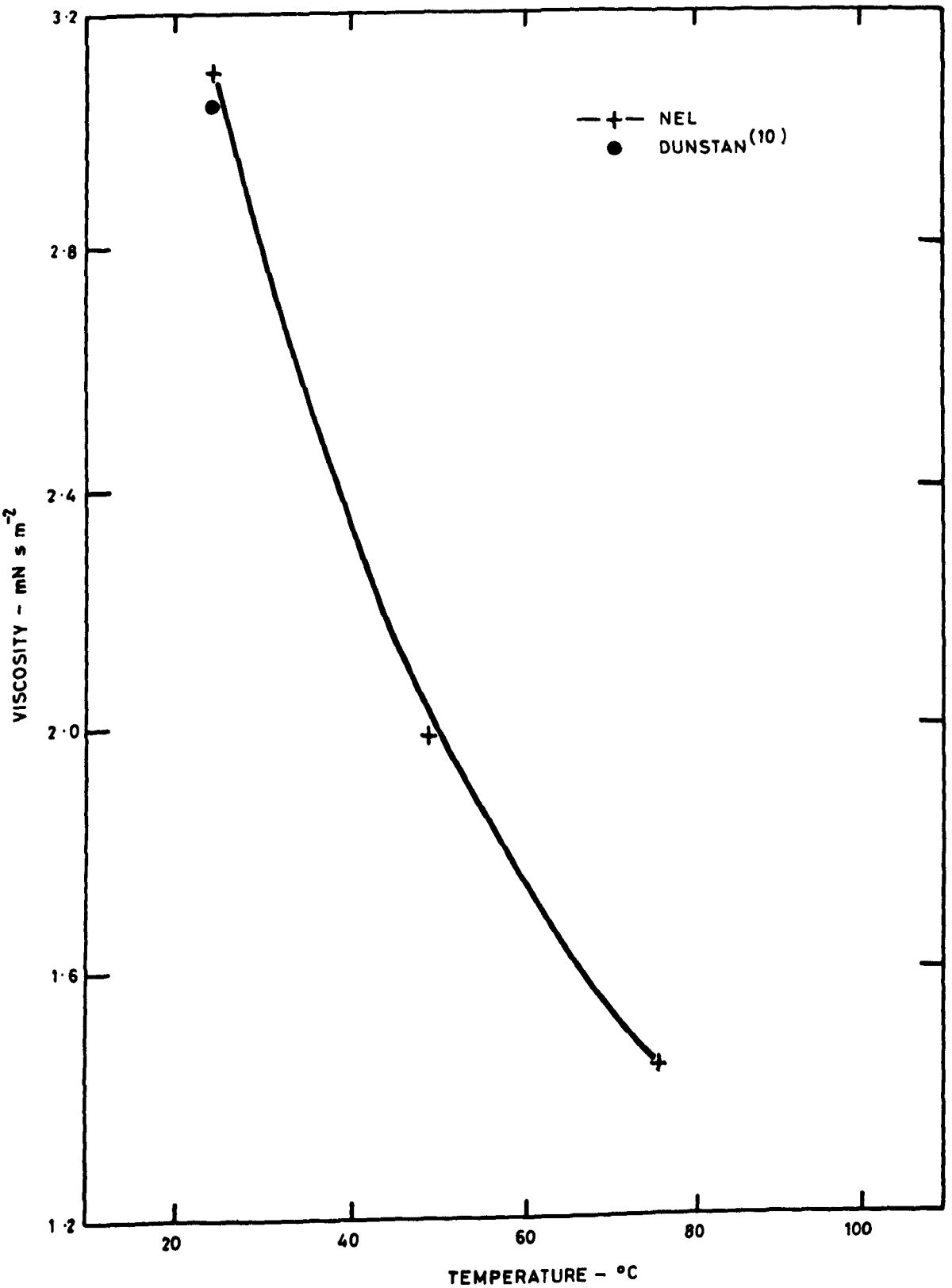

Fig. 6 Viscosity of 1,5-Dibromopentane

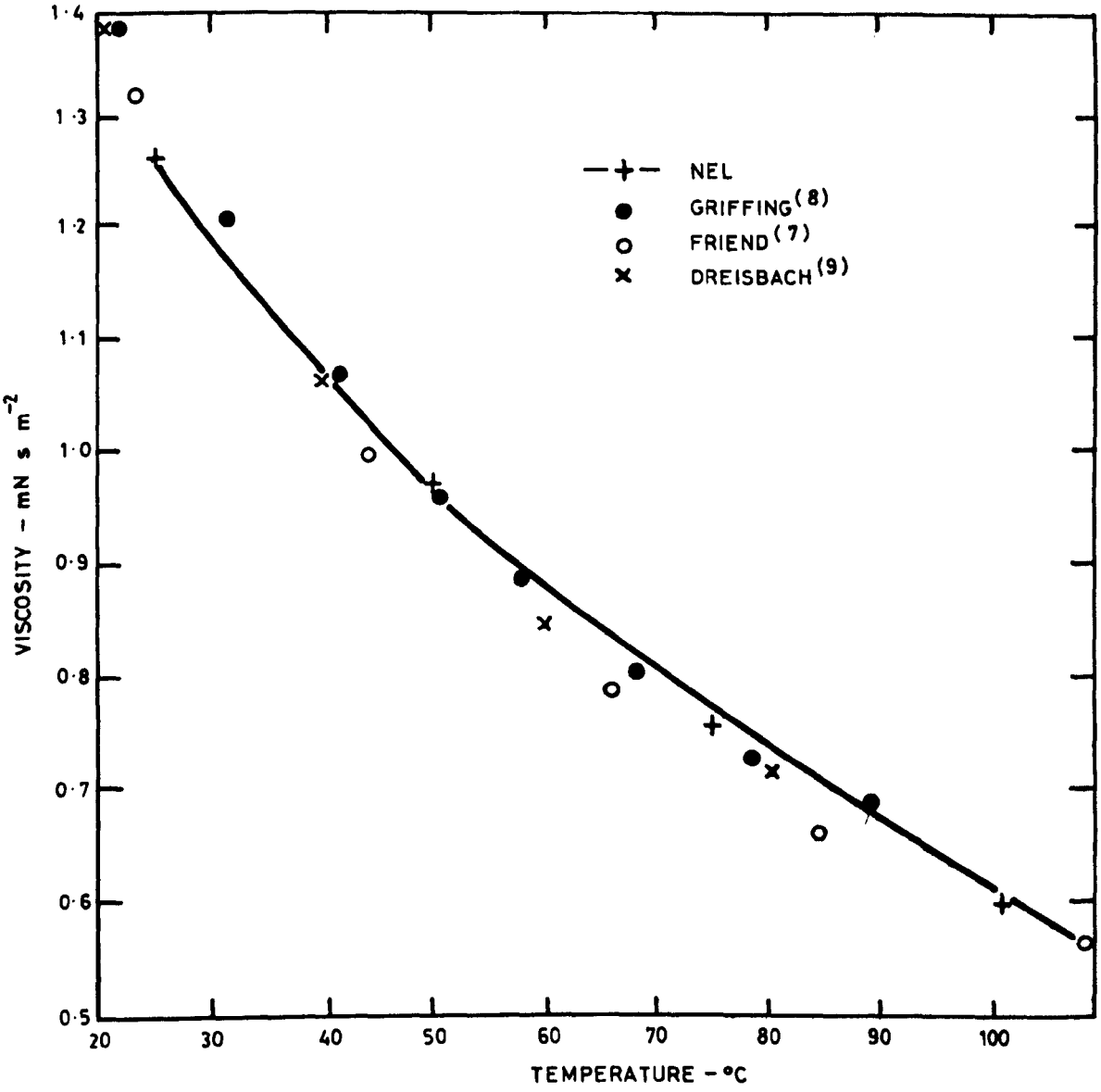

Fig. 7 Viscosity of 1,2-Dichlorobenzene

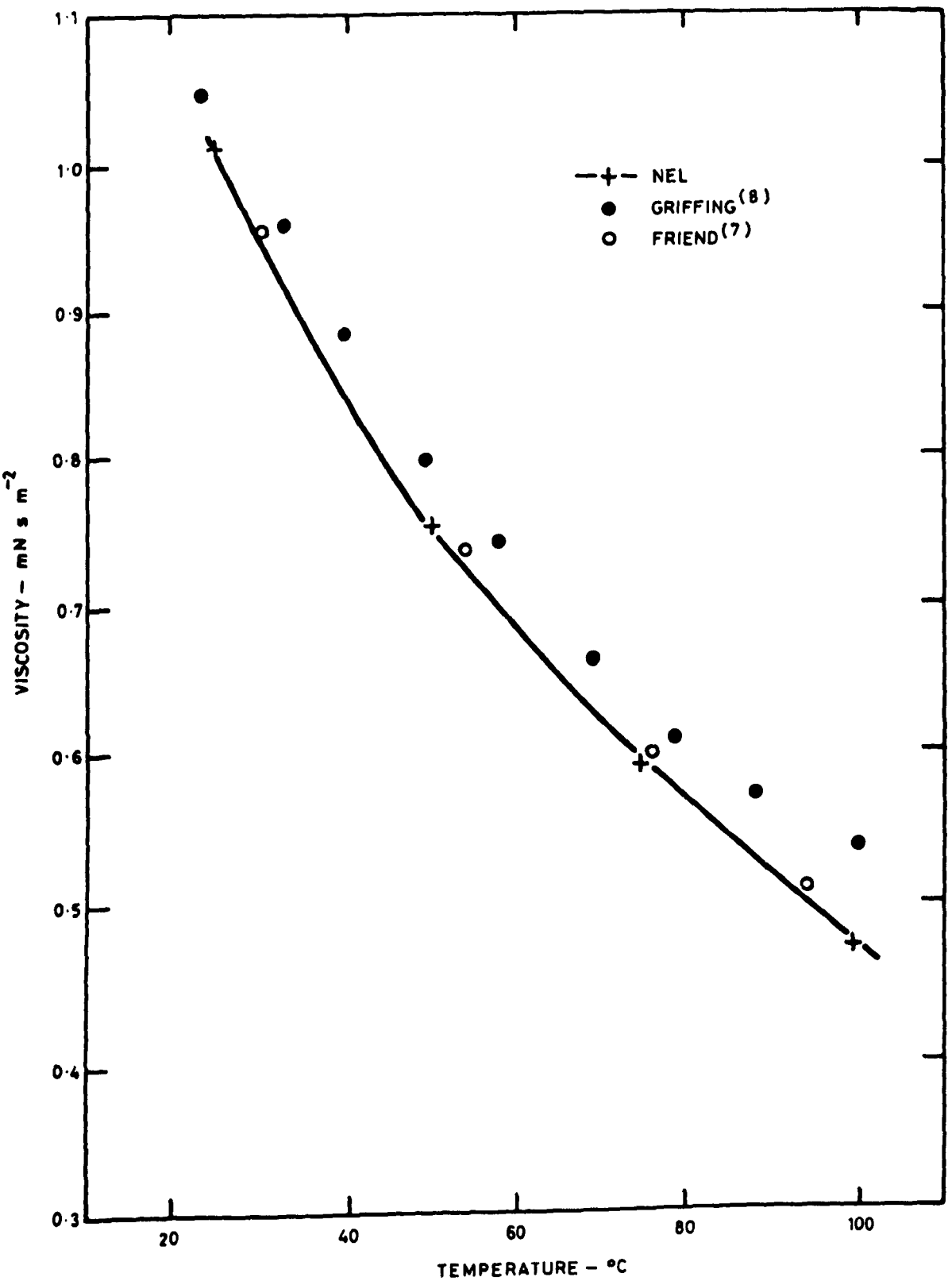

Fig. 8 Viscosity of 1,3-Dichlorobenzene

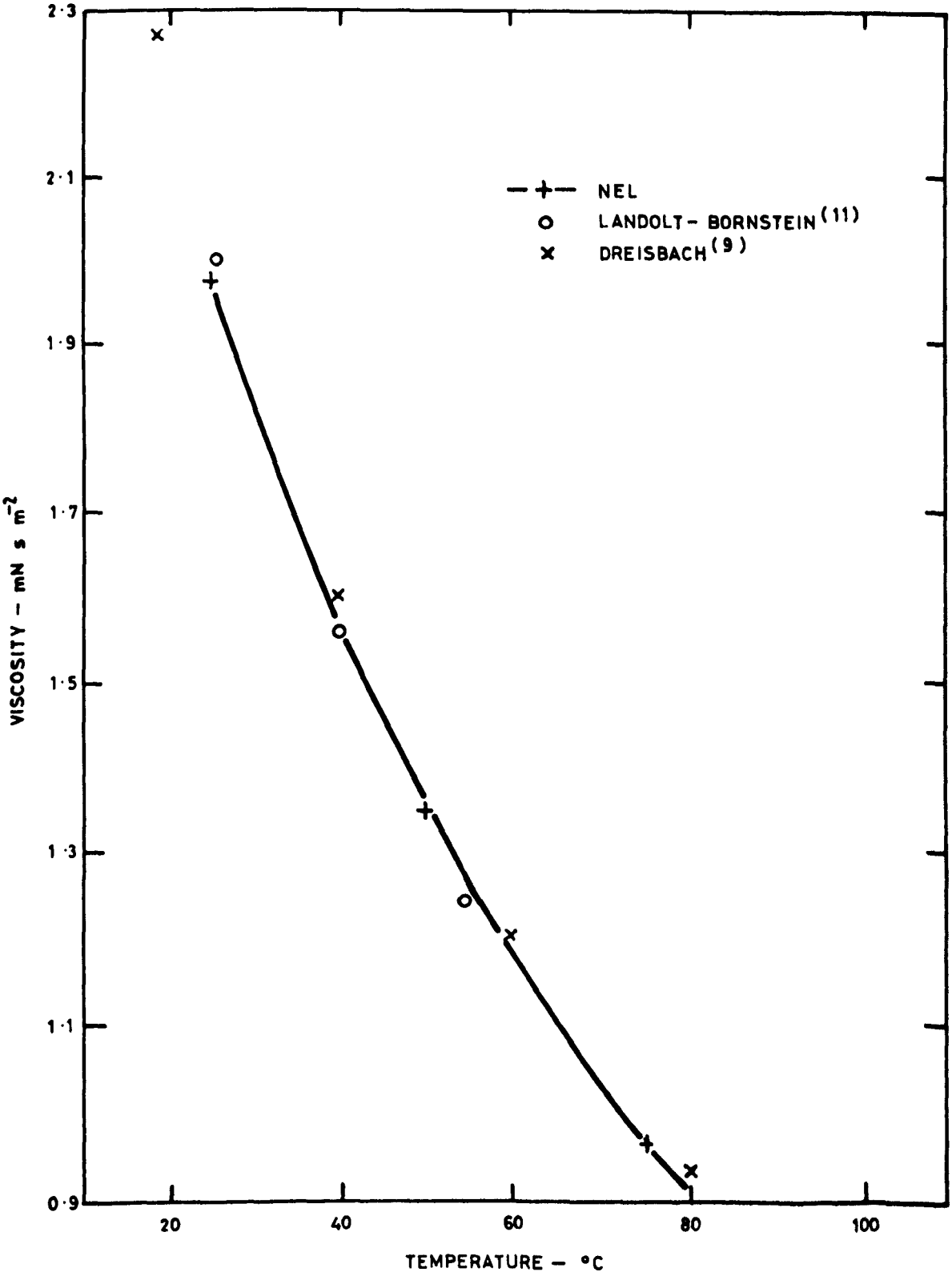

Fig. 9 Viscosity of Bromocyclohexane

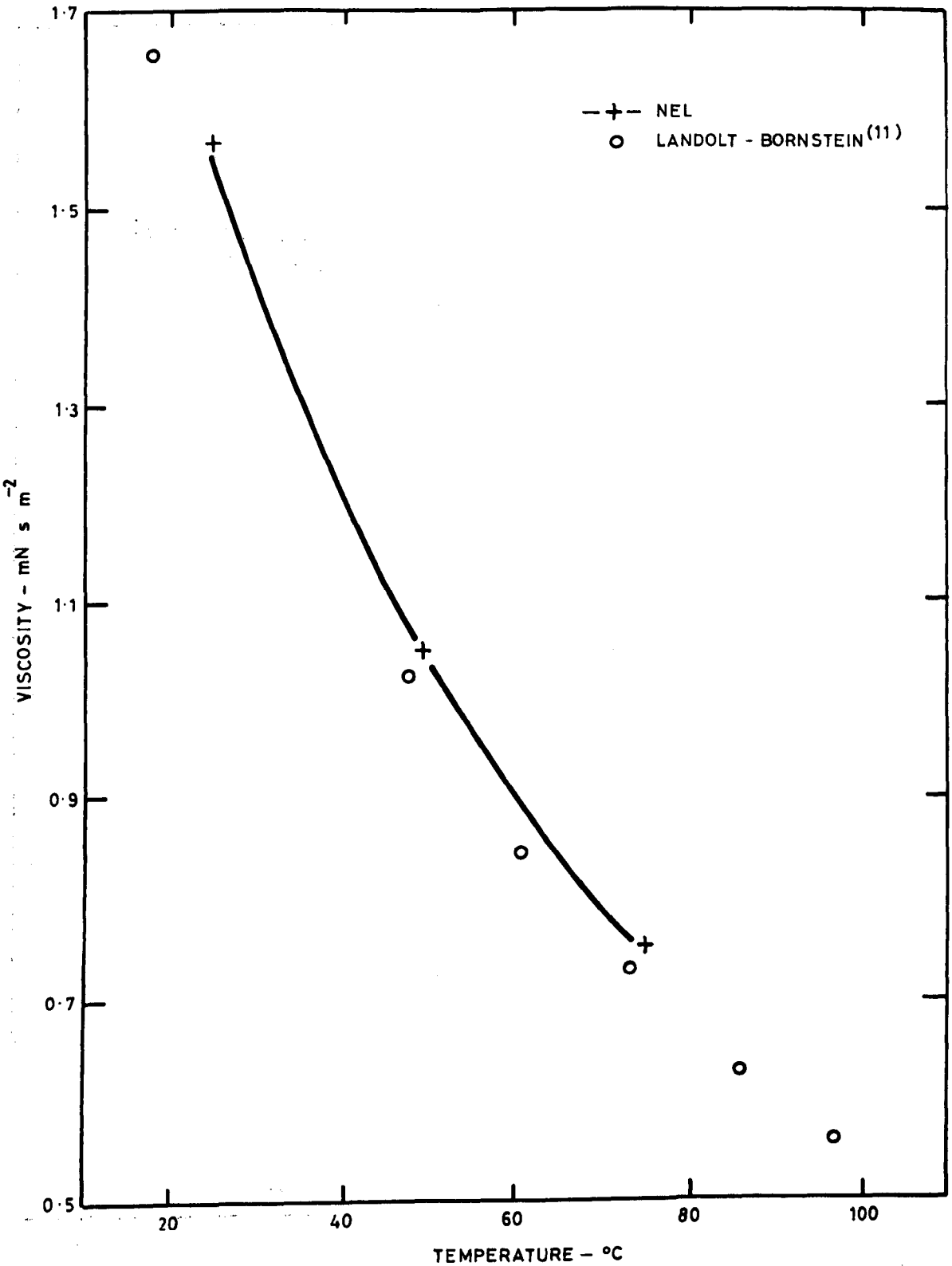

Fig. 10. Viscosity of Chlorocyclohexane

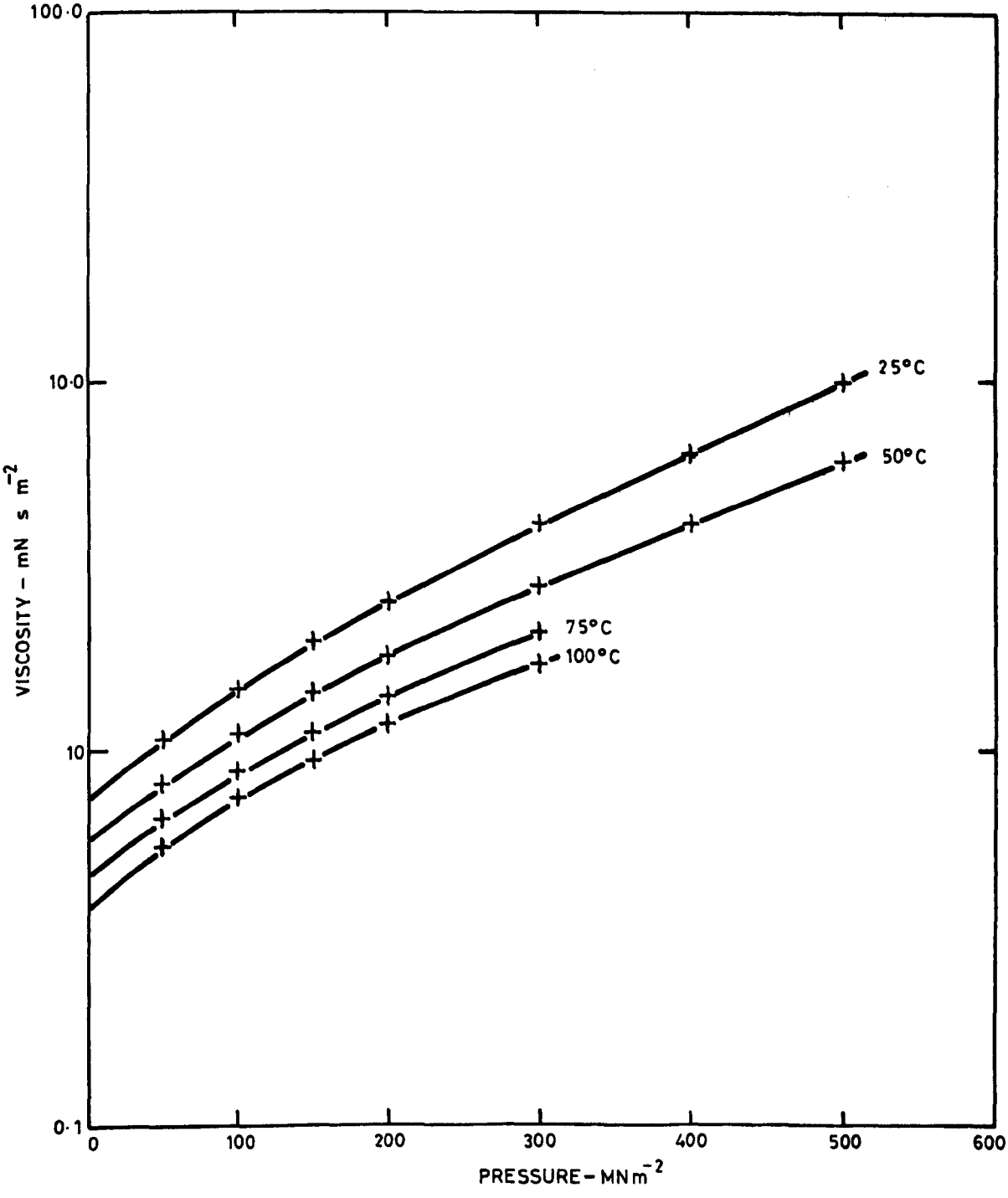

Fig. 11 Viscosity of 1-Bromopentane

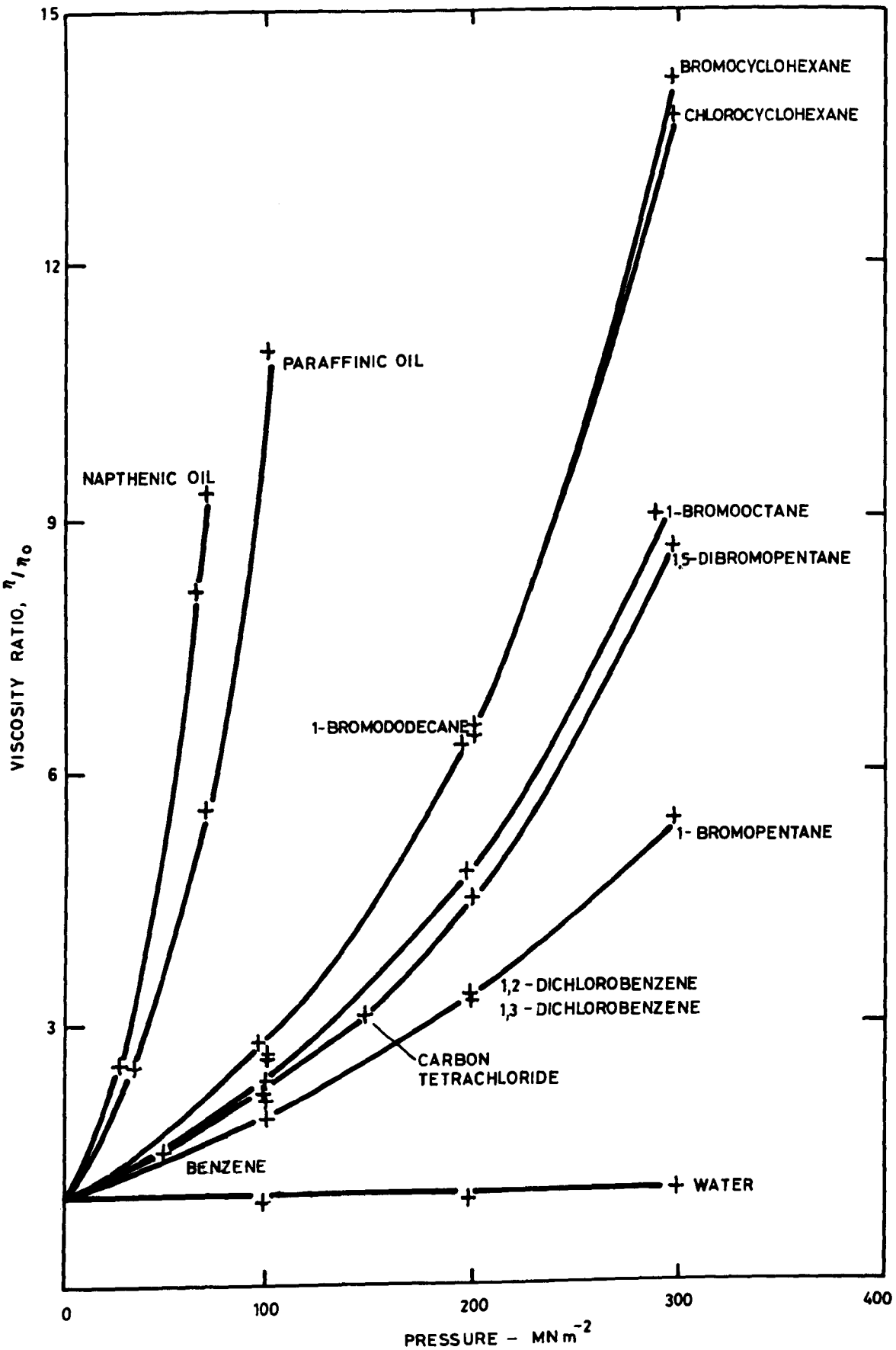

Fig. 12 Viscosity Ratios at 25°C

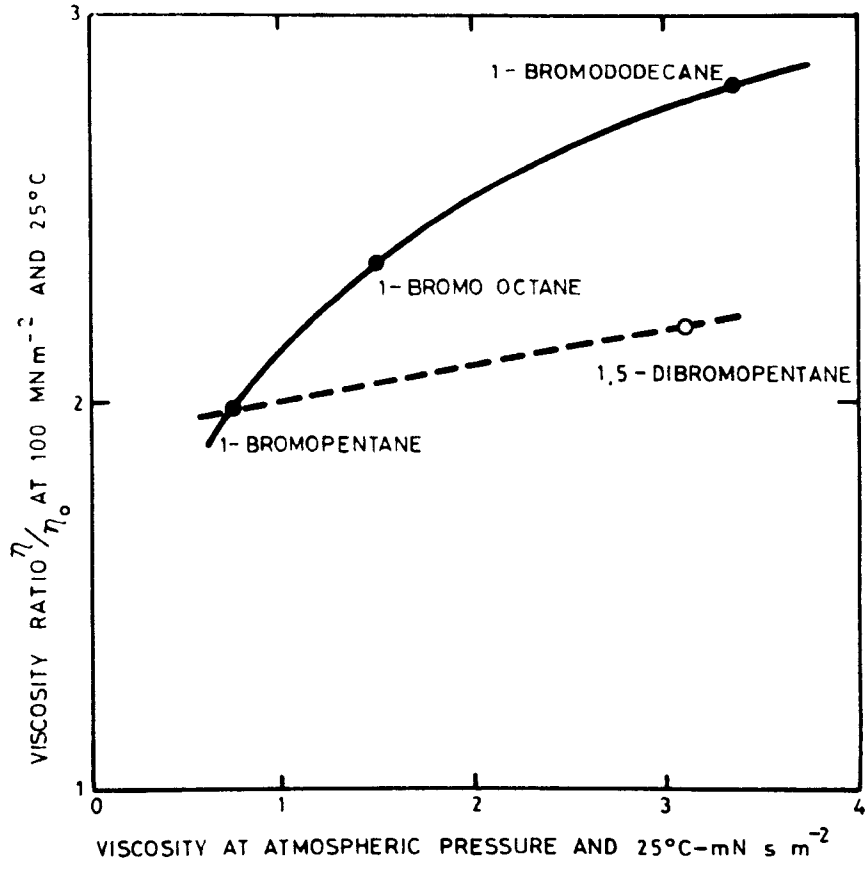

Fig. 13 Viscosity Ratios of Bromoalkanes

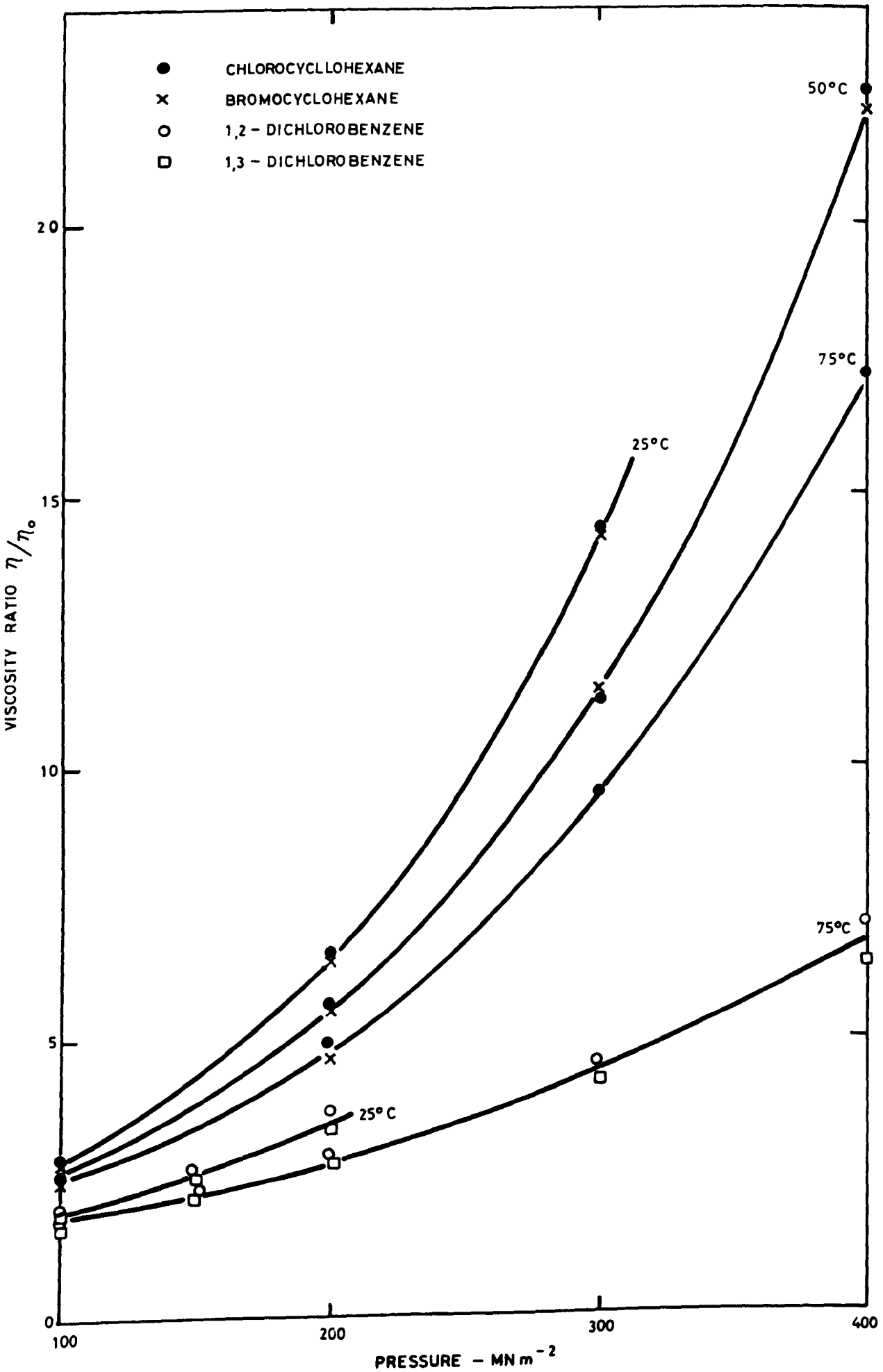

Fig. 14 Viscosity Ratios of Liquids Having Similar Molecules

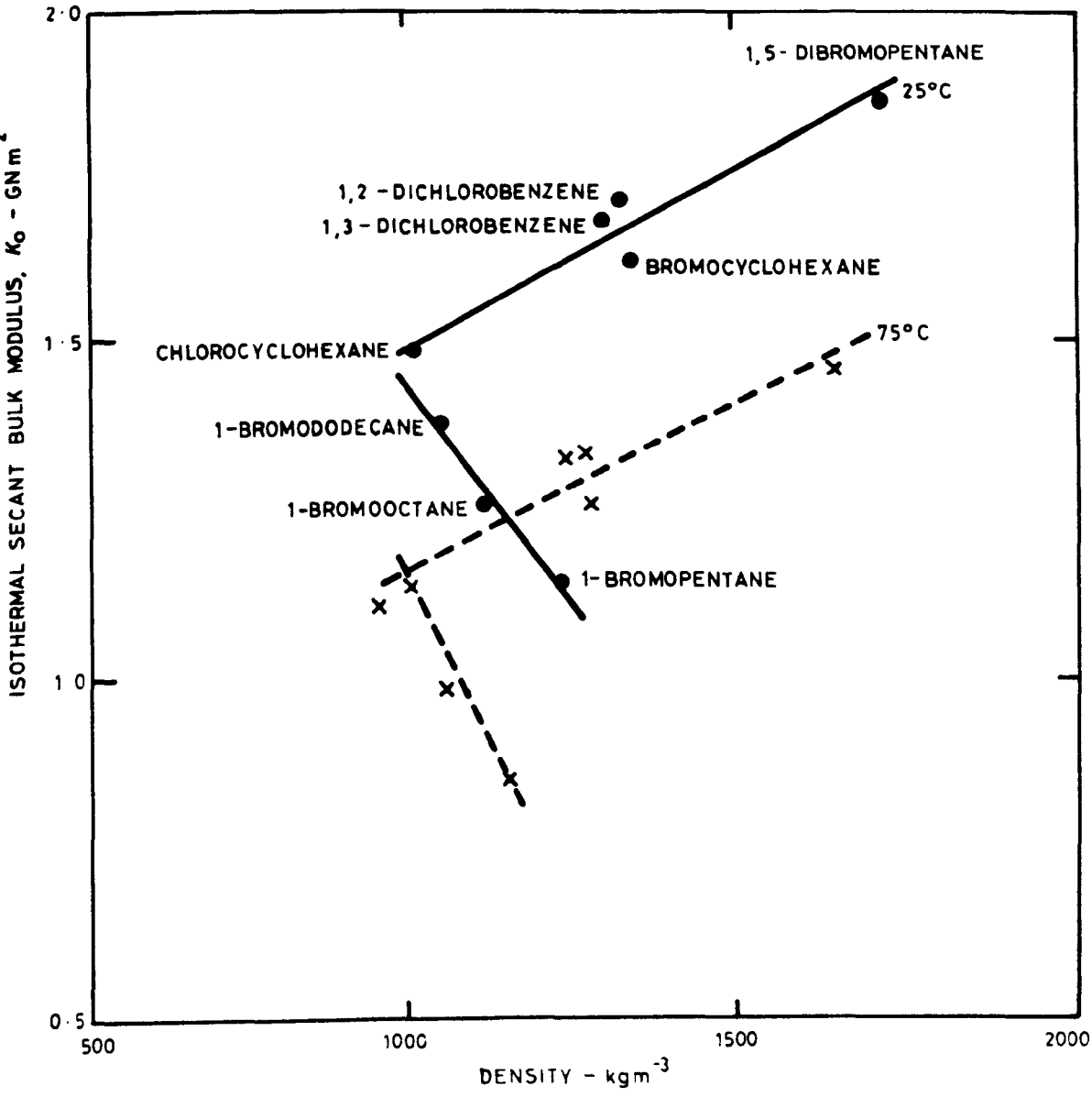

Fig. 15 Relations Between Bulk Modulus and Density at Atmospheric Pressure

RE 45004 500 12/75 NEL 604 CL

ISDALE, J D and SPENCE, C M.

High pressure viscosities and densities of eight halogenated hydrocarbons.

NEL Report No 604. East Kilbride, Glasgow: National Engineering Laboratory. December 1975.
33 pages (14 figures) 30 cm.

Measurements of the viscosity and density of eight halogenated hydrocarbons are presented for temperatures between 25 and 100°C and for pressures up to 500 MN m^{-2}. The new measurements agree well with published data at atmospheric pressure. The influence of chemical structure on the relationships between viscosity and pressure and between bulk modulus and density is examined.

ISDALE, J D and SPENCE, C M.

High pressure viscosities and densities of eight halogenated hydrocarbons.

NEL Report No 604. East Kilbride, Glasgow: National Engineering Laboratory. December 1975.
33 pages (14 figures) 30 cm.

Measurements of the viscosity and density of eight halogenated hydrocarbons are presented for temperatures between 25 and 100°C and for pressures up to 500 MN m^{-2}. The new measurements agree well with published data at atmospheric pressure. The influence of chemical structure on the relationships between viscosity and pressure and between bulk modulus and density is examined.

ISDALE, J D and SPENCE, C M.

High pressure viscosities and densities of eight halogenated hydrocarbons.

NEL Report No 604. East Kilbride, Glasgow: National Engineering Laboratory. December 1975.
33 pages (14 figures) 30 cm.

Measurements of the viscosity and density of eight halogenated hydrocarbons are presented for temperatures between 25 and 100°C and for pressures up to 500 MN m^{-2}. The new measurements agree well with published data at atmospheric pressure. The influence of chemical structure on the relationships between viscosity and pressure and between bulk modulus and density is examined.

ISDALE, J D and SPENCE, C M.

High pressure viscosities and densities of eight halogenated hydrocarbons.

NEL Report No 604. East Kilbride, Glasgow: National Engineering Laboratory. December 1975.
33 pages (14 figures) 30 cm.

Measurements of the viscosity and density of eight halogenated hydrocarbons are presented for temperatures between 25 and 100°C and for pressures up to 500 MN m^{-2}. The new measurements agree well with published data at atmospheric pressure. The influence of chemical structure on the relationships between viscosity and pressure and between bulk modulus and density is examined.

NEL PUBLICATIONS

The following reports are available on request from NEL

NEAL, A N. A method for the analysis of incompressible flow on an axisymmetric surface through a pump or fan blade row. *NEL Report* No 589

Advances in thermal and mechanical design of shell-and-tube heat exchangers: Report of a meeting at NEL, 28 November 1973. *NEL Report* No 590

ISDALE, J D, BRUNTON, W C and SPENCE, C M. Bulk modulus measurement and prediction. *NEL Report* No 591

ISDALE, J D and SPENCE, C M. A self-centring falling body viscometer for high pressures. *NEL Report* No 592

CRAWFORD, H. An automatic press for the production of stepped shafts. *NEL Report* No 593

SCOTT, D and SMITH, A I. Improvement of design and materials by failure analysis and the prognostic approach to reliability. *NEL Report* No 594

POOK, L P. Basic statistics of fatigue crack growth. *NEL Report* No 595

GREENAN, A F. Fatigue crack growth characteristics of a superplastic aluminium-zinc alloy. *NEL Report* No 596

SCOTT, R W W. The use and maintenance of weighing machines in high accuracy liquid flow calibration systems. *NEL Report* No 597

HENDRY, J C. Computer program for design and stressing of composite extrusion containers. *NEL Report* No 598

BIENIASZ, B. The dropwise condensation of steam on a gold-plated tube at atmospheric pressure. *NEL Report* No 599

UNDERWOOD, J H. J_{Ic} test results from two steels. *NEL Report* No 600

JAMIESON, D T., IRVING, J B and TUDHOPE, J S. The thermal conductivity of petroleum products: A survey to 1974. *NEL Report* No 601

HASLAM, G H. The fatigue strength of phosphor bronze thick-walled cylinders. *NEL Report* No 602

JAMIESON, D T., IRVING, J B and TUDHOPE, J S. Prediction of the thermal conductivity of petroleum and petroleum products. *NEL Report* No 603

NEL Report No 591

NATIONAL ENGINEERING LABORATORY

Bulk Modulus Measurement and Prediction

J D ISDALE, W C BRUNTON and C M SPENCE

DEPARTMENT OF INDUSTRY
JUNE 1975

Issued by

NATIONAL ENGINEERING LABORATORY,
EAST KILBRIDE, GLASGOW

DEPARTMENT OF INDUSTRY

NATIONAL ENGINEERING LABORATORY

BULK MODULUS MEASUREMENT AND PREDICTION

by

J D Isdale, B Sc, W C Brunton, and C M Spence

(Fluids Group: Properties of Fluids Division)

SUMMARY

Three methods of measuring bulk modulus at low, medium and high pressures are described, and measurements of water, crude oil, and six typical hydraulic fluids are given at pressures up to 600 MN m^{-2} for temperatures between 25 and 75°C. The variation of bulk modulus with pressure and temperature is examined and the accuracy of various methods of estimation is assessed.

BLANK PAGE IN ORIGINAL

CONTENTS

Distribution Group: Fluid properties data

NOTATION

A	Constant in equation (13)
a_i	Constants in Chebyshev series
B	Constant in equation (13)
b_i	Constants in Chebyshev series
C	Sound velocity
C_p	Specific heat
c_i	Constants in Chebyshev series
K	Thermodynamic or tangent bulk modulus
$\overline{K}$	Secant bulk modulus
K_o	Constant in equation (12)
m	Constant in equation (12)
n	Constant in equation (12)
P	Pressure
P_o	Atmospheric pressure
P'	Maximum pressure in equation (9)
P''	Minimum pressure in equation (9)
T	Absolute temperature
$T_i(\chi)$	Chebyshev series
T'	Maximum temperature in equation (10)
T''	Minimum temperature in equation (10)
V	Specific volume at pressure P
V_o	Specific volume at atmospheric pressure
a	Volume thermal expansion coefficient
β_s	Isentropic tangent compressibility
β_T	Isothermal tangent compressibility
ρ	Density

1 INTRODUCTION

Compressibility and its reciprocal, bulk modulus, are fluid properties which relate to volume change due to pressure. The increasing use of hydraulic systems has resulted in a need for reliable bulk modulus data for several different types of liquid. These data are used by system designers to calculate volume changes of the fluids, so that accurate values are essential if an optimum design is to be produced. Accurate values are also required when liquids are metered under pressure. In this case volume changes are usually relatively small; however, since large volumes are involved the effect can be of importance, for example in the metering of crude oil.

Bulk modulus may be defined in two ways. For engineering purposes the most convenient form is the secant bulk modulus $\bar{K}$ defined by

$$\bar{K} = \frac{V_o(P - P_o)}{V_o - V} .$$

If the secant bulk modulus is known volume change may be calculated directly.

The thermodynamic or tangent bulk modulus, K, is defined by

$$K = -V \frac{dV}{dP} .$$

To obtain volume changes from this definition integration must be carried out between the required pressures. Both moduli may be defined for isothermal or isentropic changes.

A considerable amount of data has already been produced here using the NEL Bulk Modulus Tester[1] but this instrument cannot be used at low or high pressures because volume changes at low pressure are so small and seal friction at high pressure is so large. The pressure range over which measurements can be made has therefore been extended to higher and lower pressures using different techniques. The purpose of the investigations described here was to compare results from the three methods, and to use this data to assess the accuracy of different methods for predicting bulk modulus over a wide range of temperature and pressure. The bulk modulus of six hydraulic fluids and a sample of crude oil were measured. The hydraulic fluids included three mineral oils, a water glycol mixture and two phosphate esters. Measurements of water were also made to check the accuracy of the sound velocity and bellows compression methods. The results are given in the form of the isothermal secant bulk modulus.

2 BULK MODULUS MEASUREMENT

The measurement of bulk modulus at low pressures by a direct method using the displacement of a piston or bellows, is complicated by the flexure and movement of the rubber seals used to contain the liquid. Since the volume changes of the liquid are so low, the slightest movement of an O-ring in its groove, for example, can cause serious errors in the volume measurement. Small bubbles of air or gas adhering to container walls can also lead to large errors at low pressure. For these reasons direct methods are usually limited to higher pressures where the total volume change of the liquid is large compared with volume changes from these sources.

Bulk modulus values derived from sound velocity measurements are not prone to errors of this sort if the method described in the following section is used. The method is similar to those used by Davis and Gordon[2] and by Vedam and Holton[3] and does not require volume measurement except at atmospheric pressure. Values derived from sound velocity measurements are usually limited to the isentropic tangent form; however this method allows isothermal and isentropic values to be calculated for both secant and tangent forms, and also provides thermal expansion coefficients and densities over the complete temperature and pressure range.

2.1 Sound Velocity Method

In non-dispersive liquids the conversion of sound velocity to compressibility may be carried out using the following relationships[2,3].

$$\beta_S = \frac{1}{\rho C^2} , \tag{1}$$

$$\beta_T = \beta_S + \frac{T\alpha^2}{\rho C_p} , \tag{2}$$

and

$$\beta_T = -\frac{1}{V}\left(\frac{\partial V}{\partial P}\right)_T = \frac{1}{\rho}\left(\frac{\partial \rho}{\partial P}\right)_T . \tag{3}$$

Equations (2) and (3) give

$$\left(\frac{\partial \rho}{\partial P}\right)_T = \frac{1}{C^2} + \frac{T\alpha^2}{C_p} . \tag{4}$$

Integrating equation (4) with respect to P gives

$$\rho(P_1,T) = \rho(P_0,T) + \int_{P_0}^{P_1} \frac{1}{C^2}\, dP + T\int_{P_0}^{P_1} \frac{\alpha^2}{C_p}\, dP \tag{5}$$

where $\rho(P_0,T)$ is density at pressure P_0 and temperature T

$\rho(P_1,T)$ is density at pressure P_1 and temperature T.

To evaluate the density given by equation (5), expressions for the variation with pressure of sound velocity, thermal expansion coefficient and specific heat are required. The first of these is obtained by fitting a suitable equation which can be integrated to experimental measurements of sound velocity. The variation of thermal expansion can be obtained from the additional relationship

$$\left(\frac{\partial \alpha}{\partial P}\right)_T = -\left(\frac{\partial \beta_T}{\partial T}\right)_P . \tag{6}$$

The right-hand side of equation (6) can be obtained directly from measurements of sound velocity, density and specific heat at atmospheric pressure using equations (1) and (2), and α_P can therefore be approximated over a small pressure range by

$$\alpha_P = \left(\frac{\partial \alpha}{\partial P}\right)_{T,P_0}\left(P - P_0\right) + \alpha_{P_0} \tag{7}$$

The variation of α with temperature can therefore be calculated at atmospheric pressure P_0 and at P_1 using equation (7). Substituting $(\partial\alpha/\partial T)_P$ obtained in this way in the expression

$$\left(\frac{\partial C_p}{\partial P}\right)_T = -\left(\frac{T}{\rho}\right)\left\{\left(\frac{\partial \alpha}{\partial T}\right)_P + \alpha^2\right\} \tag{8}$$

together with the square of equation (7) and integrating yields the change in C_p with pressure. The variation of C_p with pressure calculated in this way is so small that C_p can be assumed constant over the pressure ranges considered. Equation (5) can therefore be integrated using a constant value of C_p and the square of equation (7) as before. Equations (1), (2), (3) and (5) therefore allow the density, and both isentropic and isothermal compressibilities to be obtained over a small range of pressure by the above process; repetition of the calculations over successive pressure increments allows the pressure range to be extended as required. The method therefore requires three sets of experimental values.

a Sound velocity under pressure for several isotherms

b Density at atmospheric pressure and several temperatures

c Specific heat at atmospheric pressure.

The measured values of sound velocity are fitted along isotherms by an equation of the form

$$\frac{1}{C^2} = \sum_{i=o}^{i}{}' a_i T_1 \left\{ \frac{2P - (P' + P'')}{P' - P''} \right\} \qquad (9)$$

In the tests the maximum deviation between measured and fitted values was 0.3 m s^{-1}. Isobaric specific volumes and compressibilities are fitted by the equations

$$V = \sum_{i=o}^{2}{}' b_i T_1 \left\{ \frac{2T - (T' + T'')}{T' - T''} \right\} \qquad (10)$$

and

$$\beta_T = \sum_{i=o}^{2}{}' c_i T_1 \left\{ \frac{2T - (T' + T'')}{T' - T''} \right\} \qquad (11)$$

The thermal expansion coefficient, a, is then calculated from equation (10), and $\partial\beta_T/\partial T$ from equation (11). The resulting expressions together with equation (9) allow both integrations of equation (5) to be carried out analytically, thus yielding density at pressure P_1. Since density and expansion coefficient at P_1 allow β_S and β_T to be calculated from equations (1) and (2), repetition of the process over further small pressure intervals, P_1 to P_2 and so on, clearly permits the calculation of both compressibilities and also density over the full temperature and pressure range of the velocity measurements.

The apparatus used to measure the sound velocity is shown diagrammatically in Fig. 1. The main component is a velocity meter, shown in Fig. 2, which was developed for oceanographic studies and was modified for NEL to measure sound velocities over the range 950-1650 m s^{-1} at a frequency of 5 MHz. The instrument was checked in distilled water over the temperature range 20-75°C for pressures of 0.1013 -10.342 MN m^{-2}. The results at atmospheric pressure were compared with those given by Yazgan[4] and agreed with them to within 0.1 per cent up to 44°C and within 0.25 per cent for higher temperatures; they are shown in Fig. 3.

The velocity meter is secured in a stainless steel pressure vessel (Fig. 2) and the assembly placed in a water bath where the temperature can be held constant to ±0.05K. The bath temperature is measured by a quartz thermometer and the pressure by a deadweight tester connected as shown in Fig. 1.

The densities of the samples are measured using graduated bicapillary pyknometers[5].

Values of specific heat recommended by the hydraulic oil manufacturers were used to calculate oil compressibilities and values for water were taken from Reference 6. The specific heat of the fluids did not vary significantly in the temperature range studied and a constant value was used.

2.2 NEL Bulk Modulus Tester

This method has been used extensively by Hayward[1]; it is described in detail in Reference 7 and is shown diagrammatically in Fig. 4. A metal rod is forced, by a compression machine, through an O-ring seal into a closed vessel containing the liquid. Fluid pressure in the vessel is proportional to the load on the rod and volume changes are proportional to its displacement. Corrections are applied to eliminate the effect of friction on the rod and to allow for the deflections of the compression machine and apparatus. When the isothermal secant bulk modulus is being measured the sample bottle is immersed in a constant temperature bath and the load on the rod is increased very slowly. The method is estimated to be accurate to ±2 per cent.

2.3 Bellows Compression Method

This method makes use of the change in length of sealed bellows containing the liquid to be measured. The apparatus, which is shown diagrammatically in Fig. 5, is contained in a cylindrical pressure vessel of 25 mm bore and 190 mm outside diameter. The vessel is pressurized by an air-hydro pump up to 250 MN m^{-2}, and through an intensifier for higher pressures. The complete pressure vessel is immersed in an oil bath, the temperature of which can be held constant to ±0.02K. Temperature is measured by a quartz thermometer outside the pressure vessel, and pressure is measured by a Manganin gauge calibrated by a 700 MN m^{-2} dead-weight tester. The Manganin gauge is contained in a separate pressure vessel outside the temperature bath.

The initial volume of the sample is obtained from its weight and density. The loaded bellows are mounted on their housing inside the pressure vessel and a non-magnetic stainless steel rod is attached to their free end. A small ferrite tip at the opposite end of the rod projects out of the pressure vessel and temperature bath through a length of non-magnetic high pressure tubing which is sealed at its extremity. The position of the ferrite tip is detected by a pair of coils outside the high pressure tube, and the position of these coils is measured by a micrometer head. A second pair of dummy coils, not shown in the diagram, is mounted in a fixed position remote from unwanted magnetic influences. The four coils are connected to form a bridge which, with the ferrite tip midway between the sensing coils, is initially balanced. Movement of the ferrite tip, and hence the bellows, unbalances the bridge. The sensing coils are then moved to rebalance the bridge, and their position is measured with the micrometer.

Change in length of the bellows is converted to change in volume using the effective cross-sectional area. This area was obtained by calibration with water using two different methods. For the first method the bellows were filled at atmospheric pressure and then sealed and weighed. Their length at 25°C was then measured in a small rig using a micrometer screw. Some water was then bled off or added, and the procedure repeated so that the area could be calculated directly from the changes in length and the corresponding changes in volume. The second calibration was carried out under pressure using accurate values for the volume of water[8]. The procedure here was similar to that used for measurement except that area was calculated from the known volume change. Both sets of measurements were then averaged. No significant difference between the accuracy of the two methods was detected and the maximum deviation from the mean was just under 1 per cent. Changes in dimensions of the apparatus due to temperature and pressure were both small and fell within the normal scatter of measurement.

3 RESULTS

3.1 Bulk Modulus of Water

As the sound velocity method and the bellows compression method have not been used extensively at this Laboratory measurements were made of the compressibility of water over appropriate temperature and pressure ranges to check their accuracy. Water was chosen as the test liquid because accurate values of density are available over the full temperature and pressure ranges of the experiments. At pressures up to 100 MN m^{-2} very accurate values are given by Kell and Whalley[9], and for pressures up to 800 MN m^{-2} reliable values are given by Grindley and Lind[8].

For the calculation of the sound velocity results literature values of specific heat[6] and density[10] at atmospheric pressure were used.

Measured sound velocities in water are given in Tables 1 and 2 and are shown in Figs 3 and 6 where they are compared with values quoted by Yazgan[4]. Values of bulk modulus calculated from these velocities are given in Table 3 and are compared with the measurements of Kell and Whalley[9] in Table 4. The maximum difference between the measured values and those of Kell and Whalley is 0.46 per cent and occurs at 40°C and 1 MN m^{-2}. Kell and Whalley's values are estimated to be accurate to ±0.05 per cent and though the new measurements are about 0.2 per cent below these values, the agreement is very satisfactory and confirms the accuracy of the sound velocity method.

As the available values of specific heat for hydraulic oils are often not accurate, the effect of errors in specific heat on measurements made by the sound velocity method was examined. Values of specific heat used in the calculations for water were perturbed by amounts ranging from +5 per cent at the minimum temperature to −5 per cent at the maximum temperature. The resulting values of bulk modulus were found to deviate from the original results by a maximum of 0.27 per cent at 60°C and 4.14 MN m^{-2}.

These results show that the method can give accurate bulk moduli using comparatively inaccurate values of specific heat.

Values for water obtained by the bellows method are given in Table 3 and also in Table 5 where they are compared with those of Grindley and Lind. At the lowest pressure employed using this method, 100 MN m^{-2}, the movement of the bellows is comparatively small and accuracy is therefore limited. At higher pressures the bellows movement is larger and the deflection can be measured with greater precision so that higher accuracy is to be expected. This is reflected in the comparison shown in Table 5; however the new measurements differ from those of Grindley and Lind (which are estimated to be accurate to ±0.5 per cent) with a standard deviation of 2.4 per cent. An accuracy of this order is quite satisfactory for most engineering purposes.

3.2 Bulk Modulus of Hydraulic Fluids and Crude Oil

The hydraulic fluids selected for measurement represented most of the types currently in use. A description of them and some of their properties are given in Table 6.

When it was possible each was measured by the three methods available. The sound velocity method is limited to liquids of viscosity less than about 50 MN s m^{-2} with the present apparatus because of high viscous dissipation of the sound wave, so three of the fluids could not be measured by this method. Sound velocities for the other fluids are given in Table 7, and the complete series of bulk modulus results are given in Table 8. Fig. 7 shows the results for fluid M3.

Measurements have also been made on a Middle East crude oil using both sound velocity and bulk modulus tester methods. This oil was in equilibrium at atmospheric pressure with its dissolved gases and corresponded as closely as possible to the condition of a sample taken from storage prior to metering. Results for this oil are shown on Figs 8 and 9.

4 BULK MODULUS EQUATIONS AND PREDICTIONS

4.1 Equations for Test Results

Over the full pressure range the data can be fitted by a quadratic expression

$$\bar{K} = K_0 + mP + nP^2. \qquad (12)$$

The constants and standard deviations obtained in fitting the data by this equation along all the available isotherms are given in Table 9 and the results are illustrated for fluid G1 in Fig. 10. All the measurements made were used and the results obtained by the sound velocity method were given twice the weight allocated to the other methods. In the pressure range covered by the sound velocity method and the bulk modulus tester, that is up to 137.9 MN m^{-2}, a linear equation in pressure ($n = 0$) fitted the data within the experimental accuracy. Sound velocity results were again double weighted. Constants of the linear pressure equation are given in Table 10 and are illustrated for fluid M1 in Fig. 11. The numerical values of the constants given for both of these equations give bulk modulus directly in GN m^{-2} if the pressure is applied in MN m^{-2}.

For many liquids bulk modulus varies logarithmically with temperature[7,11]; however, for the liquids tested and within the temperature range and accuracy of this study, it decreases linearly with temperature. This is illustrated in Figs 12 and 13 at 1.48 and 10.35 MN m^{-2} respectively.

Also shown in Fig. 12 is the anomalous behaviour of water. The slope of the water glycol fluid, G1, is greater than that of the phosphate esters, whose slopes are in turn greater than those of the mineral oils.

At pressures of 1.48 and 103.52 MN m^{-2} the present results have been fitted by the equation

$$K = A + BT. \tag{13}$$

Values obtained for the constants are given in Table 11. In this case the numerical values of the constants give bulk modulus in GN m^{-2} if the temperature is applied in °C.

4.2 Assessment of Predictions

Three methods of predicting bulk modulus are examined using the new measurements. The first method has been developed by Hayward[7] and is in the form of equations which are valid in the ranges 5-100°C and 0-140 MN m^{-2}. The second method was developed by Wright[12] and is in the form of charts covering the ranges -18-260°C and 0-700 MN m^{-2}. Both methods were derived for hydraulic mineral oils. The third method, which has also been described by Hayward[13], is based on equation (2) and can be applied to fire-resistant fluids.

For the mineral oils Hayward's method gives more accurate predictions than Wright's at pressures below 200 MN m^{-2}, though for fluid M2, the high viscosity mineral oil, there was little to choose between the two methods in this region. At higher pressures Wright's method becomes more accurate and Hayward's method gives values up to 24 per cent too low at 500 MN m^{-2}, a pressure which is of course well above the maximum for the method. Fig. 14 shows a comparison of the two methods at 25°C for fluid M1. For these three oils at pressures below 200 MN m^{-2} the maximum error shown by Hayward's method is 4.7 per cent, and at pressures of 200 MN m^{-2} and above, the maximum error produced by Wright's method is 3.6 per cent.

For the fire-resistant fluids the only method available is that described by Hayward[13]. If Wright's method is applied to these fluids quite large errors are obtained, 10-15 per cent low for the water glycol fluid G1 and 50 per cent or more high for the phosphate esters. Hayward's method works well in the specified pressure range for the water glycol fluid and gives an error of only 8 per cent at 500 MN m^{-2}, as illustrated in Fig. 15. Predictions for the phosphate esters however are less accurate with a maximum error of 8.9 per cent at 103 MN m^{-2} in the case of fluid P2, and 4.1 per cent for P1 at 68.95 MN m^{-2}.

Estimates for crude oils are conventionally made using tables from API Standard 1101[14] and this method is compared with the measured values in Fig. 8. At 26.66°C it over-estimates the bulk modulus by 10 per cent, while at the maximum temperature of the tables, 53.33°C, values 15 per cent low are obtained. Extrapolation to higher temperatures would clearly produce quite large errors for this sample. A method specially developed for crude oils has been proposed by Downer and Gardiner[15] and values calculated by their method are also shown in Fig. 8. In this case the errors at corresponding temperatures are less than 5 per cent and extrapolation to higher temperatures would not lead to such large differences. Both of these methods are limited however in that they do not allow for the variation of bulk modulus with pressure. This variation is quite large in the pressure range examined here and is shown in Fig. 9 along with estimates by Hayward's and Wright's methods.

5 CONCLUSIONS

1 Two methods of measuring bulk modulus have been developed which can give experimental values at lower and higher pressures than the original NEL Bulk Modulus Tester.

2 At low pressures, a region where direct (mechanical) methods are unreliable, the sound velocity method can provide very accurate values.

3 The linear bulk modulus equation can be applied to the present results for hydraulic fluids up to 140 MN m^{-2}, a pressure higher than that usually recommended. At higher pressures a quadratic expression is necessary.

4 Within the accuracy of the present measurements bulk modulus decreases linearly with temperature for the six liquids examined.

5 Hayward's generalized equations[7] provide the best estimates for mineral oils at pressures up to 200 MN m^{-2}. At higher pressures Wright's method works well.

6 For the fire-resistant fluids Wright's method is not applicable but the method described by Hayward[13] works reasonably well. The estimates for the water glycol fluid were, however, very accurate.

7 API Standard 1101 can either over or underestimate the bulk modulus of the crude oil examined depending on the temperature, and would produce quite large errors if used for extrapolation to higher temperatures. Downer and Gardiner's correlation is more accurate but neither method allows for the variation of bulk modulus with pressure, which is similar to that of other mineral oils.

REFERENCES

1 HAYWARD, A. T. J. The truth about liquids under pressure. *Engineering*, 1964, **198**(5133), 314-316.

2 DAVIS, L. A. and GORDON, R. B. Compression of mercury at high pressure. *J. Chem. Phys.*, 1967, **46**(7), 2650-2660.

3 VEDAM, R. and HOLTON, G. Specific volumes of water at high pressures, obtained from ultrasonic-propagation measurements. *J. Acoust. Soc. Amer.*, 1968, **43**(1), 108-116.

4 YAZGAN, E. Precise measurement of the velocity of sound in liquids as a function of temperature and pressure by a new electrical method. Ph D. Thesis. Glasgow: University of Glasgow, 1966.

5 INSTITUTE OF PETROLEUM. *IP Standard 189/69*, 1973. London: Institute of Petroleum.

6 OSBORNE, N. S., STIMSON, H. F. and GINNINGS, D. C. Measurement of heat capacity and heat of vaporization of water in the temperature range 0-100°C. *J. Res. natn. Bur. Stand.*, 1939, **23**, 197-270.

7 HAYWARD, A. T. J. Generalizations for isentropic and isothermal compressibility of hydraulic mineral oils. *J. Inst. Petrol*, 1970, **56**(547), 12-32.

8 GRINDLEY, T. and LIND, J. E. PVT properties of water and mercury. *J. Chem. Phys.*, 1971, **54**(9), 3983-3989.

9 KELL, G. S. and WHALLEY, E. The PVT properties of water. 1 – liquid water in the temperature range 0-150°C and at pressures up to 1 *Kb*. *Phil. Trans., A*, 1965, **258**(1094), 565-614.

10 KAYE, G. W. C. and LABY, T. H. *Tables of physical and chemical constants*. 13th edition, p 30. London: Longmans Green, 1966.

11 KLAUS, E. E. and O'BRIEN, J. A. Precise measurement and prediction of bulk modulus values for fluids and lubricants. *J. bas. Engng*, 1964, **86**, 469-474.

12 WRIGHT, W. A. Prediction of bulk moduli and PVT data for petroleum oils. *ASLE Trans.*, 1967, **10**, 349-356.

13 HAYWARD, A. T. J. How to estimate the bulk modulus of hydraulic fluids. *Hydraul. Pneumat. Pwr.*, 1970, **16**(181), 28-40.

14 AMERICAN PETROLEUM INSTITUTE. *API Standard* 1101, 1960.

15 DOWNER, L. and GARDINER, K. E. S. The compressibility of crude oils. *J. Inst. Pet.*, 1972, **58**(559), 1-13.

LIST OF TABLES

LIST OF FIGURES

6 Velocity of sound in water under pressure

7 Bulk modulus of fluid M3

8 Measured and estimated bulk moduli of crude oil at 0.45 MN m^{-2}

9 Measured and estimated bulk moduli of crude oil at 43.33 °C

10 Bulk modulus of fluid G1

11 Bulk modulus of fluid M1

12 Relation between bulk modulus and temperature at 1.48 MN m^{-2} for fluids G1, M1, M3, and distilled water

13 Relation between bulk modulus and temperature at 103.52 MN m^{-2} for fluids G1, M1, M2, M3, P1, P2

14 Measured and estimated bulk moduli of fluid M1 at 25°C

15 Measured and estimated bulk moduli of fluid G1 at 25°C

TABLE 1

Velocity of Sound in Water at Atmospheric Pressure

Temperature (°C)	Velocity of sound ($m\ s^{-1}$)
26.65	1502.0
30.00	1510.1
33.01	1516.7
35.02	1521.1
38.01	1526.5
40.07	1529.9
43.00	1535.0
45.05	1539.4
48.02	1543.6
50.01	1545.9
53.08	1549.0
55.16	1550.2
58.02	1552.7
60.02	1554.1
63.00	1555.9
66.02	1557.0
68.83	1557.6
70.20	1557.7

TABLE 2

Velocity of Sound in Water Under Pressure ($m\ s^{-1}$)

Pressure ($MN\ m^{-2}$)	Temperature (°C)			
	30	40	50	60
0.101	1508.7	1529.0	1544.6	1552.9
0.791	1510.0	1530.6	1545.8	1554.2
2.170	1512.4	1534.4	1548.5	1556.7
3.549	1514.8	1536.5	1550.8	1559.4
5.617	1518.3	1540.1	1554.6	1563.7
6.996	1520.6	1541.6	1557.1	1567.4
8.375	1523.0	1543.9	1559.5	1568.4

TABLE 3

Isothermal Secant Bulk Modulus of Water (GN m^{-2})

Method of measurement	Pressure (MN m^{-2})	Temperature (°C)					
		25	30	40	50	60	75
Sound velocity	1.48	-	2.2370	2.2687	2.2741	2.2531	-
	2.86	-	2.2418	2.2741	2.2794	2.2584	-
	4.24	-	2.2466	2.2792	2.2847	2.2637	-
	5.62	-	2.2514	2.2841	2.2898	2.2691	-
	6.99	-	2.2561	2.2888	2.2948	2.2744	-
	8.37	-	2.2608	2.2933	2.2997	2.2797	-
Bellows	100	2.53	-	2.66	-	2.73	2.60
	200	2.85	-	2.96	-	3.02	2.89
	300	3.17	-	3.27	-	3.32	3.18
	400	3.49	-	3.57	-	3.62	3.47
	500	3.82	-	3.87	-	3.92	3.76

TABLE 4

Isothermal Secant Bulk Modulus of Water; Comparison of Results Obtained by Sound Velocity Method with Those of Kell and Whalley[9]

Temperature (°C)	Pressure (MN m^{-2})	Kell and Whalley (GN m^{-2})	NEL (GN m^{-2})	Difference (Per cent)
30	1.00	2.2287	2.2353	+0.30
	2.50	2.2382	2.2405	+0.10
	5.00	2.2472	2.2492	+0.09
	7.50	2.2556	2.2578	+0.10
	10.00	2.2639	2.2663	+0.11
40	1.00	2.2564	2.2668	+0.46
	2.50	2.2648	2.2727	+0.35
	5.00	2.2726	2.2819	+0.41
	7.50	2.2814	2.2905	+0.40
	10.00	2.2900	2.2986	+0.38
50	1.00	2.2683	2.2723	+0.18
	2.50	2.2765	2.2780	+0.07
	5.00	2.2844	2.2875	+0.14
	7.50	2.2918	2.2966	+0.21
	10.00	2.3002	2.3055	+0.23
60	1.00	2.2459	2.2513	+0.24
	2.50	2.2539	2.2570	+0.14
	5.00	2.2633	2.2667	+0.15
	7.50	2.2718	2.2764	+0.20
	10.00	2.2802	2.2860	+0.25

σ = 0.25%

TABLE 5

Isothermal Secant Bulk Modulus of Water; Comparison of Results Obtained by Bellows Method with Those of Grindley and Lind[8]

Temperature (°C)	Pressure (MN m^{-2})	Grindley and Lind (GN m^{-2})	NEL (GN m^{-2})	Deviation (Per cent)
25	100	2.530	2.526	0.17
	200	2.854	2.848	0.18
	300	3.250	3.171	2.44
	400	3.466	3.493	-0.78
	500	3.756	3.815	-1.57
40	100	2.586	2.661	-2.92
	200	2.908	2.964	-1.93
	300	3.219	3.266	-1.48
	400	3.516	3.569	-1.52
	500	3.805	3.872	-1.76
60	100	2.582	2.726	-5.59
	200	2.908	3.023	-3.96
	300	3.219	3.321	-3.15
	400	3.514	3.618	-2.95
	500	3.802	3.915	-2.96
75	100	2.539	2.602	-2.47
	200	2.867	2.892	-0.88
	300	3.178	3.181	-0.11
	400	3.474	3.471	0.10
	500	3.760	3.760	-0.01

σ = 2.4%

TABLE 6

Hydraulic Fluid Properties

Fluid	Description	Density at 25°C (kg m^{-3})	Viscosity* at 37.78°C (mN s m^{-2})	Specific heat* at constant pressure and 20°C (J kg^{-1} K^{-1})
M1	Mineral oil with additives to reduce oxidation, corrosion and foaming	862.7	12.3	1930
M2	Mineral oil with additives to reduce oxidation, corrosion and foaming	885.9	110.5	
M3	As above plus additive to increase wear resistance	868.3	43.4	1970
G1	Water glycol fluid with corrosion inhibiter	1071.6	36.1	2970
P1	Phosphate ester fluid with corrosion inhibiter	1263.8	46.4	1760
P2	Phosphate ester fluid with corrosion inhibiter	1316.5	86.2	1630

*Suppliers values

TABLE 7

Sound Velocity in Fluids M1, M3, and G1 ($m\ s^{-1}$)

Pressure ($MN\ m^{-2}$)	Temperature (°C)			
	25.00	35.00	43.33	55.00
		Fluid M1		
0.101	1395.8	1359.7	1330.4	1290.0
0.791	1398.6	1363.1	1333.9	1293.6
2.170	1405.3	1370.3	1341.2	1301.6
3.549	1412.4	1377.8	1348.5	1309.2
5.617	1422.3	1388.1	1359.6	1320.5
6.996	1428.8	1395.4	1367.0	1328.5
8.375	1435.7	1402.0	1373.7	1335.4
9.754	1442.1	1408.7	1380.5	1342.3
		Fluid M3		
0.101	1427.3	1395.6	1368.0	1332.3
0.791	1430.6	1398.7	1370.9	1335.5
2.170	1437.7	1405.6	1378.1	1342.6
3.549	1443.7	1412.3	1385.0	1349.8
5.617	1453.4	1422.1	1395.0	1360.5
6.996	1459.3	1428.6	1403.0	1367.2
8.375	1465.0	1435.0	1410.3	1374.6
9.754	1470.8	1441.0	1416.4	1381.2
		Fluid G1		
0.101	1703.0	1685.2	1668.2	1644.0
0.791	1704.4	1686.6	1670.2	1645.8
2.170	1707.4	1689.5	1673.1	1649.0
3.549	1710.4	1692.5	1676.6	1652.5
5.617	1714.8	1697.1	1681.1	1657.3
6.996	1717.8	1700.1	1684.1	1660.6
8.375	1720.7	1703.0	1687.2	1664.1
9.754	1723.6	1705.9	1690.4	1667.3

TABLE 8

Isothermal Secant Bulk Modulus of Fluids Tested (GN m^{-2})

Method of measurement	Pressure ($MN\ m^{-2}$)	Temperature (°C)				
		25	35	43.33	55	75
		Fluid M1				
Sound velocity	1.48	1.458	1.359	1.281	1.180	-
	2.86	1.467	1.369	1.291	1.189	-
	4.24	1.477	1.378	1.300	1.198	-
	5.62	1.486	1.387	1.309	1.207	-
	7.00	1.495	1.396	1.318	1.216	-
	8.38	1.504	1.405	1.327	1.225	-
	9.75	1.513	1.414	1.336	1.234	-
Bulk modulus tester	34.57	1.61	1.57	1.55	1.46	-
	69.05	1.85	1.74	1.73	1.59	-
	103.52	2.05	1.92	1.91	1.77	-
	138.00	2.25	2.10	2.06	1.90	-
Bellows	100	-	-	-	-	1.68
	200	2.49	-	-	-	2.13
	300	2.89	-	-	-	2.50
	400	3.25	-	-	-	2.87
	500	3.62	-	-	-	3.23
	600	4.00	-	-	-	3.56
		Fluid M2				
Bulk modulus tester	34.57	1.90	1.79	1.79	1.65	-
	69.05	2.07	1.98	1.96	1.82	-
	103.52	2.21	2.11	2.13	1.96	-
	138.00	2.41	2.29	2.30	2.12	-
Bellows	100	-	-	-	-	2.14
	200	2.48	-	-	-	2.52
	300	2.90	-	-	-	2.87
	400	3.27	-	-	-	3.25
	500	3.63	-	-	-	3.58
	600	3.92	-	-	-	3.90
		Fluid M3				
Sound velocity	1.48	1.485	1.429	1.382	1.320	-
	2.86	1.493	1.437	1.390	1.329	-
	4.24	1.501	1.445	1.399	1.337	-
	5.62	1.509	1.453	1.407	1.345	-
	7.00	1.517	1.461	1.416	1.354	-
	8.38	1.525	1.469	1.424	1.362	-
	9.75	1.532	1.477	1.432	1.371	-
Bulk modulus tester	34.57	1.77	1.73	1.66	1.53	-
	69.05	1.94	1.87	1.79	1.71	-
	103.52	2.13	2.03	2.00	1.89	-
	138.00	2.30	2.19	2.14	2.07	-
Bellows	100	-	-	-	-	-
	200	2.62	-	-	-	-
	300	3.00	-	-	-	2.70
	400	3.36	-	-	-	3.04
	500	3.69	-	-	-	3.39
	600	4.02	-	-	-	3.71

TABLE 8 (contd)

Method of measurement	Pressure ($MN\ m^{-2}$)	Temperature (°C)			
		25	35	43.33	55
		Fluid G1			
Sound velocity	1.48	2.843	2.730	2.633	2.497
	2.86	2.850	2.737	2.640	2.503
	4.24	2.857	2.744	2.647	2.510
	5.62	2.863	2.751	2.654	2.516
	7.00	2.870	2.757	2.661	2.524
	8.38	2.877	2.764	2.667	2.531
	9.75	2.883	2.770	2.674	2.539
Bulk modulus tester	34.57	2.98	2.91	2.84	2.83
	69.05	3.14	3.04	3.02	2.90
	103.52	3.35	3.17	3.11	3.07
	138.00	3.47	3.26	3.34	3.18
Bellows	100	3.25	-	-	3.03
	200	3.72	-	-	3.46
	300	4.23	-	-	3.83
	400	4.55	-	-	4.22
	500	4.86	-	-	4.54
		Fluid P1			
Bulk modulus tester	34.57	2.45	2.37	2.22	2.20
	69.05	2.66	2.56	2.48	2.34
	103.52	2.81	2.72	2.61	2.50
	138.00	3.04	2.84	2.76	2.56
Bellows	100	-	-	-	-
	200	3.15	-	-	3.08
	300	3.60	-	-	3.40
	400	3.98	-	-	3.88
	500	4.41	-	-	4.32
		Fluid P2			
Bulk modulus tester	34.57	2.54	2.46	2.37	2.20
	69.05	2.68	2.58	2.46	2.39
	103.52	2.85	2.82	2.57	2.55
	138.00	3.03	2.91	2.77	2.69
Bellows	100	-	-	-	-
	200	3.45	-	-	3.18
	300	3.83	-	-	3.62
	400	4.20	-	-	3.99
	500	4.72	-	-	4.46

TABLE 9

Constants for Quadratic Pressure Equation

Fluid	Temperature (°C)	K_0	m	n	Standard deviation (GN m^{-2})
			$\times 10^{-3}$	$\times -10^{-6}$	
M1	25	1.4583	5.5310	2.2862	0.027
M2	25	1.7988	3.8874	0.5535	0.041
M3	25	1.4849	6.1825	3.4019	0.030
G1	25	2.8312	4.9252	1.6506	0.023
G1	55	2.4986	5.4519	2.8304	0.036
P1	25	2.3505	4.3810	0.6086	0.045
P1	55	2.0028	4.9184	0.5684	0.058
P2	25	2.3365	5.3837	1.3702	0.046
P2	55	1.9689	6.1165	2.3397	0.047

TABLE 10

Constants for Linear Pressure Equation at 25°C

Fluid	K_0	m	Standard deviation (GN m^{-2})
		$\times 10^{-3}$	
M1	1.4512	5.7526	0.010
M2	1.7295	4.8440	0.013
M3	1.4796	6.2118	0.022
G1	2.8359	4.6688	0.010
P1	2.2594	5.5691	0.016
P2	2.3645	4.7569	0.010

TABLE 11

Constants for Linear Temperature Equation

Fluid	Pressure (MN m^{-2})	A	B	Standard deviation (GN m^{-2})
			$\times -10^{-2}$	
M1	1.48	1.6861	0.9262	0.003
M1	103.52	2.2587	0.8747	0.023
M2	103.52	2.4039	0.7614	0.034
M3	1.48	1.6220	0.5507	0.001
M3	103.52	2.3166	0.7683	0.013
G1	1.48	3.1327	0.1154	0.001
G1	103.52	3.5331	0.9047	0.039
P1	103.52	3.0772	0.1054	0.008
P2	103.52	3.1490	0.1141	0.057

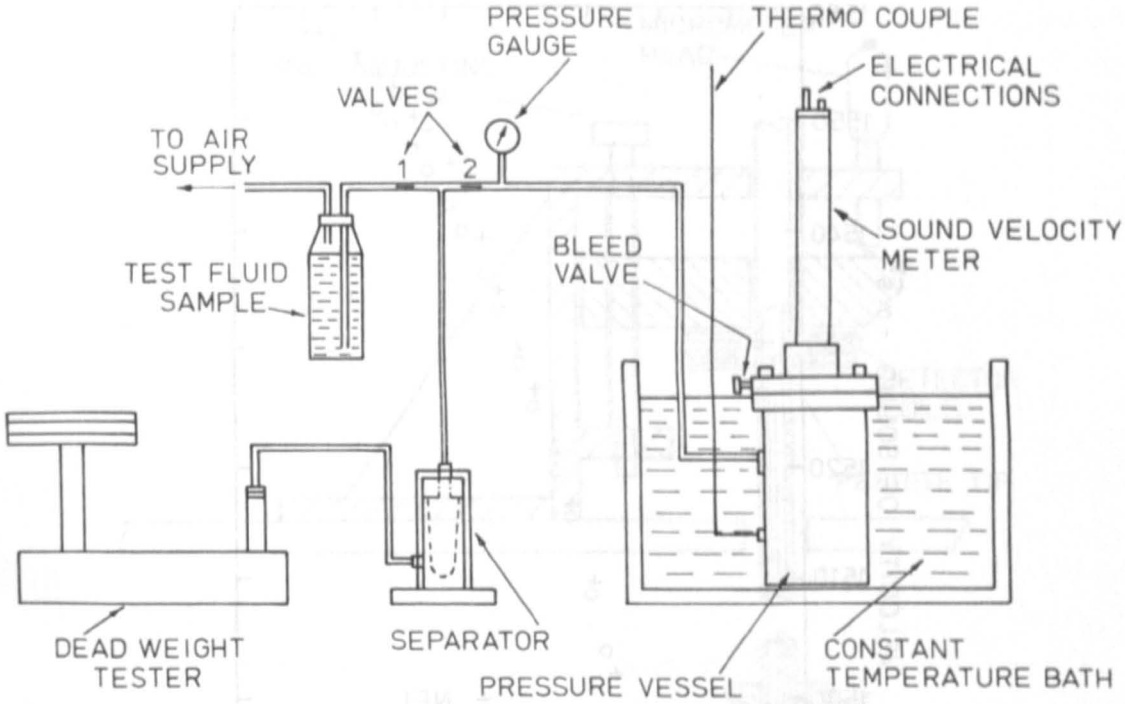

Fig. 1 Sound Velocity Apparatus

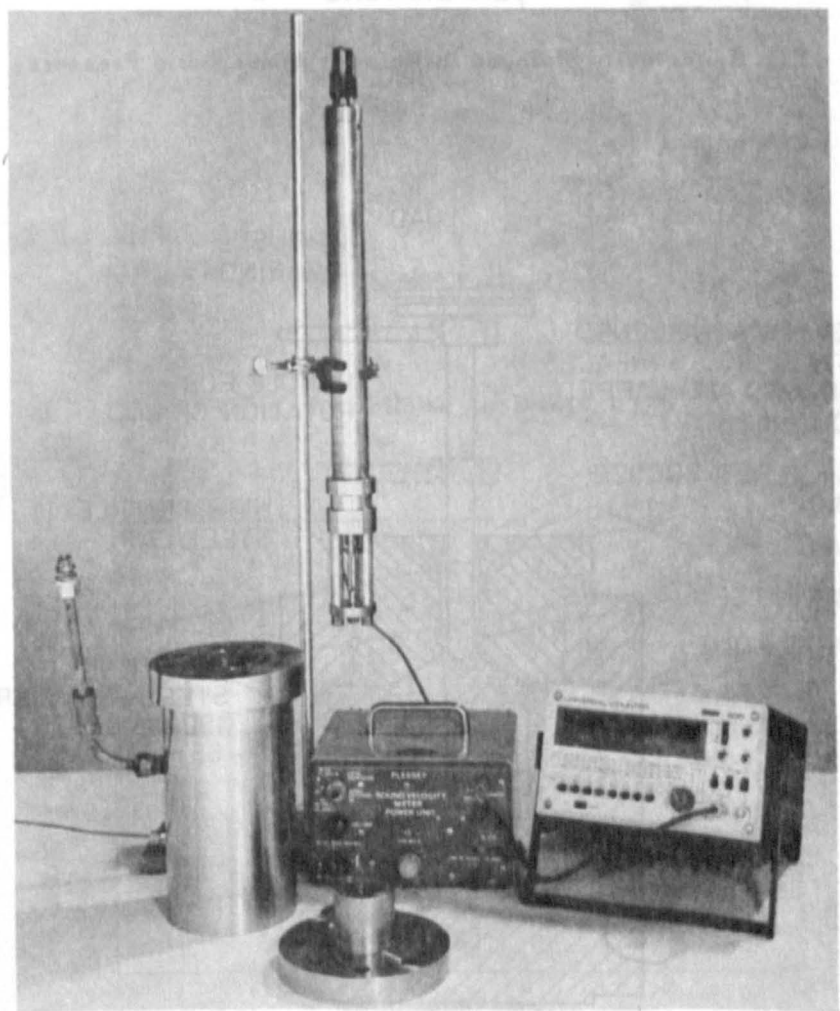

Fig. 2 Sound Velocity Meter and Pressure Vessel

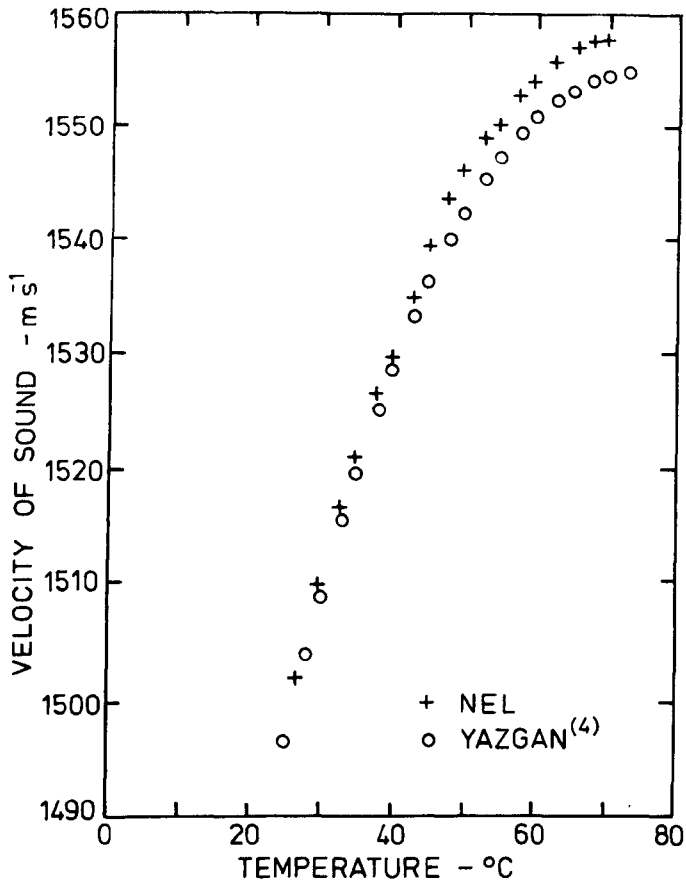

Fig. 3 Velocity of Sound in Water at Atmospheric Pressure

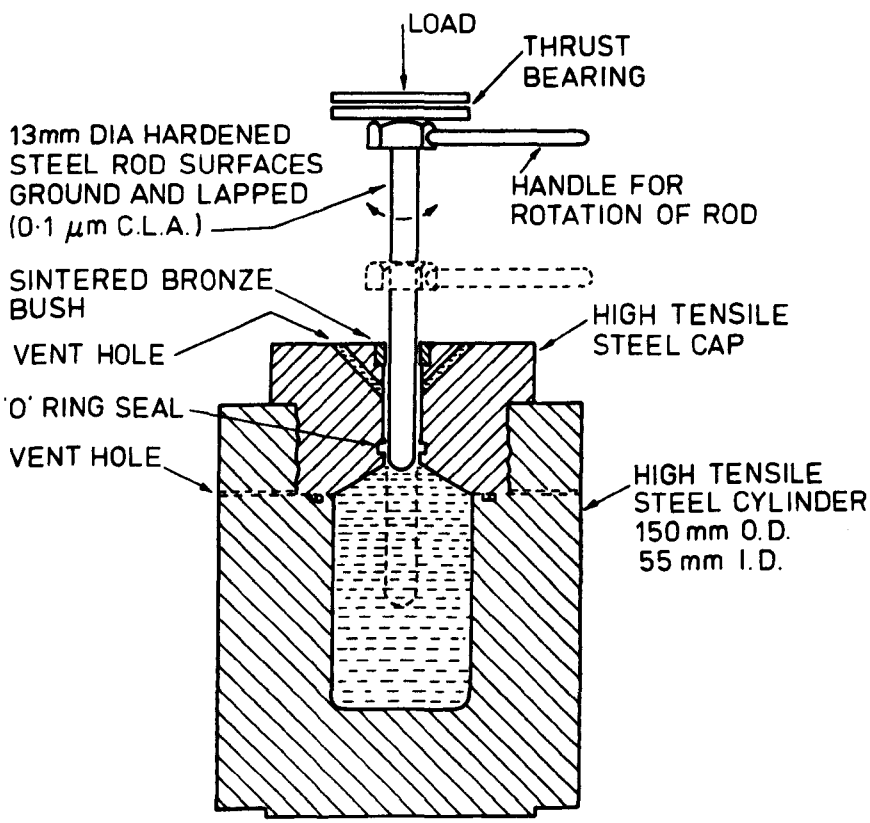

Fig. 4 NEL Bulk Modulus Tester

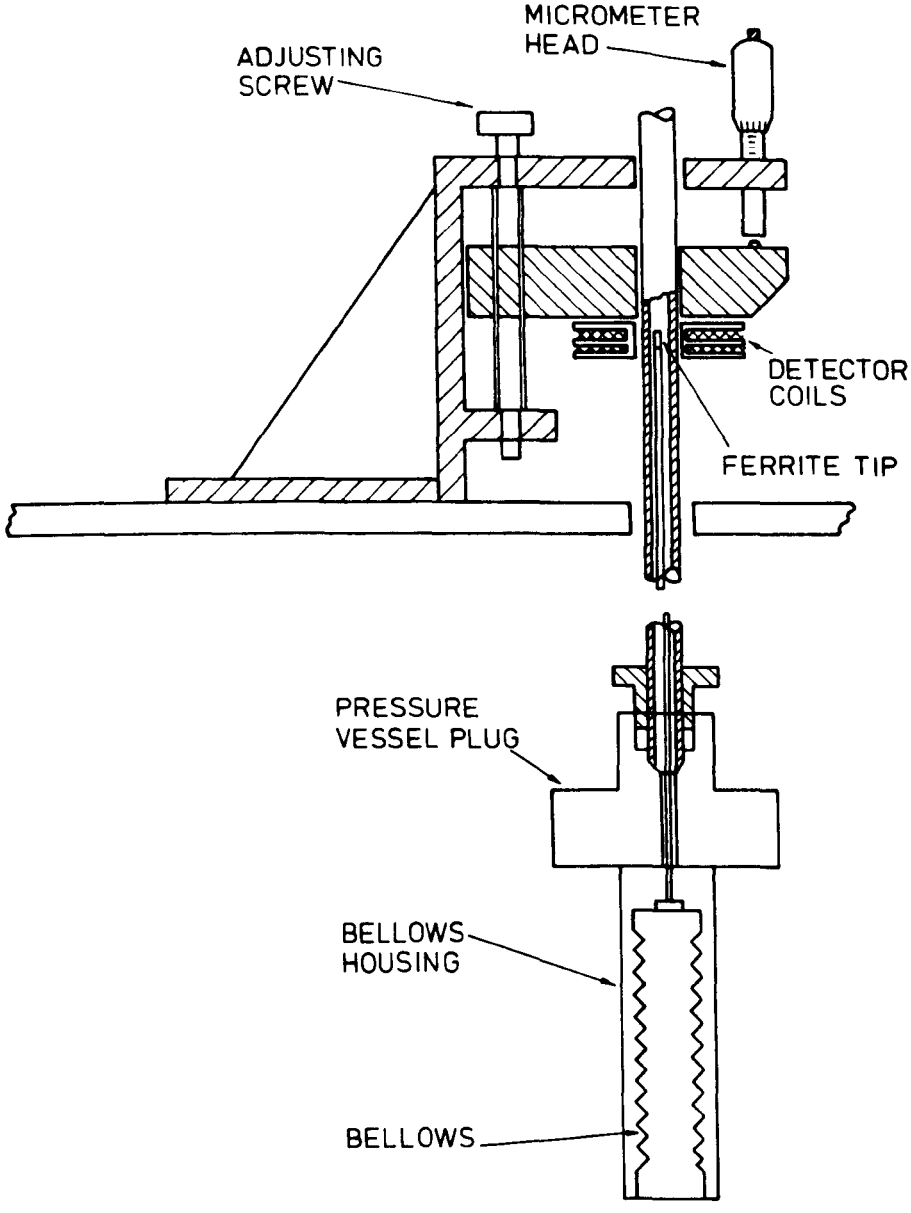

Fig. 5 Bellows Apparatus

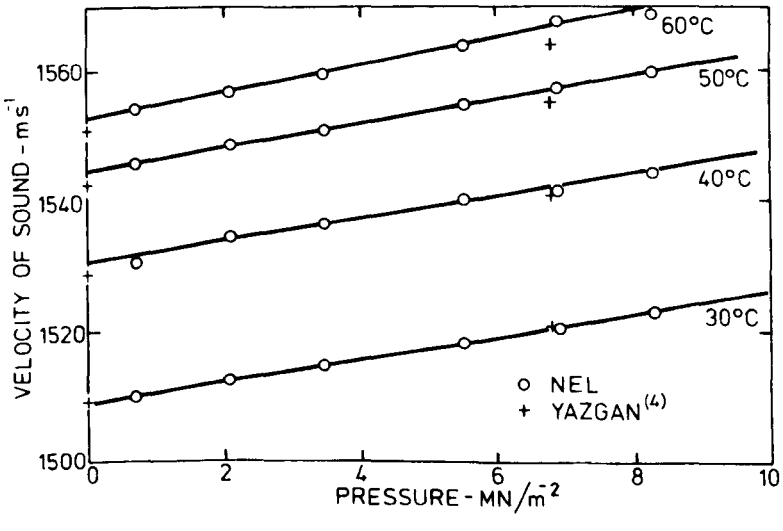

Fig. 6 Velocity of Sound in Water under Pressure

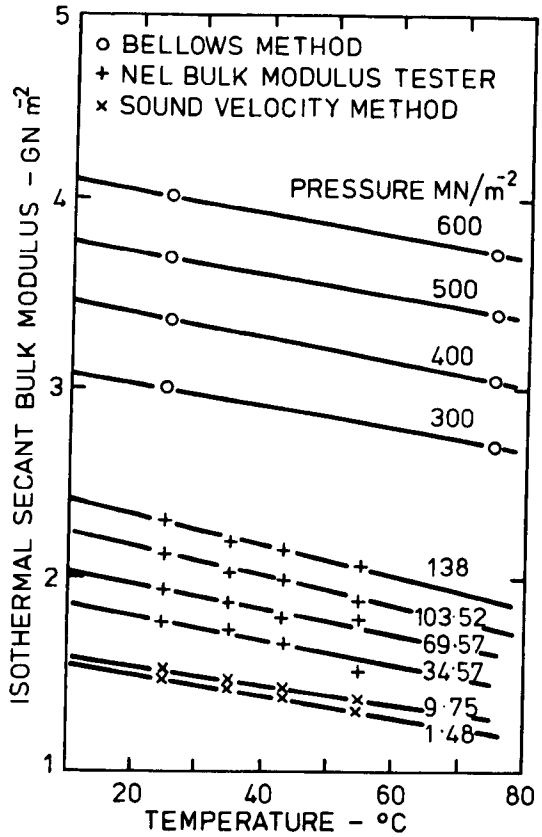

Fig. 7 Bulk Modulus of Fluid M3

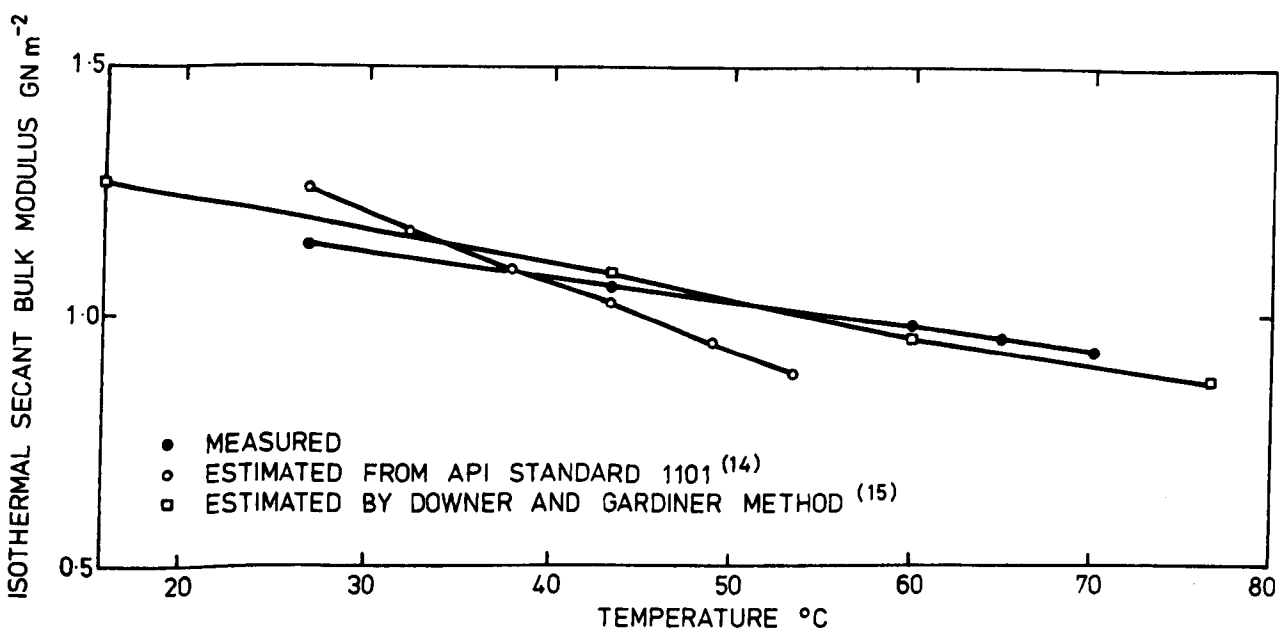

Fig. 8 Measured and Estimated Bulk Moduli of Crude Oil at 0.45 MN m^{-2}

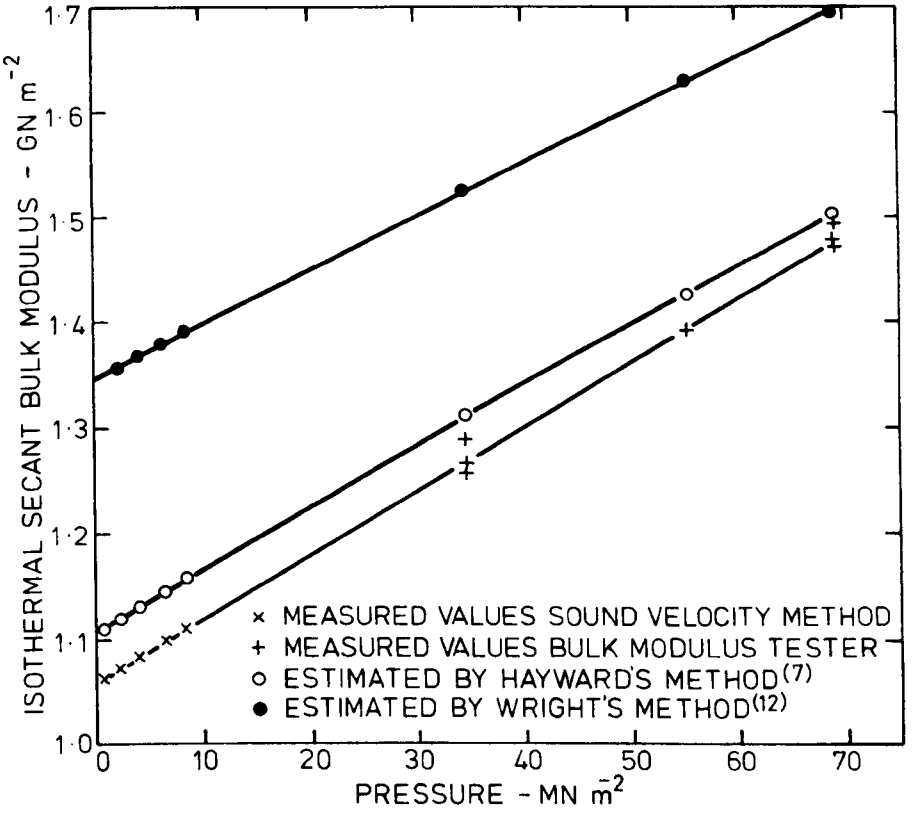

Fig. 9 Measured and Estimated Bulk Moduli of Crude Oil at 43.33°C

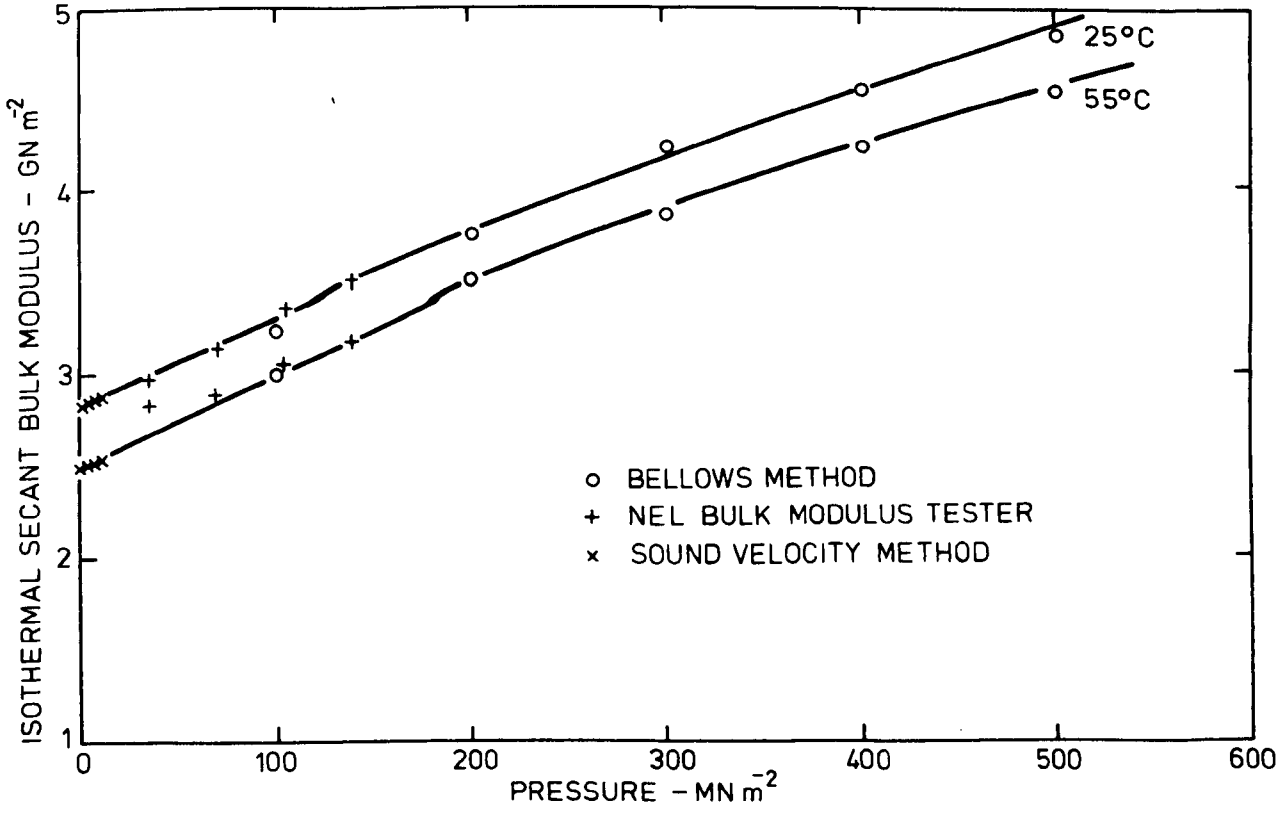

Fig. 10 Bulk Modulus of Fluid G1

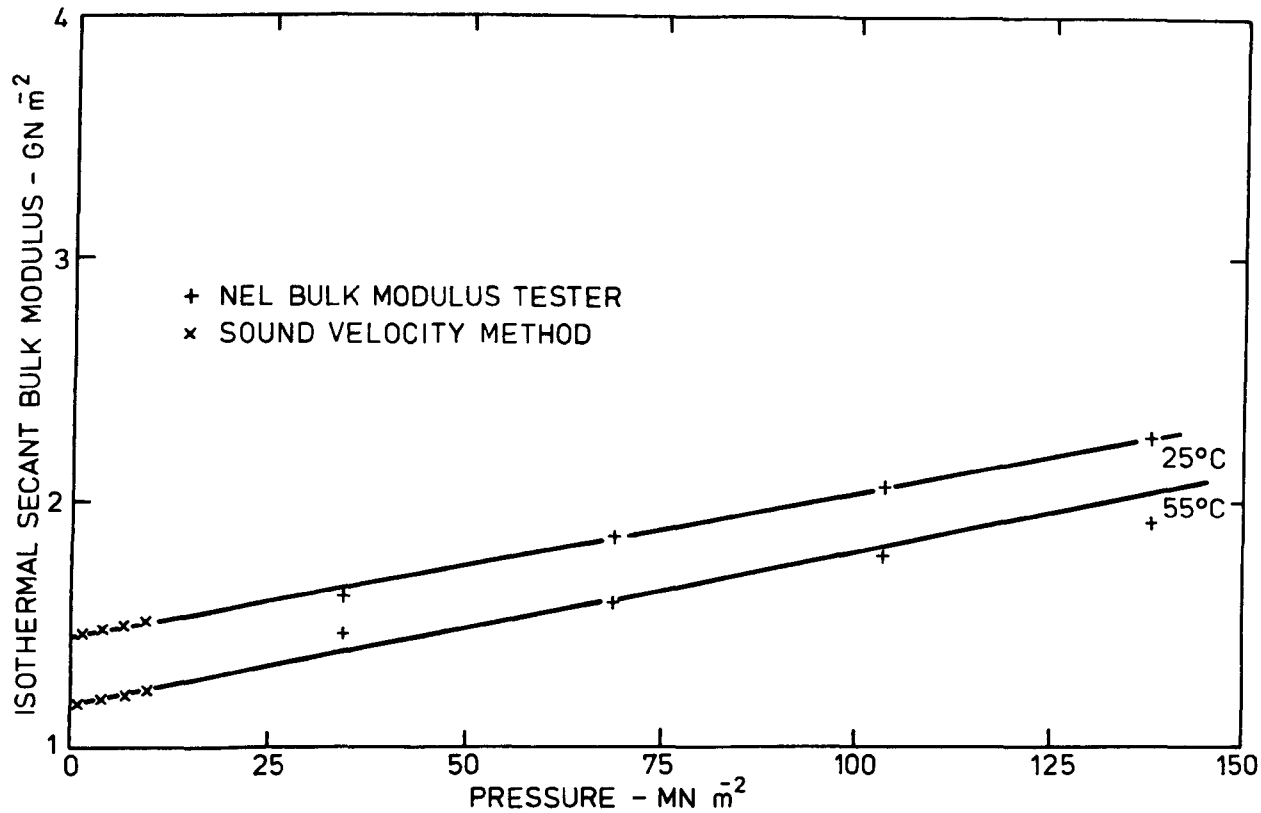

Fig. 11 Bulk Modulus of Fluid M1

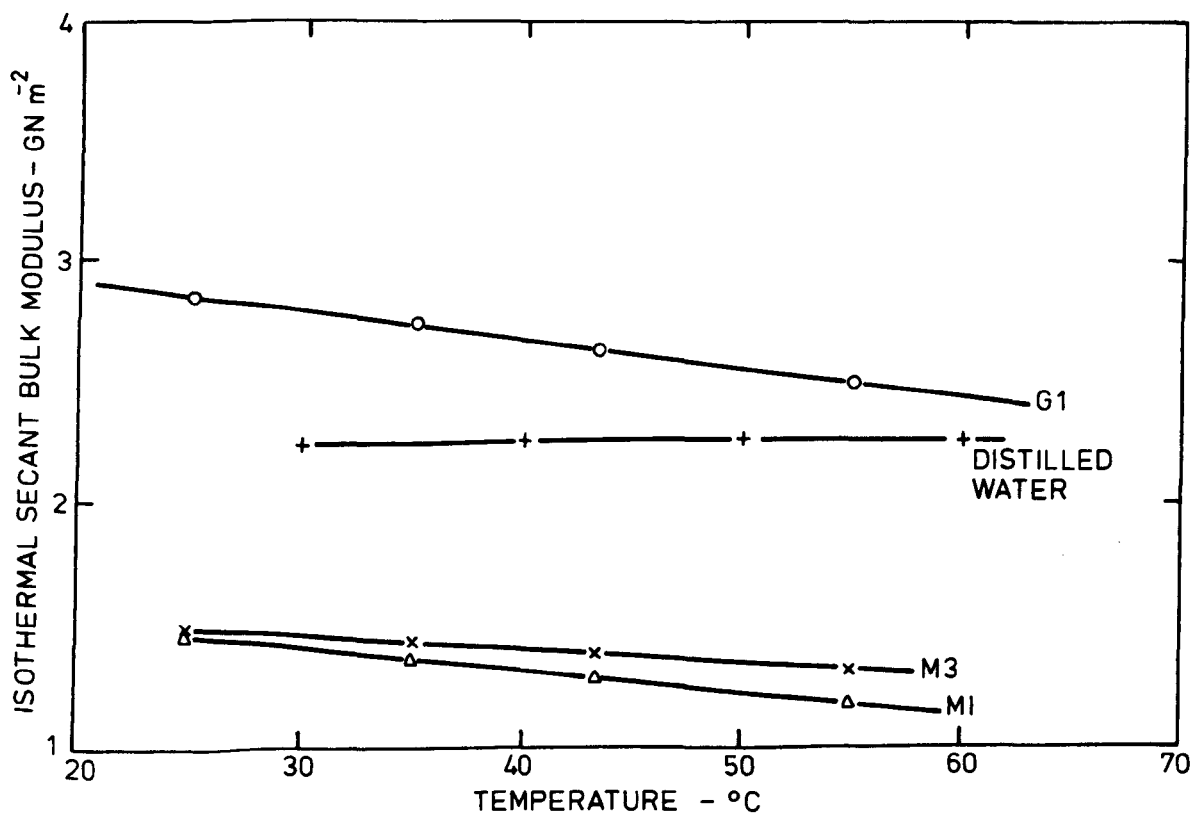

Fig. 12 Relation between Bulk Modulus and Temperature at 1.48 MN m^{-2} for Fluids G1, M1, M3, and Distilled Water

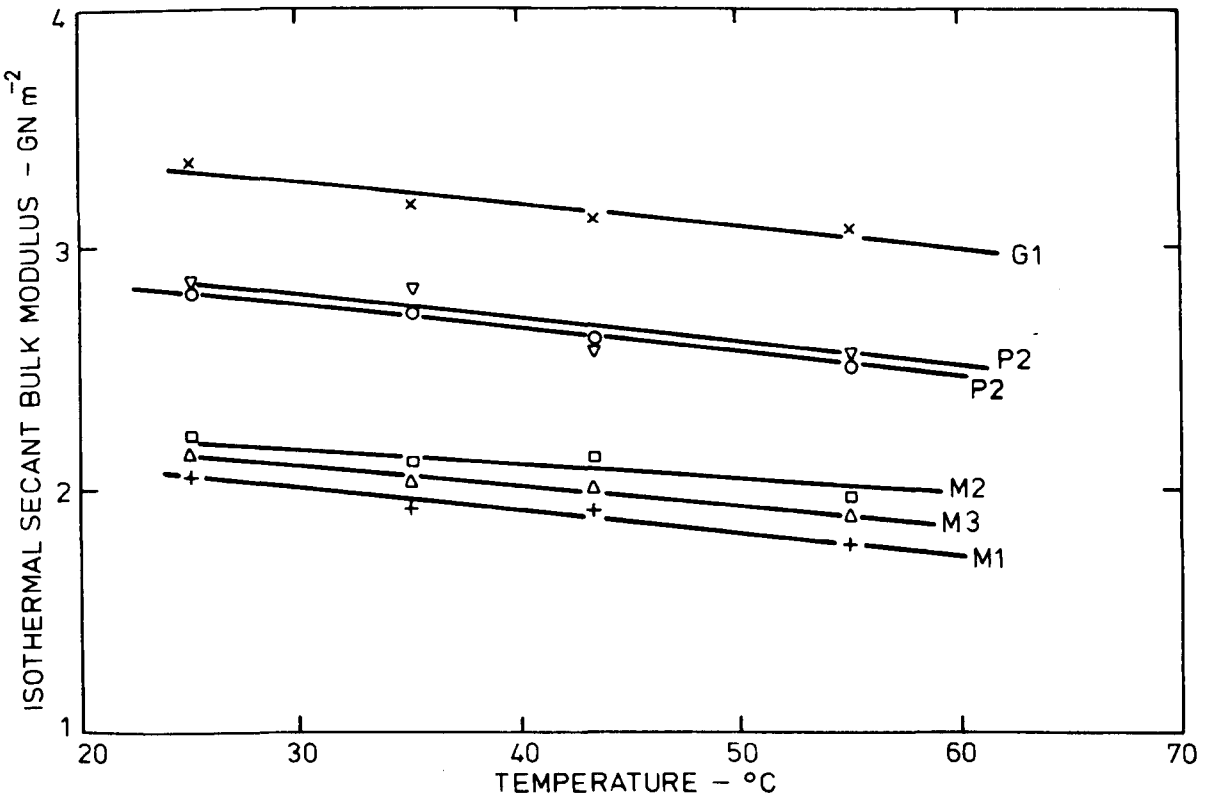

Fig. 13 Relation between Bulk Modulus and Temperature at 103.52 MN m^{-2} for Fluids G1, M1, M2, M3, P1, P2

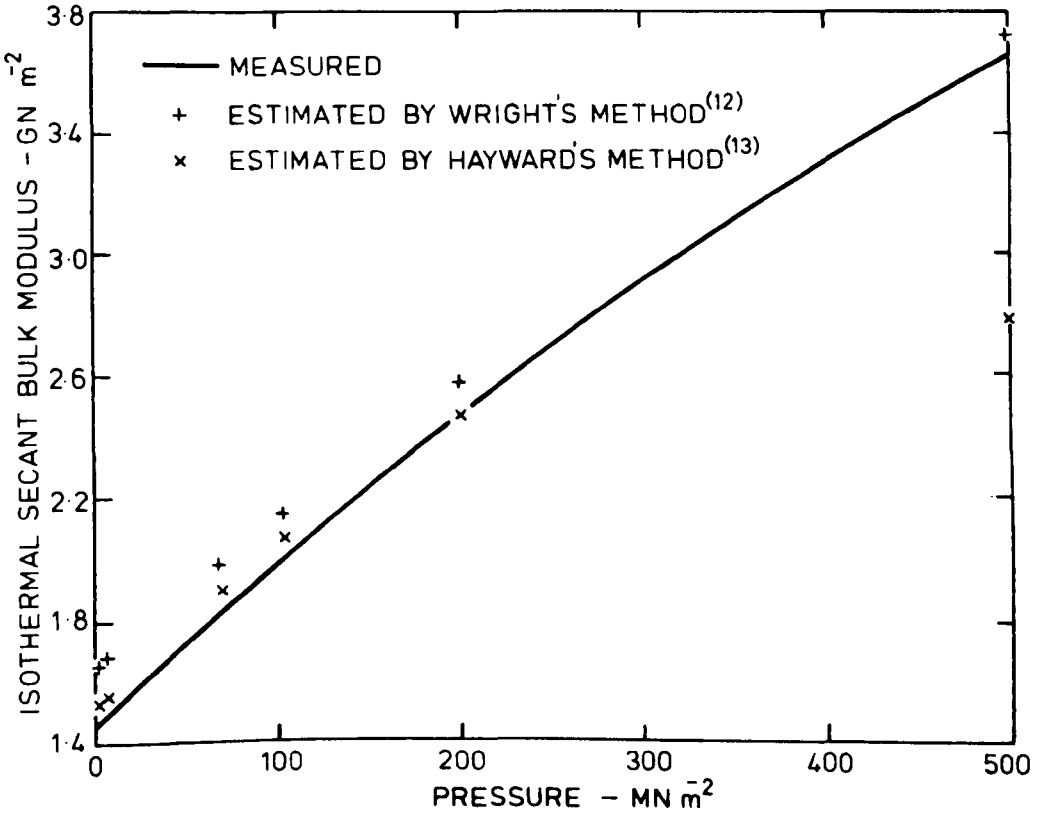

Fig. 14 Measured and Estimated Bulk Moduli of Fluid M1 at 25°C

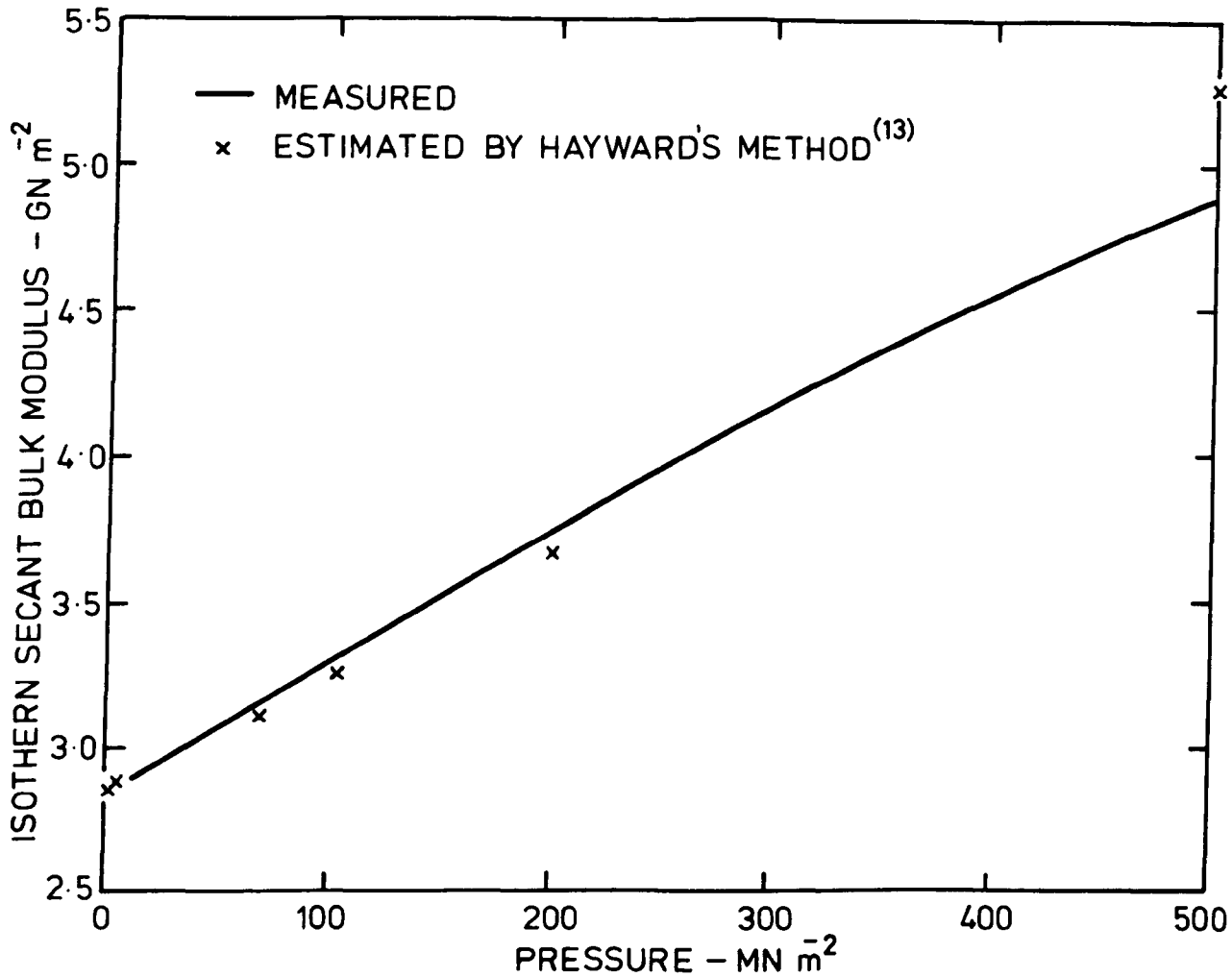

Fig. 15 Measured and Estimated Bulk Moduli of Fluid G1 at 25°C

ISDALE, J D, BRUNTON, W C and SPENCE, C M.

Bulk modulus measurement and prediction.

NEL Report No 591. East Kilbride, Glasgow: National Engineering Laboratory. June 1975.
28 pages (8 figures), 30 cm.

Three methods of measuring bulk modulus at low, medium and high pressures are described, and measurements of water, crude oil, and six typical hydraulic fluids are given at pressures up to 600 MN m^{-2} for temperatures between 25 and 75 °C. The variation of bulk modulus with pressure and temperature is examined and the accuracy of various methods of estimation is assessed.

ISDALE, J D, BRUNTON, W C and SPENCE, C M.

Bulk modulus measurement and prediction.

NEL Report No 591. East Kilbride, Glasgow: National Engineering Laboratory. June 1975.
28 pages (8 figures), 30 cm.

Three methods of measuring bulk modulus at low, medium and high pressures are described, and measurements of water, crude oil, and six typical hydraulic fluids are given at pressures up to 600 MN m^{-2} for temperatures between 25 and 75 °C. The variation of bulk modulus with pressure and temperature is examined and the accuracy of various methods of estimation is assessed.

ISDALE, J D, BRUNTON, W C and SPENCE, C M.

Bulk modulus measurement and prediction.

NEL Report No 591. East Kilbride, Glasgow: National Engineering Laboratory. June 1975.
28 pages (8 figures), 30 cm.

Three methods of measuring bulk modulus at low, medium and high pressures are described, and measurements of water, crude oil, and six typical hydraulic fluids are given at pressures up to 600 MN m^{-2} for temperatures between 25 and 75 °C. The variation of bulk modulus with pressure and temperature is examined and the accuracy of various methods of estimation is assessed.

ISDALE, J D, BRUNTON, W C and SPENCE, C M.

Bulk modulus measurement and prediction.

NEL Report No 591. East Kilbride, Glasgow: National Engineering Laboratory. June 1975.
28 pages (8 figures), 30 cm.

Three methods of measuring bulk modulus at low, medium and high pressures are described, and measurements of water, crude oil, and six typical hydraulic fluids are given at pressures up to 600 MN m^{-2} for temperatures between 25 and 75 °C. The variation of bulk modulus with pressure and temperature is examined and the accuracy of various methods of estimation is assessed.

NEL PUBLICATIONS

The following reports are available on request from NEL

McCALLUM, R and LANG, W. Combined thermal and mechanical treatments of a hot work die steel. *NEL Report* No 576

PUGH, H Ll D and CHANDLER, E F. Mechanical properties of materials under pressure. *NEL Report* No 577

Index of NEL Publications 1972-1973. *NEL Report* No 578

HENDRY, J C and MACLEAN, M S. Extrudability of a cast steel. *NEL Report* No 579

COCKCROFT, M G and MACLEAN, M S. Impact properties of cold worked mild steel. *NEL Report* No 580

THOMSON, J F. Performance of high speed steel punches in backward extrusion of cans. *NEL Report* No 581

SCOWEN, G D. Design optimization of externally pressurized gas lubricated thrust bearings for stability. *NEL Report* No 582

HOLMES, R and POOK, L P. Plain fatigue strength of a carbon manganese steel at elevated temperatures. *NEL Report* No 583

FINLAY, I C and GRANT, W D. The accuracy of some simple methods of rating evaporative coolers. *NEL Report* No 584

POOK, L P and GREENAN, A F. Preliminary tests to determine the fatigue strength of defective steel castings. *NEL Report* No 585

CRAIG, J B. Quality of response on the NEL Road Simulator. *NEL Report* No 586

MARSH, K J, MARTIN, T and McGREGOR, J. The effect of random loading and corrosive environment on the fatigue strength of fillet-welded lap joints. *NEL Report* No 587

POOK, L P. Approximate stress intensity factors for spot and similar welds. *NEL Report* No 588

NEAL, A N. A method for the analysis of incompressible flow on an axisymmetric surface through a pump or fan blade row. *NEL Report* No 589

Advances in thermal and mechanical design of shell-and-tube heat exchangers: Report of a meeting at NEL, 28 November 1973. *NEL Report* No 590